

**STRUCTURAL GEOLOGY AND TECTONIC HISTORY OF  
THE TAKU SCHIST AND SURROUNDING UNITS, NE  
PENINSULAR MALAYSIA**

**MUHAMMAD AFIQ B. MD ALI**

**FACULTY OF SCIENCE  
UNIVERSITY OF MALAYA  
KUALA LUMPUR**

**2018**

**STRUCTURAL GEOLOGY AND TECTONIC HISTORY  
OF THE TAKU SCHIST AND SURROUNDING UNITS,  
NE PENINSULAR MALAYSIA**

**MUHAMMAD AFIQ B. MD ALI**

**THESIS SUBMITTED IN FULFILMENT OF THE  
REQUIREMENTS FOR THE DEGREE OF MASTER OF  
SCIENCE**

**DEPARTMENT OF GEOLOGY  
FACULTY OF SCIENCE  
UNIVERSITY OF MALAYA  
KUALA LUMPUR**

**2018**

**UNIVERSITY OF MALAYA**  
**ORIGINAL LITERARY WORK DECLARATION**

Name of Candidate: Muhammad Afiq B. Md Ali

Registration/Matric No: SGR 130095

Name of Degree: Master of Science

Title of Thesis: Structural Geology and Tectonic History of the Taku Schist and Surrounding Units, NE Peninsular Malaysia

Field of Study: Geology

I do solemnly and sincerely declare that:

- (1) I am the sole author/writer of this Work;
- (2) This Work is original;
- (3) Any use of any work in which copyright exists was done by way of fair dealing and for permitted purposes and any excerpt or extract from, or reference to or reproduction of any copyright work has been disclosed expressly and sufficiently and the title of the Work and its authorship have been acknowledged in this Work;
- (4) I do not have any actual knowledge nor do I ought reasonably to know that the making of this work constitutes an infringement of any copyright work;
- (5) I hereby assign all and every rights in the copyright to this Work to the University of Malaya ("UM"), who henceforth shall be owner of the copyright in this Work and that any reproduction or use in any form or by any means whatsoever is prohibited without the written consent of UM having been first had and obtained;
- (6) I am fully aware that if in the course of making this Work I have infringed any copyright whether intentionally or otherwise, I may be subject to legal action or any other action as may be determined by UM.

Candidate's Signature

Date:

Subscribed and solemnly declared before,

Witness's Signature

Date:

Name:

Designation:

# **STRUCTURAL GEOLOGY AND TECTONIC HISTORY OF THE TAKU SCHIST AND SURROUNDING UNITS, NE PENINSULAR MALAYSIA**

## **ABSTRACT**

Recent studies in SE Asia have focused on extensional detachments following the Indosinian Orogeny, which have not as yet been described in Peninsular Malaysia. In this context, the study demonstrates the structural evolution of the Taku Schist with emphasis on kinematics of shear deformation by way of field and microstructural observations to explain the regional tectonic evolution of NE Peninsular Malaysia. The Taku schist represents an original Paleozoic sedimentary succession metamorphosed to amphibolite facies during Indosinian Orogeny. This is indicated by an episode of burial and metamorphism (D1), followed by top-WSW directed flattening (D2) and lastly by upright folding (D3). The overall orogenic structure by E-W directed contraction is in agreement with the evolution of continental subduction and the collision of Sibumasu and Indochina during Permo-Triassic times. For the first time, a top-SE directed shear deformation (D4) was documented, resulting in the formation of a core complex and a large-scale extensional detachment. The observed low-angle mylonitic detachment shearing is accommodated by later normal and strike-slip faulting, which forms a major NNW-SSE trending fault zone. The deformation is accompanied by greenschist-facies retrograde metamorphism, synchronous with the major exhumation of the Taku Schist and other footwall units. This includes the Stong Complex, Kemahang Granite and the Tiang Schist, separated from the Gua Musang hanging-wall by a similar top-SE detachment mechanism. The syn-kinematic intrusion of the high temperature Stong Complex during top-SE shearing and formation of young sedimentary basins in the hanging-wall indicate that the post-orogenic extension and concurrent exhumation likely occurred during Late Cretaceous – Eocene time.

Keywords: post-orogenic, extensional detachments, exhumation, Peninsular Malaysia

# **STRUKTUR GEOLOGI DAN SEJARAH TEKTONIK TAKU SCHIST DAN UNIT SEKITARAN DI TIMUR LAUT SEMENANJUNG MALAYSIA**

## **ABSTRAK**

Kajian terkini di Asia Tenggara menumpu kepada proses pembentukan detasmen berikutan episod perlanggaran Indosinia dan belum dihuraikan secara jelas bagi Semenanjung Malaysia. Dalam konteks ini, kajian evolusi struktur dan ricihan kinematik Taku Schist dilakukan berdasarkan pemerhatian kajian lapangan dan mikrostruktur bagi menjelaskan tektonik Semenanjung Malaysia. Unit Taku Schist berasal daripada batuan Paleozoik mengalami metamorfosis sehingga peringkat amphibolit-fasies akibat daripada perlanggaran Indosinia. Kajian ini menunjukkan bahawa unit Taku Schist dan sekitaran dipengaruhi oleh proses kompresi dari arah timur dan barat, melingkupi episod metamorfisma awal (D1) diikuti oleh ricihan ke arah barat daya (D2) dan berakhir dengan proses lipatan tegak (D3). Keseluruhan episod ini selaras dengan kajian evolusi subduksi dan perlanggaran benua Sibumasu dengan Indochina semasa Permo-Triasik. Ini diikuti oleh proses ricihan ke arah timur tenggara (D4) yang membentuk detasmen berskala besar serta pembentukan kompleks metamorf. Episod deformasi ini bermula dengan sesar mylonit bersudut rendah dan diikuti oleh sesar turun dan geser mendatar. Deformasi ricihan ke-arah timur tenggara (D4) diiringi oleh metamorfisma bersifat mundur sehingga peringkat greenschist-fasies serentak dengan pencungkilan Kompleks Stong, Granit Kemahang, dan Tiang Schist daripada formasi Gua Musang. Episod ini juga melingkupi intrusi syn-kinematik kompleks Stong pada suhu tinggi dan pembentukan cekungan sedimen muda sebahagian daripada unit dinding gantung. Keterangan ini menunjukkan bahawa proses pencungkilan selaras dengan canggaan D4 berlaku semasa waktu Cretaceous-Eocene.

Keywords: post-orogenic, extensional detachments, exhumation, Peninsular Malaysia

## **ACKNOWLEDGEMENTS**

This study is the result of the joint collaboration between University of Malaya, Kuala Lumpur, Malaysia (Grant no. RU011-2013) and the Netherlands Centre for Integrated Solid Earth Science, University of Utrecht, The Netherlands. The author is indebted to Dr. Iskandar Taib, Dr. Ng Tham Fatt, Dr. Liviu Matenco, and Dr. Ernst Willingshofer.

University of Malaya

## TABLE OF CONTENTS

Abstract .....	iii
Abstrak .....	iv
Acknowledgements .....	v
Table of Contents .....	vi
List of Figures .....	xi
List of Symbols and Abbreviations.....	xvi
List of Appendices .....	xvii
<b>CHAPTER 1: INTRODUCTION.....</b>	<b>1</b>
1.1 General Introduction.....	1
1.2 Problem Statement.....	1
1.3 Objective.....	3
1.4 Field Techniques.....	3
1.4.1 Measurement of Geological Structures .....	3
1.4.2 Determining the Shear Sense Criteria .....	3
1.4.3 Interpreting the Microstructural Fabric .....	4
<b>CHAPTER 2: PREVIOUS STUDIES.....</b>	<b>6</b>
2.1 General Introduction.....	6
2.2 Progression of Indosinian Orogeny .....	6
2.3 The Geology of Northern Central Belt .....	8
2.3.1 The Metamorphic Units.....	9
2.3.1.1 The Taku Schist.....	9
2.3.1.2 The Tiang Schist.....	14
2.3.2 The Sedimentary Units .....	15

2.3.2.1	The Gua Musang/ Aring Formation .....	15
2.3.2.2	The Gagau Group .....	16
2.3.3	The Igneous Plutons .....	17
2.3.3.1	The Stong Complex.....	17
2.3.3.2	The Kemahang Granite .....	20
<b>CHAPTER 3: THE TAKU SCHIST .....</b>		<b>23</b>
3.1	Introduction.....	23
3.2	The Southern Dome – 1st Sector (SSE domain) .....	28
3.2.1	Field Observation .....	28
3.2.1.1	Structural Geometries.....	28
3.2.1.2	Kinematic Transport.....	31
3.2.1.3	Contact with Overlying Unit.....	32
3.2.2	Petrographic Study .....	33
3.2.2.1	Microstructural Observation .....	33
3.2.2.2	Metamorphic Parageneses.....	38
3.3	The Central Dome – 2nd Sector .....	38
3.3.1	Field Observation .....	38
3.3.1.1	Structural Geometries.....	39
3.3.1.2	Kinematic Transport.....	44
3.3.1.3	Contact with Overlying Unit.....	45
3.3.2	Petrographic Study .....	48
3.3.2.1	Microstructural Observation .....	48
3.3.2.2	Metamorphic Parageneses.....	54
3.4	The Northern Dome – 3rd Sector .....	55
3.4.1	Field Observation .....	55

3.4.1.1	Structural Geometries.....	55
3.4.1.2	Kinematic Transport.....	59
3.4.1.3	Contact with Overlying Unit.....	60
3.4.2	Petrographic Study.....	62
3.4.2.1	Microstructural Observation.....	62
3.4.2.2	Metamorphic Parageneses.....	66
<b>CHAPTER 4: THE SURROUNDING UNITS.....</b>		<b>67</b>
4.1	Introduction.....	67
4.2	The Gua Musang/Aring Formation.....	71
4.2.1	Field Observation.....	71
4.2.1.1	Eastern Flank of the Taku Schist.....	71
4.2.1.2	Western Flank of the Taku Schist.....	77
4.2.1.3	Southern Flank of the Taku Schist.....	83
4.2.2	Petrographic Study.....	85
4.2.2.1	Micro-Structural Observation.....	85
4.2.2.2	Metamorphic Parageneses.....	93
4.3	The Panau Formation.....	94
4.4	The Boundary Range Granite.....	96
4.5	The Kemahang Granite.....	97
4.5.1	Field Observations.....	97
4.5.1.1	The Eastern Unit.....	98
4.5.1.2	The Western Unit.....	101
4.5.2	Microstructural Observation.....	106
4.5.3	Metamorphic Parageneses.....	111
4.6	The Stong Complex.....	112

4.6.1	Field Observation .....	112
4.6.1.1	Berangkat Tonalite .....	112
4.6.1.2	Kenerong Leucogranite .....	113
4.6.1.3	Noring Granite.....	119
4.6.2	Petrographic Study .....	124
4.6.2.1	Microstructural Observation .....	124
4.6.2.2	Metamorphic Parageneses.....	129
4.7	Tiang Schist .....	130
4.7.1	Field Observation .....	130
4.7.2	Petrographic Study .....	133
4.7.2.1	Microstructural Observation .....	133
4.7.2.2	Metamorphic Parageneses.....	137
<b>CHAPTER 5: STRUCTURAL ANALYSIS .....</b>		<b>138</b>
5.1	Introduction.....	138
5.2	Initial Burial Compression and Metamorphism, D1 .....	143
5.2.1	Field Observation .....	143
5.2.2	Microstructural Study.....	146
5.2.3	Top- West Directed Shearing, D2 .....	147
5.2.3.1	Field Observation .....	147
5.2.3.2	Microstructural Study.....	149
5.2.4	Late E-W Contraction, D3.....	152
5.2.4.1	Field Observation .....	152
5.2.5	Top- SE Detachment, D4 .....	154
5.2.5.1	Field Observation .....	154

<b>CHAPTER 6: DISCUSSION .....</b>	<b>161</b>
6.1 The Evolution of the Taku Schist and the Surrounding Units.....	161
6.2 Implication of Taku Extensional Detachment .....	169
<b>CHAPTER 7: CONCLUSION.....</b>	<b>176</b>
References .....	179
List of Publications and Papers Presented .....	183
Appendix A: Complementary Maps .....	187
Appendix b: Data sets .....	188

University of Malaya

## LIST OF FIGURES

Figure 1.1: Methods in determining the shear sense movement.....	4
Figure 2.1: Cartoons illustrating the formation of the Bentong–Raub Suture. ....	7
Figure 2.2: Geological map of northern part of Peninsular Malaysia.....	9
Figure 2.3: Geological map of the Taku Schist after Dawson et al. (1968).....	10
Figure 2.4: U-Pb Zircon ages of granitoid plutons across Peninsular Malaysia.....	13
Figure 2.5: Geological transect of the eastern foothills of Main Range Granite .....	15
Figure 2.6: Geological map of the Stong Complex.....	19
Figure 3.1: Geological map of the study area .....	24
Figure 3.2: The southern, central and northern domain of the Taku Schist.....	25
Figure 3.3: Taku Schist map showing the orientation of foliation plane and stretching lineation.....	26
Figure 3.4: Plot of fold axis observed in the Taku Schist unit.....	26
Figure 3.5: Taku Schist map showing the interpreted kinematic directions from shear sense analysis. ....	27
Figure 3.6: Garnet (almandine) porphyroblast in quartz-mica schist .....	29
Figure 3.7: The observed folds in the SSE domain, Taku Schist.....	30
Figure 3.8: Mylonitic exposures in SSE margin of Taku Schist.....	31
Figure 3.9: Sedimentary and volcanic rock exposure in the southern margin of Taku Schist.....	32
Figure 3.10: Photomicrograph of garnet-quartz-mica schist in SSE domain within Ulu Temiang Forest Reserve.....	33
Figure 3.11: Photomicrograph of quartz-rich schist in SSE domain within Ulu Temiang Forest Reserve.....	35
Figure 3.12: Photomicrograph of garnet-biotite schist in the SSW margin near Kg. Slow Pak Long .....	36

Figure 3.13: Photomicrograph of mylonitized biotite- granite in SSE margin near Manik Urai.....	37
Figure 3.14: Exposures across Galas River transect .....	40
Figure 3.15: Rock exposures near Temangan area .....	41
Figure 3.16: Quartz-mica schist fabric within Sokor-Taku area.....	43
Figure 3.17: Graphitic schist within Sokor-Taku area.....	44
Figure 3.18: Fault contact in Temangan area.....	46
Figure 3.19: Photomicrograph of quartz-feldspar-mica schist near Temangan iron mine. ....	48
Figure 3.20: Photomicrograph of quartz-feldspar schist in the E flank at Kg. Sg. Hau .	50
Figure 3.21: Photomicrograph of garnet-biotite schist in the WNW flank at Sokor Taku Forest Reserve.....	52
Figure 3.22: Photomicrograph of quartz-rich schist in to the W margin at Sg. Galas Basin.....	54
Figure 3.23: Compositional difference within quartz-mica schist, NNE domain of the Taku Schist.....	56
Figure 3.24: Examples of small- scale structures observed within the schist.....	57
Figure 3.25: Inclined asymmetrical folds in SSW margin of Kemahang granite. ....	58
Figure 3.26: Cataclastic schist layer contained within a fault zone .....	59
Figure 3.27: Rock exposures near to Kemahang Granite-Taku Schist contact, NNW part of Taku Schist .....	60
Figure 3.28: Photomicrograph of garnet-mica schist in the NW flank in Sokor Taku Forest Reserve.....	62
Figure 3.29: Photomicrograph of quartz-mica schist in the NE flank at Kg. Ipoh. ....	63
Figure 3.30: Photomicrograph of quartz-mica schist in the NNE flank at Kg. Ipoh. ....	65
Figure 4.1: Geological map of study area showing the overall stations .....	67
Figure 4.2: The foliation and bedding planes map of the surrounding units .....	68

Figure 4.3: The fault map of the Taku Schist and the surrounding units.....	69
Figure 4.4: Plots of fold axis observed in the surrounding units .....	69
Figure 4.5: Kinematic transport map of the surrounding uni.....	70
Figure 4.6: Examples of lithologies observed in the eastern flank, Gua Musang Formation .....	72
Figure 4.7: Sketch of a sedimentary rock exposure in Kuala Krai .....	74
Figure 4.8: Carbonaceous shale exposure in Kuala Krai .....	74
Figure 4.9: Exposures within the Lebir Fault Zone .....	75
Figure 4.10: Example of sedimentary rock exposures in the western flank, Gua Musang Formation .....	79
Figure 4.11: Schistosed oolitic limestone fabric showing S/C shear bands.....	79
Figure 4.12: Examples of folds in the western flank, Gua Musang Formation .....	81
Figure 4.13: Quartz-feldspar schist bounded between fault planes near Dabong.....	81
Figure 4.14: Rock exposures in contact with the Noring Granite near Batu Melintang. 82	
Figure 4.15: Sedimentary rock exposures in the southerly flank, Gua Musang Formation .....	84
Figure 4.16: Photomicrograph of phyllites near to the ESE margin of Taku Schist.....	85
Figure 4.17: Photomicrograph of tuffaceous siltstone in the direction toward SSE of Taku Schist.....	87
Figure 4.18: Photomicrograph of mudstone near the eastern margin of Taku Schist....	88
Figure 4.19: Photomicrograph of dacite near the eastern margin of the Taku Schist....	89
Figure 4.20: Photomicrograph of rhyolite at Sg. Galas near to the Eastern margin of Taku Schist.....	90
Figure 4.21: Photomicrograph of tuffaceous phyllite near Lebir fault zone.....	91
Figure 4.22: Photomicrograph of tuffaceous siltstone at the western flank of Gua Musang Formation. ....	92
Figure 4.23: Polymict conglomerates of Panau Formation.....	94

Figure 4.24: Faults observed in the Panau Formation.....	95
Figure 4.25: Boundary Range Granite exposure in adjacent of Panau Formation.....	96
Figure 4.26: Examples of granite rock exposures within the Lebir Fault zone at Lata Rek. ....	97
Figure 4.27: Development of foliations in Kemahang granite.....	99
Figure 4.28: Kemahang granite exposure near Taku Schist, Polytechnic Jeli.....	101
Figure 4.29: Kemahang granite exposure near Noring Granite, Kg. Sg. Rual .....	103
Figure 4.30: Photomicrograph of migmatite in the western domain of Kemahang granite .....	106
Figure 4.31: Photomicrograph of quartz-feldspar enclave in the western domain of Kemahang granite unit. ....	107
Figure 4.32: Photomicrograph of sheared Kemahang granite in the western domain of the unit.....	109
Figure 4.33: Photomicrograph of sheared Kemahang granodiorite in the eastern domain of the unit. ....	110
Figure 4.34: Photomicrograph of quartz-mica enclaves (Taku Schist), in Kemahang granite at Polytechnic Jeli. ....	111
Figure 4.35: Examples of Berangkat granodiorite exposures .....	113
Figure 4.36: Fault contact between Berangkat tonalite and Kenerong Leucogranite. ...	113
Figure 4.37: Examples of styles of intrusion observed across Sg. Kenerong.....	115
Figure 4.38: Relations between meta-sedimentary xenoliths and granite at Sg. Kenerong. ....	116
Figure 4.39: Rock exposure near Kenerong Leucogranite showing transition of quartz-mica schist into migmatite melts.....	117
Figure 4.40: Sheared meta-sedimentary and leucogranite rocks in Sg. Renyok.....	118
Figure 4.41: Examples of Noring granite exposures in G. Basor Forest Reserve .....	120
Figure 4.42: Sheared meta-sedimentary xenolith exposure in Lata Tubur .....	122

Figure 4.43: Photomicrograph of quartz-feldspar hornfels, forming xenoliths in Kenerong Leucogranite at Sg. Kenerong.....	124
Figure 4.44: Photomicrograph of calc-silicate hornfels xenolith in Kenerong Leucogranite at Sg. Renyok.....	126
Figure 4.45: Photomicrograph of sheared Berangkat tonalite at Gunung Stong, Dabong.....	127
Figure 4.46: Photomicrograph of amphibole hornfels and quartz-feldspar hornfels xenolith of Noring Granite at Lata Tubur.....	128
Figure 4.47: Folded Tiang Schist exposure on EW-highway.....	131
Figure 4.48: Photomicrograph of quartz-mica schist with pervasive shear fabrics and contact metamorphosed quartz-mica-schist near Main Range Granite.....	133
Figure 4.49: Photomicrograph of andalusite-mica-schist near Kemahang Granite.....	135
Figure 4.50: Photomicrograph of contact metamorphosed quartz-feldspathic schist near Noring Granite.....	136
Figure 5.1: Structural geology map of the study area with overall S1 Foliation.....	139
Figure 5.2: Structural geology map of the study area with overall kinematic result. ...	140
Figure 5.3: Structural and geological cross-section of the Taku Schist and surrounding units across an east-west transect.....	141
Figure 5.4: Structural and geological cross-section of the Taku Schist and surrounding unit across northwest-southeast transect.....	142
Figure 5.5: Summarize tectonic-stratigraphic plot of the Taku Schist and the surrounding units.....	157
Figure 6.1: Summarize of evidences detailed by this study and the interpreted tectonic implication.....	161
Figure 6.2: The formation of low-angle detachment fault by the formation of metamorphic core complex.....	168
Figure 6.3: Interpreted tectonic model for the Taku Schist following modification of Metcalfe (2002).....	170
Figure 6.4: Cross-section in the Northern Thailand from Chiang Mai Basin across Doi Intahonon Core Complex.....	174

## LIST OF SYMBOLS AND ABBREVIATIONS

### Mineral Descriptions:

Adl	:	Andalusite
Bt	:	Biotite
Ca	:	Calcite
Grt	:	Garnet
Hbl	:	Hornblende
Kfs	:	K-feldspar
Mcv	:	Muscovite
Plg	:	Plagioclase
Qtz	:	Quartz
Src	:	Sericite
Trm	:	Tourmaline
Ttn	:	Titanite

### Recrystallization Degrees of Quartz Aggregates:

BLG	:	Grain boundary bulging
GBM	:	Grain boundary migration
SGR	:	Grain boundary rotation

## LIST OF APPENDICES

Appendix A: Complementary map of study area	187
Appendix B: Measured field data sets	188

University of Malaya

## **CHAPTER 1: INTRODUCTION**

### **1.1 General Introduction**

The collision between two different blocks i.e. Sibumasu and Indochina plates during Late Triassic was long known as Indosinian Orogeny signifying an important geological boundary across SE Asia (Metcalf, 2000, 2013; Hutchison and Tan, 2009). Until recently, many research across SE Asia focuses on the development of post-orogenic extensional tectonics that involves major exhumation of continental units and the creation of coeval sedimentary basins (Pubellier and Morley, 2014). In Peninsular Malaysia, the progression of Indosinian Orogeny is known by continental subduction and collision between Sibumasu and Indochina block (Sukhothai Arc system and larger Indochina terrane) along the Bentong-Raub Suture Zone striking across the mid-line of Peninsular Malaysia that stretches northward across Thailand-Burma border. Previous studies have demonstrated many critical evidences of post-orogenic activities that includes regional uplift and exhumation across Peninsular and formation of young sedimentary basins during Late Cretaceous to Eocene times (Pubellier and Morley, 2014). This is in particular observed in NE Peninsular Malaysia where unexplained extensive metamorphic body (i.e. the Taku Schist) is exposed situated close to post-orogenic intrusions (i.e. the Stong Complex) and young sedimentary basins (i.e. the Gagau Group). While this post-orogenic feature are the foundations of an extensional tectonic settings of Peninsular Malaysia, the mechanics which result in formation of these important structures have not yet been recognized up to present time.

### **1.2 Problem Statement**

The selection of area of interest should starts with local structural geometries that contain a characteristic able to define the regional tectonic system. In this study, the Taku Schist is a part of Central Belt situated to the east of Bentong-Raub Suture Zone. The extension of this tectonic line however, is unclear in the northern Peninsular

Malaysia and was speculated to extend along the west margin on the Stong Complex. Nevertheless, the extension of the tectonic line across Thailand border pertaining to Paleo-Tethys suture zone has been well accepted in previous studies (Metcalf, 2000, 2013). The location of the Taku Schist is also close to the Stong Complex, which indicates a post-orogenic activities that result in intrusion and can possibly responsible for the unroofing of the Taku Schist.

The Taku Schist body is the product of high grade metamorphism, which is overlaid by sediments of Gua Musang/ Aring formation that were only affected by low grade to non regional metamorphism. However, the geological contacts between these two units are not known up to present times. Thus, the location of the Taku Schist is near to suture-zone and is affected by post-orogenic activities by unknown tectonic process that result in significant metamorphic offset with overlying sediment possibly coeval with intrusion of Stong Complex.

The long axis of Taku Schist body stretched nearly 60 km in length whereas perpendicular width ranges about 15 km in length. The interested study area also include Tiang Schist, Stong Complex and Gua Musang/ Aring Formation, which altogether spans approximately 90 km X 90 km wide stretches from east of Main Range to Eastern Boundary Granite on the westerly side. Most of the exposures of Taku Schist and surrounding unit lie within deep forest reserve from Kuala Gris – Manik Urai – Kuala Krai – Temangan – Tanah Merah, and is strong affected by deep tropical weathering.

### **1.3 Objective**

The main objective of this research is to study the structural framework of the Indosinian orogenic and post-orogenic development in NE Peninsular Malaysia. In this context, the research intent to explain:

1. The quantitative structural geometries of Taku Schist and surrounding units, integrated with kinematic transport and metamorphic analyses.
2. The mechanics of deformation geometries observed in the Taku Schist and surrounding units observed in both field and microstructures study.
3. The interpreted structures and kinematic deformation to the regional evolution the Taku Schist and the surrounding units.
4. The tectonic process that controls the evolution of the Taku Schist in relation to the surrounding units and in larger regional context.

### **1.4 Field Techniques**

#### **1.4.1 Measurement of Geological Structures**

The most important aspect of this study is arguably fieldwork, which concern on quantitative measurement throughout the areas of interest. An essential measurement of orientation of geological structures in field includes foliation, lineation, fold axes, fault planes and slickenlines. These data are assisted by sketches and photographs to construct a proper cross-cutting relationship between each deformational structure with its details.

#### **1.4.2 Determining the Shear Sense Criteria**

While kinematic movement can be inferred from sorts of classical indicators including direction of fold vergence, asymmetric boudinages and passive markers, a more comprehensive method in determining shear sense movement by Simpson and Schmid (1983) were implemented into this study. The required plane in observing the

shear criteria should be parallel to stretching lineation and perpendicular to foliation plane (Figure 1.1). Following shear sense indicators such as S/C and S/C' shear bands as well as rotated porphyroblasts, the movement can be inferred either plunging toward or against the direction of inclination of the foliation plane.

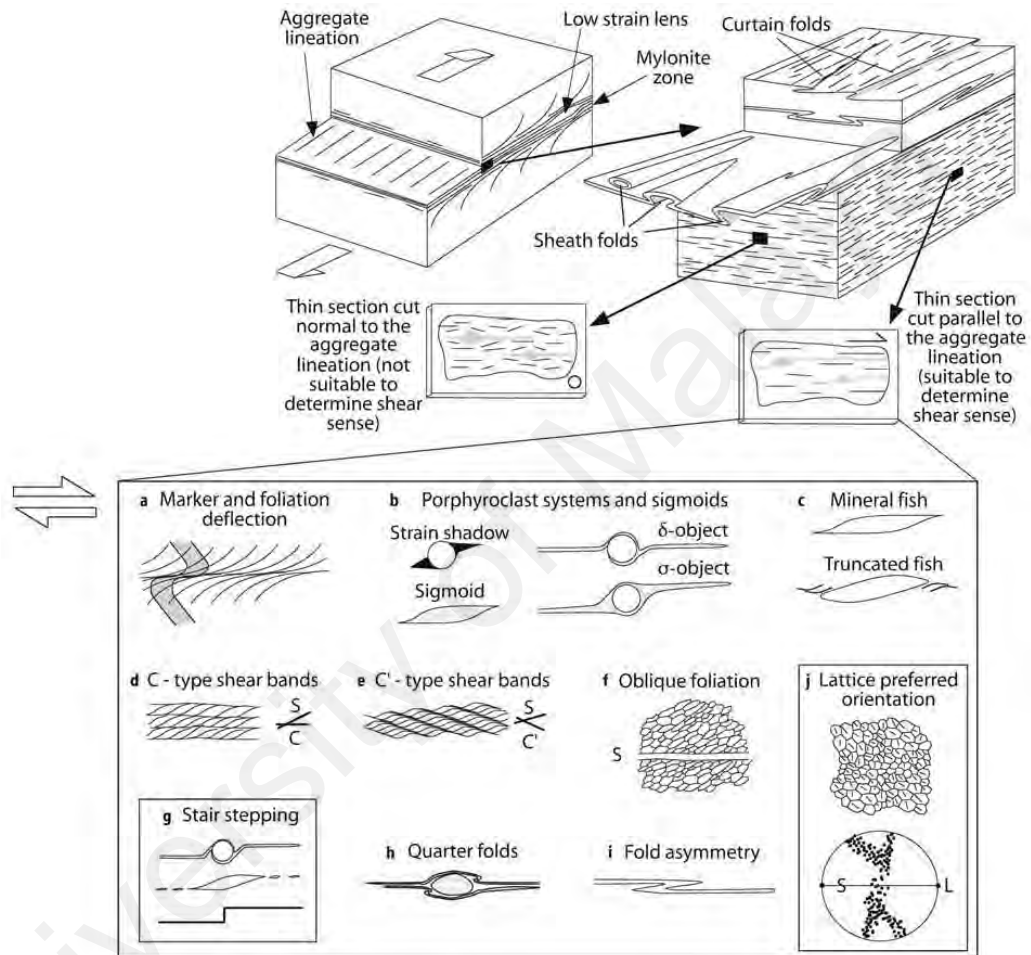


**Figure 1.1: Methods in determining the shear sense movement (Passchier, 2000). Applied in both field and microscopic analysis in this study.**

### 1.4.3 Interpreting the Microstructural Fabric

Following Moore (1970) and Passchier (2000), a principal classification based on mutual arrangements of grains and fabrics were used in this study to describe the size distributions of grains aggregates i.e. equigranular, inequigranular and seriate textures, where the geometry of the grain boundary can be described as polygonal, interlobate or ameboid shapes. Special terms used in describing textures of rocks in this study include

granoblastic (mosaic of approximately equal-dimensional mineral grains), flaser (lenses of quartz separated by bands of finely crystalline), and mylonitic (fine grained rocks with marked laminated and presence of small megacryst). Foliation cleavage defined by a preferred orientation of inequant fabric elements forming a layer of parallel surfaces in a rock were distinguished and classified accordingly to discuss the main processes involved in their development, such as fine-slaty cleavage or coarse-gneissic cleavages. The fabric elements in domainal structures forming the foliation cleavage are also described by the spacing, shapes and proportion.

The dynamic recrystallization of quartz is used as reference for this study to demonstrate temperature constraint of crystal-plastic deformation (Passchier, 2003). Three different types of recrystallization mechanism include grain boundary bulging, sub-grain rotation and grain boundary migration. The grain boundary bulging recrystallization (BLG) operates around 250-300 °C which is characterized by development of core-mantle structure with serrated boundaries and patchy undulose extinction. Grain boundary rotation (SGR) operates around 400-500 °C following progressive misorientations of subgrain and the formation of new grains showing lattice-preferred orientation and sweeping undulose extinction. Grain boundary migration (GBM) operates at high temperature around 500-700 °C characterized by amoeboid shapes of quartz aggregates with lobated outline assembled in variable grains sizes and devoid of undulose extinction or subgrains development.

## **CHAPTER 2: PREVIOUS STUDIES**

### **2.1 General Introduction**

The Peninsular Malaysia has long been recognized to comprise of three major N-S belts i.e. Western, Central and Eastern belts separated based on differences in magmatism, stratigraphy, structures and metamorphism (e.g. Hutchison, 1973; Metcalfe, 2000 & 2013). These three different belts were assembled following the progression of Indosinian Orogeny during Permo-Triassic times. The late Triassic collision between two continental plates (Sibumasu and Indochina) led to formation of the Bentong-Raub Suture Zone of Peninsular Malaysia.

### **2.2 Progression of Indosinian Orogeny**

The Western and Eastern belts of Peninsular Malaysia represent the lateral extensions of the Sibumasu and Indochina terranes to the north across the border with Thailand, sutured together as a result of the Indosinian Orogeny (Metcalfe, 2000). Stratigraphic and biogeographic affinities indicate that the Paleo-Tethys Ocean was once separated Sibumasu from Indochina up to the Early Permian, until which time both blocks shows different climatic affinities. While the Sibumasu terrane was subjected to cold climatic conditions and had stratigraphic affinities to Gondwanaland, the Indochina block was subjected to a warm climate and has stratigraphic affinities to Cathaysia. In agreement with rapid northward movement of the Sibumasu plate toward Indochina during the Permo-Triassic indicated by Paleo-magnetic data (Ritcher et al. 1999), this period represents the closure of the Paleo-Tethys ocean by eastward subduction underneath Indochina block (Figure 2.1 a, b). During this process, the developing accretionary prism separates the Semanggol foredeep basin on west, from the Gua Musang-Semantan volcanoclastic forearc basin on east (Figure 2.1 a, b). This accretionary prism contains heterogeneous remnants of the Paleo-Tethys Ocean continuously accreted toward the west by eastward subduction.

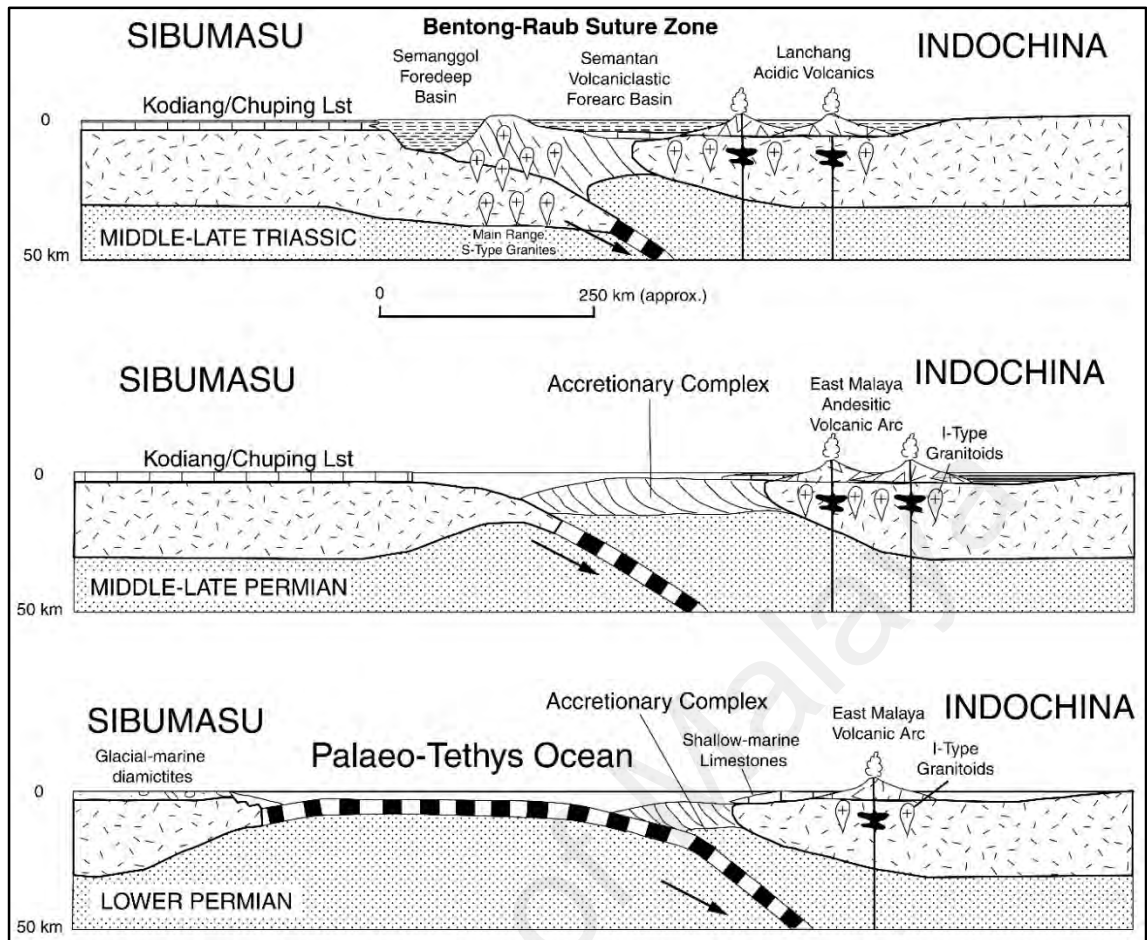


**Figure 2.1: Cartoons illustrating the formation of the Bentong–Raub Suture (Metcalf, 2000). The initial subduction of the Palaeo-Tethys Ocean led to collision of the Sibumasu and Indochina terranes.**

The amalgamation between the Sibumasu and Indochina terranes of the Western and Eastern belts of Peninsular Malaysia occur in the Late Triassic along the N-S trending Bentong-Raub Suture Zone (Figure 2.1 c). According to Metcalfe (2000), the rocks within suture zone comprise a mixture of ribbon bedded cherts, argillites, turbiditic rhymites, melange and serpentinites. These Paleozoic-derived rocks attain higher metamorphic degree during regional metamorphism in a thickened accretionary prism as a result of orogenic processes, while neighboring Mesozoic sediments were metamorphosed to a lesser degree. Major S- type granite intrusions of the Main Range were then emplaced into the overlying accretionary prism and the thickened part of the Sibumasu lithospheric crust.

Isostatic uplift following the conclusion of the Late Triassic orogeny resulted in the contemporaneous accumulation of thick continental molasse deposited within intermontane basins. Situated within Central Belt, these basins were known to have formed during Jurassic – Cretaceous times due to pull-apart basin mechanics (Harbury, 1990; Shuib, 2000). Extension and normal faulting was in response to preceding thrust tectonics and the intrusion of Main Range granite batholiths. These basins were then inverted after deposition following major, regional uplift observed throughout the Peninsula coeval with the intrusion of Late Cretaceous plutons along the Central Belt. In the north, Shuib (2000) suggest that the emplacement of Stong Complex is associated with intense shearing by a NW-SE trending fault zone with sinistral transpressive kinematics, further correlated by Shuib (2009) with movement along the major Lebir fault zone as well as the Bok Bak and Bukit Tinggi faults. Major shearing is supported by K: Ar ages (Bignell and Snelling, 1977) combined with newer thermochronology data (Cottam, 2013) throughout the Peninsula suggesting that a tectonic event in the Late Cretaceous which resulted in deep exhumation of the entire landmass.

### **2.3 The Geology of Northern Central Belt**

Two elliptical bodies striking NNW-SSE represent the Stong Complex (a series of mafic to intermediate intrusions of Cretaceous age) and the metapelitic/metavolcanic Taku Schist, which has undergone high grade (amphibolite facies) metamorphism, is surrounded by weakly metamorphosed to unmetamorphosed sediments of the Gua Musang Formation (Figure 2.2). On both margins of the central belt lie two granitic batholith complexes, namely the Main Range Granite (Western belt) and the Boundary Range Granite (Eastern belt). Overall, the structural framework in the northern part of central belt is affected by episodes of transpressional and transtensional strike-slip

deformations.

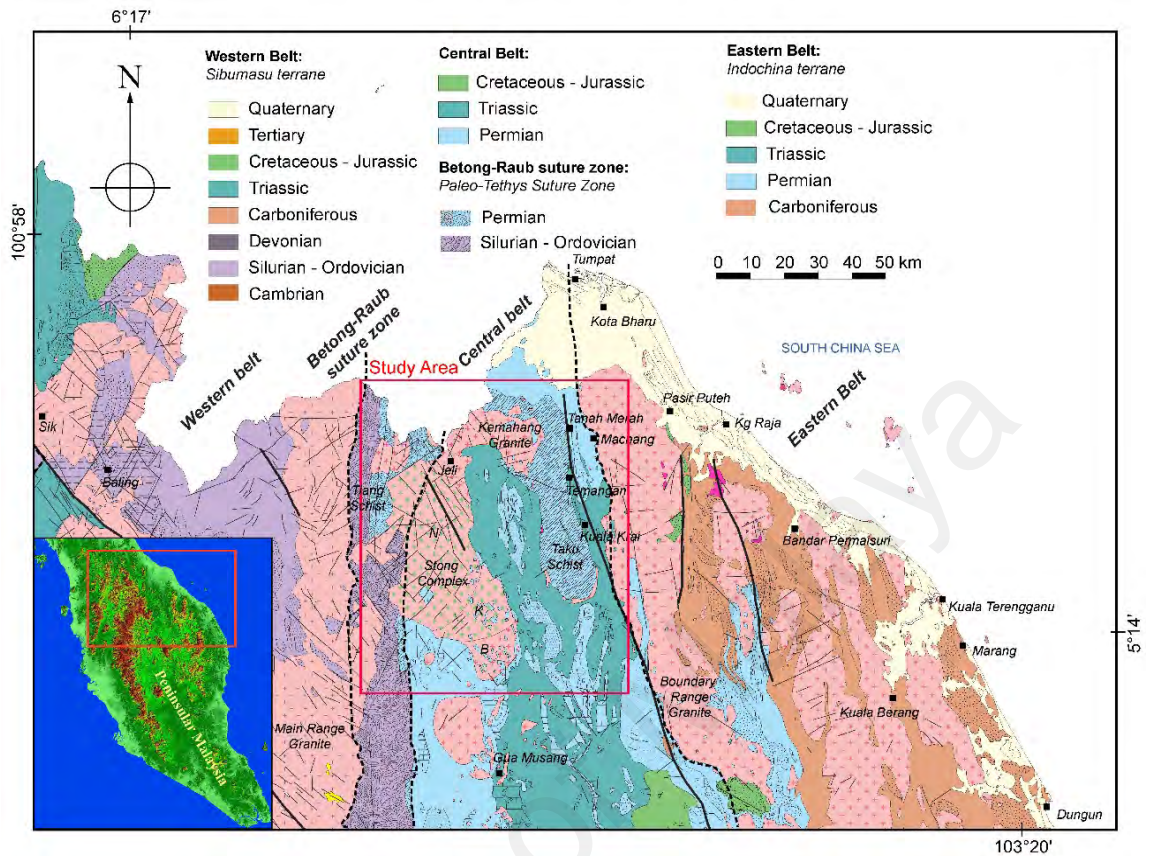


**Figure 2.2: Geological map of northern part of Peninsular Malaysia (modified after Tate, 2008) in the overall Peninsular Malaysia. The marked rectangles indicate the location of study area.**

### 2.3.1 The Metamorphic Units

#### 2.3.1.1 The Taku Schist

The most extensive product of deep-seated regional metamorphism as product of Indosinian Orogeny in Peninsular Malaysia is the Taku Schist. The Taku Schist is exposed as a body elongated along a NNW-SSE trend with an anticlinal dome shaped structure that plunges toward the southern end (Figure 2.3). The unit continues northward across Thai border and is recognized by Buke Ta unit (The Malaysian and Thai Working Groups, 2006). Despite the roughly symmetrical anticlinal shapes of unit, the eastern limb dips steeper than the western limb, from the diagram of Hutchison

(1973), which indicates slight easterly vergence. The body dips gently beneath surrounding low-grade metamorphosed Permo-Triassic sediments, which forms synclinal structures (Figure 2.3). These Permo-Triassic sediments, in turn, are bounded on the west by the Stong igneous complex, which forms an area of high relief.

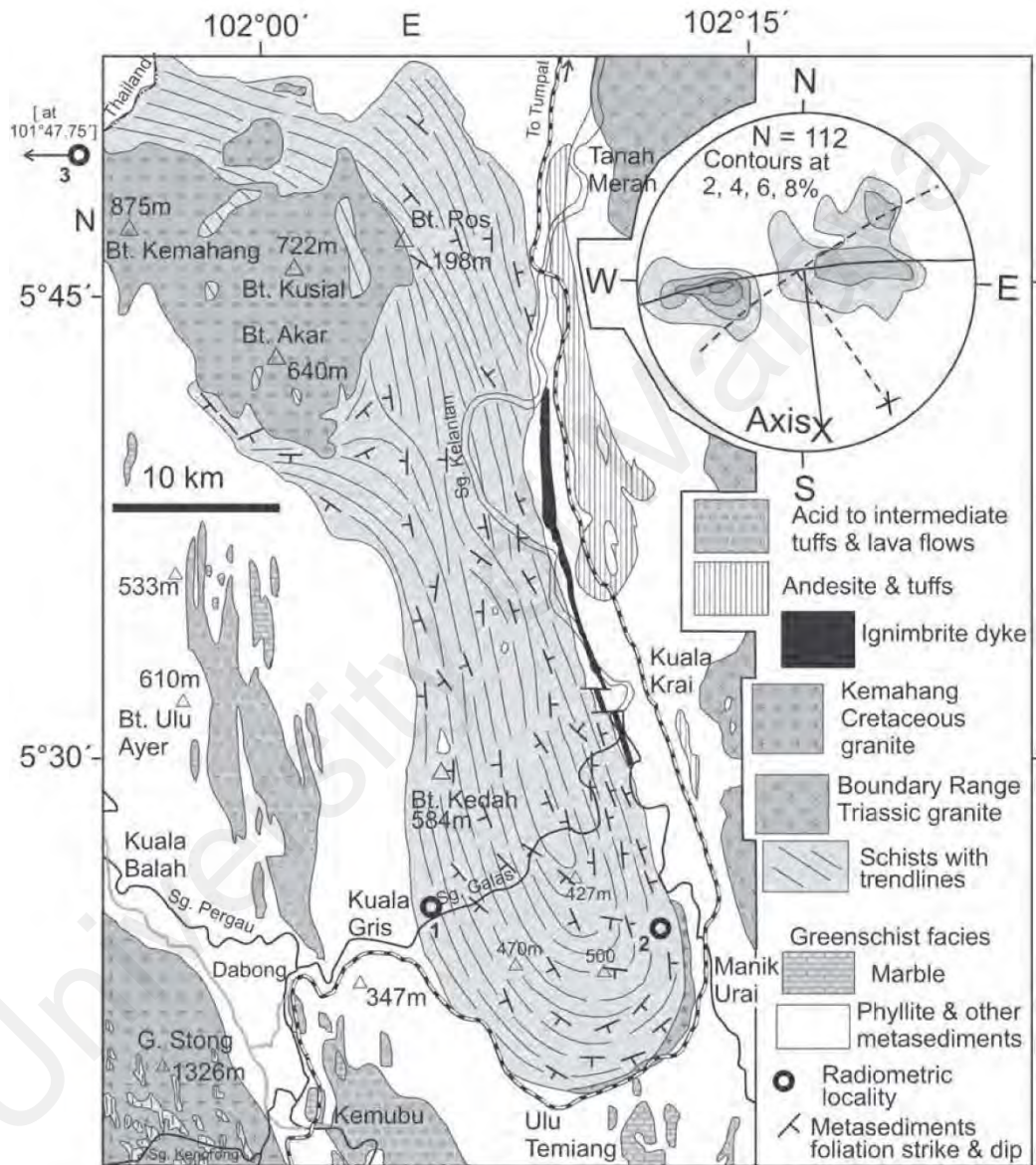


**Figure 2.3: Geological map of the Taku Schist after Dawson et al. (1968). Notice the anticlinal dome shaped body of the metamorphic Taku Schist unit.**

The Taku Schist is composed primarily of metamorphosed argillaceous and arenaceous rocks, interbedded or intruded by mafic components (Figure 2.3). The resulting lithologies are dominantly garnet-mica schist and quartz-mica-schist with assemblages of quartz, muscovite, feldspar and garnet (almandine) minerals (MacDonald, 1968, Hutchison, 1973). The schistose fabric is defined by preferentially aligned muscovite and biotite minerals accompanied with rotated, poikiloblastic garnet containing quartz as either inclusions or strain shadows. Apart from garnet, secondary minerals developed resulting from metamorphism include extensive occurrences of chlorite, widespread but diminutive amounts of tourmaline as well as a local occurrence of kyanite near Temangan (MacDonald, 1968). Contact metamorphic aureoles adjoining the granite in the north contain occurrences of silimanite, andalusite and cordierite. The degree of metamorphism attained within most of the Taku Schist is the Garnet Zone in Barrovian Metamorphism although a higher degrees of metamorphism can be inferred from occurrence of minor metamorphic minerals (i.e. kyanite, silimanite, andalusite and cordierite minerals). According to Hutchison, 1973, the Taku Schist experienced high temperature metamorphism with a variable intensity of shearing stresses.

The mafic components of Taku Schist include narrow bands of amphibole schist as well as localized occurrences of serpentinite schist and pyroxene schist (Figure 2.3, MacDonald, 1968). On the banks of Sg. Galas, amphibolites occur together with mica schist. These contain assemblages of hornblende, clinozoisite, quartz, feldspar, epidote with minor tremolite, garnet and biotite. These bands of amphibolitic schist are in proximity with occurrences of pyroxene schist, which is dominantly quartz-diopside-sphene-plagioclase. Occurrences of amphibolite near the Kemahang granitic unit has also been observed, which resulted from heat influx from the intrusion.

A localized ultramafic exposure observed by MacDonald (1968) includes the serpentinite-schist observed in the headwater of Sg. Taku proximate to the contact with shales (Figure 2.3). He describes the rocks as dark greenish color, with antigorite as main forming sheet-silicate and exhibit strong schistosed fabric. In addition, an interfoliated band of biotite-granite gneiss and schist (Hutchison, 1973) ranging up to 1 km in width is found at the southern margin, and is strongly cataclastic and display mortar textures containing a fine grained sericitized matrix.

The nature of the geological contact between the Taku Schist and the surrounding Gua Musang/Semantan Formation has been a matter of controversy. Aw (1974), MacDonald (1968) and Hutchison (1973) referring to sharp increases from non-metamorphosed sediments to amphibolitic grade schist described an unconformity or tectonic disconformities. However, since no definite unconformity was observed and the presence of apparent structural conformity between the two units, Khoo and Lim (1983) suggest a conformable contact with an increase of Barrovian metamorphic zonation across the units. This gradational increase was hypothesized across a southeast transect, near Manik Urai, based on a change from chlorite grade within outlying sediments to the appearance of biotite in the Taku Schist.

Bignell and Snelling (1977) indicate late Triassic,  $212 \pm 8$  Ma ages of metamorphism for the Taku Schist, obtained from biotite K-Ar geochronology in the western edge of the dome. However, K:Ar analyses of biotite minerals from schist enclaves within Kemahang granite indicate a Late Cretaceous age of of metamorphism, about  $107 \pm 3$  Ma. Ng et. al. (2015) provided newer U-Pb ages of the Kemahang granite intrusions, showing Late Triassic ages ( $226.7 \pm 2.2$  Ma in Figure 2.4) equivalent to the Berangkat tonalite sub-unit of the Stong complex which give an age of  $220.4 \pm 3.9$  Ma. The age is in contrast with other sub-units in the north that indicates late Cretaceous ages of

intrusion for the Kenerong leucogranite ( $83.9 \pm 0.8$  Ma) and Noring granite ( $75.7 \pm 0.6$  Ma). Furthermore, thermochronology analysis by Cottam (2013) also indicates a major period of tectonism within Cretaceous age between 100 Ma – 90 Ma in response regional uplift and prolonged exhumation.

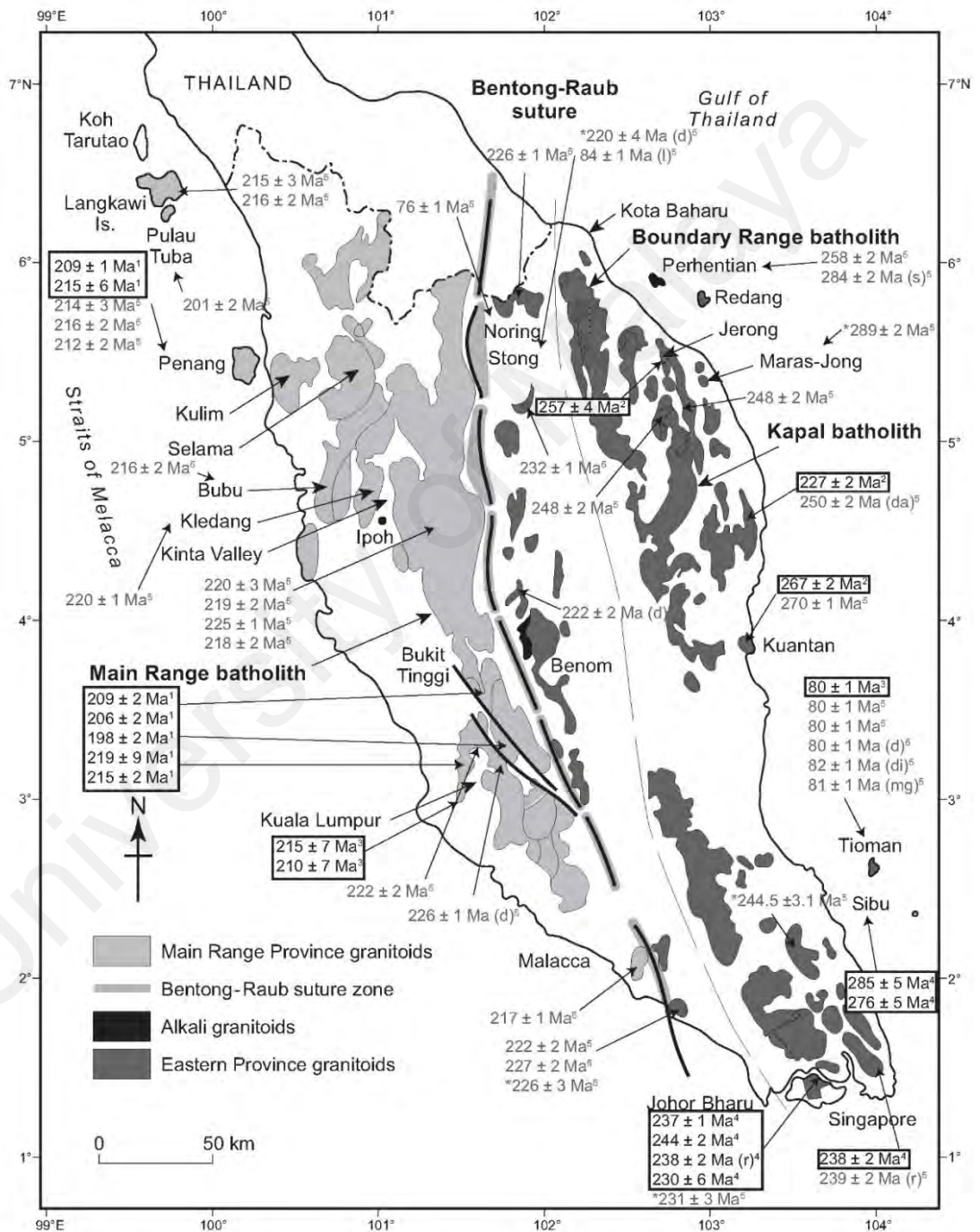


Figure 2.4: U-Pb Zircon ages of granitoid plutons across Peninsular Malaysia (after Ng et. al, 2015)

According to Shuib (2009), the amphibolitic grade metamorphism of Taku Schist continues further to west as migmatized amphibolite resulted from mantle upwelling from adiabatic decompression occurred during Indosinian orogeny in late Triassic. Subsequent regional uplift resulted in the development of an anticlinal open fold structure across the Taku Schist. The exhumation of the Taku Schist was synchronous with the emplacement of the late Cretaceous Stong Complex granitoids within a shear zone by sinistral transpressive movement indicated by the presence of boudinage, ptygmatic folds and migmatization (Figure 2.5; Hutchison and Tan, 2009; Shuib, 2009).

### **2.3.1.2 The Tiang Schist**

The unit represent the lower Paleozoic series of Richardson (1946) representing the lateral prolongation of Karak Formation/ Bentong group in the south, which forms the eastern foothills of the Main Range Granite and overlain by Permo-Triassic sediments (Figure 2.2; Lee et al., 2004 and Lee, 2009). The compositions are mainly comprised of quartz-, quartz-mica-, graphitic- and amphibolitic schist displaying well-developed schistose fabric affected by strong folding (Richardson, 1946). Apart from schist, phyllite and hornfels have also been described. The amphibole- schist is primarily composed of actinolite with minor quartz, chlorite and epidote is interpreted as basic-ultrabasic protolith. Hutchison (1973) also mentioned the presence of intrusive ultrabasic rocks such as peridotite, pyroxenite and dolerite forming ophiolitic suite associated with this schist unit. The schist is oriented in NNW-SSE striking direction and metamorphosed up to greenschist facies (Hutchison, 1973). The overlying Permo-Triassic sediments are formerly known as the Older Arenaceous Series of Richardson (1946) which is composed of conglomerate, sandstones and cherts, and is associated with tuffaceous rocks. According to Tjia (1969) and Shuib (2009), the schist series were affected by strong transpressive deformation of both dextral and sinistral shearing proceeded with NNW-SSE trending reverse oblique faults. Along the E-W highway

near Batu Melintang, the Galas Fault Zone forms a mylonitic shear zones displaying well-developed S/C fabric that indicate top –SW kinematic transport (Figure 2.4, Shuib, 2009). The fault zone controls the emplacement of both the Stong Complex and the Kemahang Granite under sinistral transpressive movement.

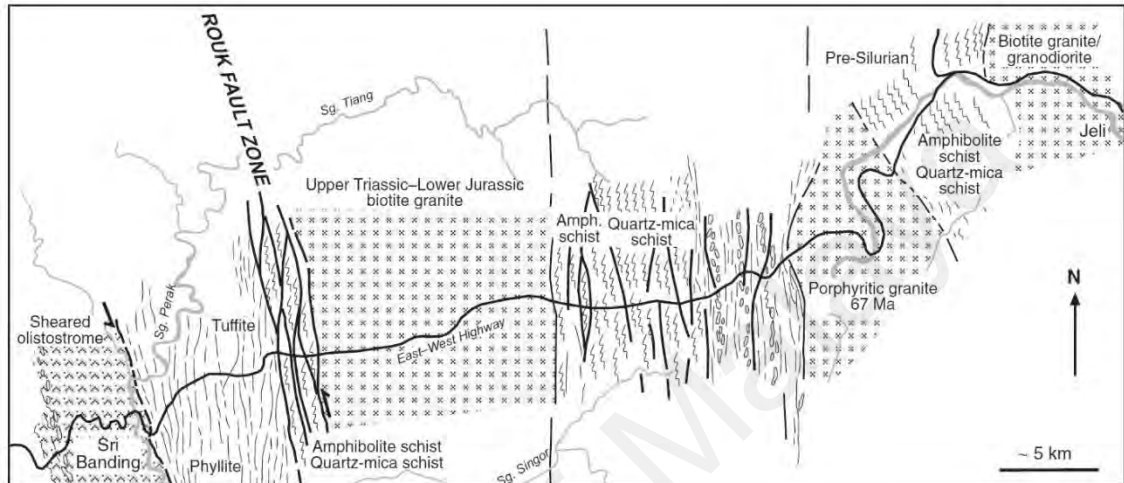


**Figure 2.5: Geological transect of the eastern foothills of Main Range Granite (Shuib, 2009). The lower Paleozoic schist on foothills of Main Range Granite were cut by NNW-SSE trending fault zone indicating sinistral sense of shear toward southwest direction.**

## 2.3.2 The Sedimentary Units

### 2.3.2.1 The Gua Musang/ Aring Formation

In Kelantan, the sediments of the Gua Musang/ Aring Formation are mainly composed of argillaceous rocks accompanied with variable amounts of carbonaceous and calcareous material (Figure 2.2). The calcareous material is often occur as bands of crystalline limestone. These sediments generally strike along NS-trend, where the bedding planes were isoclinally folded. Near the margin with granites, contact metamorphism has transformed argillitic rocks into hornfels (Figure 2.2). The regional metamorphism is, in contrast, mild, resulting in low grade slates, phyllite, quartzites and marbles. In addition, acidic volcanic rocks cover extensive parts within the unit, with rhyolites and trachytic tuff being most common accompanied with minor dacite to

andesite rocks. The volcanic rocks displays porphyritic textures in presence of quartz and sanidine/ orthoclase phenocrysts within a matrix of quartz, feldspar and mica. Near the southern margin of the Taku Schist, the tuffaceous shales noticeably altered into green chloritic phyllites whereas in the Temangan area, the shales are strongly brecciated in contact with Taku Schist.

According to Lee et al. (2004), the sediments of the Gua Musang Formation were deposited in a shallow marine environment, affected by contemporaneous sub-aerial acidic volcanism that ranges from rhyolitic to dacitic. Deepening of the basins toward the south results in the deposition of turbidites of the equivalent argillitic Semantan Formation. Stratigraphic and fossils study shows that these two sub-units were deposited during Late Permian up to Late Triassic within a forearc basin that suggests easterly-directed subduction. According to a study by Shuib (2009), the sediments form slaty cleavages and develop three stages deformations from isoclinally folds to overturned, upright fold structures.

The NNW-SSE-trending fault east of the Taku Schist is recognized as the Lebir Fault, recognized through strong lineaments on DEM imagery correspond to the eastern boundary of the Central Belt (Aw, 1974; Tjia, 1969, 1996). The fault zone extends to 4 km in width, containing three discrete shear zones in non-metamorphosed Semantan Formation.

#### **2.3.2.2 The Gagau Group**

This unit represents the Jurassic and Cretaceous continental deposits equivalent to Tembeling Formation in the south, and bounded by the Lebir Fault Zone and Boundary Range Granite. The sediments are composed of coarse oxidized sandstone and polymict conglomerates deposits with an absence of metamorphic cleavage, where the bedding planes are steeply oriented (Rishworth, 1974). It is inferred that these sediments were

deposited in low-lying intermontane basins with close proximity toward fluvial, lacustrine and deltaic environments, and represent the molasse deposits of an orogeny (Burton, 1973). Meanwhile, Tjia (1996) and Shuib (2009) link the formation of these continental basins to dextral, transtensional pull-apart tectonics. This is followed by an episode of inversion, caused by sinistral transpressional kinematics contemporaneous with widespread uplift and regional exhumation across the Peninsula.

### **2.3.3 The Igneous Plutons**

#### **2.3.3.1 The Stong Complex**

The igneous complex is situated to the west of the Taku Schist where the topography is dominated by hilly terrain striking NNW-SSE and form a sigmoidal outline (Figure 2.5). It is composed of three sub-units in order of decreasing age; the Berangkat Tonalite, the Kenerong Leucogranite and the Noring Granite, the earliest two being highly deformed (Singh, 1984). The earliest intrusion, the Berangkat Tonalite, consists of mafic, megacrystic tonalite containing large K-feldspar within matrix of biotite and hornblende. The next intrusive episode gave rise to the Kenerong Leucogranite, cuts the Berangkat Tonalite and consists of a series of crosscutting veins, comprised of leucogranite and biotite granite. Both the Berangkat Tonalite and the Kenerong Leucogranite show metamorphic foliation, unlike the last unit emplaced, the Noring Granite. The latter form the largest sub-plutonic unit, typified by pink megacrystic biotite granite containing large K-feldspar minerals. Where the Noring granite intrudes the earlier Kenerong Leucogranite, dense biotite schlieren zones are found. Both the Berangkat Tonalite and the Noring Granite have similar mineralogical and textural features, which correspond to I-type signature of Eastern Belt granitoids (Ghani, 2000, 2009).

Enclaves present within the granitic plutons signify country rocks comprised of metapelites, metaarenites, pure to impure marble, as well as amphibolite rocks present within southern part of the complex (MacDonald 1968; Singh, 1984). Prior to the intrusion of the granites, regional metamorphism of up to lower greenschist facies resulted in the production of slaty cleavage within these metapelites. The highly folded phyllite observed nearest to the pluton, developed biotite porphyroblasts before transforming into graphitic schist (Singh, 1984). In the Kenerong Leucogranite, the enclaves consist of finely banded hornblende-quartz schist, staurolite-garnet-biotite schist, fine-grained biotite-muscovite schist, diopside-phlogopite marble and sillimanite-garnet-biotite gneiss. Within blastose garnet (almandine) minerals, the inclusion trains are oriented oblique to main foliation plane. According to Hutchison (1973, 2009), the attained metamorphism reaches up to upper amphibolite facies, high enough to cause anatexis. This is also supported by presence of ptygmatic veins that signify the migmatite nature of enclaves.

The intrusion and high temperature metamorphism of the Kenerong Leucogranite occurred during late Cretaceous, constrained by isotope geochronology. Three Rb-Sr analyses of samples of the Kenerong leucogranite resulted in ages of  $79 \pm 3$  Ma with an initial ratio of  $^{87}\text{Sr}/^{86}\text{Sr}$  ratio of 0.70801 whereas samples from the Noring Granite define an isochron of  $90 \pm 3$  Ma with initial ratio of 0.70865 (Bignell and Snelling, 1977). K-Ar ages obtained from muscovite and biotite within Noring granite define ages of  $65 \pm 2$  Ma and  $70 \pm 2$  Ma respectively. This is also supported by newer U-Pb ages obtained within the three sub-units of the Stong Complex by Ng et al. (2015) in Figure 2.4, where a Late Triassic age is indicated for the Berangkat tonalite ( $231.8 \pm 1.8$  Ma) as well as Late Cretaceous ages for the Kenerong Leucogranite ( $83.9 \pm 0.8$  Ma) and the Noring Granite ( $75.7 \pm 0.6$  Ma).

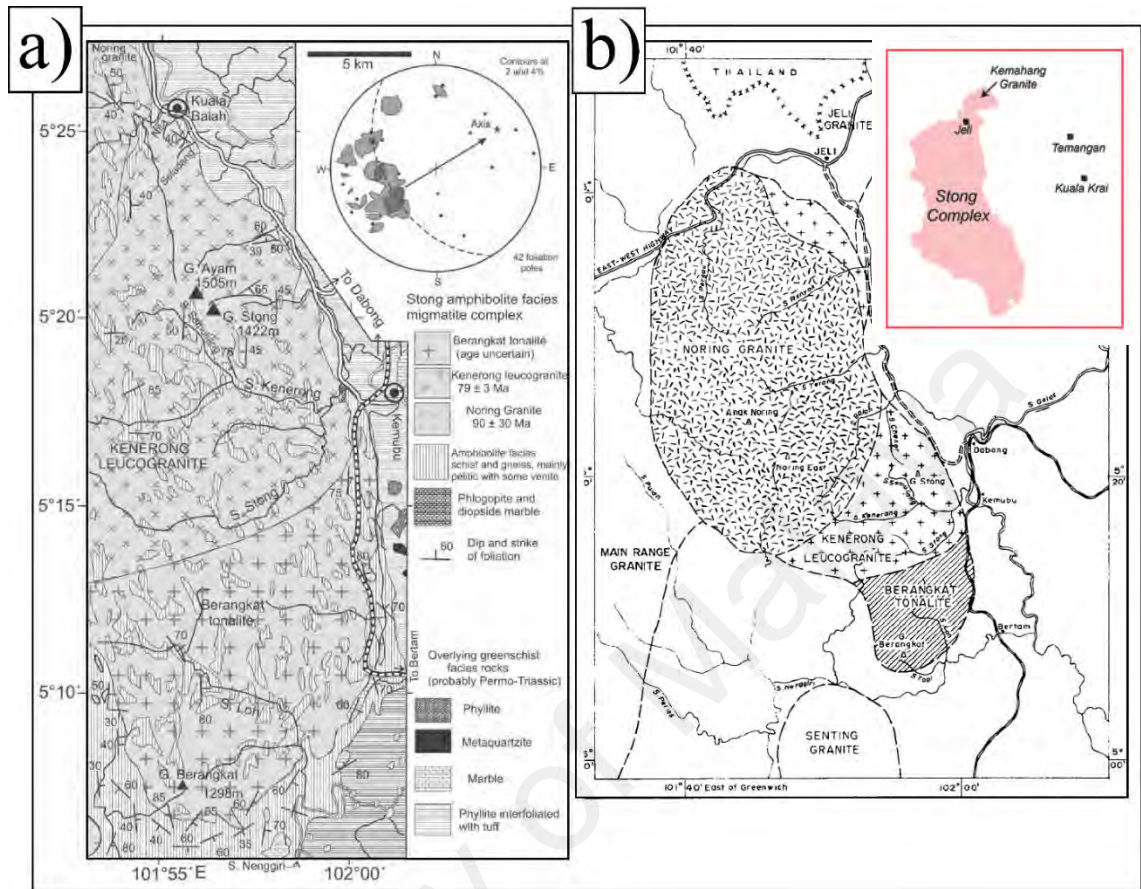


**Figure 2.6: Geological map of the Stong Complex. (a) The southern part of Stong Complex showing separation between schist-gneiss host rock with overlying phyllitic Permo-Triassic sediments (after Dawson et al., 1968) and (b) Separation of sub-unit in Stong Complex (modified after Singh, 1984). Notice the location of Stong Complex in the study area**

Umor and Mohamad (2002) characterize the Stong Complex as peraluminous, shoshonite to K-rich calc-alkaline series suggesting emplacement within an anorogenic tectonic environment. The granite originates from partial melting of meta-basalt to meta-tonalite where the magma is enriched with mantle component and undergone continuous differentiation to form the three sub-plutons; the Berangkat Tonalite, Noring Granite and Kenerong Leucogranite in order of emplacement. The earliest interpretation was based on the relationship between a series of sub-parallel vein injection into meta-sedimentary host rocks at Sg. Renyok as part of Kenerong Leucogranite sub-unit as described by Singh (1984). The earliest thin granitic veins were injected into meta-

pelitic enclaves, which were subsequently crosscut by larger veins. Both structures were affected by intense deformation that resulted in the development of boudinaged veins sub-parallel to the metamorphic foliation fabric and ptygmatic veins. This shearing deformation is interpreted as D1 and D2 by Ibrahim Abdullah (2003) and as a sinistral transpressive event by Shuib (2009), which he further describes as a syn-kinematic intrusion via lit-par-lit into NNW-SSE trending shear zones. Heat influx derived from dynamothermal metamorphism of intense sinistral transpressive shearing resulted in metamorphic foliation containing intra-folial folds that envelops the asymmetric boudins of granitic veins. A later episode of granite intrusion in the final relaxation stages crosscuts earlier granitic veins, which lacks any deformation fabrics (Singh, 1984; Shuib, 2009). The last stages of deformation (D3) recognized by Ibrahim Abdullah (2003) forms NS- trending faults associated with dextral kinematic movement, where axis of drag fold structures plunges toward the SE.

Hutchison (2009) equates the migmatitic features such as ptygmatic folds and granitic boudins observed in the Kenerong Leucogranite with similar features in the well-studied metamorphic core complex of the Inthanon Zone in Thailand. The location of this core complex in relation to suture zone of the Indosinan orogeny is situated in the western side of the Nan-Utarradit – Chiang Mai Suture Zone, while the Stong Complex is located to the east of the Bentong- Raub Suture Zone. The metamorphism and deformation associated with emplacement of Stong complex also occurred during Cretaceous time whereas the regional metamorphism of the Inthanon core complex resulted from Triassic Indosinian Orogeny.

#### **2.3.3.2 The Kemahang Granite**

This pluton occupies the northernmost part of the Central Belt in Peninsular Malaysia and continues across the border into Thailand as the Sukhirin Granite unit. It

intruded into the northwestern part of the Taku Schist, bordered by Gua Musang Formation and is laterally continuous with Stong Complex to the west (MacDonald, 1968). Typified by coarse-grained porphyritic granodiorite, the granite displays large K-feldspar phenocryst enveloped within biotite-rich matrix. Near Stong Complex plutons, shearing deformation within granite led to appearance of augen textures that developed from both quartz and feldspar minerals, enveloped within biotite sheet silicates forming S/C shear fabrics (MacDonald, 1968; Shuib, 2009). In the presence of metamorphic foliation, the quartz crystals are fractured and partly recrystallized. This is also observed in microgranite in the westernmost part of unit, which displays strongly schistosed fabrics (MacDonald, 1968). Khoo (1980) infers that the appearance of catclastic granite gneisses arises from a shear/ fault zone that developed after granitic emplacement. This is in agreement with K-Ar ages of Bignell and Snelling (1977) that define an apparent ages of shearing during  $107 \pm 3$  Ma, where recent U-Pb analysis of Ng et al. (2015) also indicates granitic emplacement in Late Triassic ( $226.7 \pm 2.2$  Ma in Figure 2.4). Shuib (2009) interprets this shearing as the result of movement along the NNW-SSE trending Galas Fault Zone, resulting in steeply dipping mylonite rock that indicates top-to-the-southwest sense of shear. However, he suggested that the emplacement of Kemahang granite was coeval with Stong Complex.

At present, the nature of the intrusion of the Kemahang granitic into the Taku Schist is still speculative, either by deep-seated catazonal emplacement (MacDonald, 1968; Hutchison, 1973) or by mesozonal intrusion preceding a metamorphic event (Khoo, 1980). The former interpretation is based on syn-kinematic characters observed by lit-par-lit granitic intrusions in appearance of gneissose fabric within parts of unit. This include migmatization of granitic gneiss with complete conformity with schist body (Hutchison, 1973). In contrast, Khoo (1980) proposed a typical non-synkinematic intrusion that was the result of contact metamorphism of the proximal parts of the Taku

Schist. These arguments are mostly based on the report of MacDonald (1968) which states the presence of schist enclaves within cataclastic granite, quartz-feldspathic and amphibolite hornfels in the adjoining Taku Schist as well as presence of andalusite as an anti-stress mineral.

University of Malaya

## CHAPTER 3: THE TAKU SCHIST

### 3.1 Introduction

The study area stretches about 90 x 90 kilometers in distances within second-third of the northern Kelantan of Peninsular Malaysia. The long axis of Taku Schist unit stretches about 60 kilometers in distances with perpendicular distance ranges around 15 kilometers (Figure 3.1). The study area also includes the surrounding units of the Taku Schist, i.e. the Gua Musang/Aring Formation, Stong Complex, Kemahang Granite and Tiang Schist (Figure 3.1). Both Main Range Granite and Boundary Range Granite mark the boundaries on both western and eastern margin of study area. The results are based on field and microstructural observations, which covers field observation around 250 rocks exposures and the study of 70 thin sections made from samples collected across the study area.

The Taku Schist is divided into three domains; south, central and north sectors, where each domain contains a unique representative of Taku Schist unit which is relatively homogeneous (Figure 3.1). Geological observations within the three domains were describe in detail (Figure 3.2), which comprises of field observations, kinematic analyses and contact with overlying units.

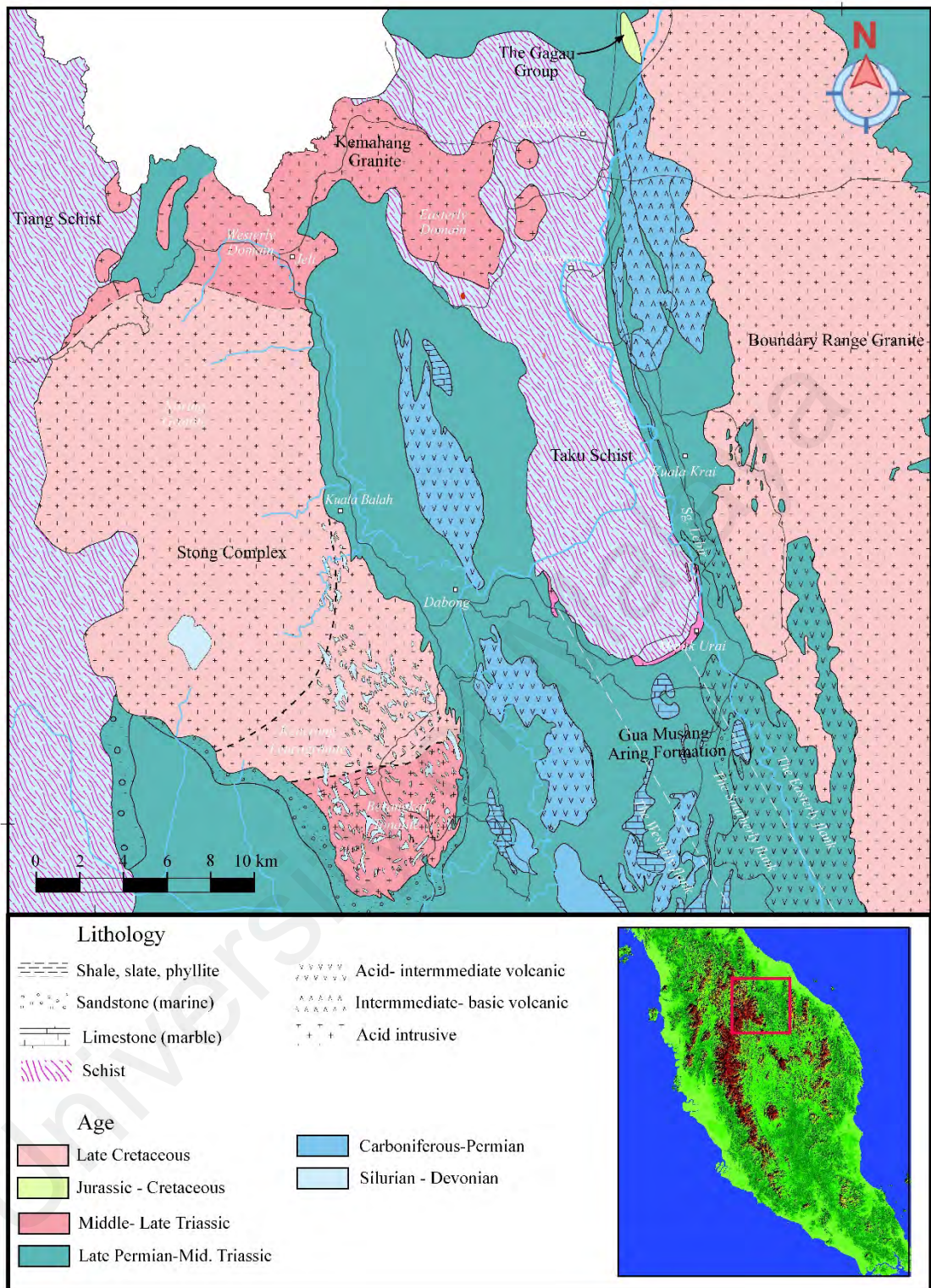


**Figure 3.1: Geological map of the study area (modified after Tate et. al, 2008). The studied area includes the Taku Schist and surrounding units comprising of Gua Musang/Aring Formation, the Stong Complex, the Tiang Schist and Boundary Range Granite**

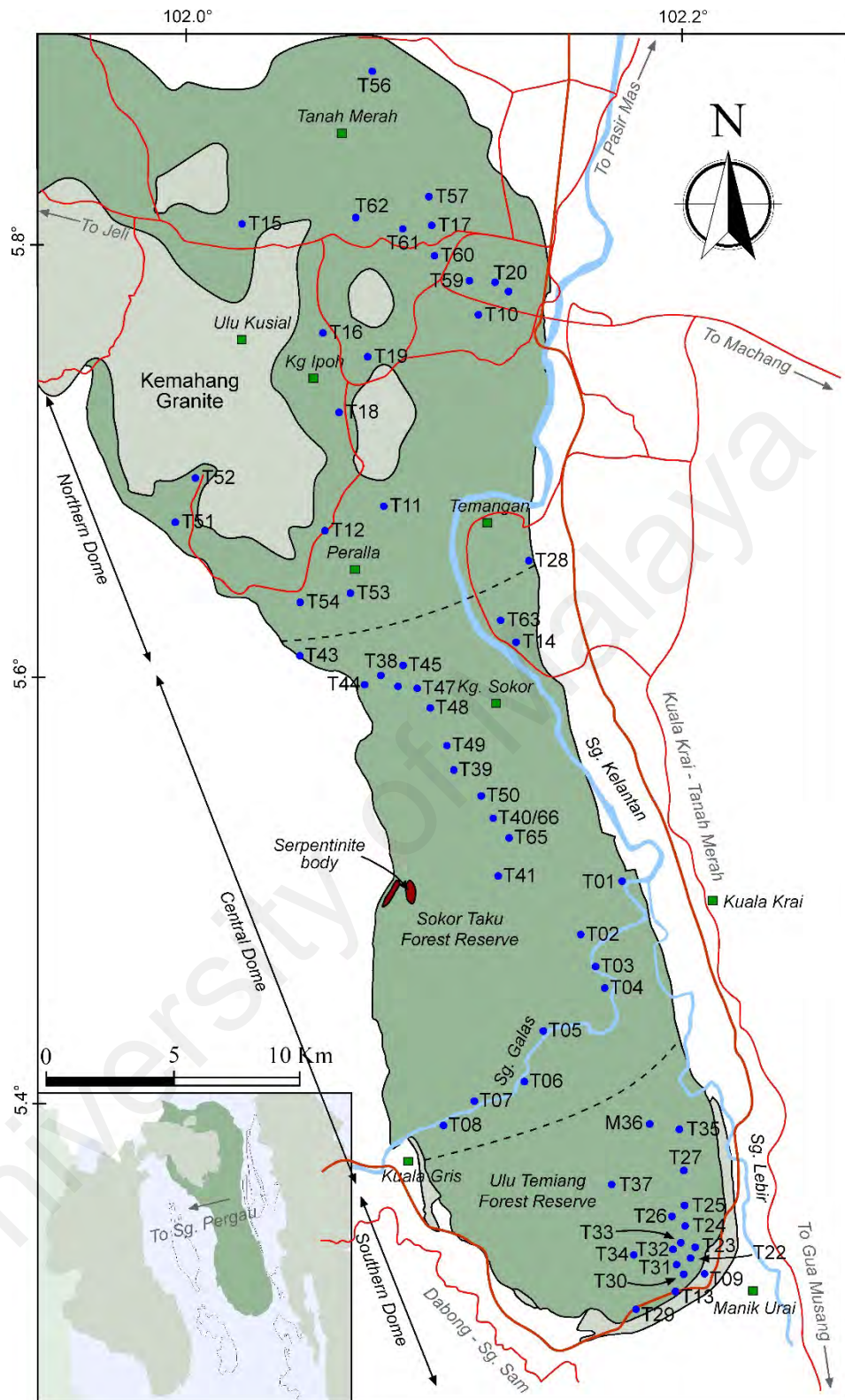


**Figure 3.2: The southern, central and northern domain of the Taku Schist. The blue dot is the location of outcrops investigated in this study.**

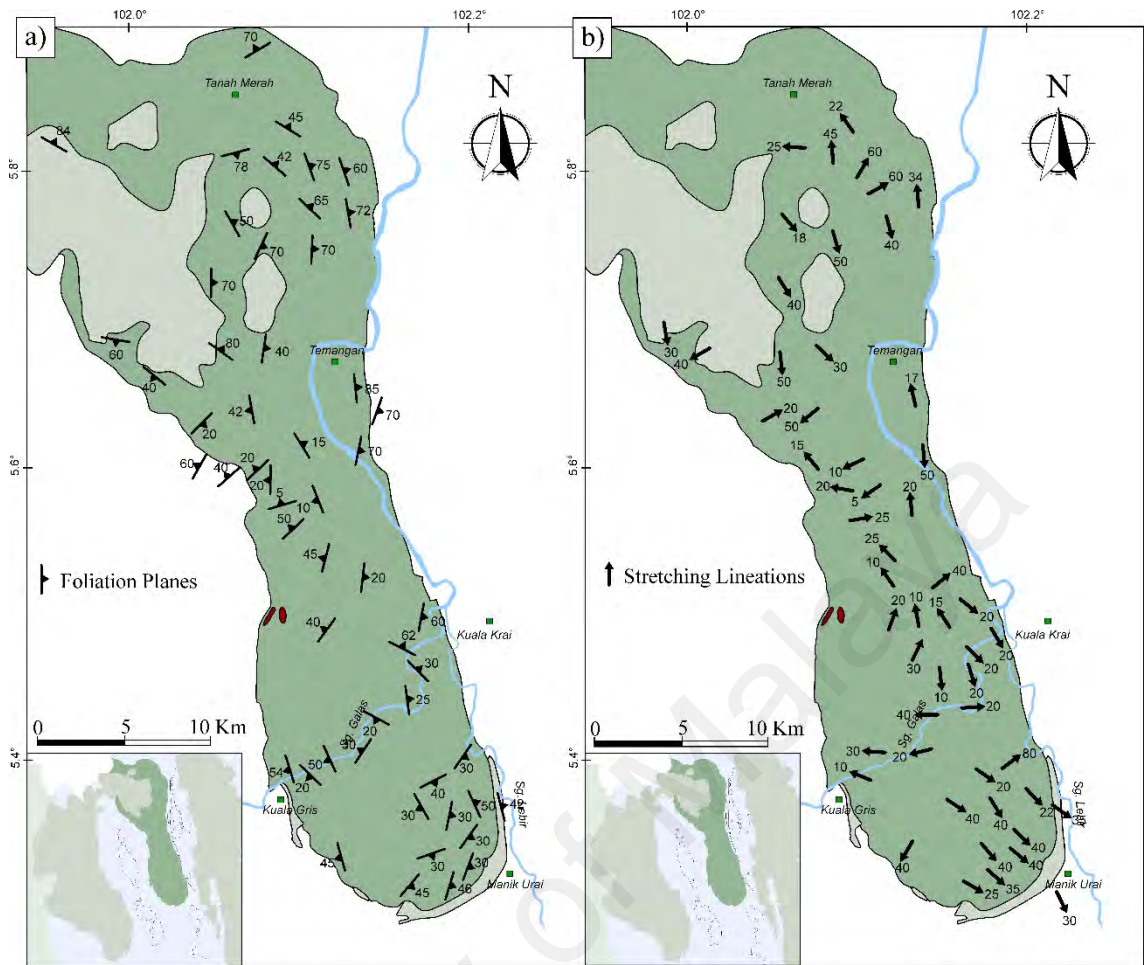


**Figure 3.3: Taku Schist map showing the orientation of (a) foliation plane and (b) stretching lineation**

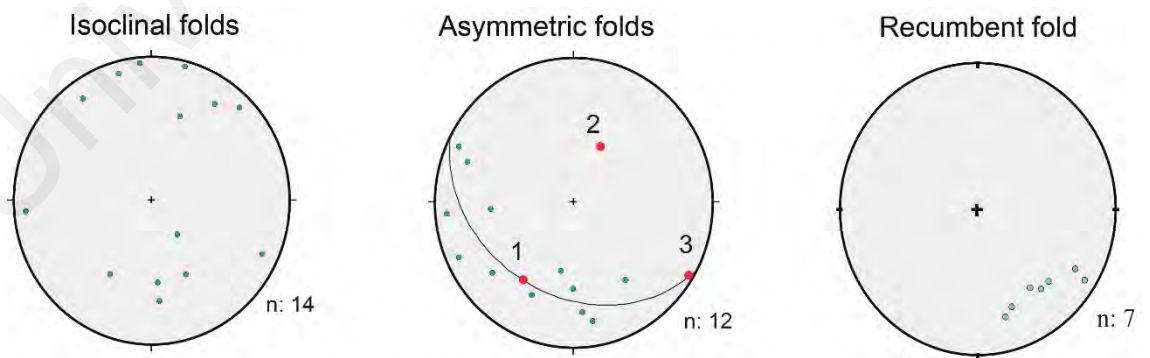


**Figure 3.4: Plot of fold axis observed in the Taku Schist unit**

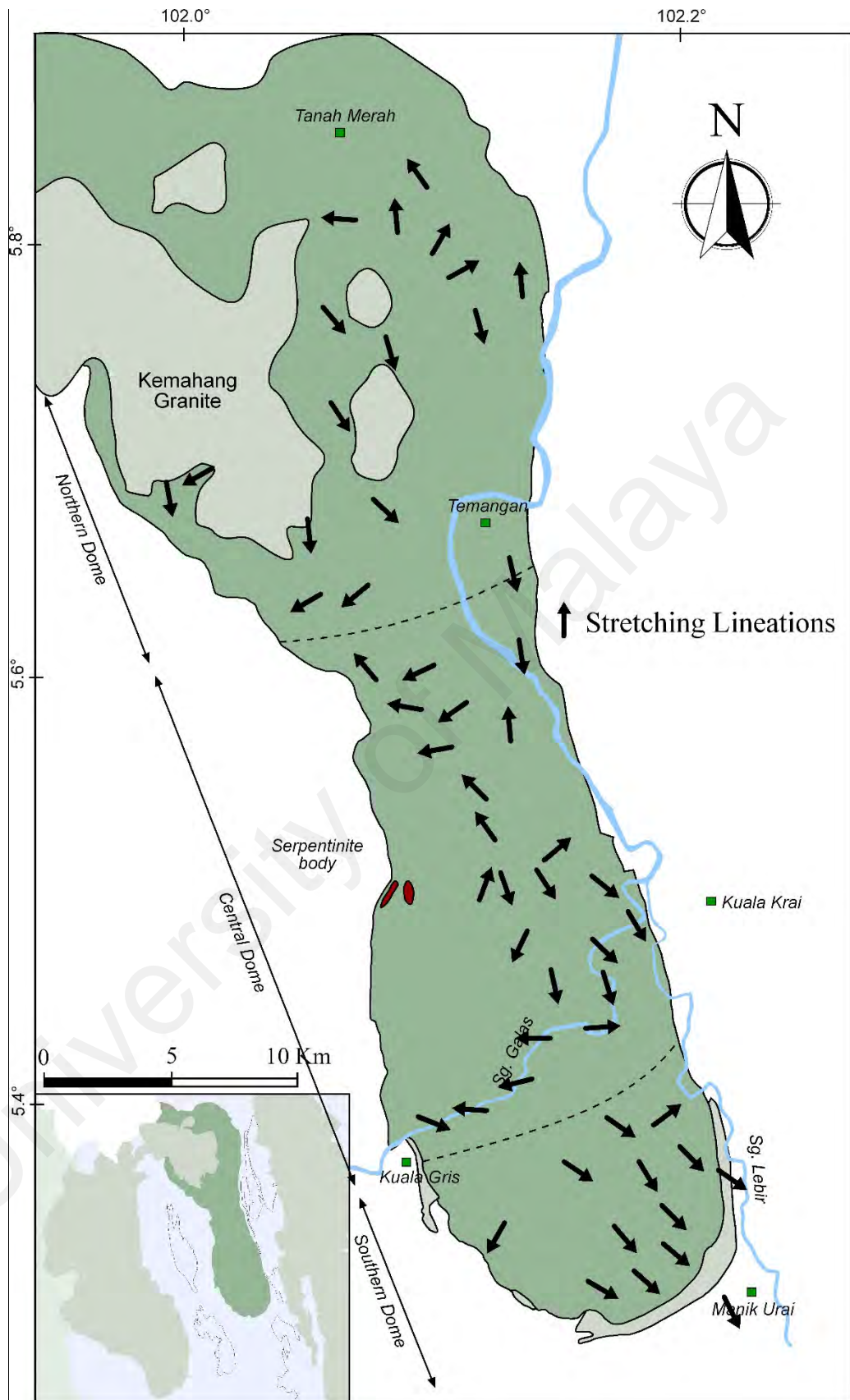


**Figure 3.5: Taku Schist map showing the interpreted kinematic directions from shear sense analysis.**

### **3.2 The Southern Dome – 1st Sector (SSE domain)**

This domain covers areas across Ulu Temiang Forest reserve situated south of Sg. Galas Basin and bounded by railway line that stretches from Olak Jerai to Manik Urai (Figure 3.2). In the easterly flank of the Taku Schist, the schist exposures are found within off road tracks whereas in the westerly flank, the exposures are within oil palm plantations and are deeply weathered. The domain covers about 20 exposures with 7 thin section samples (Figure 3.2).

#### **3.2.1 Field Observation**

##### **3.2.1.1 Structural Geometries**

The lower part of SSE domain observed in Ulu Temiang Forest Reserve is dominated by light greyish, quartz-mica schist and whitish quartz-rich schist displaying well-developed schistosity. The S1 foliation strikes NNE-SSW sub-parallel to the outline of the Taku Schist that defined the cylindrical curvature of the dome structure (Figure 3.3 a). The orientation of S1 foliations is inclined toward SSE direction at low angle, with steepening towards the margin of the unit. The schistosity is defined by preferred alignment of muscovite and biotite and it develops pervasive stretching lineation (L1) plunging towards SSE at low angles. The plunge direction of the stretching lineation is relatively uniform throughout the entire area (Figure 3.3 b). The S1 foliations are commonly crosscut by steeply inclined C'-shear planes and result in various asymmetric structures. The penetrative cleavage development is stronger in mica-rich lithology and often forms contorted/ crenulated schist fabric. Quartz veins oriented parallel to foliation planes (S1) are common and are often boudinaged into sigmoidal shape that usually indicate dextral movement.

Part of the exposures across the SSE domain contains numerous blastose garnet (almandine), enveloped by quartz-mica matrix. This is particularly observed in the

upper reach of Sg. Mei, where it contains numerous, exceptionally large blastose garnet up to 30 mm in diameter (Figure 3.6). Thus, the minerals assemblages of quartz-mica schist within SSE domain comprise of quartz-K-feldspar-muscovite-biotite-garnet (almandine), which indicate metamorphism at amphibolite- facies.

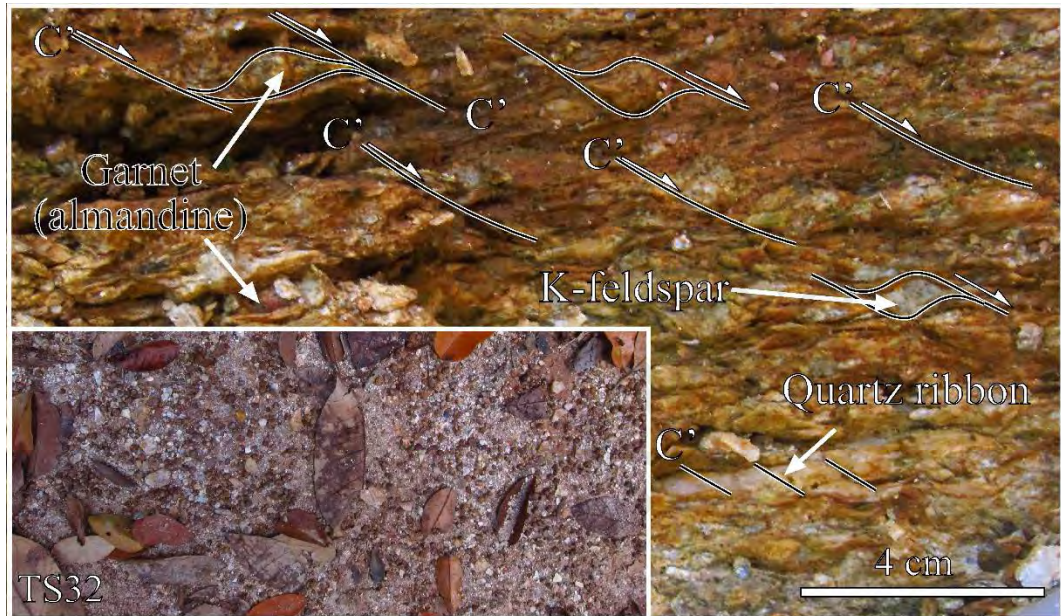


**Figure 3.6: Garnet (almandine) porphyroblast in quartz-mica schist. The garnet is enveloped by matrix with well-developed S/C' fabric. Inset shows garnet grains scattered on the ground.**

Folds observed throughout the SSE part of Ulu Temiang Forest Reserve occur as either as centimeters-scale intra-folial folds or meter-scale recumbent folds (Figure 3.7). The former are asymmetrical folds with isoclinal hinge closures (F1), where the layering most likely represents the strata of original bedding planes (S0). The axial planes are oriented almost parallel to the S1 foliations. The recumbent folds (F2) show symmetrical limbs with gentle hinge closures. The axial planes are low-lying with inclination towards the W. This fold consistently plunges towards SSE direction, which is sub-parallel to the observed stretching lineation (L1).

The exposures near to the SSE margin of the Taku Schist in contact with Gua Musang Formation are typified by occurrences of quartz-mica and quartz-rich schists

that contain lit-par-lit injections of biotite granite veins. Part of the exposure develops mylonitic fabrics, where the S1 foliations strikes along NNE-SSW with intermediate dip towards the E (Figure 3.8a). The rocks contain aligned quartz-muscovite bands. The stretching lineation (L1) plunges towards SE direction at low angle. The exposure is cut by steeply eastward dipping faults striking NNE-SSW (Figure 3.8). The areas in the SSW margin are typified by purplish mica- rich schist, where the S1 foliation strikes in NW-SE direction with low dip angle towards the W. It is accompanied with well-developed stretching lineation (L1) that plunges towards SW direction at low angle.

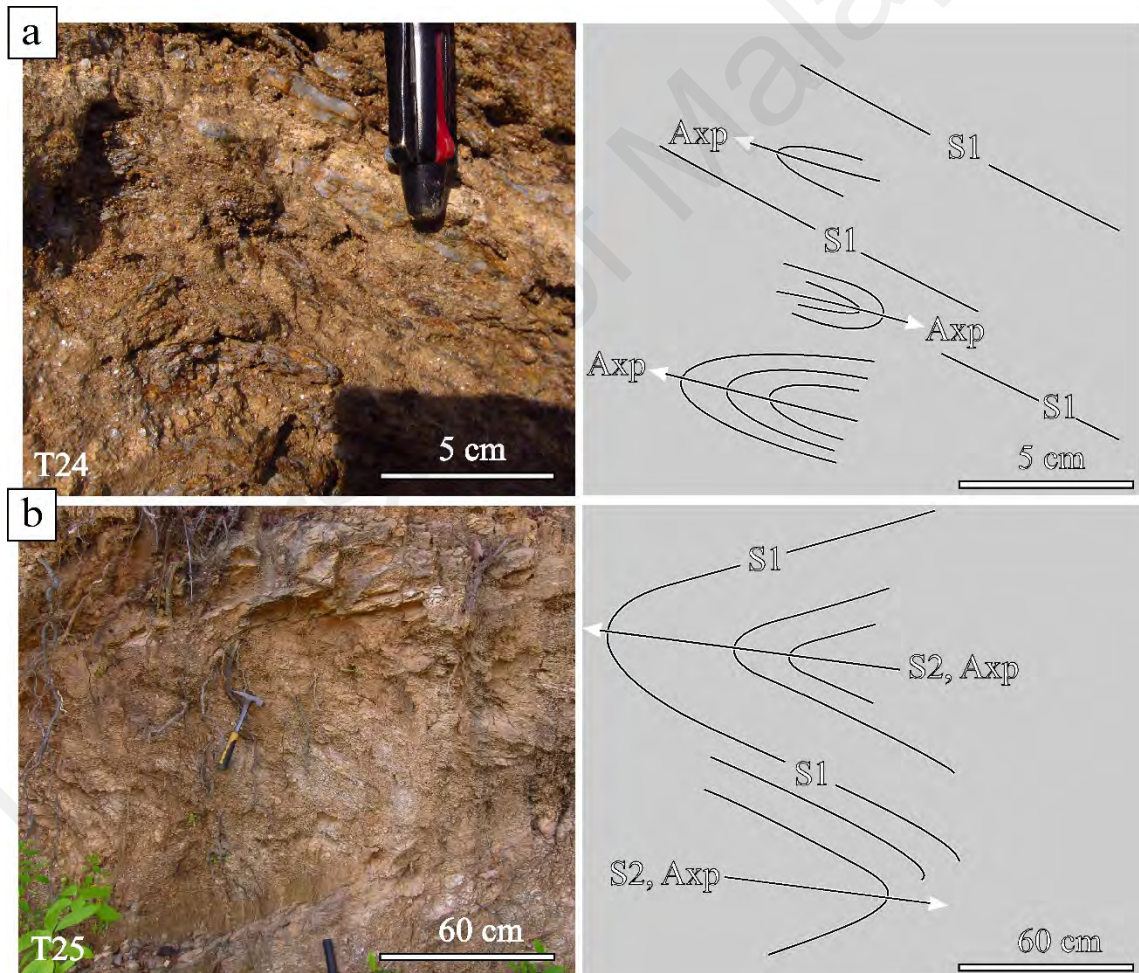


**Figure 3.7: The observed folds in the SSE domain, Taku Schist; (a) intra-folial bands of quartz-rich layers folded into symmetrical isoclinal folds, (b) symmetrical recumbent folds with gentle closures in quartz-mica schist.**

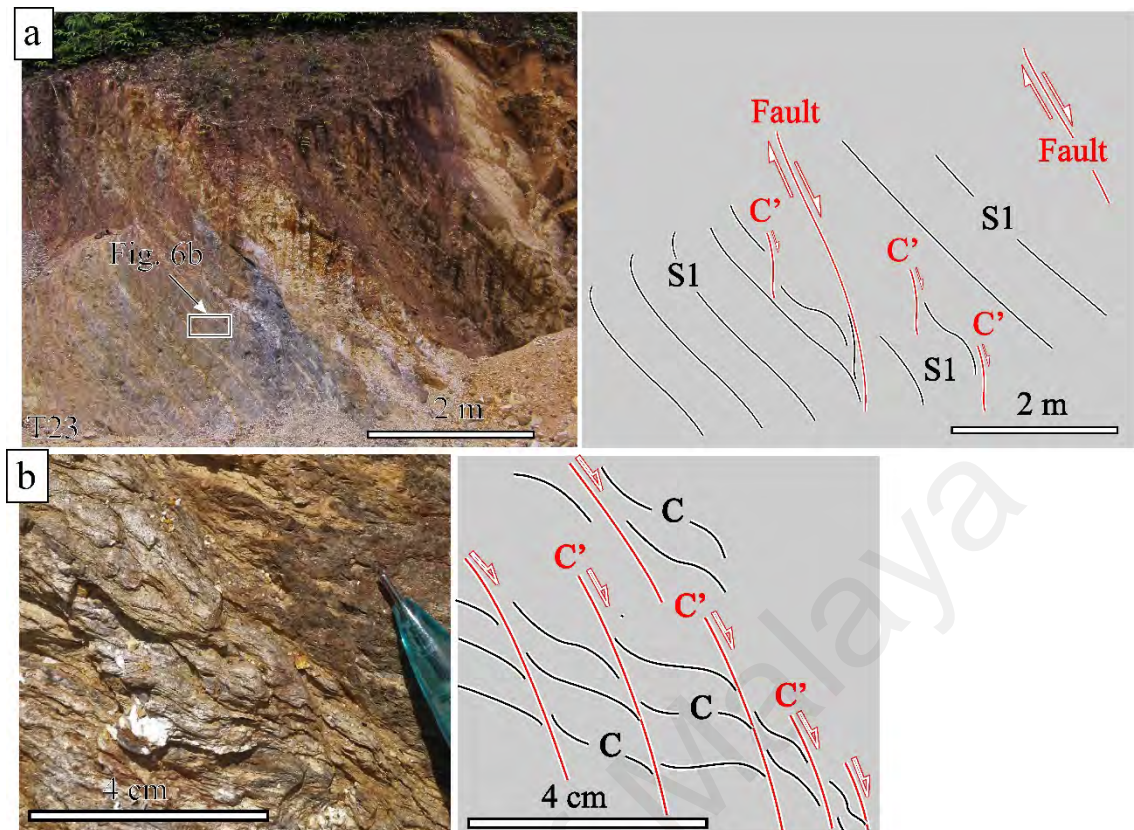


**Figure 3.8: Mylonitic exposures in SSE margin of Taku Schist; (a) Lit-par-lit injection of light-colored biotite-granite into dark quartz mica schist, (b) a strongly foliated quartz-rich schist**

### 3.2.1.2 Kinematic Transport

Rocks in the SSE domain show well-developed stretching lineation, demarcated by preferred alignment of muscovite and biotite that consistently plunges towards SE at low-angle ( $130^\circ \rightarrow 30^\circ$ ). Kinematic analysis on well-developed S/C' shear bands and minor S/C shear bands as well as  $\sigma$ -type garnet porphyroblast observed parallel to the stretching lineation (L1) indicate a uniform top-SE sense of shear (Figure 3.5, Figure 3.8a). Similar top-SE shears are also observed in ultramylonite located nearest to the SSE margin that contain lit-par-lit biotite-granite veins injections ( $132^\circ \rightarrow 35^\circ$  in Figure 3.8c). This is in contrast with exposures near the SW domain where top-SW shears ( $210^\circ \rightarrow 40^\circ$ ) are recorded. In addition, faults observed at the SSE margin also indicate a dextral normal oblique movement towards the S ( $190^\circ \rightarrow 30^\circ$  in Figure 3.8a).

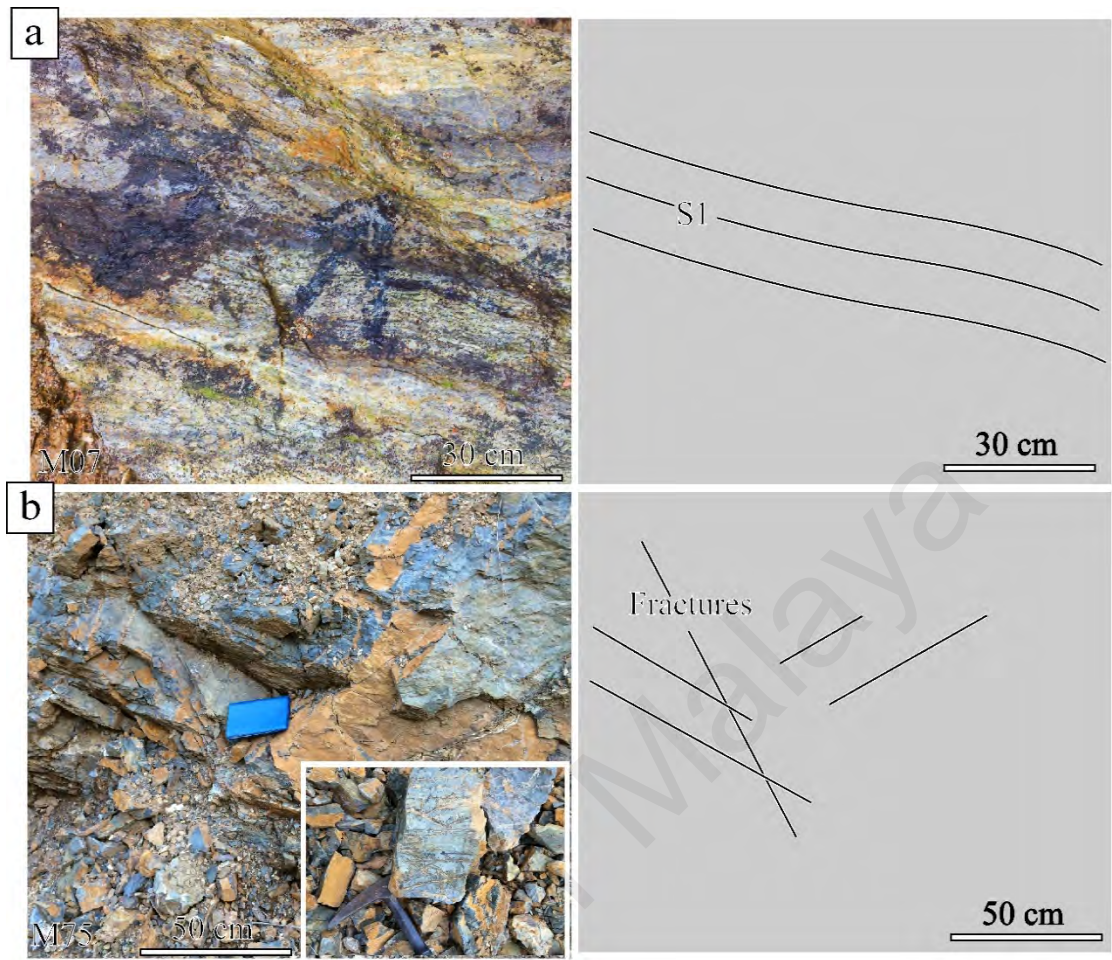


**Figure 3.9: Sedimentary and volcanic rock exposure in the southern margin of Taku Schist; (a) quartz-feldspar mylonitic phyllites situated in the SSE margin and, (b) strongly fractured tuffaceous agglomerate situated in the SSW margin of the Taku Schist**

### 3.2.1.3 Contact with Overlying Unit

The transition from the Taku Schist toward Gua Musang Formation in the SSE domain was observed by the occurrence of garnet-bearing quartz-mica schist and quartz-rich schist, which changes toward quartzo-feldspathic phyllite within a separation of less than 10 meter. The grayish phyllites signify the Gua Musang Formation particularly observed in the lower reaches of Sg. Mei in Manik Urai area (Figure 3.2). Here the rocks are strongly folded and crenulated, and in parts develop mylonitic fabrics (Figure 3.9). The S1 foliations strike NW-SE with sub-vertical dips towards NE., There is pervasive mineral alignment (L1) that plunges towards SSE at low to intermediate angles. The phyllite is cut by steeply dipping, NNW-SSE trending

faults, where kinematic analysis indicates dextral normal kinematics towards SE direction. The phyllite is also in contact with shaly mudstone showing weakly developed penetrative cleavage. The contact at SW margin shows sharp changes from quartz-mica schist to strongly brecciated volcanic agglomerate (Figure 8).

### 3.2.2 Petrographic Study

#### 3.2.2.1 Microstructural Observation

- Garnet- quartz-mica schist; Ulu Temiang. Lination:  $135 \rightarrow 30^\circ$ .  
Major: Qtz, Mcv. Minor: Bt, Kfs, Grt, Chl, Src. Trace: Trm, Zr.

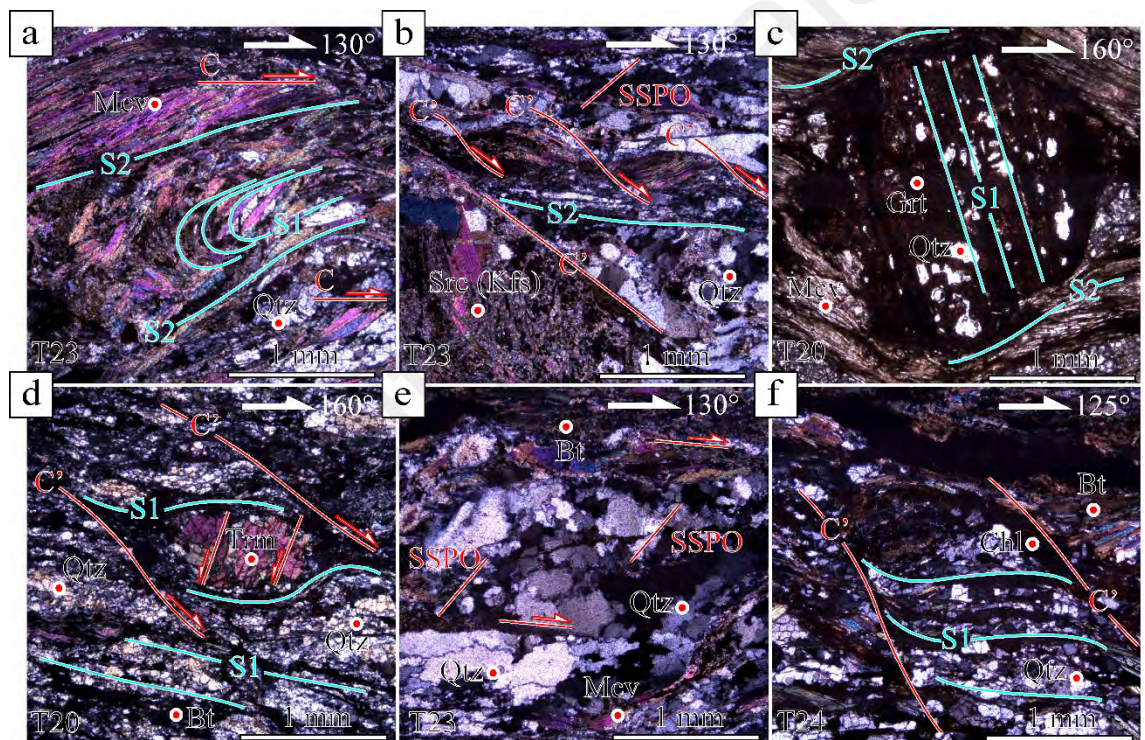


**Figure 3.10: Photomicrograph of garnet-quartz-mica schist in SSE domain within Ulu Temiang Forest Reserve.**

The garnet-bearing quartz-mica schist characterizes the rocks observed within many parts in SE domain of the Taku Schist. The rock is dominantly composed of quartz and muscovite minerals showing varying abundances in different thin sections. The quartz aggregates are coarse-grained and show shape preferred orientation. They are interlayered with muscovite with preferred alignment and this define the wide,

disjunctive foliations that often form compositional bands. Muscovite is the main sheet silicate in addition to some biotite and chlorite. The quartz aggregates often show flattened and inequigranular shapes with interlobated-bulged to serrated outline, where the extinction varies from wavy to patchy. The coarse quartz aggregates arrange in continuous elongated of flaser bands, where the sub-grains stacked between the boundaries shows strong preferred orientation (SSPO). All of above indicators suggest recrystallization mechanism mainly by subgrain rotation (SGR) in addition to minor grain boundary bulging (BLG).

In addition to S/C shear bands, the development of C'-shear bands are prominent where it occur as smooth distinctive arrays to fine anastomosed arrays that crosscut the S-foliation. The crosscutting C'-shear bands result in pervasive shape preferred orientation of quartz aggregates. In part, it occurs as steeply micro-fault. The C'-shear bands control many kinematic features including lenticular mica (muscovite) fishes and the development of rotated garnet, tourmaline and K-feldspar porphyroblast/ prophyroclast . All of these indicators suggest dextral sense of shear towards SE direction. The garnet (almandine) porphyroblasts show large hexagonal shapes that are enveloped by mica forming  $\sigma$ - type structure rotated in clockwise/ dextral manner. Inclusions contained within garnet porphyroblast comprise of fine quartz and muscovite occurring as parallel or spiral layers discontinuous to the foliation fabric in surrounding matrix. Tourmaline forms rotated  $\sigma$ - type porphyroblast align sub-parallel to the foliation and is often fractured. Large K-feldspar prophyroclast are affected by sericitization.

- Quartz- rich schist; Ulu. Temiang Forest Reserve.

Lineation: 132 → 30°. Major: Qtz. Minor: Mcv, Bt. Trace: Trm.

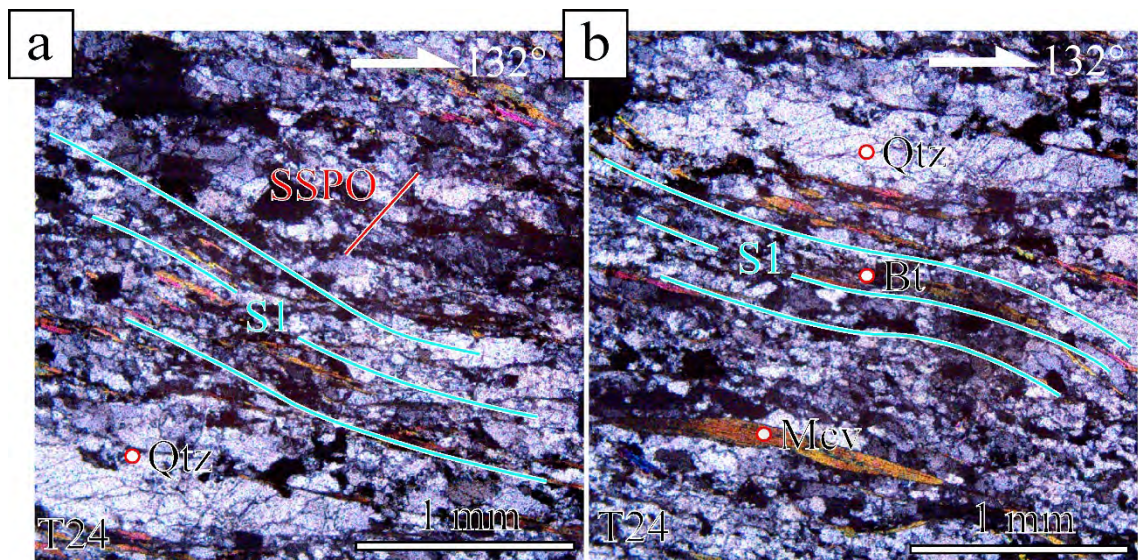


**Figure 3.11: Photomicrograph of quartz-rich schist in SSE domain within Ulu Temiang Forest Reserve.**

The samples contain high amount of quartz, as observed in few parts across the southern dome of the unit. The continuous, disjunctive foliation is defined by preferred alignment of fine muscovite as well as some biotite. The quartz aggregates varies from fine- to medium-grained. They are sub-rounded equigranular to inequigranular interlobated in shape and display shape preferred orientation parallel to the foliations. Both patchy- and wavy- type of extinction have been observed within the quartz aggregates. Weak sub-grain and neocryst shape preferred orientation suggests recrystallization mechanism in quartz aggregates operates mostly by grain boundary rotation (SGR). The presence of interlobated/serrated outline and patchy-type of extinction, it is inferred that quartz aggregates were also affected by grain boundary bulging recrystallization (BLG). There are also some S/C shear bands and muscovite fishes that indicate dextral sense of shear towards SE direction.

- Garnet- biotite schist; Kg. Slow Pak Long. Lineation:  $210 \rightarrow 40^\circ$ .

Major: Qtz, Bt. Minor: Grt, Mcv, Chl. Trace: Trm.

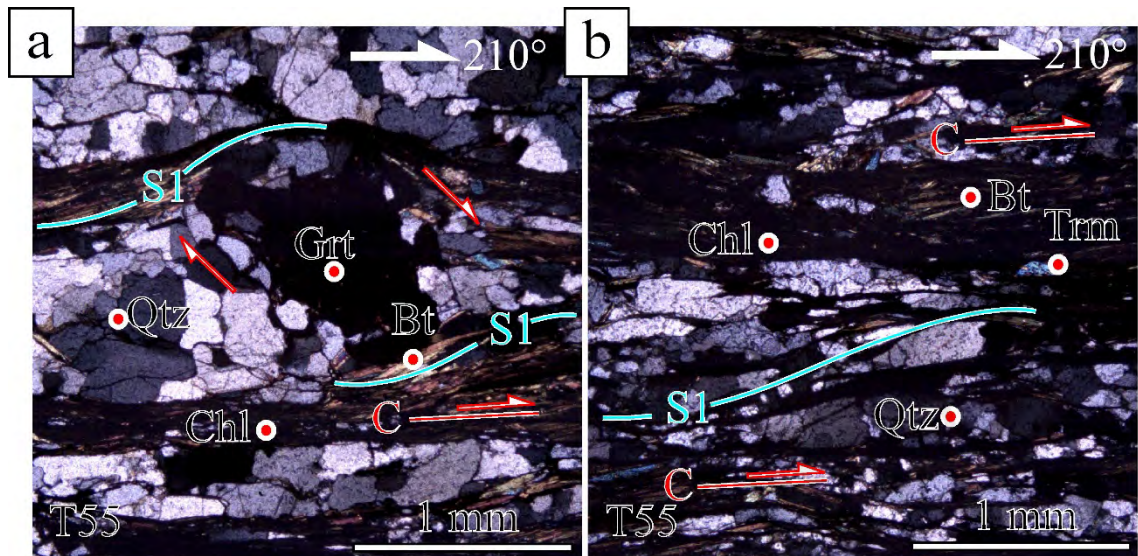


**Figure 3.12: Photomicrograph of garnet-biotite schist in the SSW margin near Kg. Slow Pak Long**

The sample was obtained near to the SSW margin in contact with severely fractured agglomerate. The rock develops continuous disjunctive foliation formed by preferred orientation and alignment of quartz and biotite. The sheet silicates also include chlorite and muscovite. In some parts, occurrences of isoclinal folds are observed within the sheet silicates. The quartz aggregates varies from fine- to coarse-grained with inequigranular shapes and they dominantly show wavy extinction, where the contact between the aggregates are often interlobated and bulged. This indicates recrystallization mechanism in quartz aggregates operates dominantly by grain boundary bulging (BLG). Kinematic analyses on S/C shear bands on biotite and garnet prophyroblast suggest dextral sense of shear towards SW direction.

- Mylonitized biotite-granite (Courtesy of Twan Daanen, U. Utrecht) ; Manik Urai  
 Lineation:  $146^\circ \rightarrow 43^\circ$ .  
 Major: Plg, Kfs, Qtz, Bt. Minor: Mcv, Src.

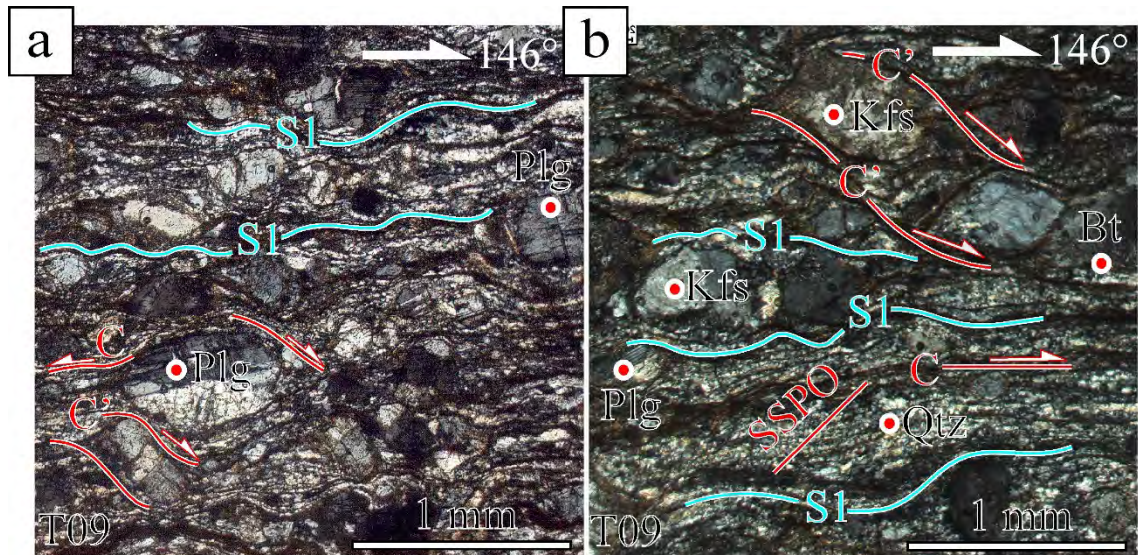


**Figure 3.13: Photomicrograph of mylonitized biotite- granite in SSE margin near Manik Urai**

The sample composed of quartz, K-feldspar, plagioclase and mica, and is consistent with an original granite protolith. The finely spaced foliation is defined by preferred alignment of continuous biotite bands interlayered with quartz and feldspathic aggregates. There are many plagioclase and K-feldspar clasts enveloped by micas forming  $\sigma$ -type prophyroclast showing dextral sense of shear. The feldspar prophyroclasts are often fractured, displaying deform twinning in plagioclase and patchy extinctions in K-feldspar. Some of the feldspar prophyroclast shows serrated boundaries, which indicate minor bulging (BLG) recrystallization. The fine quartz subgrains show strong shape preferred orientation (SSPO) oblique to S1 foliation fabric suggesting recrystallization by subgrain rotation (SGR). There is also secondary alteration as shown by sericitization of feldspar and oxidization of biotite.

### **3.2.2.2 Metamorphic Parageneses**

The rocks in the southern domain comprise of quartz-mica, garnet-quartz-mica and quartz- rich schists. This suggests a general assemblage that consists of muscovite-biotite-garnet minerals indicating prograde metamorphism to the amphibolite- facies (M1). This is responsible for the creation of spaced or spaced continuous foliations (S1), where in parts it develops compositional layering. The prograde metamorphism is also responsible for the development of large garnet (almandine) porphyroblasts in the quartz-mica schist. The porphyroblasts contain either straight or spiral quartz inclusions. The spiral inclusions possibly indicate concurrent prograde metamorphism with shear deformation (D1).

The schist samples also feature a different retrograde metamorphism (M2) indicated by the presence of chlorite that developed in C or C'-shear bands that correspond to (D2) deformation. It indicates a general assemblage of biotite-muscovite-chlorite minerals. This metamorphism however does not result in new development of blastose mineral. Inclusions within former garnet are discontinuous with external foliation fabrics, suggesting an overprinted S1 foliation fabric within SSE domain of unit.

## **3.3 The Central Dome – 2nd Sector**

### **3.3.1 Field Observation**

This domain covers areas across Sokor Taku Forest Reserve, the Galas river basin and Temangan (Figure 3.1). About 35 outcrops and 11 thin sections samples are studied in this domain. Although the exposures are limited because most areas are situated in primary forest, the condition of rock exposures is better than the intensely weathered sedimentary rocks of the overlying unit.

### 3.3.1.1 Structural Geometries

An east-west transect across Taku Schist in contact with the overlying units was made along a boat transect across Galas River for about 30 kilometers in distance. The foliations (S1) are oriented along NW-SE strikes with dips towards both NE and SW directions, which signify a regional antiformal structures of the Taku Schist (Figure 3.3a). The dipping angles accordingly decreases from intermediate angle ( $\sim 50^\circ$ ) to low angle ( $\sim 10^\circ$ ) in the direction toward the crest of Taku Schist antiform. The lithologies are mostly consist of quartz-mica schist in addition to quartz-rich and amphibole schist. The quartz-mica (biotite) schist is mostly observed in the easterly flank (Figure 3.14b), which changes to amphibole schist in the west-proximate of anticlinal crest while the light-colored quartz-rich schist is mostly observed towards the limit of the westerly flank (Figure 3.14e). Stretching lineations (L1) were observed by preferred alignment of biotite and muscovite where the plunges are consistently low angle and directed towards ENE and WSW direction (Figure 3.3b). The amount of biotite increases toward Taku Schist antiform where it displays disjunctive penetrative cleavage. This is in contrast with crenulated cleavage fabrics of quartz-rich schist in the westerly flank. The amphibole schist display finely foliated hornblende with the presence of garnet and clinozoisite (Figure 3.14c). The abundance of garnet decreases toward west proximate with a corresponding increase in clinozoisite. Folds structures were not observed during boat transect possibly resulted from the lack of exposures.

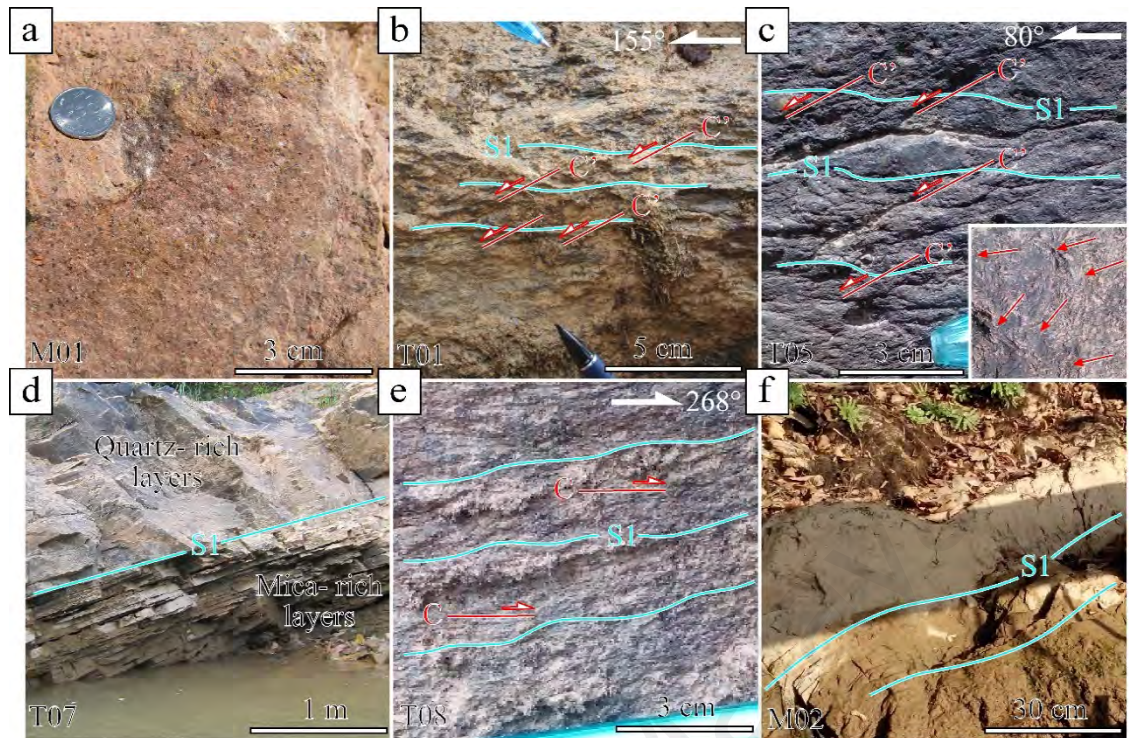


**Figure 3.14: Exposures across Galas River transect; (a) massive rhyolite in contact with (b) quartz-biotite schist at E-margin; (c) amphibole schist on the anticlinal crest of unit, the inset shows clinozoisite lineations; (d) compositional differences of schist layers (e) S/C shear bands in W-margin and (f) slaty-phyllitic rock exposure near to the contact.**

Exposures of easterly margin of the Taku Schist are observed along road parallel to the bending of Kelantan River in the Kuala Hau-Temangan areas (Figure 3.2). The lithologies comprise mainly of quartz-mica and quartz-feldspar schists with the absence of blastose garnet. The orientation of foliation fabric (S1) dominantly strikes along WNW-ESE direction, with low to intermediate inclination angles toward NNE or SSW direction (Figure 3.3a, Figure 3.14a). The fabric displays preferred alignment of muscovite flakes defining stretching lineation (L1) consistently plunges toward SE direction at low angles (Figure 3.3b).

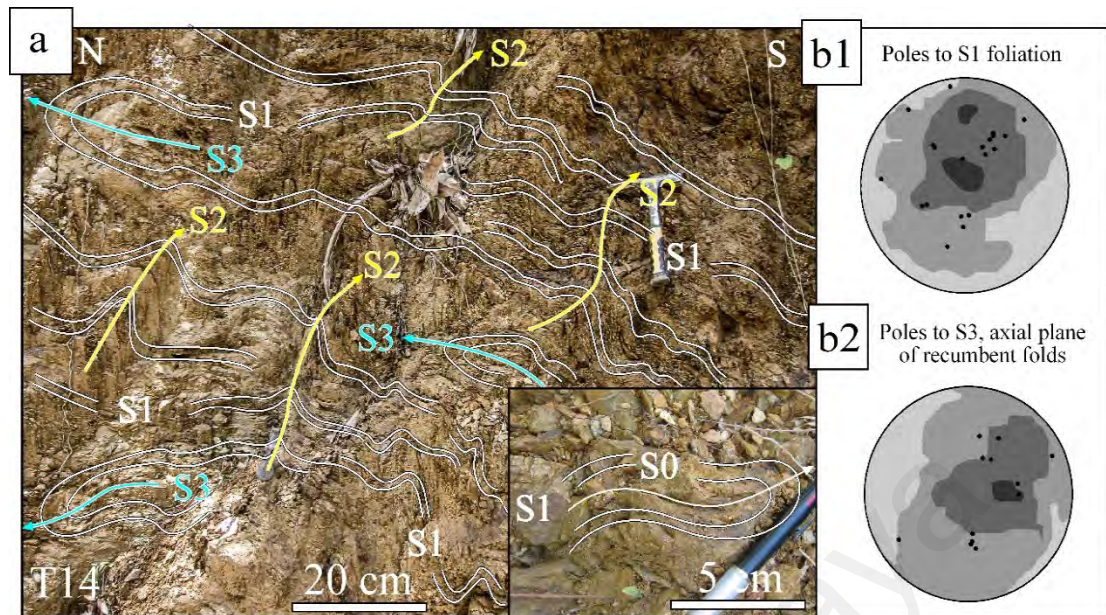


**Figure 3.15: Rock exposures near Temangan area. (a) Orientation of refolded fold structures showing the relation between S1, S2 and S3, (b) stereographic projection of (1) S1 foliation planes and (2) Poles to axial plane cleavages of recumbent fold structures**

In the same Temangan areas, the exposures shows re-folding of S1 foliation and in part results in the development of crenulated schistosity. Detail measurement of S1 foliations suggests similar dipping inclination toward both NNE and SSW directions (Figure 3.15b1), which suggests symmetric fold structures (F2 in this case). The axial planes of these folds are consistently inclined toward NE direction at low angles with horizontal axis, suggesting a recumbent-type of fold structures (Figure 3.15b2). In addition, the folds show gentle to intermediate hinge closures, where the axes plunge toward ESE direction sub-parallel to plunge of the stretching lineation (L1). Relics of centimeter scale asymmetric folds (F1) are presented within limbs of these larger symmetrical folds (F2) (Figure 3.15a). These former folds show sub-vertical axial planes inclined toward NW or NE direction, and plunges toward WNW direction with consistent westerly vergencies directions.

Good schist exposures are also observed in Sungei Hijau iron mine near Temangan where they are in contact with sedimentary rocks of the Gua Musang Formation (Figure

3.2, Figure 3.19). The lithologies are dominantly quartz-mica and quartz-feldspar schists where the foliations (S1) strike along NS- direction with sub-vertical dips towards the E (Figure 3.3). The stretching lineations (L1) are observable by alignment of white micas and are plunging towards SE at intermediate angles (Figure 3.3b). The schist is composed of quartz, muscovite and K-feldspar, minor staurolite and the absence of blastose garnet. Many NS- trending faults cut the exposures where the orientations are similar to S1 foliation planes associated with low angle striations plunging toward SE direction (Figure 3.19).

Many exposures are observed along the off-road tracks in the Sokor Taku Forest Reserve that stretches about 80 kilometers in distance, starting from the Sokor River through Taku River and ends in the Galas River basin. The lithologies are composed mainly of quartz-mica, in addition to quartz-, quartz-feldspar-, graphitic-, calc-silicate schists and schistosed marble. The quartz-mica schist is often bluish-green in color containing abundant blastose garnet and lesser tourmaline. The orientation of foliations (S1) in general strikes NNW-SSE sub-parallel with the long axis of the Taku Schist body, although localized orientation inconsistency are observed across the transect (Figure 3.3a). The S1 foliation planes inclined either towards WSW or NE with low-intermediate dipping angles on both flanks of the central domain, which define the regional antiformal structure of the Taku Schist (Figure 3.3a). The stretching lineation (L1) demarcated by alignment of biotite and muscovite flakes shows highly inconsistent plunge directions (SW-W-NW-NE-E-SE) associated with low-plunging angles (Figure 3.3b).

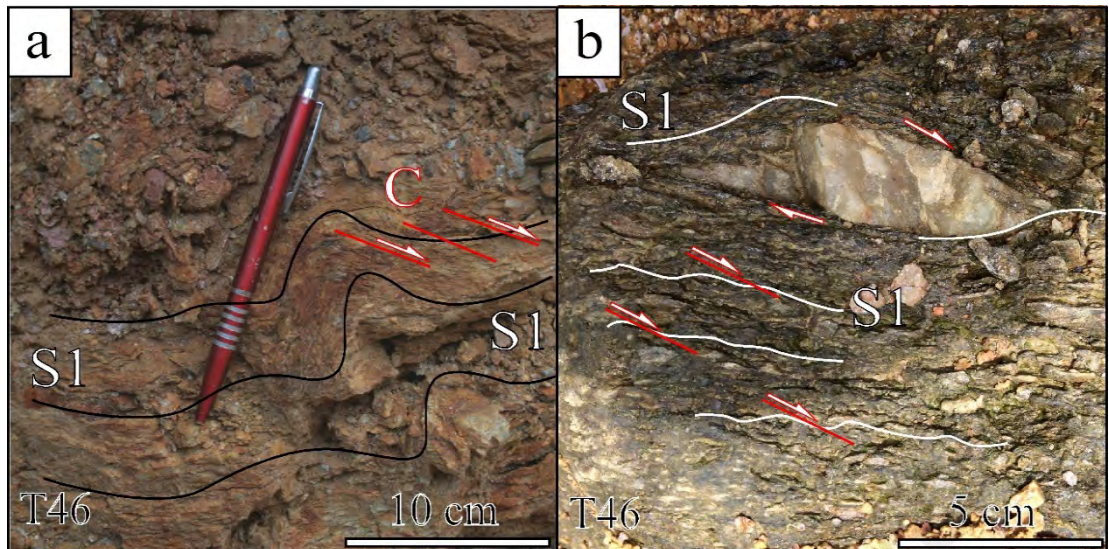


**Figure 3.16: Quartz-mica schist fabric within Sokor-Taku area. (a) C-shear bands and small asymmetric fold structures; (b) rotated marble prophyroclast. Both kinematic indicators indicate dextral sense of shear.**

In addition to transposed isoclinal folds (F1) widely observed within the schist, two other types of folds are observed across the transect: asymmetric folds with steeply inclined axial plane (F2); and symmetric folds with sub-horizontal axial plane (F3). The former upright, asymmetrical folds are prevailing across the transect displaying tight hinge closures that plunge towards the WSW. The asymmetry arises from steep westerly dipping limbs in relationship to shallow easterly dipping limbs, which suggest west-directed vergence. This asymmetric vergence is also related to steeply inclined C'-shear planes striking NNE-SSW that cut the S1 foliation. It results in the development of boudinage and prophyroclast of marble. The symmetrical folds (F3) in contrast are localized, occurring in few exposures that result in complex re-folded foliation fabrics (Figure 3.18). In addition, an exposure in east proximate of the anticlinal crest near Kg. Sokor shows a leucogranitic injection into graphitic schist parallel to the S1 foliation planes, which is further folded into Z-shaped asymmetries (red patches in Figure 3.1, Figure 3.17).

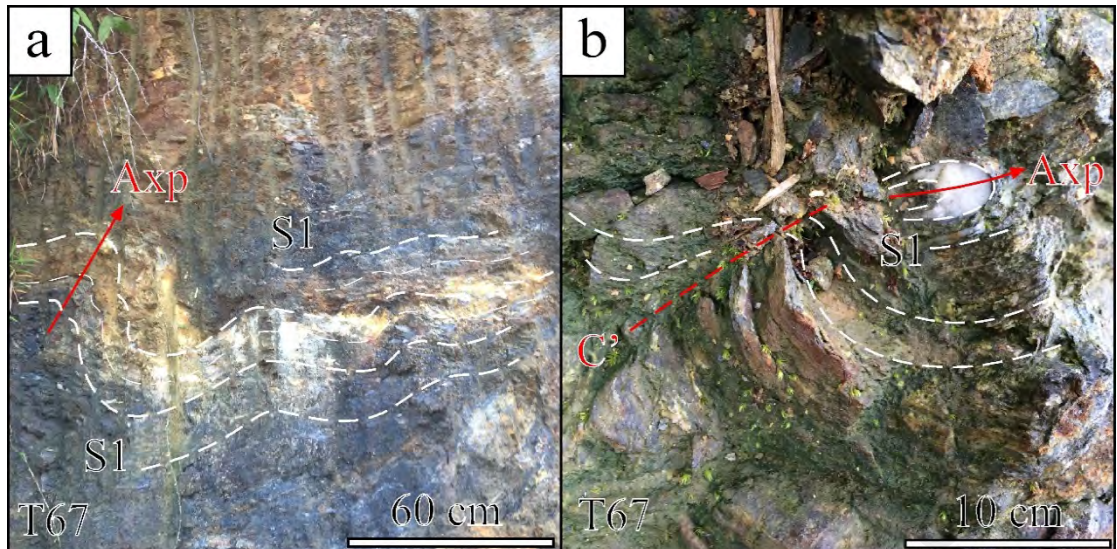


**Figure 3.17: Graphitic schist within Sokor-Taku area. (a) Biotite-leucogranite veins injections align sub-parallel to foliation planes affected by folding and (b) Isoclinal fold aligned sub-parallel to S1 foliation cuts by steep C'- shear bands.**

### 3.3.1.2 Kinematic Transport

The EW transect across Sg. Galas basin indicates three directions of kinematic transport, which includes WNW, NE, and SE sense of shears (Figure 3.5). The S/C shear bands in amphibole and quartz-rich schists situated in the anticlinal crest and parts of the westerly flanks indicate dominant top-WNW shear directions (Figure 3.14c and Figure 3.14e) in addition to a single top-NE shear observed in the east proximate to the anticlinal crest. Exposures situated on the easterly flanks show top-SE shears as determined from S/C' shear bands (Figure 3.14b), where it shows a uniform kinematic direction in contrast with former WNW and NE directed kinematics.

Despite the inconsistent plunge directions of the stretching lineations (L1) observed across the Sokor Taku Forest Reserve (Figure 3.3b), kinematic analysis on S/C and S/C' shear bands as well as garnet prophyroclast suggest low angle shears towards WSW, NE and SE directions (Figure 3.5). The WSW and NE shears are associated with the occurrences of asymmetrical upright folds with gentle to tight hinge closures. These shears are mostly inferred from C'- shear planes, marble boudinages and prophyroclast

(Figure 3.16). However, the axes of stretching lineation (L1) are inconsistent with  $\sim 30^\circ$  degrees variation in orientations (Fig. 3.3b and Fig. 3.15). The latter top-SE shears are similarly determined from S/C' and S/C shear bands as well as garnet porphyroblasts. The foliation associated with this kinematic often strikes ENE-WSW and cut by C'-shear bands striking NNW-SSE parallel to fault planes (Figure 3.18). Both C'-shear and fault planes show similar kinematic movement of top-SE or dextral normal towards the SE. While the faults often drag-fold the quartz-mica schist following the kinematic direction, the S1 foliation associated with this kinematic often developed into symmetrical open folds with sub-horizontal axial planes (F2). The plunge of these fold axes are sub-parallel to the plunge of the stretching lineations (L2). In addition, it is observed that the earlier upright asymmetrical folds (F1) were re-folded by the recumbent symmetrical folds (F2) pertaining to the top-SE deformation (Figure 3.18).

### **3.3.1.3 Contact with Overlying Unit**

The contact between Gua Musang Formation and the Taku Schist across Sg. Galas Basin was interpreted from lithological changes from a massive, non-deformed rhyolite to quartz-biotite schist in the east of Sg. Galas Basin (Figure 3.14a and Figure 3.14b). The westerly margin shows lithological changes from phyllitic mudstone to quartz-rich schist (Figure 3.14e and Figure 3.14f). The rhyolite represents the acidic volcanic rocks of Gua Musang Formation unaffected by significant metamorphism. A minor EW-striking sinistral strike-slip fault cuts through the rhyolite exposure.

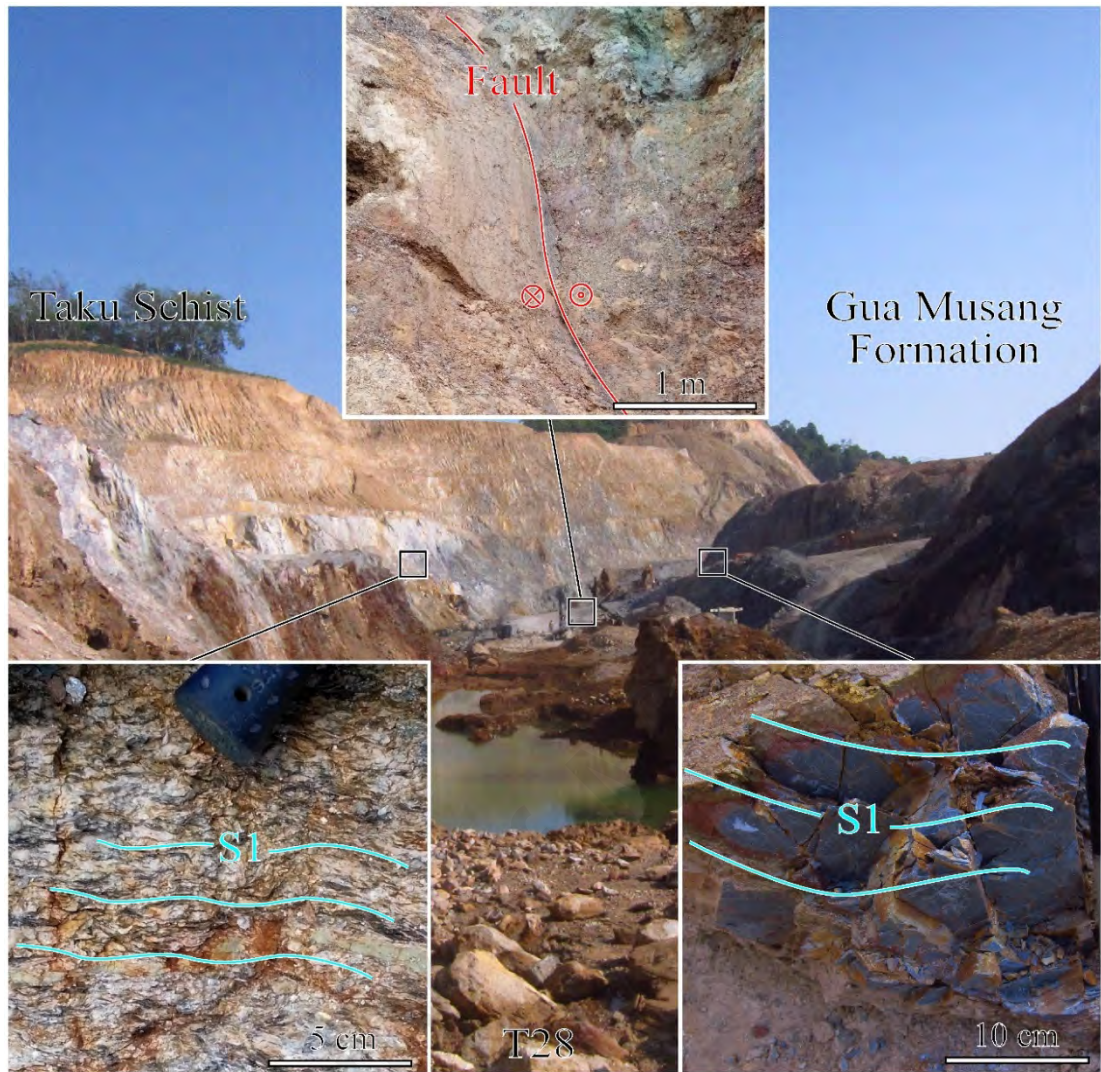


**Figure 3.18: Fault contact in Temangan area. The strike slip fault separates quartz-feldspar schist from mudstone.**

The aerial view of Sg. Kelantan shows sudden looped shapes within part of the river near Temangan area where the river initially flow within easterly boundary margin of the Taku Schist bends laterally and flow along the westerly margin of Gua Musang Formation (Figure 3.2). Field observation near Temangan iron mine shows a major faults responsible for separation between the quartz-feldspar schist of the Taku Schist from shales and mudstone of the Gua Musang Formation (Figure 3.18). This is indicated by presence of steeply inclined NS-trending faults in both units. The faults show low plunging striations indicative of strike-slip, which contain cataclastic quartz-mica schist or mudstone. Kinematic analysis on the faults based on Riedel shear suggest dextral shears towards SE direction ( $165^{\circ} \rightarrow 20^{\circ}$ ). The kinematic is comparable to

sense of shear observed in the quartz-mica schist, where analysis on S/C' shear bands suggests top-SE shears (Figure 3.5). Both schist and mudstone exposures indicate structural conformity. Both have steeply inclined S1 foliation/ bedding plane (S0) striking NS direction, but the schist shows significant penetrative cleavage development.

University of Malaya

### 3.3.2 Petrographic Study

#### 3.3.2.1 Microstructural Observation

- Quartz-mica-feldspar schist; Sungei Hijau iron mine

Lination:  $160^\circ \rightarrow 45^\circ$ .

Major: Qtz, Mcv, Kfs (Src). Minor: Bt. Trace: Zr.

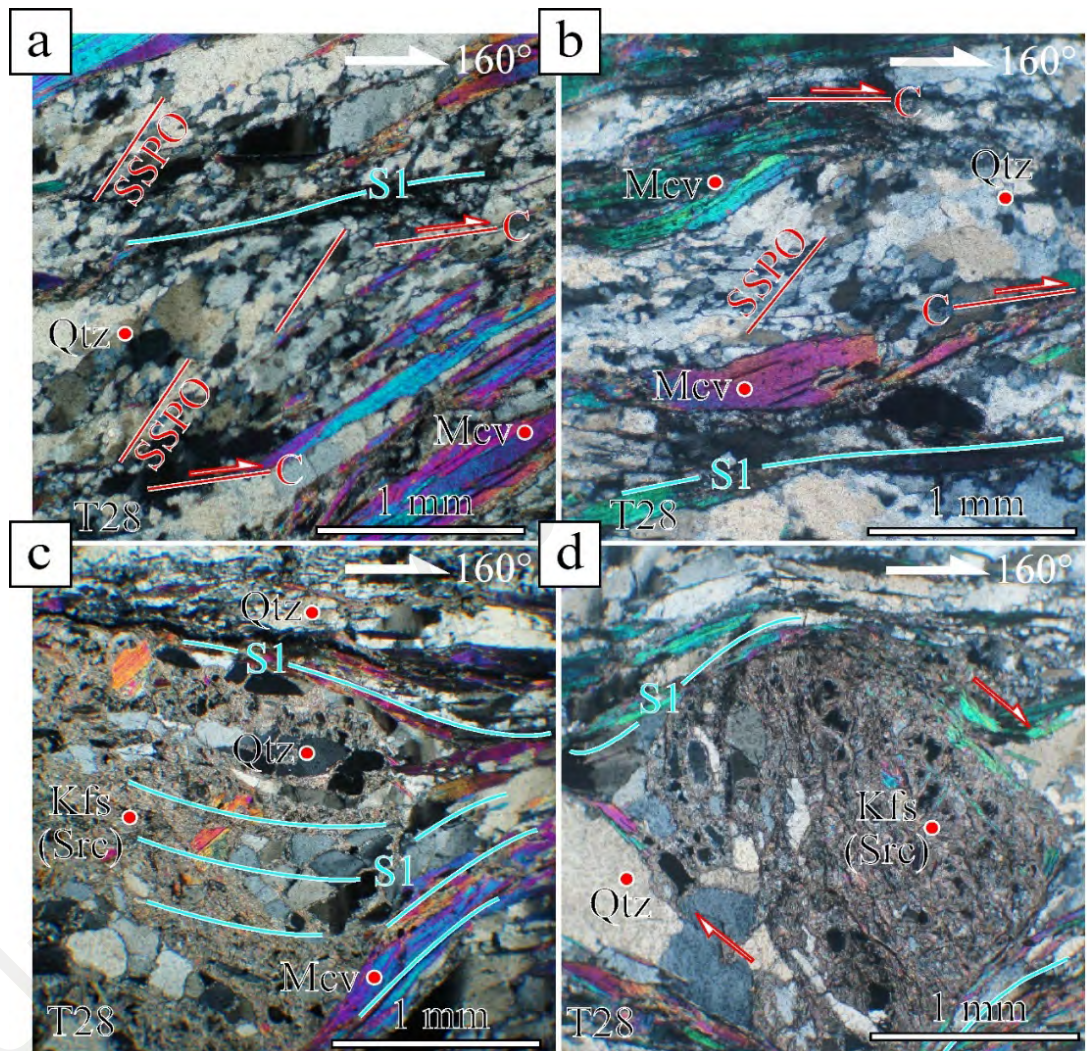


**Figure 3.19: Photomicrograph of quartz-feldspar-mica schist near to E margin near Temangan iron mine.**

The schist samples obtained nearest to the contact with overlying sedimentary rocks show wide disjunctive spacing forming compositionally layered foliation fabric that composed dominantly of quartz and feldspar. The quartz aggregates are coarse grained, with elongated shapes and bulged to interlobated outline and show wavy-type of

extinction. Fine quartz sub-grain and neocryst aggregates occur between large quartz aggregates, as well as envelopes the K-feldspar prophyroclasts. It indicates that the recrystallization mechanism operated within the quartz aggregates is mainly by subgrain rotation (SGR), which is responsible for strong shapes preferred orientation (SSPO) of quartz sub-grains and neocrysts oriented oblique to foliation plane (S1).

There are many large prophyroclast up to 5 millimeter in diameter, where some of these were affected by intense secondary alteration obliterating its primary features. Two types of prophyroclast observed from shapes outlines include the large square-shaped prophyroclast and a sub-rounded clast made up of equigranular quartz aggregates. The former clasts are completely transformed to sericite containing quartz inclusions oriented oblique to S1 foliation. From the clast shape, it is inferred that they are relict K-feldspar clasts. The prophyroclasts are rotated clockwise in agreement with dextral sense of shear observed in muscovite fishes. Both structures are in close association with C'-shear bands, which similarly indicate dextral shear. Thus, the overall dextral sense of shear indicates kinematic transport towards ESE direction.

- Quartz-feldspar-mica schist; Kg. Sg. Hau. Lineation:  $160^\circ \rightarrow 24^\circ$ .

Major: Qtz, Kfs. Minor: Mcv, Bt, Chl

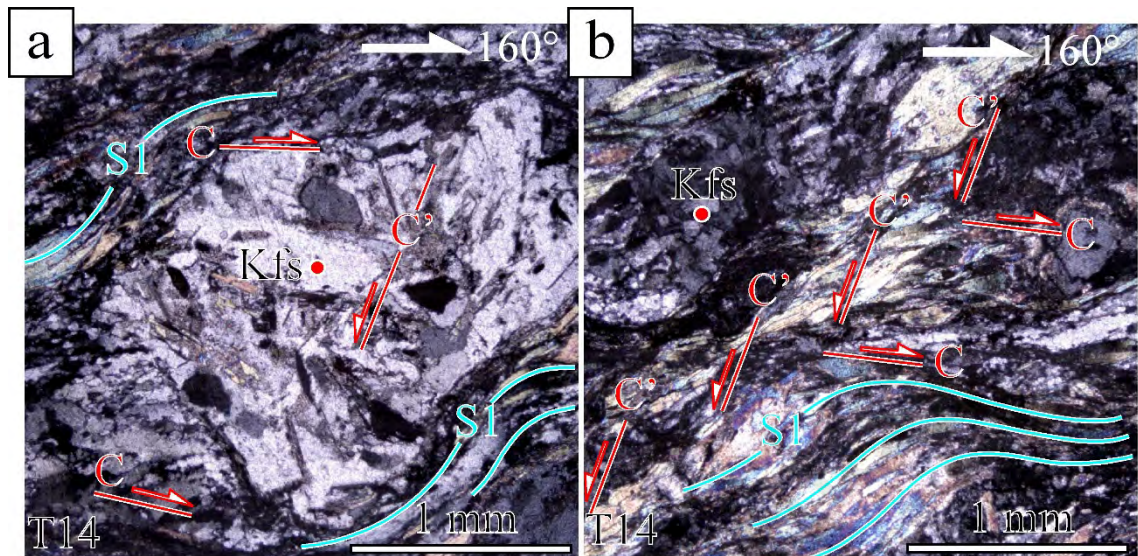


**Figure 3.20: Photomicrograph of quartz-feldspar schist in the E flank at Kg. Sg. Hau**

The sample is primarily composed of coarse grained quartz and K-feldspar with some muscovite, biotite and chlorite assembled into dense cleavage zones. The foliation fabric is mainly controlled by both S/C and S/C' shear bands that results in appearance of crenulated-like schistosity. The fabric envelops numerous large K-feldspar within muscovite forming prophyroclastic structures. In addition, trace minerals identified are zircon and titanite, which are also aligned parallel to the foliations. The large quartz aggregates are strongly elongated along foliations. It has interlobated to amoeboid boundaries and wavy extinction. Fine recrystallized quartz and quartz sub-grain aggregates are stacked in between these aggregates of relict quartz. This indicates recrystallization by subgrain rotation (SGR), although some of the aggregates boundaries are serrated suggesting minor recrystallization by grain boundary bulging (BLG).

The fabric also contains numerous K-feldspar porphyroclast about 2 millimeter in diameter often fractured. The fractures are often at high angles to the foliation and show antithetic displacements. The K-feldspar porphyroclasts are affected by sericitization along the fractures. Biotite inclusions in the K-feldspar are randomly oriented, and secondary chlorite grains are observed in the strain shadows. The K-feldspar shows patchy extinction. The clockwise rotation of the porphyroclast, as well as dextral sense of shear observed from S/C shears bands and muscovite fishes indicate kinematic movement towards SE direction.

University of Malaya

- Garnet-biotite schist; Sg. Taku, Sokor Forest Reserve.

Lineation:  $52^\circ \rightarrow 10^\circ$  (T45) and  $345^\circ \rightarrow 30^\circ$  (T41).

Major: Qtz, Bt, Grt. Minor: Mcv, Chl.

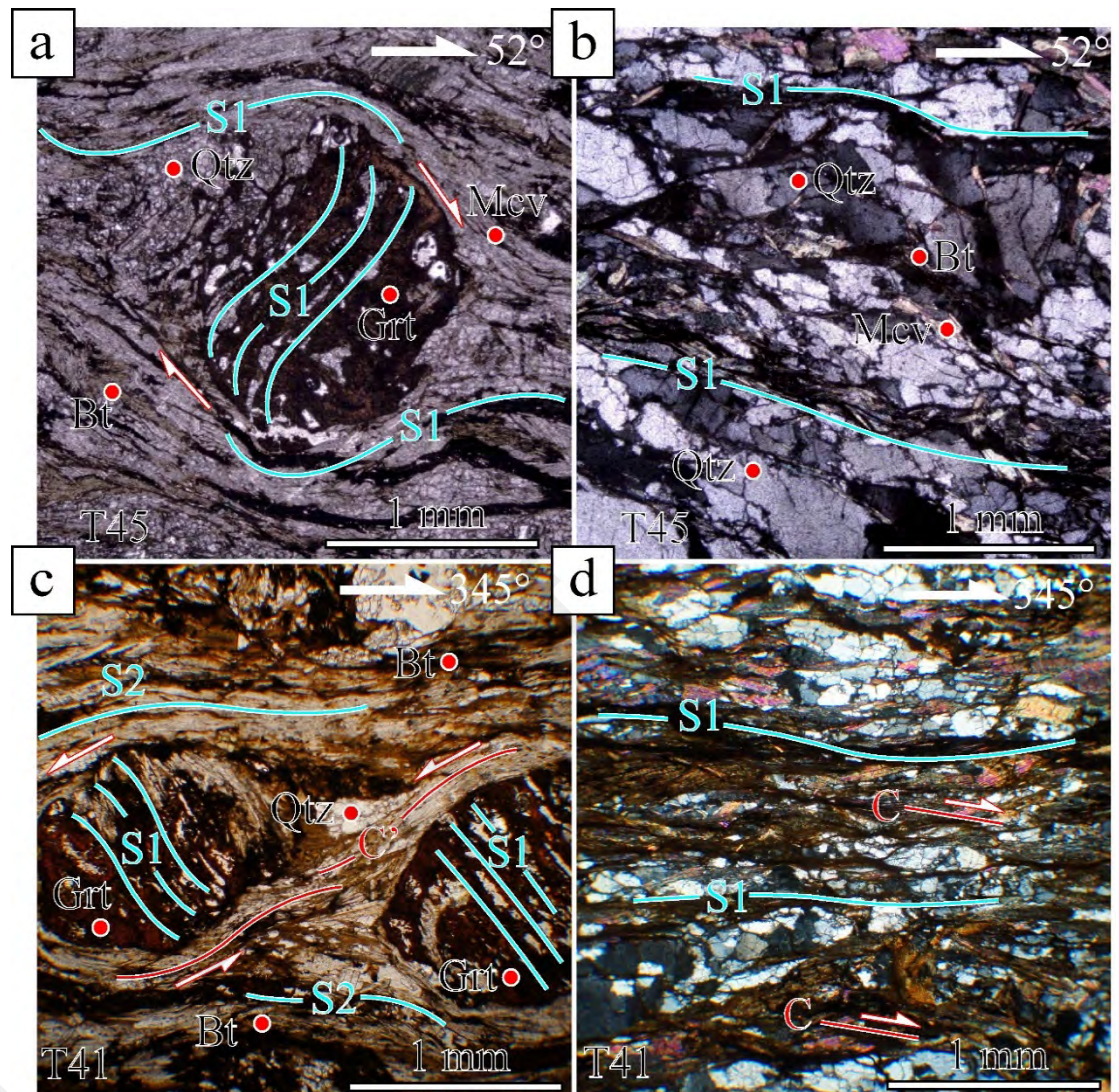


**Figure 3.21: Photomicrograph of garnet-biotite schist in the WNW flank at Sokor Taku Forest Reserve.**

The foliations of the garnet-bearing quartz-biotite schist are defined by finely spaced disjunctive cleavage showing compositional layering of alternating biotite and quartz aggregates, which often anastomose. The biotite-rich matrix envelops numerous poikiloblastic garnet (almandine) about 1.5 mm in diameter into  $\sigma$ - porphyroblasts. The quartz aggregates possess equigranular shapes with serrated to bulged outlines along

contacts, where it shows dominantly patchy-types of extinction as well as minor wavy extinction. This indicates recrystallization mechanism by grain boundary bulging (BLG) responsible for development of fine neocrysts stacked in between quartz grains. The quartz aggregates in part of the sample (S.31.3.2) also define a weak preferred orientation that indicates a former recrystallization mechanism by subgrain rotation (SGR).

The garnet (almandine) porphyroblasts contain fine quartz inclusions that form parallel layers with slight curve towards the edge. These inclusion layers are either continuous (see S.31.3.2) or discontinuous to the foliation of the surrounding matrix. The garnet porphyroblasts indicate clockwise rotation or dextral sense of shears, similar to the muscovite/mica-fishes. In latter case of S.31.3.8, arrays of C'-shear bands cut the S foliations and folded the foliation, where a dextral shears is indicated. All of the indicators suggest dextral kinematics towards SE directions in S.31.3.8 and NE direction in S.31.3.2.

- Quartz-rich Schist; Sg. Galas Basin. Lineation:  $275^\circ \rightarrow 30^\circ$ .

Major: Qtz. Minor: Mcv, Bt.

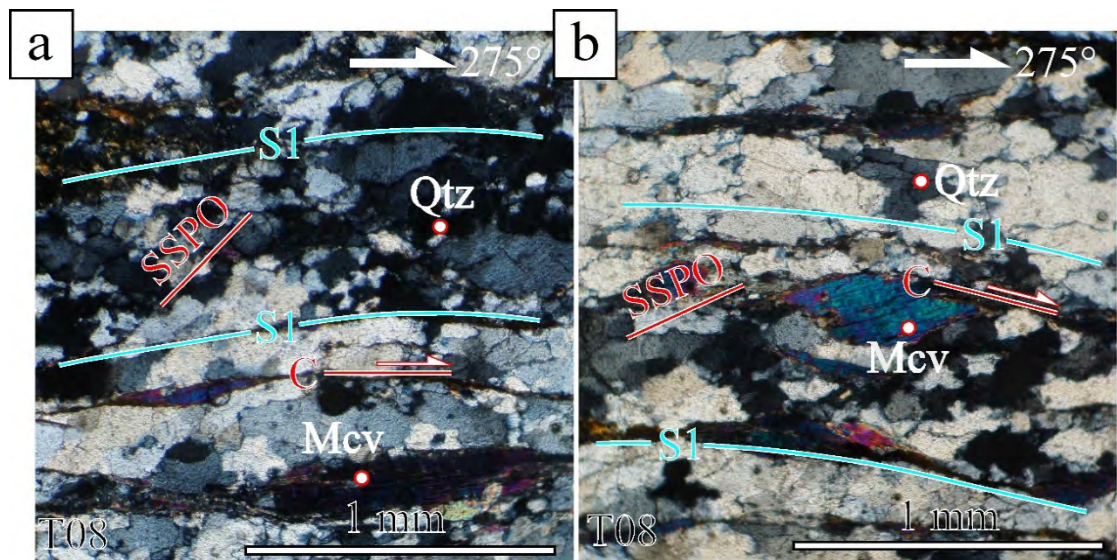


**Figure 3.22: Photomicrograph of quartz-rich schist in to the W margin at Sg. Galas Basin.**

The sample was obtained from the western flank of Taku Schist in the upper reaches of Sg. Galas Basin. It contains mostly of quartz aggregates interlayer with fine muscovite and biotite showing preferred alignment and defines continuous disjunctive foliation fabric. The quartz aggregates vary from fine- to coarse- grained, equigranular and have interlobated outlines. They also exhibit wavy extinction and weak preferred sub-grains orientations indicative of recrystallization mechanism by subgrain rotation (SGR). By inferring the orientation of oblique quartz sub-grains in respect to foliation fabric, the derived sense of shears is sinistral towards NW direction.

### 3.3.2.2 Metamorphic Parageneses

Samples in both E and WNW part of the central domain comprise of quartz-mica, garnet-quartz-mica, quartz-feldspar and quartz-rich schists. The mineral assemblage of muscovite-biotite-garnet indicates a prograde metamorphism (M1) to amphibolite facies, responsible for development of spaced disjunctive schistosity. This is related to

occurrences of subgrain rotation (SGR) observed in some of the samples obtained from NNW-domain associated with D1 shear deformation. The metamorphism is also responsible for development of foliation fabric within garnet recognized by straight orientation of quartz inclusions.

Samples obtained near to the E margin contain feldspars porphyroclasts that show sericitization and fracturing. Some of these minerals are completely sericitized. Parts of muscovite grains also show transformation to chlorite. This feature indicates retrograde metamorphism (M2) associated with D2 shear deformation. In addition, the metamorphism is also responsible for discontinuous relationship between internal foliation contained within garnet porphyroblasts with the foliation fabric on surrounding matrix.

### **3.4 The Northern Dome – 3rd Sector**

#### **3.4.1 Field Observation**

The northern domain of the Taku Schist covers areas from Ayer Lanas to Tanah Merah, and reaching the Kelantan River. It also covers the areas on northern parts of Temangan and Sokor Taku Forest Reserve. Field study comprised of 16 exposures with 4 thin sections (Fig. 3.2).

##### **3.4.1.1 Structural Geometries**

The areas close to Tanah Merah provide the most accessible Taku Schist outcrops despite affected by intense weathering, where exposures are mostly observed near to the ongoing housing projects. The exposures comprised mostly quartz-mica schists, where the foliation (S1) is defined by preferred alignment of muscovite, chlorite and biotite. The S1 foliations on average strike NNW-SSE with moderate to steep dips towards NE, where the orientation follows the outlying curvature of the northern dome (Figure

3.3a). The rocks display well-developed schistosity containing low angles stretching lineations (L1) plunging toward SW, SE, NE and W directions (Figure 3.3b).

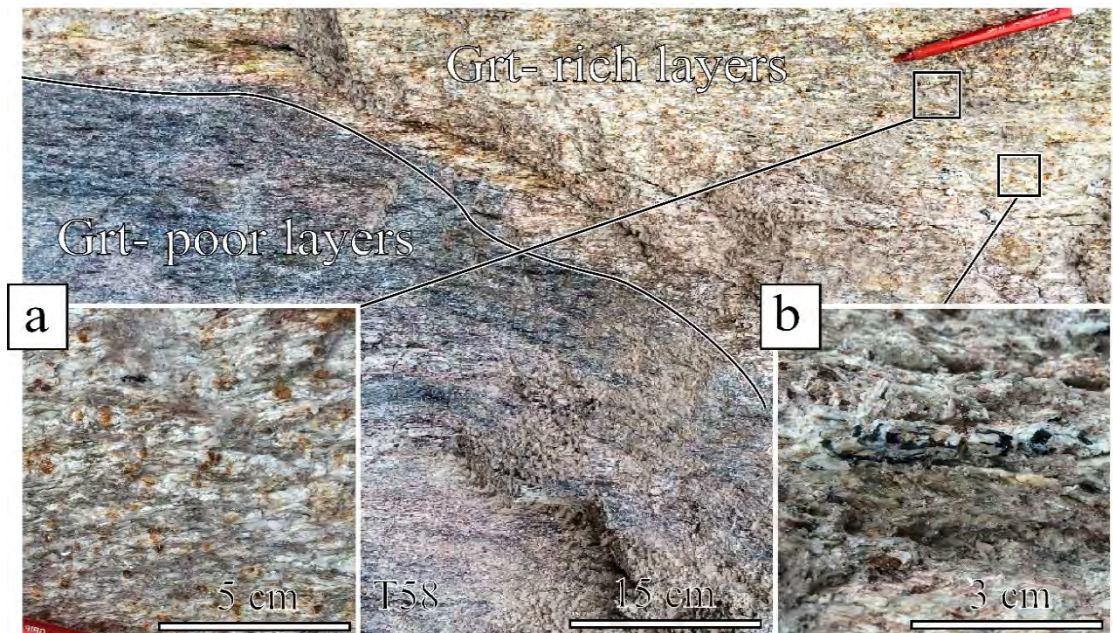


**Figure 3.23: Compositional difference within quartz-mica schist, NNE domain of the Taku Schist. The blastose minerals include (a) garnet (almandine) porphyroblast and (b) prismatic tourmaline minerals. The amount of garnet is higher in whitish schist layer in comparison to dark-greyish layers.**

The quartz-mica schist in Tanah Merah is often bluish-green colored, possibly indicates primary chlorite. It contains numerous blastose garnet (almandine) in contrast to the purplish-brown color of quartz-rich schist (Figure 3.24). A common blastose mineral in the schist but less abundant is tourmaline, recognized by its prismatic shape although it does not show preferred orientation (Figure 3.24). The quartz-mica schist also contains centimeter thick intercalation of quartz and marble layers that often develop asymmetrical boudins, rotated porphyroblasts or Z- shapes asymmetrical folds with transposed limbs (Figure 3.25).

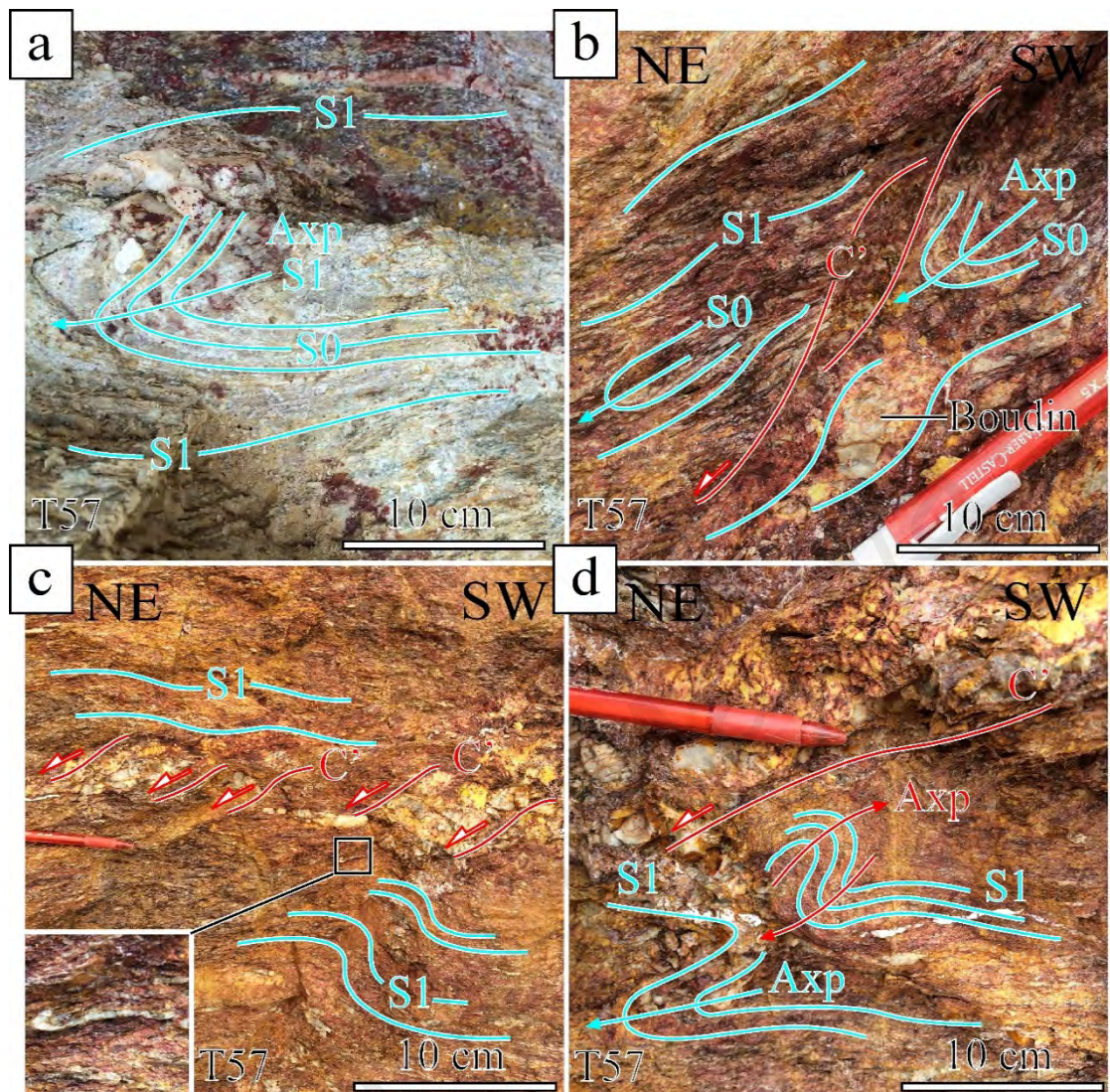


**Figure 3.24: Examples of small- scale structures observed within the schist; tight-isoclinal folds in (a), (b), (c) and (d) shows an axial plane oriented parallel to S1 foliation. Steep C'- shear bands crosscut S1 foliation by sinistral manners, where in (b), it results in development of asymmetrical boudinages of marble layers.**

Millimeter-scale symmetric tight to isoclinal folds with transposed limbs (F1) usually develop in quartz or marble layers, where the axial planes are sub-parallel to S1 foliation planes. The schist exposures also develop centimeter-meter scale asymmetrical folds characterized by tight to gentle hinge closures with asymmetrical limbs (F2), where the axial planes are steeply dipping and strike along NS direction. The fold axis plunges either towards NW or towards SE directions, perpendicular to the stretching lineation (L1) and indicate westerly vergence (Figure 3.26). The occurrence of these

asymmetrical folds and other asymmetrical boudins are usually related by crosscutting shear planes (fault plane in Figure 3.25). In the areas near to the SSW margin of Kemahang granite (Keralla, Tanah Merah), pervasive development of asymmetrical folds was observed in dark-greyish mica-rich schist where it develop contorted and crenulated fabrics. This is in contrast to the quartz-rich layers where foliations are folded into a gentle, large-scale asymmetrical fold. The folds are cut by arrays of NS-trending faults, where it drags folded the layers in proximity.

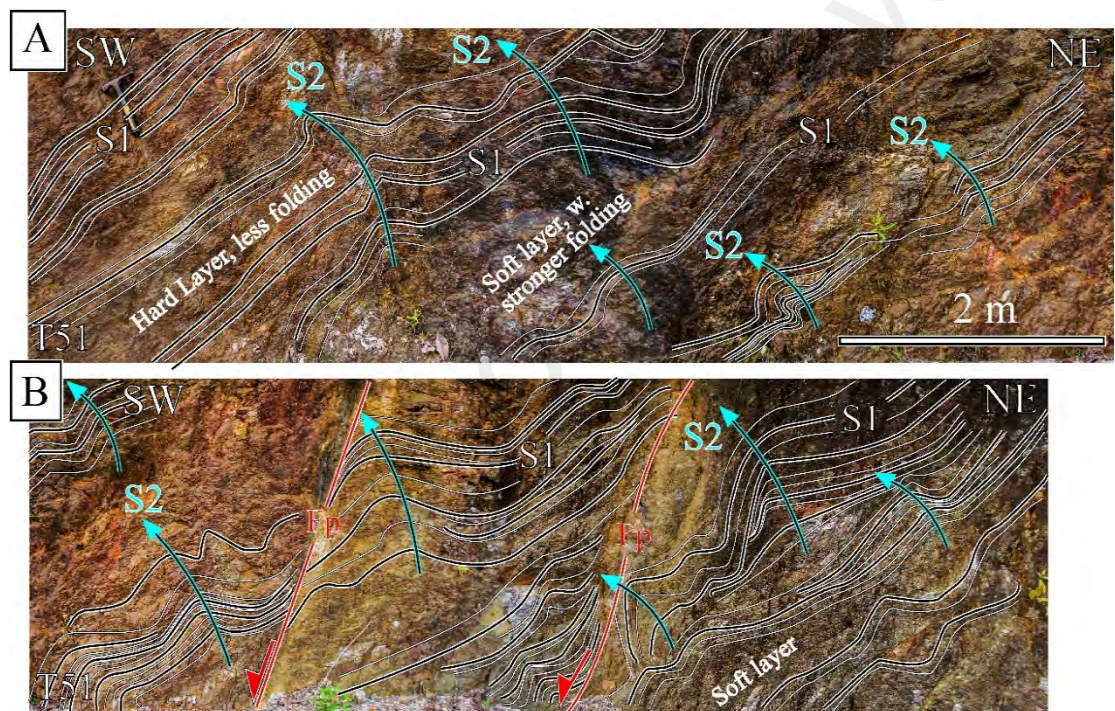


**Figure 3.25: Inclined asymmetrical folds in SSW margin of Kemahang granite. Notice the development of fold is stronger in the argillaceous layer.**

The exposures in the northern domain also show many large, steeply inclined NNW-SSE trending faults cutting the foliations. The faults are accompanied often by low-plunging striations. The schist fabrics in proximity to the fault planes are usually affected by chloritization and are folded following the kinematic of these faults. In addition, the faults also contain centimeters- scale cataclastic quartz-mica schist (Figure 3.26).

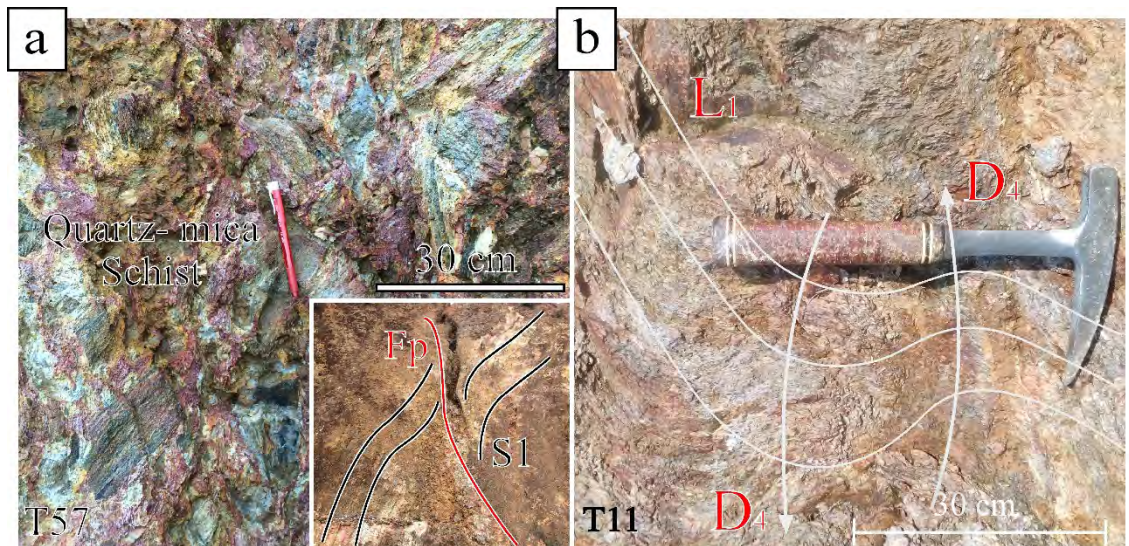


**Figure 3.26: (a) Cataclastic schist layer contained within a fault zone. The inset shows a fault drag folded the S1 foliation. (b) Folded L1 stretching lineation by subsequent fold episode.**

#### 3.4.1.2 Kinematic Transport

Kinematic analysis in the northern domain of Taku Schist shows four directions of shear that include top-WSW, NE and SSE directions (Figure 3.5). The areas around Tanah Merah and Keralla- Kg. Ipoh show top-WSW and NE shears determined from S/C and S/C' shear bands as well as rotated garnet porphyroblasts (Figure 3.5, Figure 3.25). The S1 foliation typically shows crosscutting C'-shear planes and strong development of inclined asymmetrical folds (F2) with consistent westerly vergence. Similar sense of shear is also associated with schist exposures near to the contact with Kemahang granite (Figure 3.28).

Some of the exposures in Tanah Merah and Kg. Ipoh (on the eastern flank of Kemahang granite) show top SSE and NNW shears interpreted from S/C' shear bands in quartz-mica schist (Figure 3.5). The kinematic is comparable to the crosscutting faults, where Riedel shear analysis indicates dextral oblique movement towards ESE direction. Chloritization, brecciation of the quartz-mica schist and drag-folding of schist layers in proximities are observed, associated with the faults. In exposures showing top-

SW shears, occurrence of L1 stretching lineation folded into recumbent structures (F3) plunging towards SSE direction are also observed (Figure 3.27).

### 3.4.1.3 Contact with Overlying Unit

Near the entrance of Sokor Taku off-road track, a change from a purplish slate into whitish quartz mica-schist in about 100 meter separation indicates the contact between the western margin of the Taku Schist with the overlying Gua Musang Formation (Figure 3.2). The S1 foliation on both exposures strikes NNW-SSE with dips towards NE. Despite the observed structural conformity, the foliation dip angles in quartz-mica schist are shallower in comparison to the overlying slates (Figure 3.3a). While the kinematic analysis on the quartz-mica schist indicates top WNW shears (Figure 3.5), the slates exposures shows development of asymmetrical tight folds indicating westerly-vergence direction (F2).

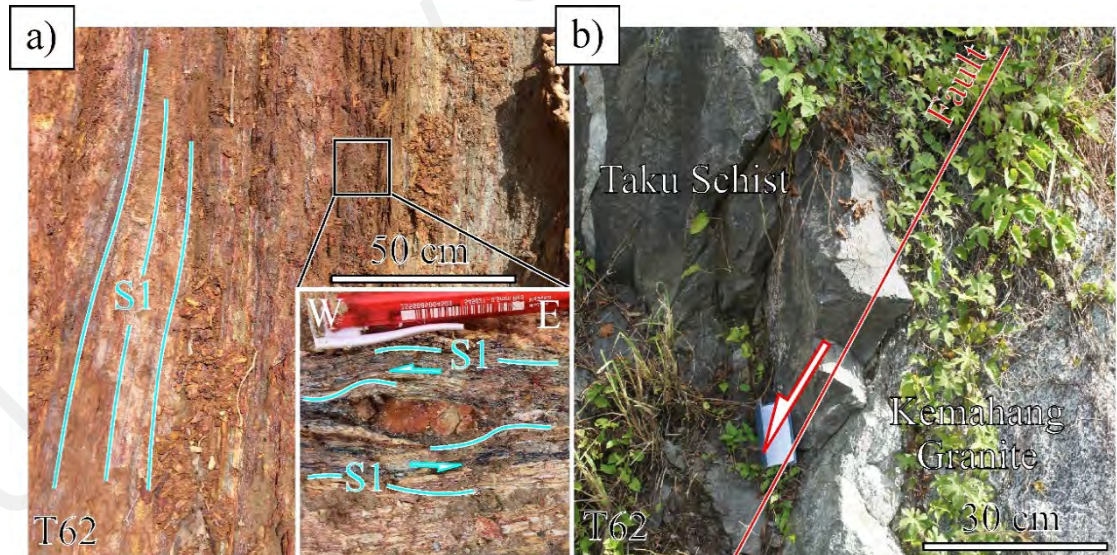


**Figure 3.27: Rock exposures near to Kemahang Granite-Taku Schist contact, NNW part of Taku Schist: (a) a mylonitic contact or (b) fault contact.**

The schist exposure located near to the eastern margin of Kemahang granite along the Tanah Merah – Jeli road displays thinly elongated bands of quartz-feldspar and quartz-mica defining mylonitic fabric (Figure 3.28a). The foliation strikes NNE-SSW

with sub-vertical dips towards SE. Kinematic analysis on marble prophyroclast indicates top-W direction of shear ( $274^{\circ} \rightarrow 25^{\circ}$  in Figure 3.28a). Similar mylonitic schist fabrics are observed around Peralla-Kg. Ipoh, where it indicates top-WNW shear and minor top-NE shears.

Evidence of fault contact between the Kemahang granite and the Taku Schist is observed outside of unit area, in western domain of Kemahang granite near Sebarang Bina Quarry. The exposure shows a NNW-SSE trending fault that is responsible for separation between the granodiorite of Kemahang granite with quartz-mica hornfels of the Taku Schist (Figure 3.28b). Kinematic analysis of this fault plane suggests dextral normal oblique movement toward ESE direction, suggesting that the Taku Schist were down-faulted in relationship to Kemahang Granite. Comparable SE directed kinematic movements are observed in surrounding faults where they show secondary chloritization as well as quartz-mica hornfels in the footwall.

### 3.4.2 Petrographic Study

#### 3.4.2.1 Microstructural Observation

- Garnet-mica-schist; Lintasan Unggul Sdn. Bhd, Sokor Taku Forest Reserve.

Lination:  $240^\circ \rightarrow 50^\circ$ .

Major: Qtz, Mcv, Bt. Minor: Grt, Trm.

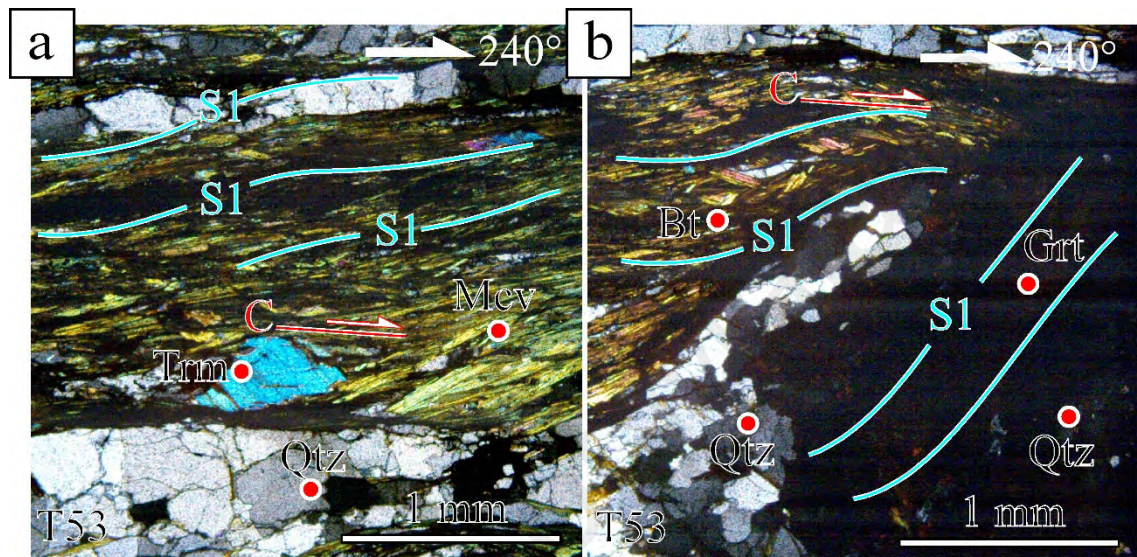


**Figure 3.28: Photomicrograph of garnet-mica schist in the NW flank in Sokor Taku Forest Reserve.**

The sample was obtained from the NW part of Sokor Taku Forest Reserve, where it shows a well-developed compositional layering between ribbon quartz alternating with biotite and muscovite that forms a spaced disjunctive foliation fabric. The quartz are fine- to medium- grained and it forms inequigranular aggregates with interlobated boundaries and wavy extinction. The main recrystallization mechanism in quartz is subgrain rotation (SGR), although the quartz aggregates display weak oblique shape preferred orientation (SSPO). Some of the aggregates show bulged and serrated outline that indicates minor grain boundary bulging recrystallization (BLG). The sheet silicates are dominantly biotite forming S/C shear band/s that indicate dextral sense of shear. Garnet (almandine) minerals are enveloped by the matrix and form  $\sigma$ - porphyroblast. They contain quartz inclusions forming spiral layers that continues with the foliation

fabric of the surrounding matrix. The foliation is cut by incipient normal faults in alternation to C'- shear bands. Both the porphyroblasts and C'-shear bands suggest dextral kinematic towards SW direction.

- Quartz-mica schist: Kg. Ipoh. Lineation:  $130^\circ \rightarrow 18^\circ$ .

Major: Qtz, Bt, Mcv. Minor: Trm

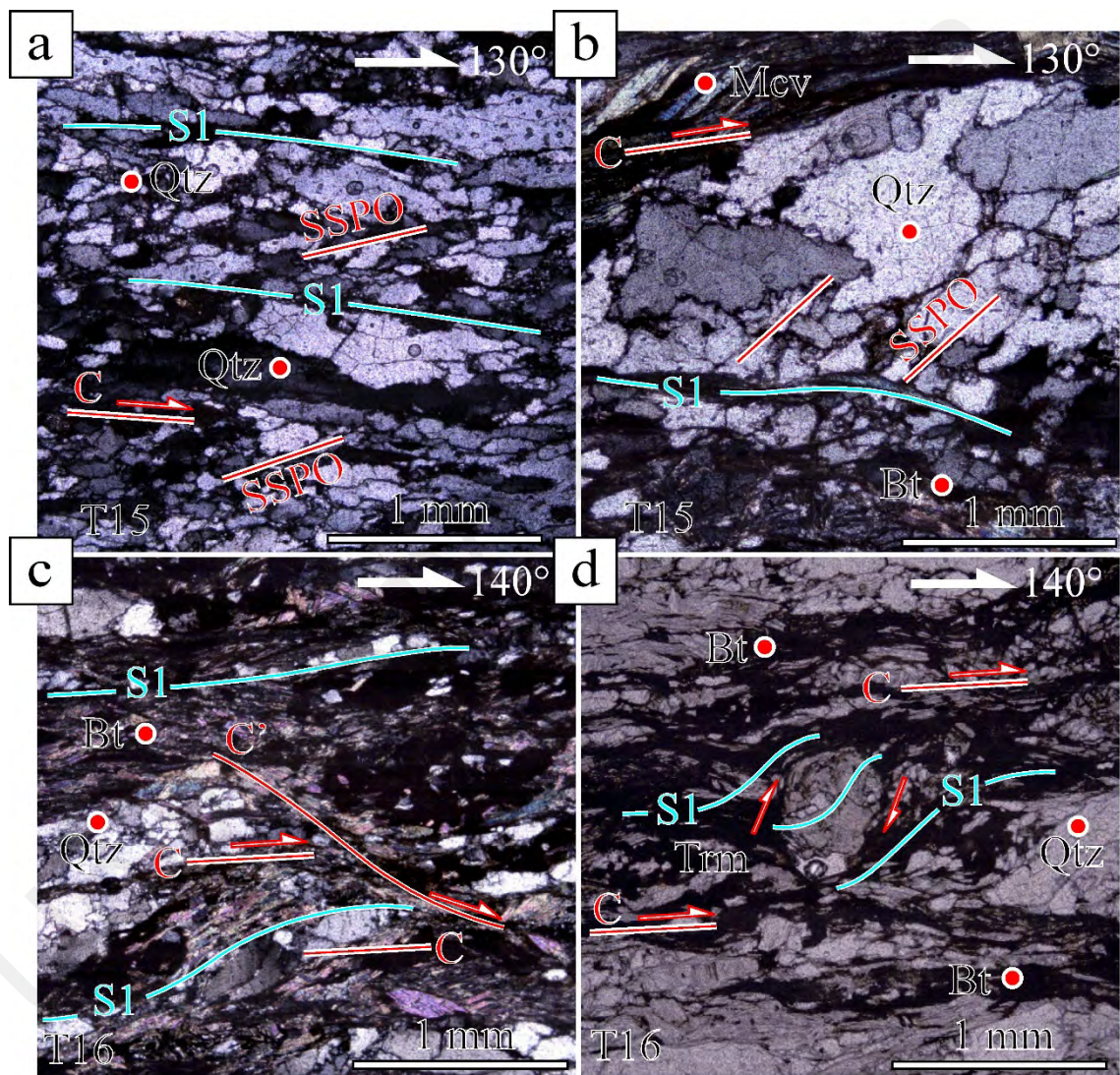


**Figure 3.29: Photomicrograph of quartz-mica schist in the NE flank at Kg. Ipoh.**

The samples are comprised of quartz -rich schist and quartz- mica schist obtained near to the Kemahang granite. The quartz –rich schist are composed of elongated quartz aggregates interlayered with minor biotite and muscovite defining a continuous disjunctive foliation. The quartz are fine- to coarse- grained with interlobated outline boundaries and possess patchy- types of extinction. While the coarse-grained aggregates are elongated along S1 foliation, the finer grains aggregates define shapes preferred orientation (SSPO) align oblique to S1 foliation. These oblique oriented aggregates indicate an interrelation of recrystallization mechanism between grain boundary bulging (BLG) and subgrain rotation (SGR), where it indicates dextral shear towards SE direction.

The quartz–mica schist shows compositional layering with alternating layers rich in quartz aggregates and biotite defining space disjunctive schistosity. The quartz aggregates are coarse-grained with equigranular shapes that possess both wavy-type and patchy-type of extinction. The outline boundaries are serrated and bulged and shows presences of fine neocryst indicates recrystallization mechanism via grain boundary bulging (BLG) and grain boundary rotation (SGR). There are also tourmaline that contains quartz inclusions, which forms  $\sigma$ - porphyroblasts. Analysis of  $\sigma$ - porphyroblasts, as well as S/C and S/C' shear bands suggest dextral sense of shears with top towards SE direction.

- Quartz-mica schist; Kg. Ipoh. Lineation:  $235^\circ \rightarrow 10^\circ$ .

Major: Qtz, Mcv. Minor: Kfs, Grt, Bt, Chl, Trm. Trace: Zr.

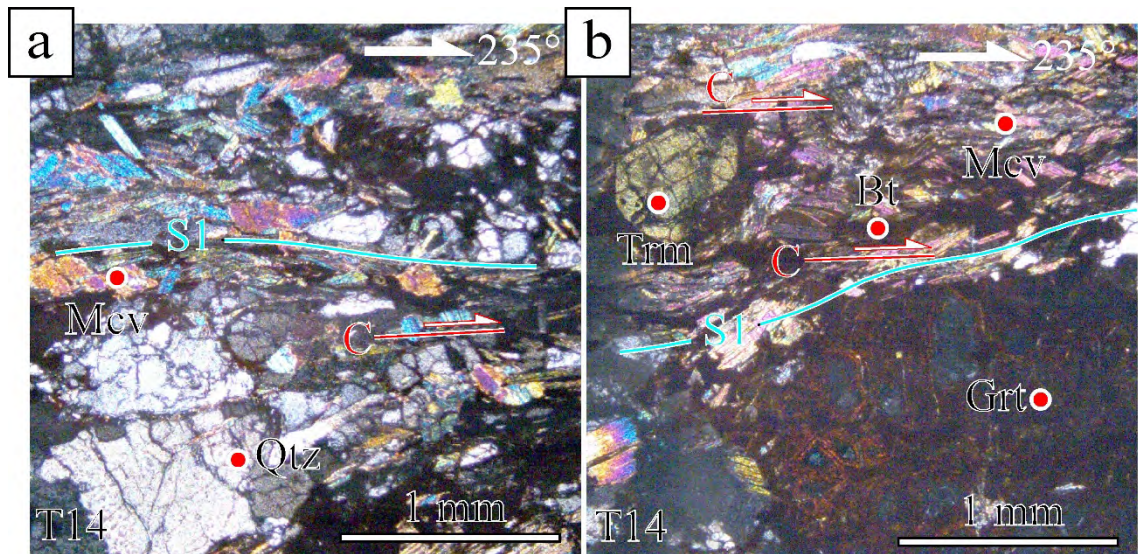


**Figure 3.30: Photomicrograph of quartz-mica schist in the NNE flank at Kg. Ipoh.**

The sample is composed of quartz ribbon interlayered with thick muscovite and biotite forming compositional foliation fabric or spaced disjunctive schistosity. The fabric are crosscut by fault which separate mica-rich in the upper left and quartz-rich in the lower right part of sample, aligned in parallel to S1. The mica-rich fabric envelops many large garnet (almandine) forming  $\sigma$ - type of porphyroblasts. The garnet contains spiral inclusions of small quartz grains parallel with foliation fabric on surrounding matrix. The sample also contains large K-feldspar porphyroclast that are affected by sericitization. Tourmaline develops either in surrounding matrix or on top of garnet, which does not shows preferred alignment along foliation. The quartz is equigranular with serrated boundary and wavy extinction. It also shows weak oblique preferred shapes orientation, which indicates recrystallization mechanism by subgrain rotation (SGR) and grain boundary bulging (BLG). The kinematic analysis on both garnet and K-feldspar porphyroblast/clast as well as S/C shear bands indicates dextral top towards SW shear.

#### **3.4.2.2 Metamorphic Parageneses**

The prograde metamorphism (M1) is responsible for development of spaced disjunctive schistosity in quartz-mica schist forming compositional bands or continuous disjunctive schistosity in quartz-rich samples. These samples display an assemblage of biotite-muscovite-garnet (almandine) minerals suggesting prograde metamorphism up to amphibolite-facies. The sheet silicates comprises of biotite and muscovite that forms S/C shears bands enveloping many garnet porphyroblast suggesting D1 deformation is associated with prograde metamorphism (M1). This deformation is also associated with sigmoidal quartz inclusions contained within garnet minerals, which shows continuation with foliation fabric of the surrounding matrix. Despite close proximity to the Kemahang granite, the samples do not show features related to contact metamorphism.

## CHAPTER 4: THE SURROUNDING UNITS

### 4.1 Introduction

Rocks of the Gua Musang/Aring Formation overlain by both the Taku Schist and Stong Complex metamorphic bodies. The Kemahang granite intrudes the Taku Schist as well as the Tiang Schist. The Kemahang granite is intruded by the Stong Complex. Detail geological observation has been done throughout these four units with emphasis on kinematic analysis (Figure 4.1, Figure 4.2 and Figure 4.3).

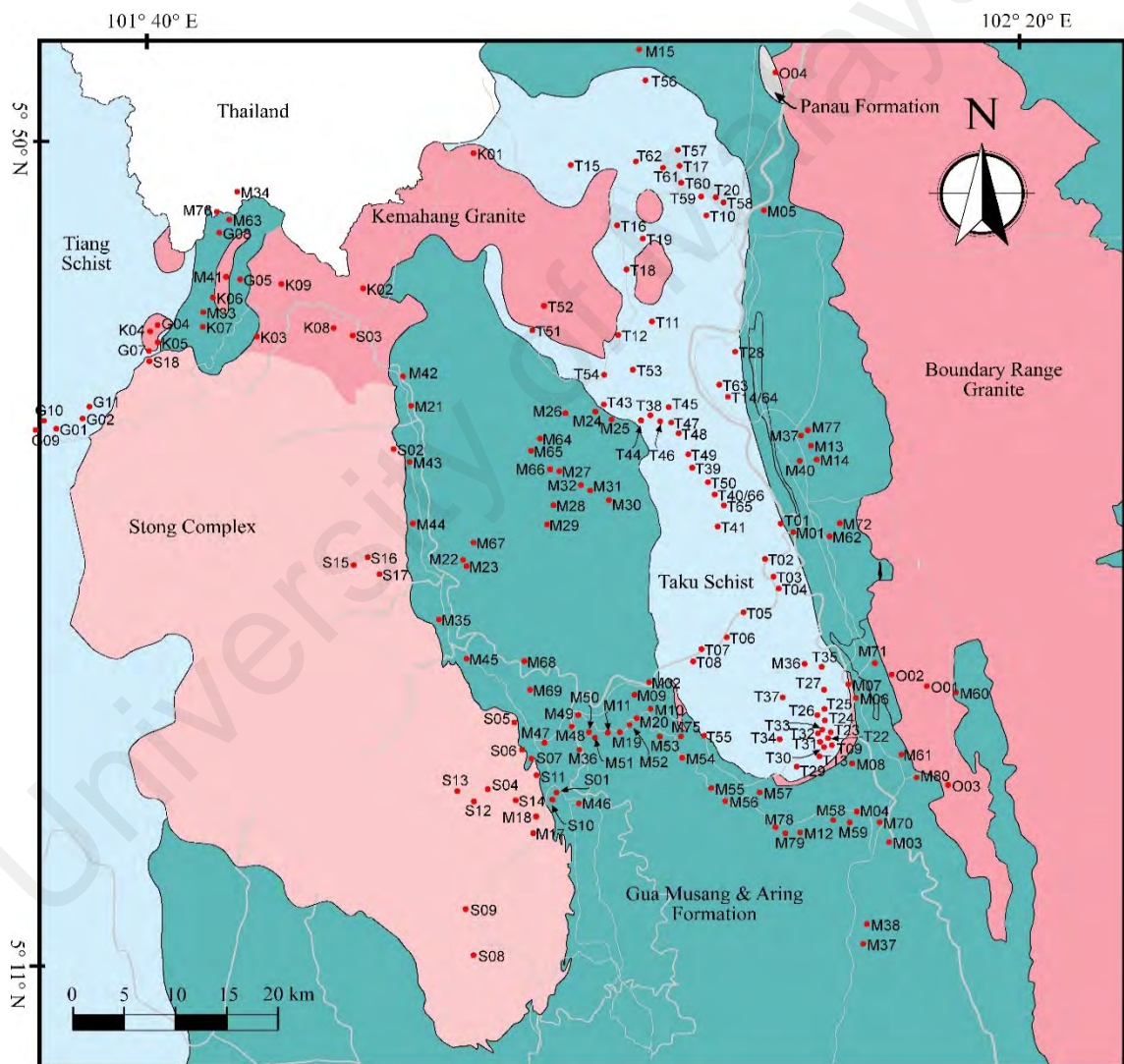


**Figure 4.1:** Geological map of study area showing the overall stations. The Gua Musang Formation includes the easterly, westerly and southerly flanks; the Kemahang Granite includes the westerly and easterly domain; and the Stong Complex consists of Berangkat, Kenerong and Noring sub-units.

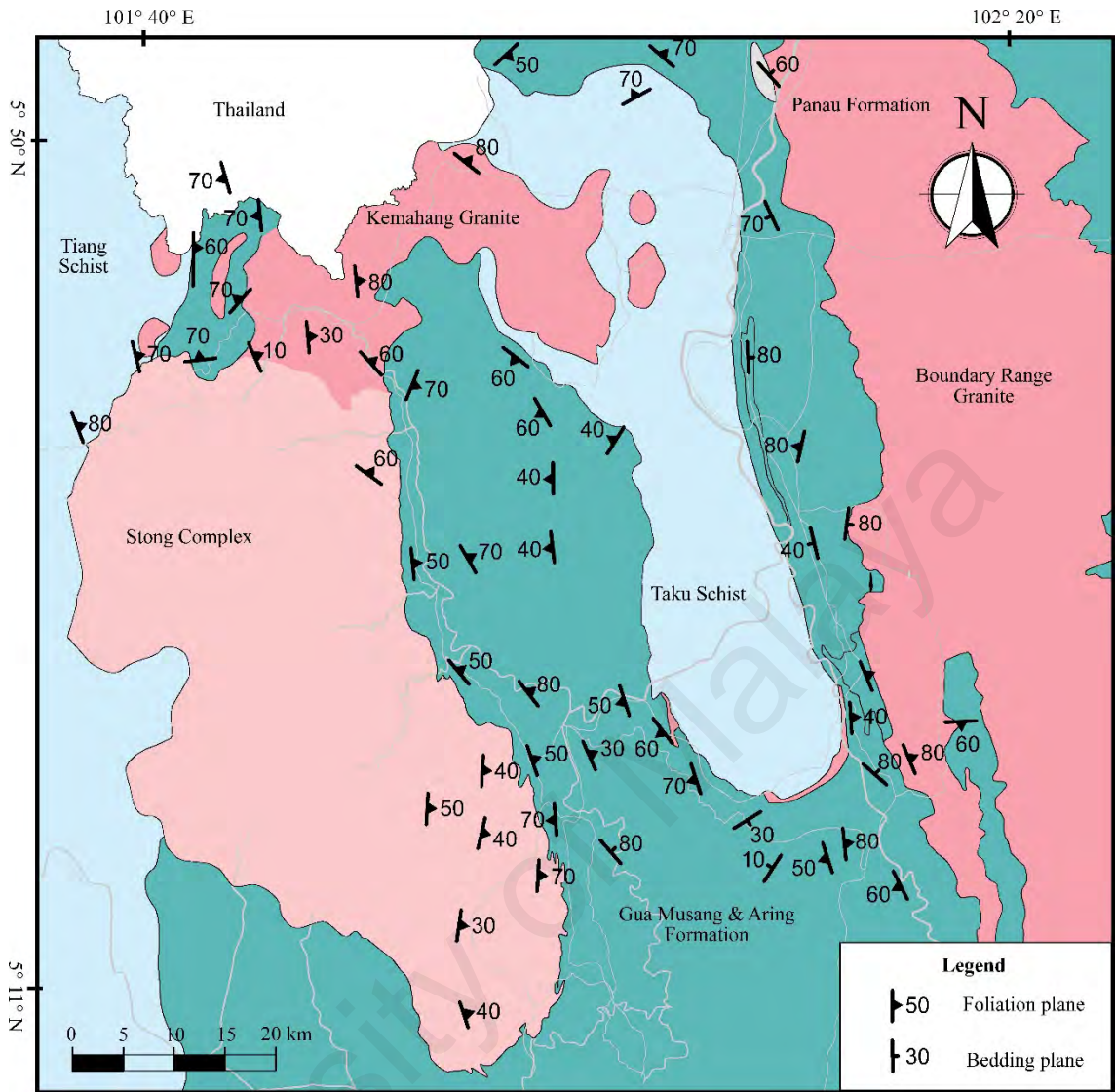


**Figure 4.2: The foliation and bedding planes map of the surrounding units**

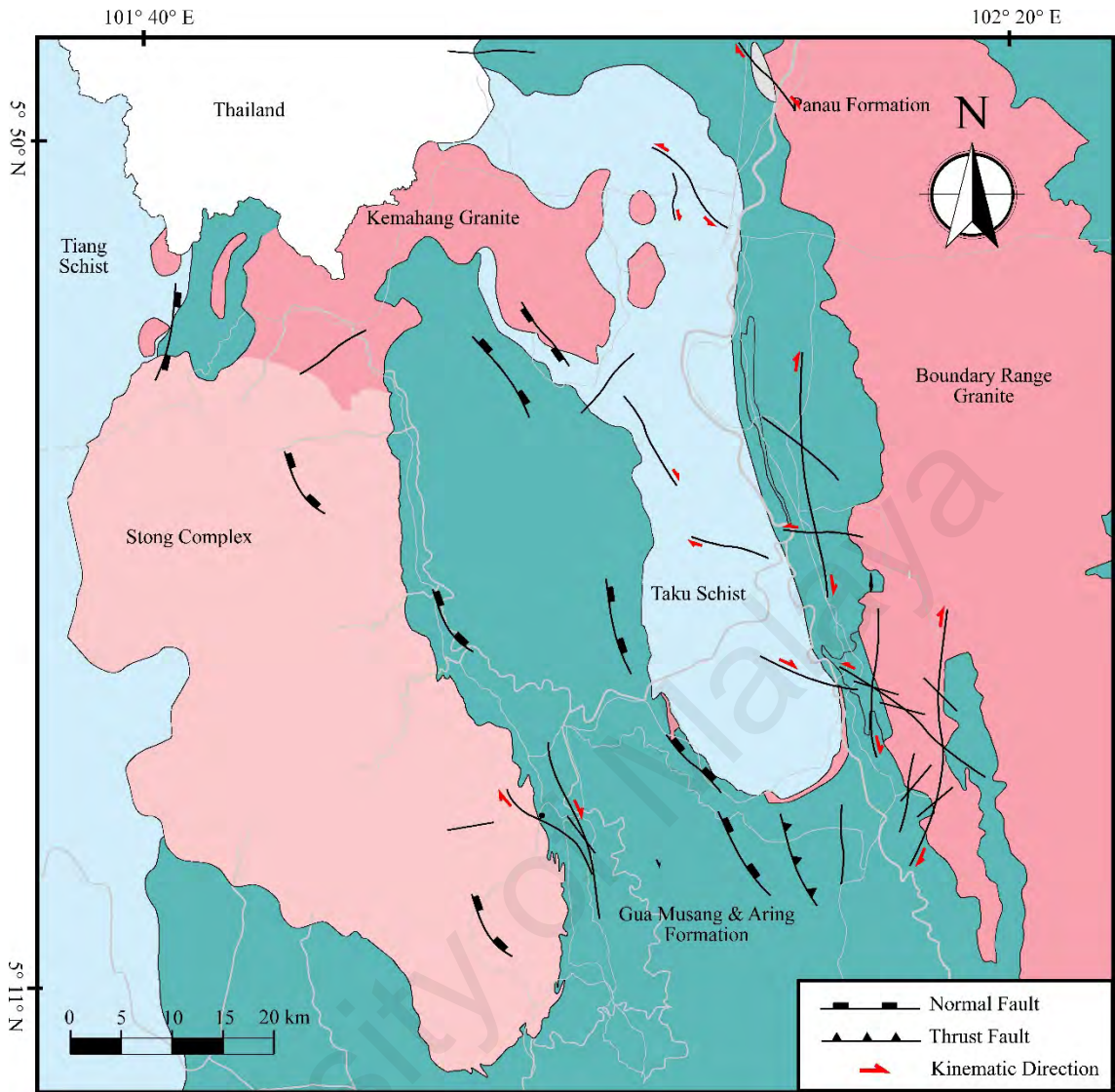


**Figure 4.3: The fault map of the Taku Schist and the surrounding units**

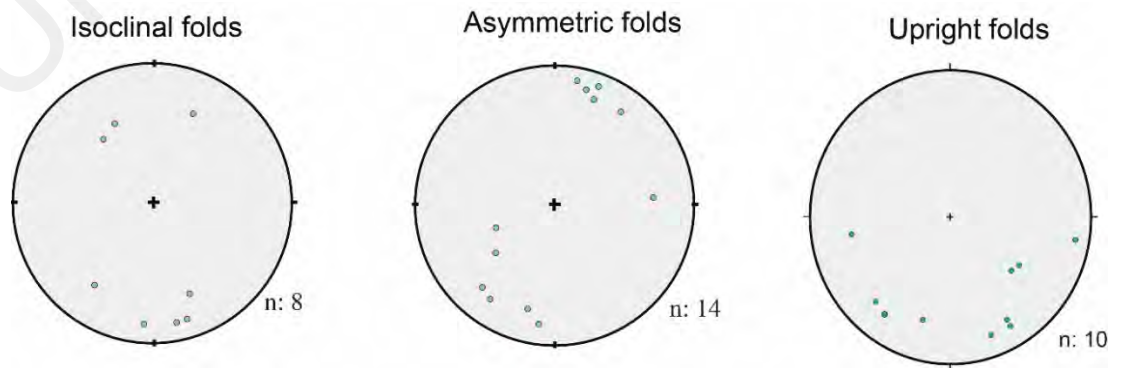


**Figure 4.4: Plots of fold axis observed in the surrounding units**

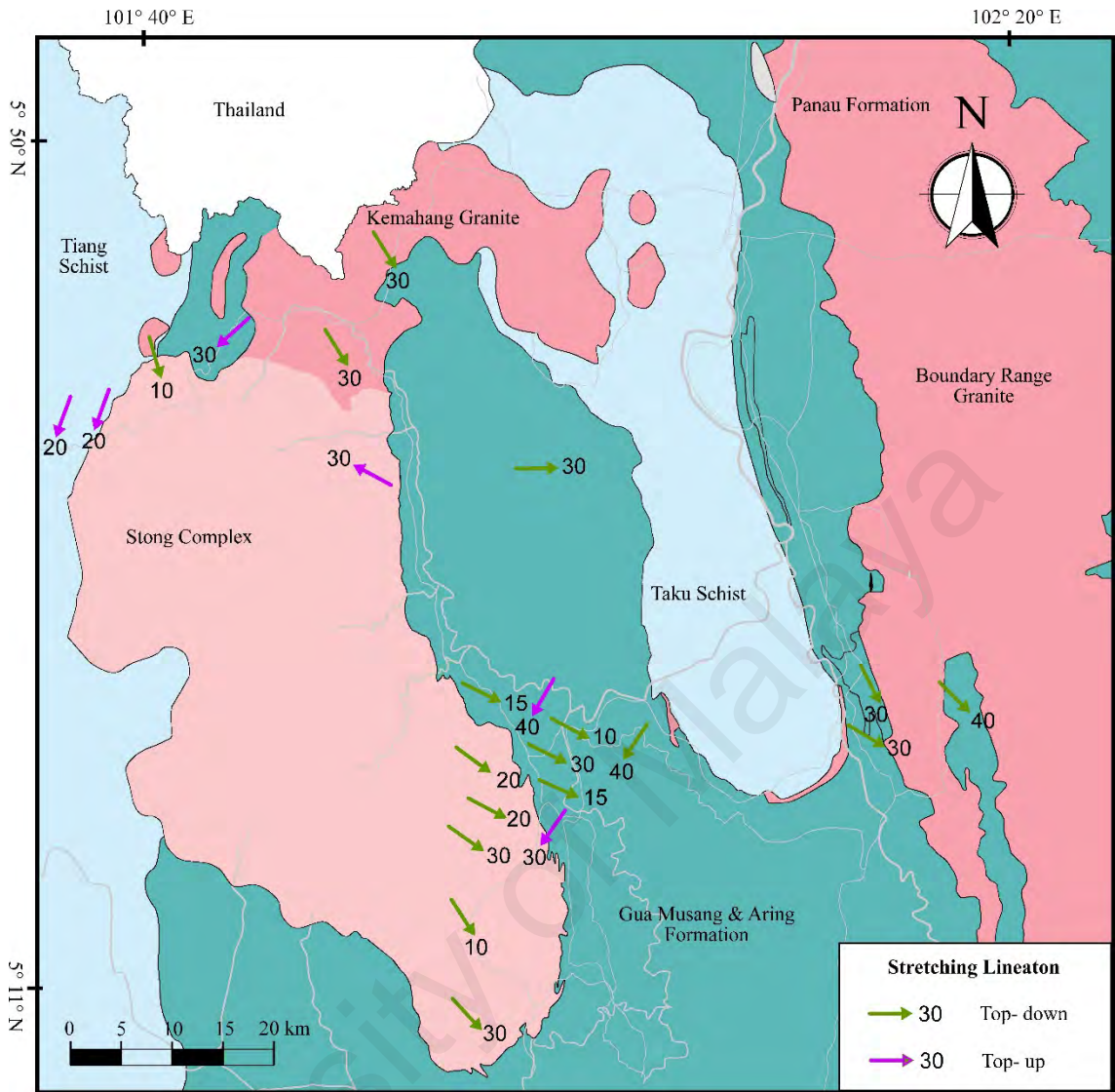


**Figure 4.5: Kinematic transport map of the surrounding unit. Green arrows indicate top- down toward direction of stretching lineation whereas purple arrows indicate top- up against direction of stretching lineation.**

## **4.2 The Gua Musang/Aring Formation**

### **4.2.1 Field Observation**

#### **4.2.1.1 Eastern Flank of the Taku Schist**

The orientation of foliation and bedding planes at the eastern flank of the Taku Schist strikes NNW-SSE and dipping towards E direction (Figure 4.2). The foliation strikes sub-parallel to the boundary between the units and comparable to orientation observed in the Taku Schist. The sedimentary rocks comprise mainly of light greyish, carbonaceous to calcareous mudstones as well as tuffaceous sandstones and minor limestones, acid to intermediate volcanics such as rhyolite, dacites and andesites (Figure 4.1 and Figure 4.6). The rocks display very weak, in part absence in penetrative cleavage development, which differ from the well-developed schist fabric of the Taku Schist. Extensive occurrences of NNW-SSE trending faults and shear zones along Kuala Krai; Gua Musang Road signifies the Lebir Fault Zone (Figure 4.3). This fault zone observed to affects the nearby exposures and represents the contact with the Boundary Range granite of Eastern belt.

In the west proximate of Lebir Fault Zone along the Kuala Krai-Gua Musang road, the sedimentary rocks are primarily tuffaceous mudstone containing whitish K-feldspar phenocryst and devoid of penetrative cleavage (Figure 4.6 a, b). Numerous NNW-SSE and minor E-W trending faults occur as parallel-fault arrays associated with large faults that folded the layers in proximity (Figure 4.7, Figure 4.8). This result in upright, open asymmetrical folds with easterly- directed vergence. The crosscutting faults/shear zones is also related to localize increase of penetrative cleavage development up to fine phyllites within the rocks in parts affected by strong chloritisation (Figure 4.9b). Kinematic inferences from Riedel shears indicates dominant dextral normal to ESE direction ( $110^\circ \rightarrow 25^\circ$ ) and minor sinistral thrust oblique towards NW direction ( $330^\circ \rightarrow 25^\circ$  in Figure 4.3). Northward to Kuala Krai, occurrences of NW-SE trending fault

planes/ zones display anastomosing structures that cut through tuffaceous sandstone and formed cataclasites. Foliation fishes and K-feldspar prophyroclasts formed related to crosscutting C'- shear planes. Kinematic analysis indicates a sinistral shear top towards west direction ( $260^\circ \rightarrow 14^\circ$ ).

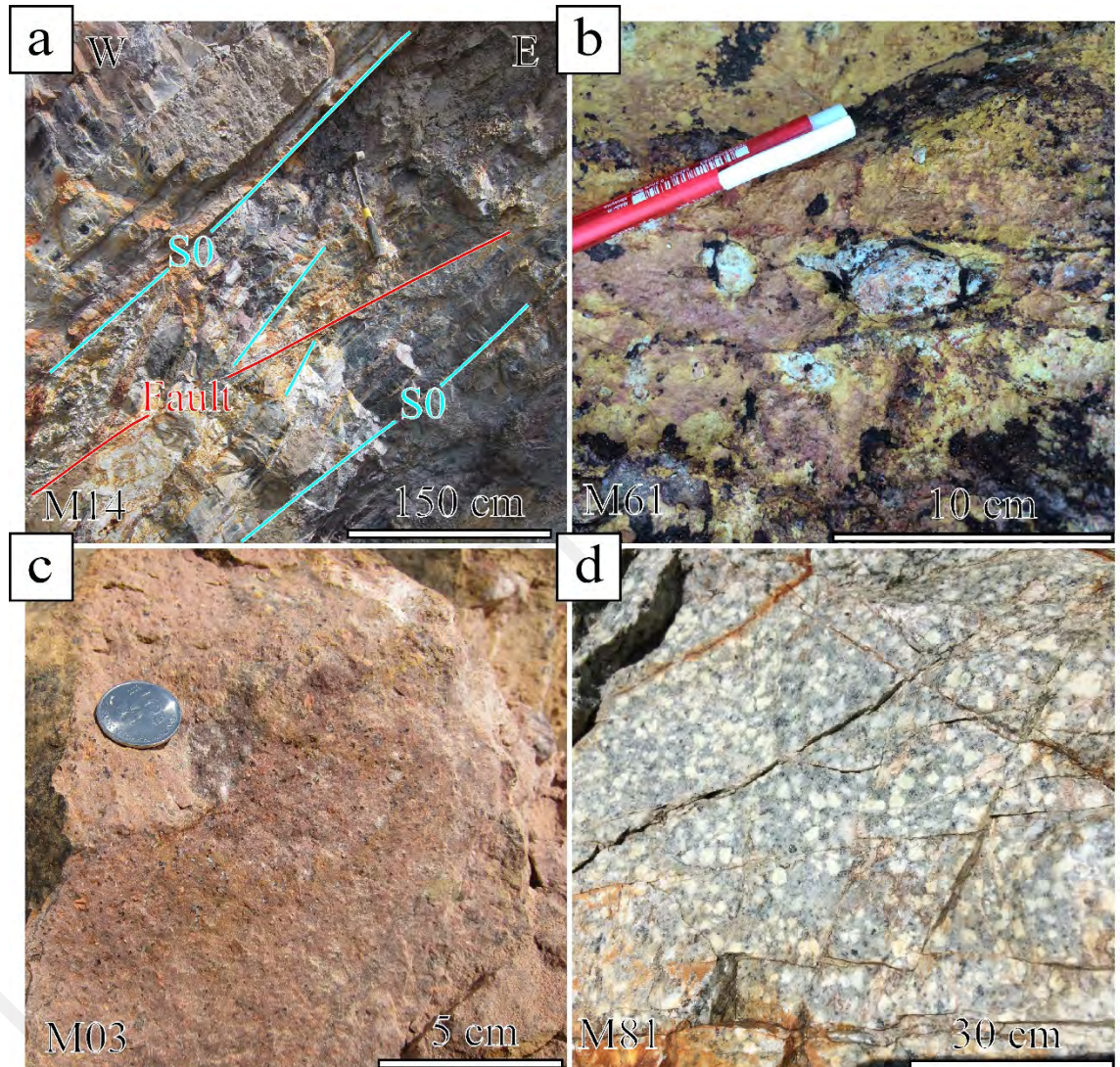


**Figure 4.6: Examples of lithologies observed in the eastern flank, Gua Musang Formation; (a) Carbonaceous/ calcareous mudstones affected by faulting, (b) tuffaceous rhyolite, (c) rhyolite and (d) dacite/andesite.**

Near Kg. Manik Urai Baru, a dark-reddish shale exposure with bedding plane (S0) striking N-S and dipping at low angle towards the E (M60, Figure 4.1; Figure 4.2) is in contact with granite of the Boundary Range along a five meter thick sub-vertical shear zone trending E-W. The shear zone contains brecciated granite clasts wrapped into well-

developed S/C fabrics and prophyroclasts (Figure 4.9a). The schistosed fabric contains pervasive mineral lineations plunging towards ESE at low angles. Kinematic analysis suggests top-ESE or dextral strike-slip toward ESE ( $110^\circ \rightarrow 30^\circ$  in Figure 4.5). The reddish shales, granite and shear zones, are cut for about 10 m by a large discrete fault and is associated with strong smell of sulphur. The N-S striking fault dips towards E at moderate angle. , Analysis using Riedel shears indicate a thrust sinistral movement toward WNW- direction ( $308^\circ \rightarrow 40^\circ$ , Figure 4.3).

#### *Sedimentary rock exposures in Kuala Krai*

Sedimentary rocks exposed by housing projects in Kuala Krai are commonly affected by deep tropical weathering obliterating their structural features. They are primarily mudstone-siltstone containing varying carbonaceous to tuffaceous components, the latter observed by the presence of angular feldspar fragments within a reddish matrix (Figure 4.6 a, b). Preserved sedimentary features such as mud-drapes indicates incipient degrees of metamorphism. Incipient metamorphic layering (S1) observed in parallel to the bedding planes (S0). The S1 foliation has average strike of NNW-SSE with steep dips towards both ENE and SSW directions (Figure 4.2 and Figure 4.7). The exposures contain centimeters scale isoclinal folds of bedding plane (S0), where the axial plane (F1) strike parallel to S1 foliations. In addition, three other types of fold recognized includes Z- shaped asymmetrical fold (F2), upright symmetrical fold (F3) and recumbent symmetrical folds (F4) (Figure 4.4).

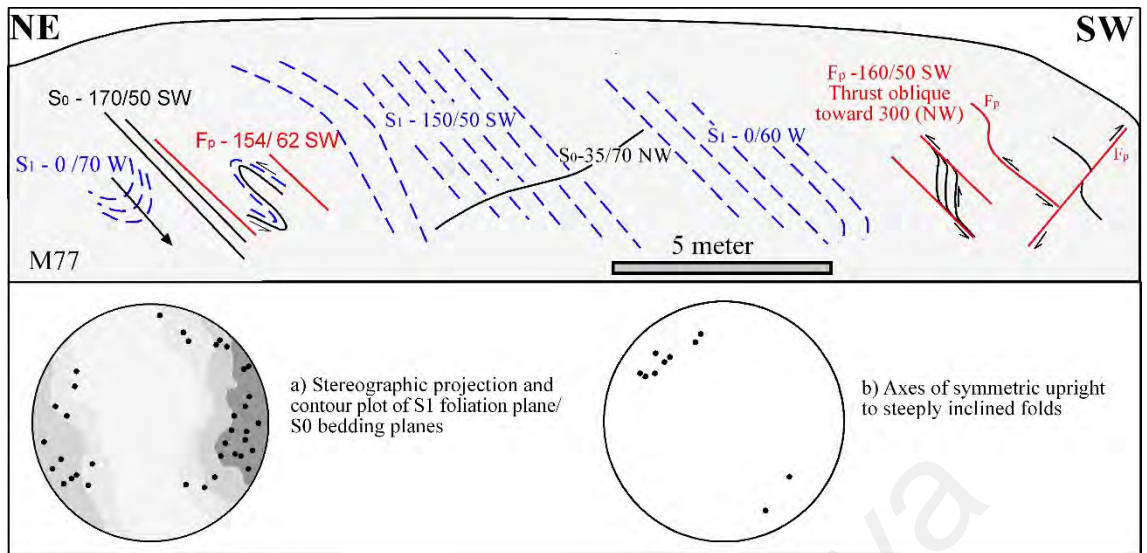


**Figure 4.7:** Sketch of a sedimentary rock exposure in Kuala Krai, showing the relation between bedding, foliation and faulting with stereographic plot of foliation/bedding planes and axes of symmetrical upright folds.

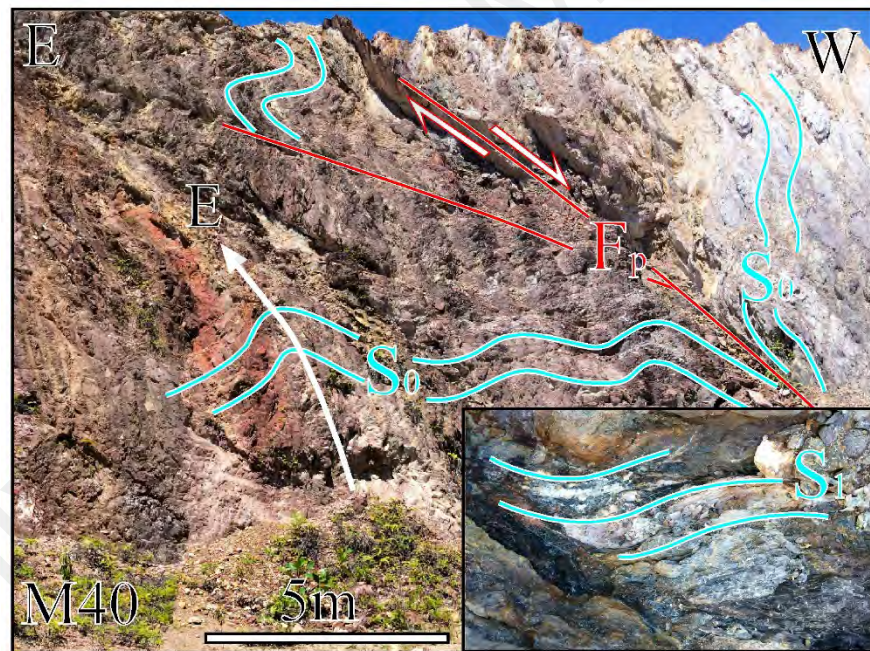


**Figure 4.8:** Carbonaceous shale exposure in Kuala Krai. The folded strata are cut by normal faults. The inset shows localized cleavage intensification within a fault zone.

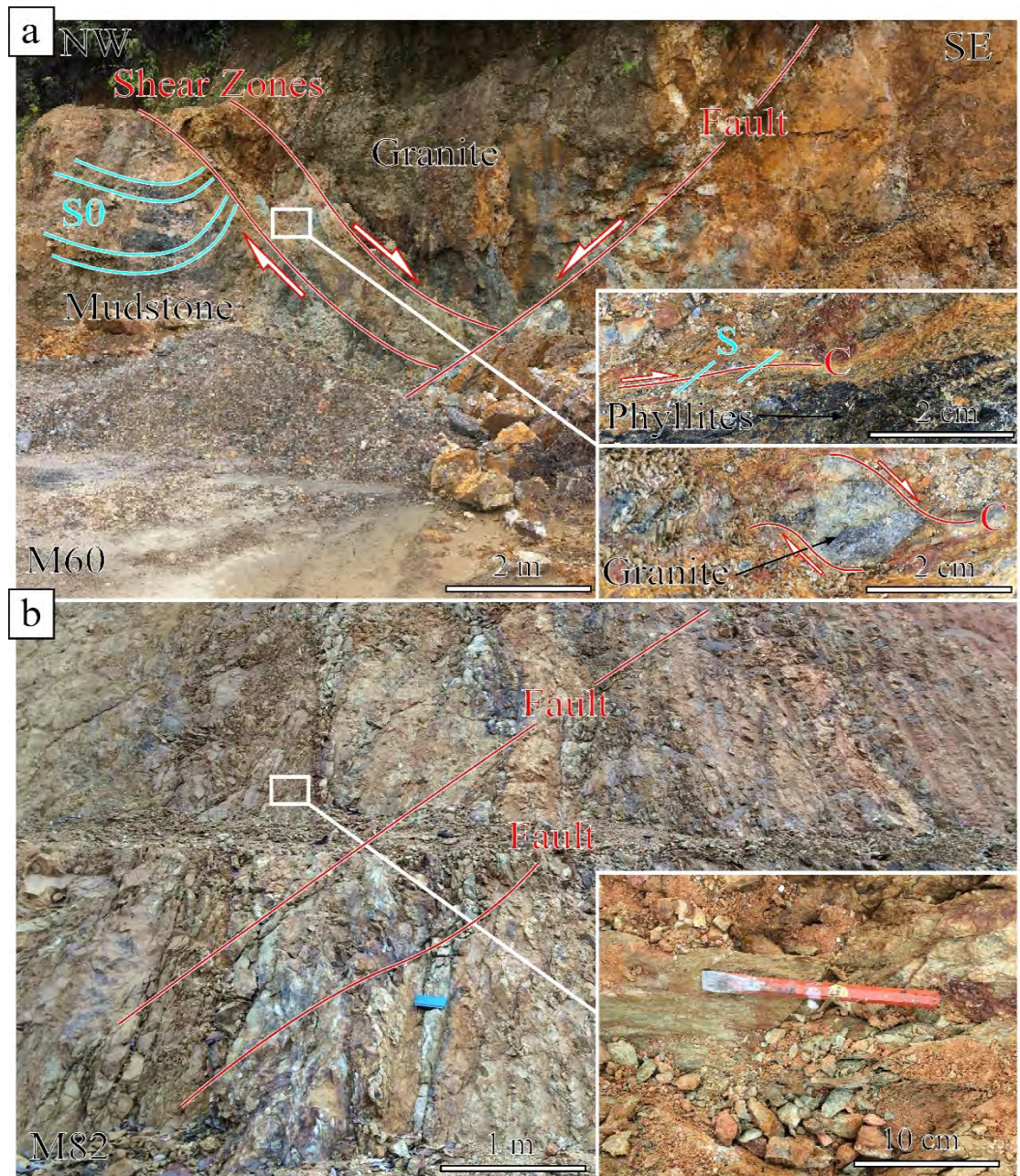


**Figure 4.9: Exposures within the Lebir Fault Zone. (a) Fault contact between shales of Gua Musang Formation and Boundary Range Granite, further cut by a later normal fault, (b) brittle-ductile transition faulting showing increase in phyllitic cleavage within tuffaceous mudstone.**

The Z-shape asymmetrical folds (F2) develop in response to crosscutting C'-shear plane striking N-S. The axial planes (F2) are steeply inclined striking WNW-ESE direction with fold axes plunge steeply towards WNW direction (Figure 4.4b). Commonly, the NW dipping flanks are steeper than opposing -NE dipping flanks suggesting westerly vergence. The third type of fold (F3) is widely observed as upright

symmetrical open folds. The axial plane cleavage forms a newly developed foliation (S2), striking NNE-SSW and dip almost vertically, mostly toward NNW, where the hinges are oriented along NW-SE (Figure 4.4, Figure 4.8). This S2 foliation cut both S1 foliation and bedding plane (S0), while retaining an older, re-folded asymmetrical fold showing Z-shape asymmetries (F2). Some of these folds are quite large, ranging up to 20 metres in amplitude. The last variant of fold (F4) commonly observed within N/S facing outcrops is recumbent, symmetrical to asymmetrical structures ranging about 5 metres in amplitude. The axial planes are striking NW-SE and dip towards NE at low-angle. These folds similarly plunges at low angles towards both –SSE or –NW (Figure 4.4).

The folds are crosscut by both normal and strike-slip faults, particularly near margin of Taku Schist. Field observation indicate the dominant orientation strikes NS to NW-SE direction, where the analyses on striations and Riedel planes suggest kinematic movement by dextral normal oblique toward –SE (Figure 4.3, Figure 4.8). Minor EW striking fault with similar kinematic movement were also observed. The fault zone also includes other minor kinematic reading such as sinistral thrust oblique toward NW direction and dextral kinematic toward SE. The fault also results in intensification of cleavage development to form phyllitic cleavages, where the S1 foliation near to fault planes are folded into S- shapes structures (Figure 4.8). The faults cut through the upright, symmetrical folds at high angle whereas the recumbent symmetrical folds are cut by lower dipping faults, results in asymmetric shapes vergence following the direction of fault movement (Figure 4.8).

The faulting continues toward the lower reaches of Sg. Galas along the Taku Schist border affecting the rhyolitic rocks exposures. Characterized by light-reddish color, the rhyolite contains non-deformed K-feldspar and quartz grains (Figure 4.6c). Analysis of

the fault indicates sinistral normal oblique toward northwest ( $340^\circ$ ) direction. Similar rhyolitic rocks near Temangan were also faulted, fractured and chloritized. The dacite near Tanah Merah is composed primarily of quartz in addition to epidote and chlorite (Figure 4.6d) and is similarly cut by NNW-SSE fault with oblique thrust towards NE (Figure 4.3).

#### **4.2.1.2 Western Flank of the Taku Schist**

In contact with the Stong Complex and Kemahang granite (Figure 4.1), the sedimentary rocks comprise mainly of carbonaceous mudstone and siltstone and minor tuffs. The development of penetrative cleavage varies from fine phyllitic cleavage to shale-slaty cleavage with general foliation orientation along NNW-SSE strikes accompanied with SW and NE plunging mineral lineation (Figure 4.2 and Figure 4.5).

Exposures along EW transect from Stong Complex to Taku Schist (Dabong – Kg. Pak Abu road in Figure 4.1) comprise dominantly of carbonaceous-tuffaceous mudstones and localized limestones (marble, oolites) (Figure 4.10 a, c, d and Figure 4.11). Most rocks display phyllitic fabric crosscut by incipient C- cleavage resulting in two sets of penetrative cleavage. The S1 foliations strike NNW-SSE and dip steeply towards both ENE-WSW directions (Figure 4.2). Occasionally, occurrence of low-angle, symmetrical open folds with axis striking WNW-ESE and plunge sub-parallel to the mineral lineations. The mineral lineations are observed in a few exposures and analysis indicates low angle shears towards SE direction ( $125^\circ \rightarrow 15^\circ$  in Figure 4.5). Localize occurrence of oolitic limestone observed to develop shistosity containing oolite enclosed by chlorite and muscovite, which indicates top -NE directed kinematics ( $30^\circ \rightarrow 45^\circ$  in Figure 4.5 and Figure 4.11).

Rocks along the Jeli- Gua Musang expressway are composed of carbonaceous/calcareous mudstone, sandstone (Figure 4.10b), marble and tuffs. The fabric changes

from slate to fine phyllite in direction toward the Stong Complex. On average, the foliation (S1) strikes NW-SE with a high angle dips towards both NE and SW directions (Figure 4.2). There are three types of folds; cm-meter scale symmetrical isoclinal folds, meter scale asymmetrical upright folds and large symmetrical open folds (Figure 4.4). The symmetrical isoclinal fold contains primary bedding plane (S0), where the axial plane oriented parallel to S1 foliation plane (Figure 4.12a). The latter steeply inclined, asymmetrical folds folded the S1 foliation and have consistent westerly vergence (Figure 4.12b). The symmetrical recumbent open fold in particular observed in close proximity with the Stong Complex (Figure 4.12c).

Several localized NW-SE striking shear zones are observed near the margin of Kenerong Leucogranite to cut the main S1 foliations (Figure 4.3). It results in amplification of penetrative cleavage that develop into quartz-mica schist from an original phyllitic rocks observed along Kuala Balah – Dabong road. Localize occurrence of quartz-feldspar schist displaying whitish colored fabrics. The well-developed stretching lineation of these fault rocks indicates strong top-SE shears. One of the exposures display narrow (~ 100 cm) shear zones bounded by fault planes, with both faults indicates a top- SE shear (Figure 4.5 and Figure 4.13).

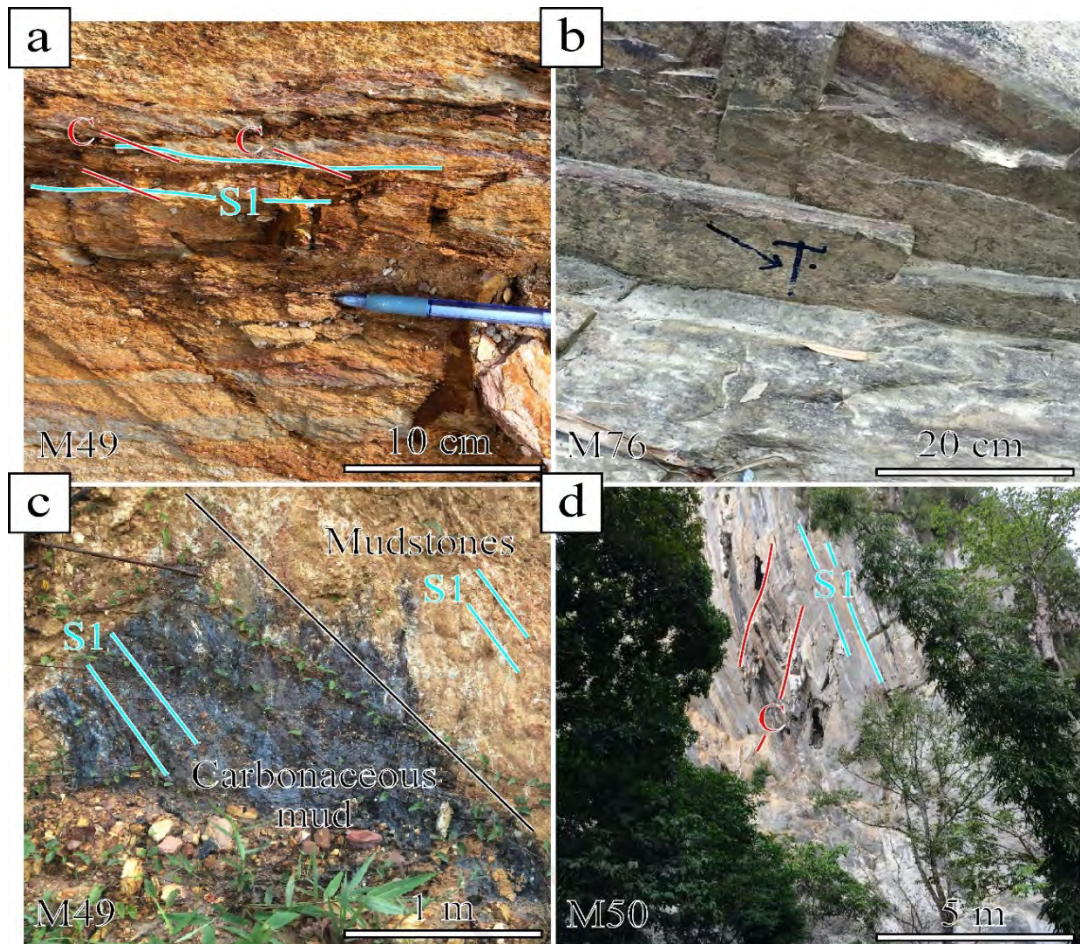


**Figure 4.10:** Example of sedimentary rock exposures in the western flank, Gua Musang Formation; (a) phyllitic mudstones, (b) quartz hornfels, (c) carbonaceous mudstones and (d) limestone

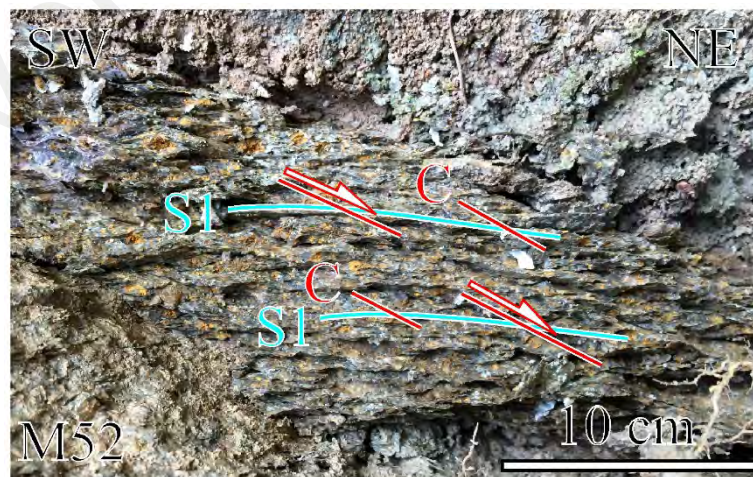


**Figure 4.11:** Schistosed oolitic limestone fabric showing well-developed S/C shear bands, indicating top-NE shears.

Shear zones are not limited to near the margin of Stong Complex but also present far away such as in CNMM gold mine, western Sokor Taku Forest Reserve. The greyish-purple colored sheared quartz-mica schist strikes along NS- direction and steeply dipping towards the E (M65, Figure 4.1; Figure 4.2). The stretching lineations plunge towards the E at low angles. The schist also contains large quartz prophyroclast within matrix with well-developed S/C fabrics indicates probable tuffaceous origin. In addition, large foliation fishes observed controlled by crosscutting NE-SW striking C-shear planes. Kinematic analysis suggests top -E shear ( $90^\circ \rightarrow 30^\circ$ , Figure 4.5). The surrounding tuffaceous siltstone and mudstone display weakly penetrative S1 foliations sub-parallel to bedding plane (S0), with NW-SE strike and easterly vergence (Figure 4.2). The orientation is comparable to the schistosed oolitic limestone outside the mining area. In all cases, the rocks display two apparent sets of cleavage, the latter being the C- plane oriented at oblique angles. Steeply dipping fault planes trending NNE-SSW cut the siltstone exposure, showing normal dextral oblique movement toward ENE- direction ( $70^\circ \rightarrow 30^\circ$ , Figure 4.3).

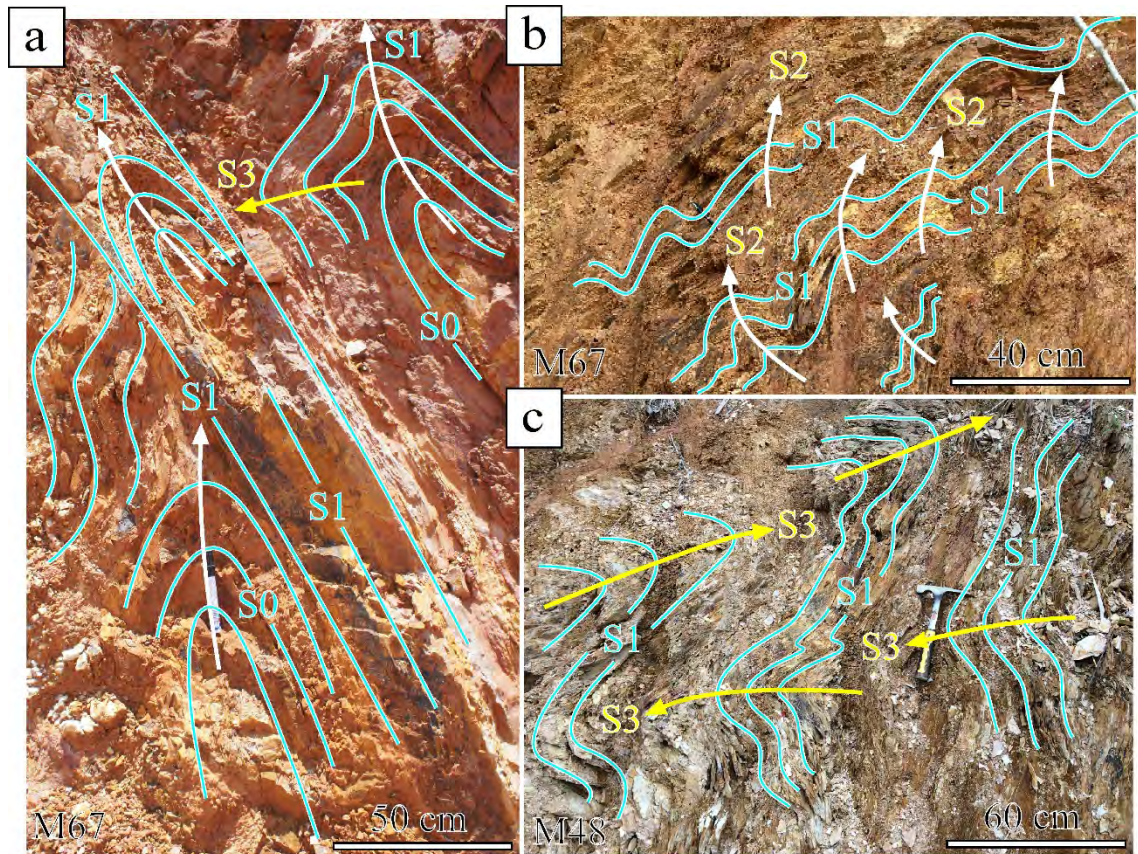


**Figure 4.12: Examples of folds in the western flank, Gua Musang Formation; (a) a tight to isoclinal fold of bedding planes, (b) an asymmetrical, steeply inclined fold, (c) symmetrical recumbent folds.**



**Figure 4.13: Quartz-feldspar schist bounded between fault planes in mudstone exposure near Dabong.**

The Gua Musang Formation in the NNW part of the study area is bounded on both sides by the Tiang Schist, Kemahang and Noring granite (Figure 4.1). The geological map shows that localized Kemahang granite exposure is surrounded by sedimentary rocks. In the field, the sedimentary rocks are mainly arenaceous, with some calcareous and argillaceous rocks. Penetrative foliations (S1) are weakly developed or absent. A localized occurrence of bedded hornfels along the NNW margin of the Noring granite was observed, containing an alternation between quartz and quartz-biotite hornfels (S0) striking NW-SE direction and dips towards NE-direction at intermediate angles (Figure 4.2 and Figure 4.14a). The siltstone beds show very gentle buckle folds. This bedded hornfels is not directly in contact with the Noring granite, but is separated by a zone of mylonitic Kemahang granite (Figure 4.14b), with pervasive foliations striking NNW-SSE and is associated with top-SE shear.

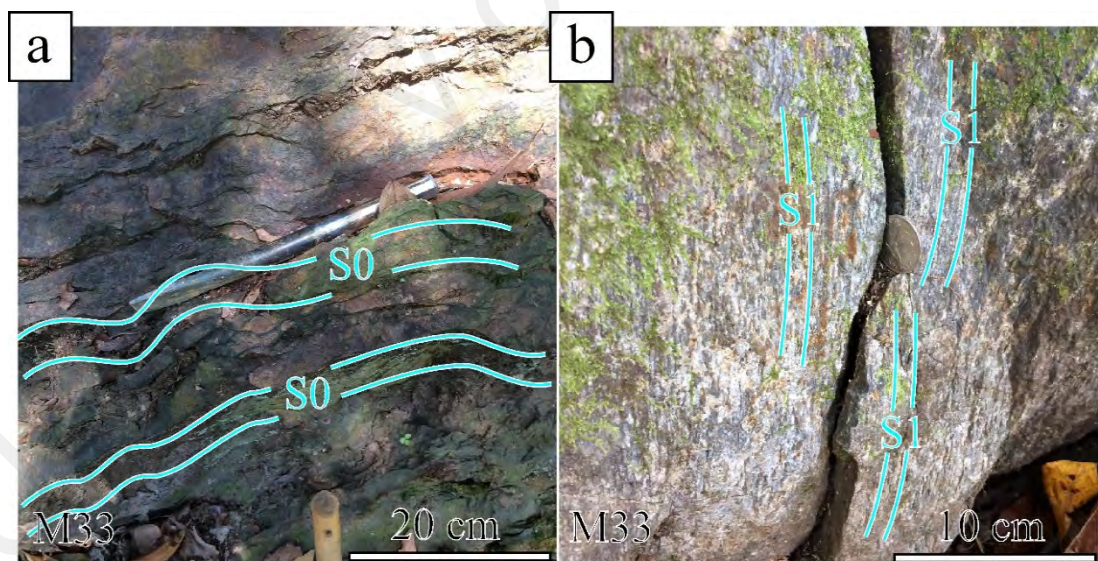


**Figure 4.14: Rock exposures in contact with the Noring Granite, near Batu Melintang. (a) Bedded hornfels metamorphosed from siltstone and sandstone and (b) strongly sheared mylonitic quartz-feldspar granodiorite.**

Areas near to Sg. Kalai gold mine situated close to Thailand border are comprised of quartz hornfels, marbles and phyllitic mudstones (e.g. Figure 4.10b). The penetrative metamorphic foliation (S1) is steeply dipping and strikes along NNE-SSW direction

(Figure 4.2). The foliation is weakly developed and contains relics of elongated mud drapes of dark mud laminae. A scarce occurrence of mineral lineation (L1) plunges towards the SE at low angles was also observed (Figure 4.5). The contact metamorphism and resulting quartz hornfels are likely to occur during the intrusion of the granitic pluton. Occurrences of purplish-red phyllitic mudstone were also observed further away which are unaffected by contact metamorphism. The mudstone is in close contact with quartz-mica schist of the Tiang Schist unit (Figure 4.1 and Figure 4.2)

#### **4.2.1.3 Southern Flank of the Taku Schist**

Field observation from Kg. Pak Abu up to Sg. Sam road (M56, Figure 4.1) indicates the presence of carbonaceous shale and absence of penetrative cleavage development (Figure 4.15b). The NE-SW striking bedding planes (S0) are dipping towards both NE and SW, although the dip towards SW is steeper than NE, showing an easterly vergence fold (Figure 4.2, Figure 5.1). This is also recorded in the exposure at Kg. Slow Pak Long where a sub-horizontal bedding (S0) is folded forming a large inclined S- shape structure. The fold is largely symmetrical, with open hinges closure about 100-meter amplitude verging towards east and plunges toward southwest (Figure 4.15a; Figure 4.4). The folding resulted in the formation of NE-SW trending axial plane cleavages crosscutting the bedding plane. In addition, occurrences of shale beds unaffected by metamorphism was similarly observed near Kuala Balah, at 2 kilometers from E margin of Kenerong leucogranite or migmatite exposure. The beddings (S0) are almost vertical and striking NW-SE, crosscut by faults, which result in the formation of kink folds plunging towards SE at low angles. An agglomerate exposure was also observed near the SW margin of the Taku Schist (Figure 4.10, TS.) It is highly fractured and affected by strong chloritization.

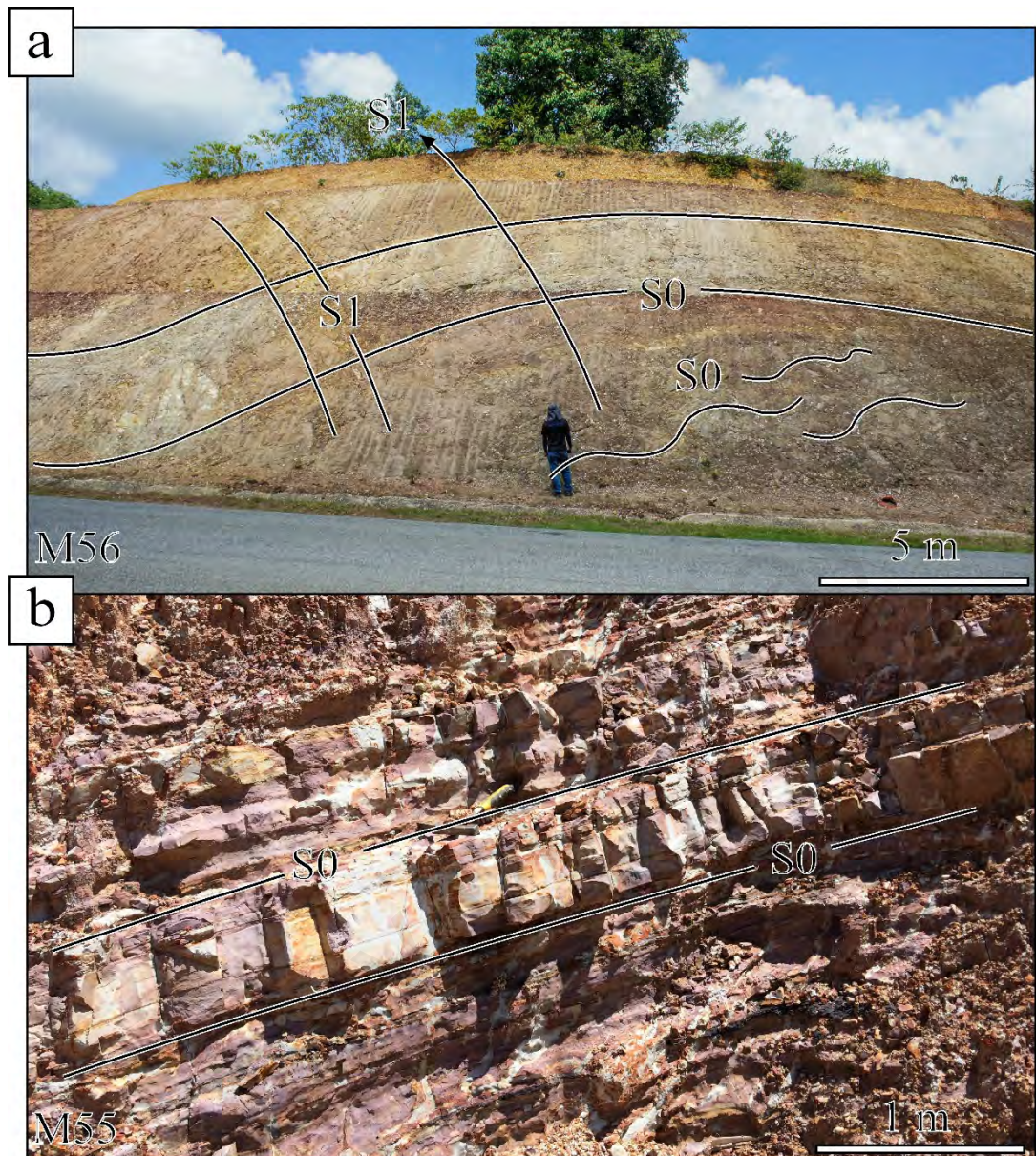


**Figure 4.15: Sedimentary rock exposures in the southerly flank, Gua Musang Formation; (a) a large upright fold with symmetric flanks and associated axial plane cleavages and (b) carbonaceous shale beds.**

At Kg. Sg. Sam a strongly folded carbonaceous phyllite exposure was observed. The S1 foliations have NNW-SSE strikes and intermediate to steep dip angles (Figure 4.2). C'-shear planes striking NE-SW controls the development of pervasive upright, open asymmetric folds as well as crenulations. These folds plunge towards SW and have west-vergence direction. This exposure is near contact between the Taku Schist and sedimentary rocks.

## 4.2.2 Petrographic Study

### 4.2.2.1 Micro-Structural Observation

- Quartz –feldspar phyllite, Phyllitic mudstone; Manik Urai Lama.

Lination:  $160^\circ \rightarrow 42^\circ$ ;  $125^\circ \rightarrow 50^\circ$ .

(Quartz-feldspar phyllite) Major: Qtz, Kfs, Bt, Src. Minor: Plg, Mev.

(Phyllitic Mudstone) Major: Src. Minor: Qtz.

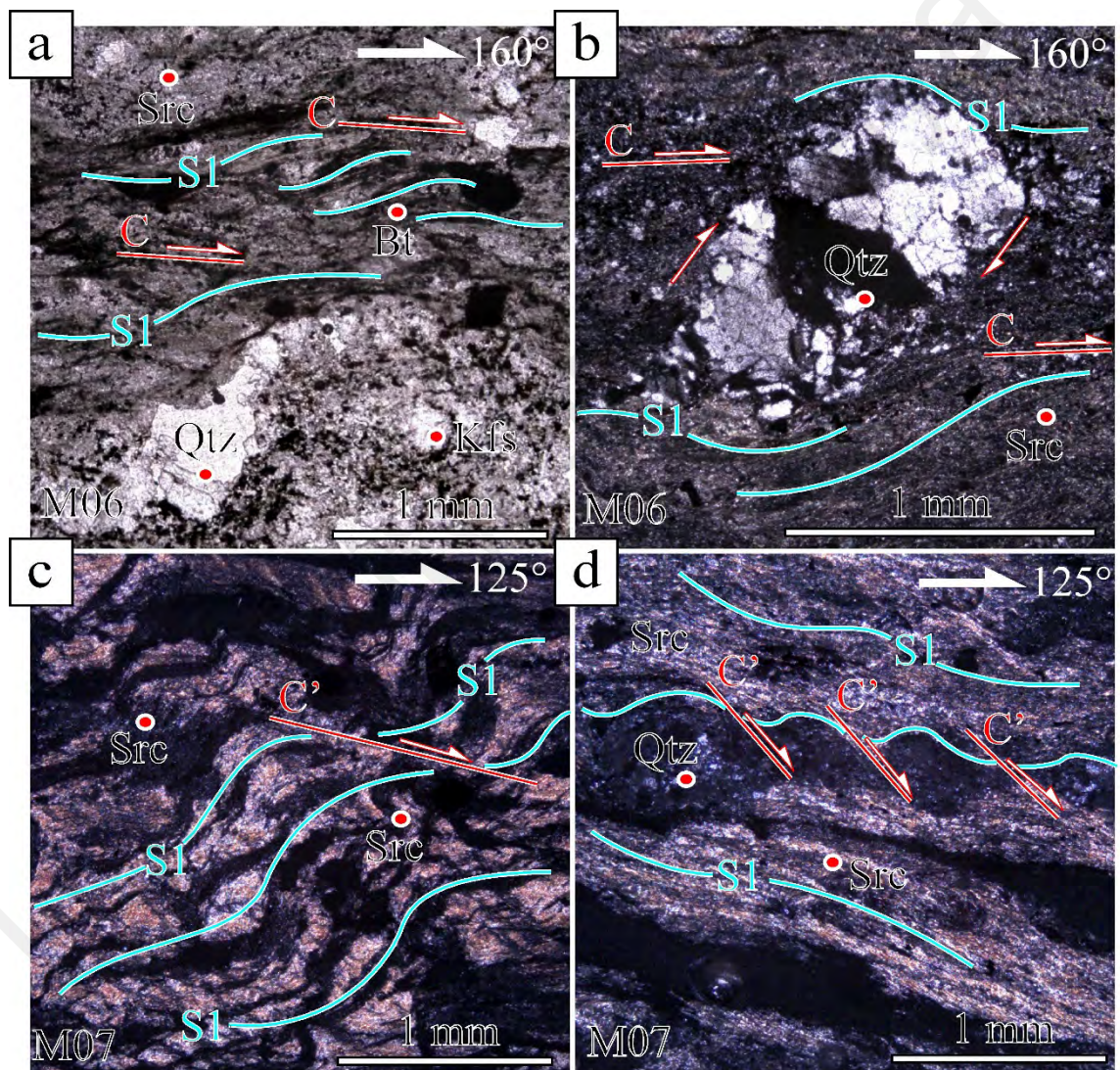


**Figure 4.16: Photomicrograph of phyllites near to the ESE margin of Taku Schist comprising of (a, b) quartz-feldspar phyllite and (c, d) phyllitic mudstone.**

Located near the ESE margin of the Taku Schist, the quartz-feldspar phyllite (Figure 4.16a, b) displays pervasive penetrative cleavages comprising of quartz and feldspar (plagioclase and K-feldspar) prophyroclast enveloped within fine matrix of quartz, feldspar, muscovite and sericite. In part, the sericitic micas contain relict muscovite showing a strongly preferred alignment, which define the continuous crenulated phyllitic foliations. Most of the prophyroclast are comprised of quartz minerals that often fractured, resulting appearance of patchy- type extinction where the mineral outlines are serrated and bulged. This characterizes minor recrystallization within quartz minerals by grain boundary bulging (BLG) mechanism. The rotated prophyroclast is also related to crosscutting incipient C'- shear bands, where both indicate top-right shear towards SE direction ( $162^\circ \rightarrow 42^\circ$ ).

Another sample obtained in proximity is phyllitic mudstone (Figure 4.16c, d) displays intense crenulated phyllitic foliations composed entirely of sericite and fine muscovites that exhibit strong preferred alignment. This defines the foliation which is strongly crenulated, kinked and folded into asymmetrical Z- shapes. Arrays of extinction bands occur parallel to C'- shear bands. A thin elongated ribbon quartz is enclosed within thick layer of sheet silicates. Analyses of S/C' shear bands suggest a top-right movement towards SE ( $162^\circ \rightarrow 42^\circ$ ).

- Tuffaceous siltstone; Ulu. Temiang

Major: Src, Qtz. Minor: Kfs, Bt, Chl.

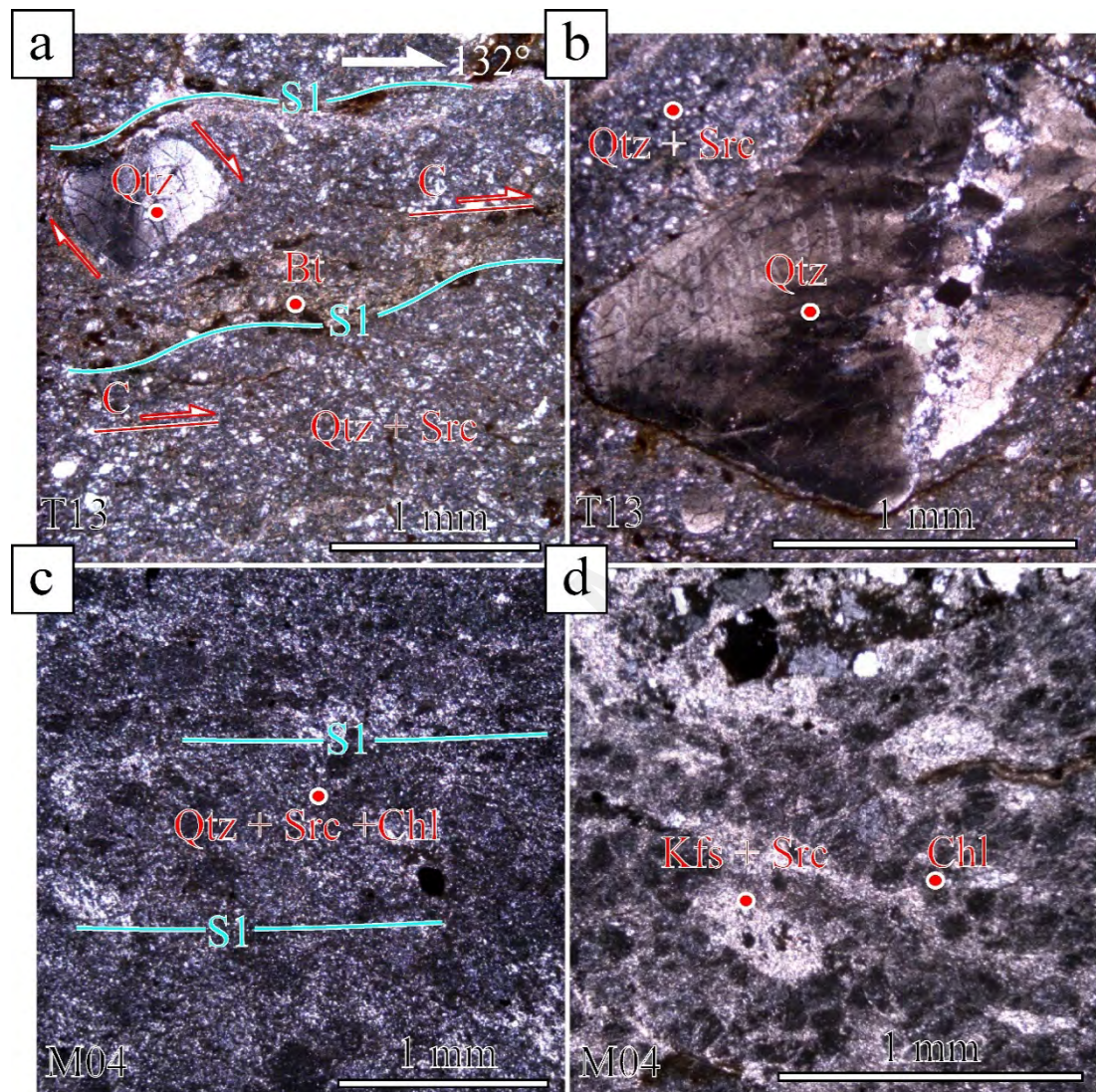


**Figure 4.17: Photomicrograph of tuffaceous siltstone in the direction toward SSE of Taku Schist**

Two samples obtained at the SSE flank of Taku Schist, one located close to the margin (T13 in Figure 4.17a, b) and the other is about 1 km away (M04 in Figure 4.17c, d). Both show weak foliations and containing quartz and K-feldspar clasts enclosed within fine sericite and quartz matrix. Despite similar composition, the sample near the SSE margin (T13) shows coarser quartz aggregates with observable shape preferred orientation defining the foliation. The clasts are fractured and develop patchy type of

extinction (Figure 4.17a, b). This fabric is in contrast with sample no M04 which shows sericite matrix with fine, anomalous blue chlorite and devoid of foliation (Figure 4.17c, d).

- Mudstone; Sg. Hijau Iron Mine, Temangan  
Major: Src, Chl, Qtz.

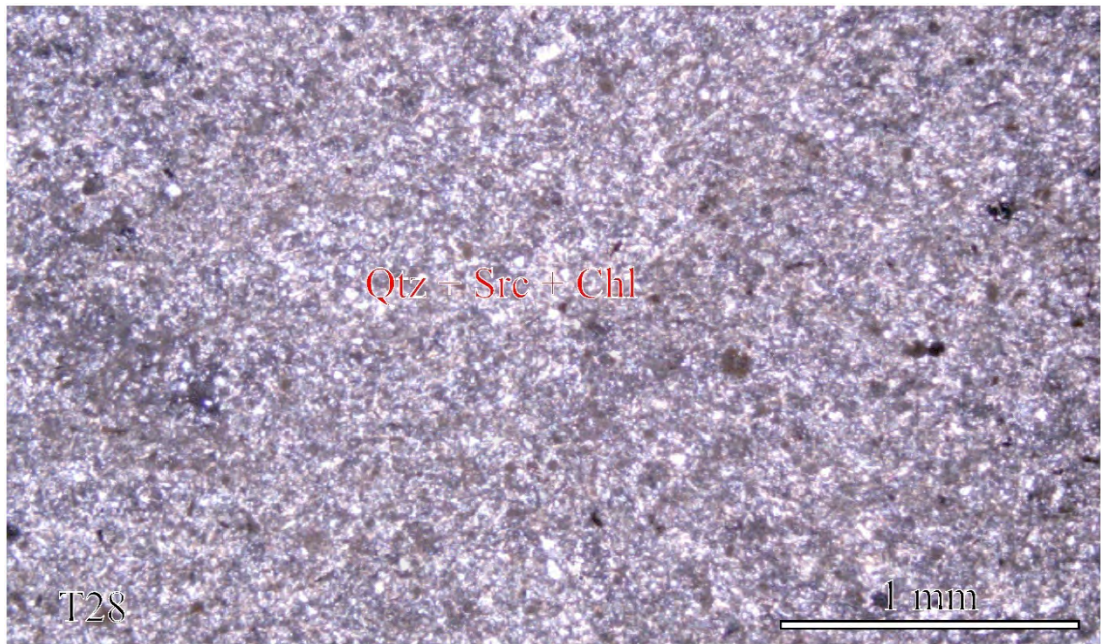


**Figure 4.18: Photomicrograph of mudstone near the eastern margin of Taku Schist.**

The mudstone sample in Figure 4.18 was obtained at the eastern margin of the Taku Schist. It is composed of fine quartz aggregates, fine chlorite and sericite that do not show preferred orientations. The absence of foliation is in contrast with the fabric of the Taku Schist.

- Dacite; Tanah Merah

Major: Kfs, Plg, Qtz, Minor: Bt, Src, Chl, Hbl.

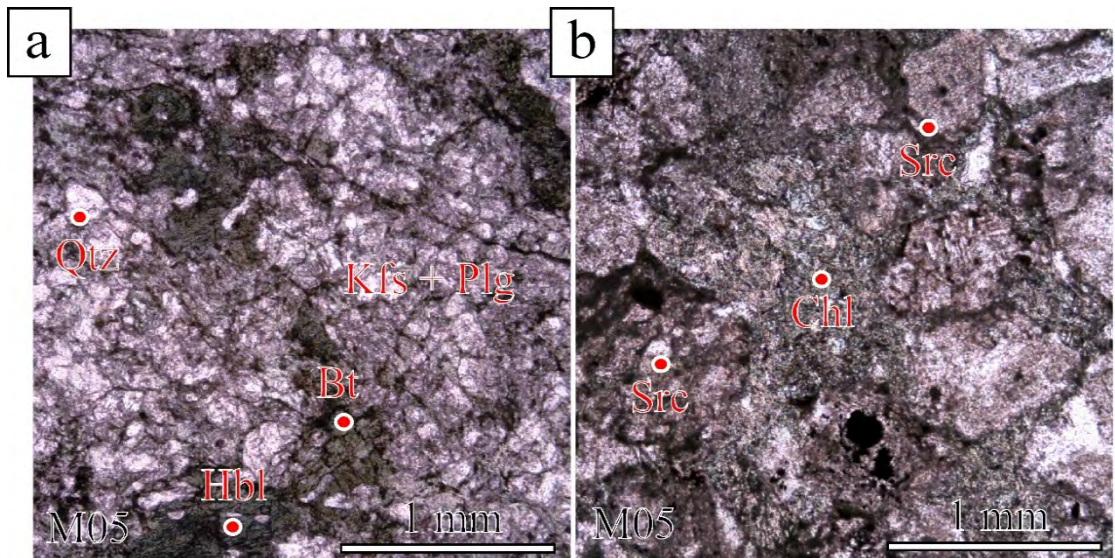


**Figure 4.19: Photomicrograph of dacite near the eastern margin of the Taku Schist.**

The dacite is composed of coarse, equigranular aggregates of K-feldspar, plagioclase and quartz (Figure 4.19) with lesser biotite and hornblende. There is no shape preferred orientation and foliation is absent. Most of the minerals are altered, such as sericitization of K-feldspar and plagioclase and chloritization of biotite.

- Rhyolite; Sg. Galas Basin

Major: Qtz, Kfs, Plg.

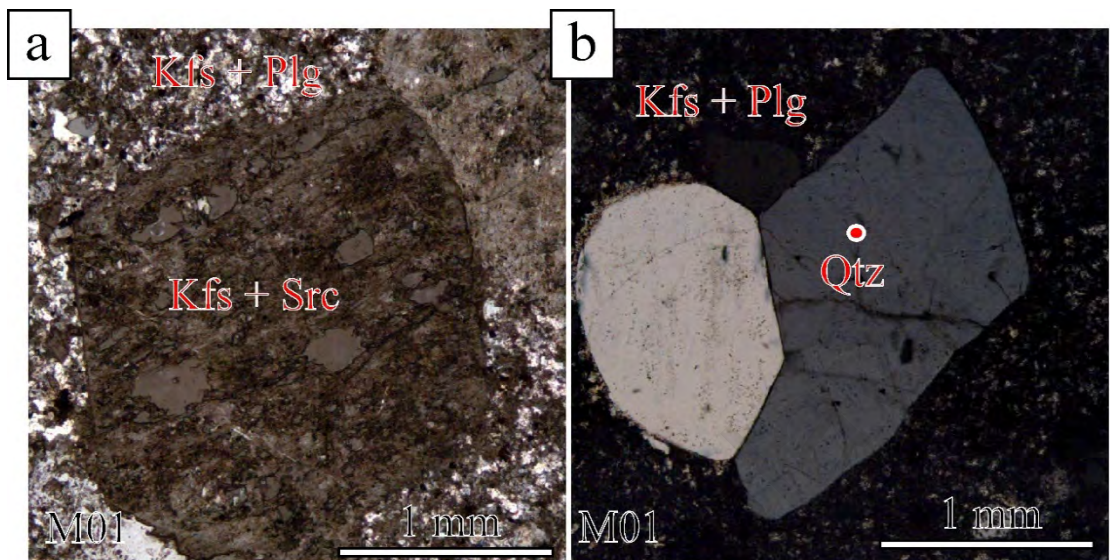


**Figure 4.20: Photomicrograph of rhyolite at Sg. Galas near to the Eastern margin of Taku Schist.**

The rhyolite sample (Figure 4.20) was obtained near to to E margin of Taku Schist in Sg. Galas basin, which was mapped as an ignimbrite ridge by Aw (1977). The rhyolite contains quartz, K-feldspar and plagioclase that form many medium-grained, euhedral phenocrysts enclosed by fine matrix. There is no foliation. The feldspars are sesriticized.

- Tuffaceous phyllite; Lata Rek. Lineation:  $125^\circ \rightarrow 10^\circ$ .

Major: Qtz, Src. Minor: Kfs, Mcv.

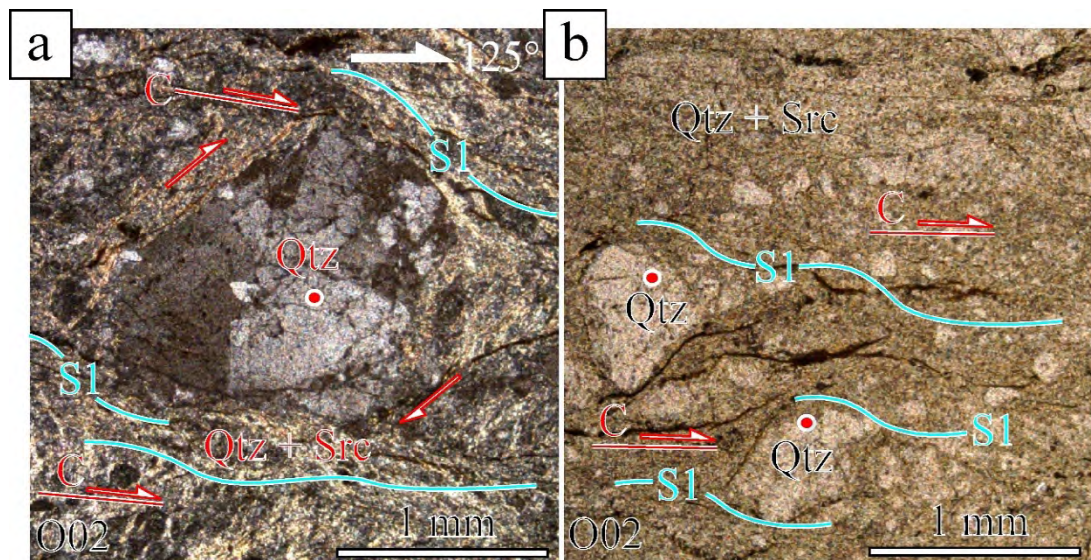


**Figure 4.21: Photomicrograph of tuffaceous phyllite near Lebir fault zone.**

The sample was obtained near the Lebir Fault zone, SSE of the Taku Schist (Figure 4.21). The tuffaceous phyllite displays strong preferred alignment of fine-grained muscovite and sericite together with quartz aggregates defining phyllitic foliation (S1). The fine to medium quartz grains shows bulged to serrated outlines elongated along the foliation. Individual grains within the aggregates are inequigranular with interlobated contact displaying patchy extinction indicating bulging (BLG) mechanism of recrystallization. The fine micas envelop medium-grained K-feldspar into  $\sigma$ -type prophyroclast indicating top-right movement, directed towards SE ( $125^\circ \rightarrow 10^\circ$ ).

- Tuffaceous siltstone; Dabong. Lination:  $120^\circ \rightarrow 18^\circ$ .

Major: Src, Qtz, Kfs, Plg. Minor: Chl.

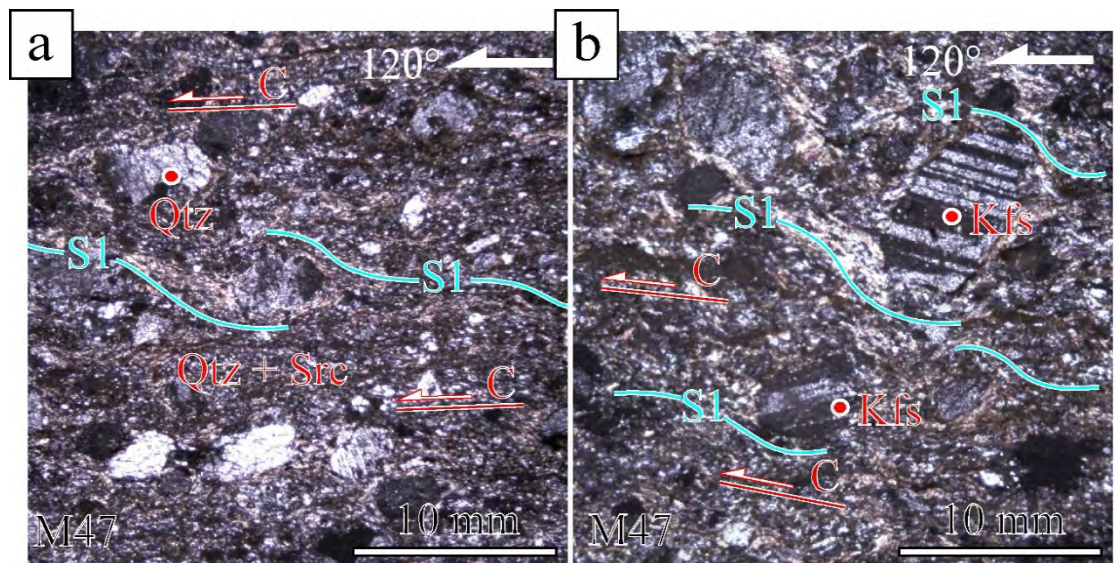


**Figure 4.22: Photomicrograph of tuffaceous siltstone at the western flank of Gua Musang Formation.**

A tuffaceous siltstone sample from the western flank near to the Stong Complex is comprising of medium-grained feldspar clast enclosed within fine matrix of quartz, sericite and chlorite (Figure 4.22). The fine quartz aggregates display shape preferred orientation, the sericite and chlorite show continuous alignment defining fine phyllitic foliation. The clast comprised of K-feldspar and plagioclase, the latter shows albite twinning. Minor K-feldspar clasts indicate patchy extinction and fractures at right angles. The feldspars are enveloped by the foliated matrix forming  $\sigma$ - shape prophyroclast where it indicates a sinistral kinematic movement or top to SE shear.

#### 4.2.2.2 Metamorphic Parageneses

Samples obtained within the eastern flank of Taku Schist, including both E and SSE margins show weak development of penetrative cleavages up to slate cleavage. This is in contrast with samples obtained in ESE margin (M06, M07) and far-off SSE flanks near Lebir fault zone (O02) as well as westerly flanks of Taku Schist which have phyllitic foliation (S1). In all of the samples, the prograde metamorphism (M1) is at most of sub-greenschist facies indicated by assemblages of quartz-plagioclase-sericite-muscovite-chlorite minerals. The foliation (S1) is defined by preferred alignment of sericite accompanied by weak shape preferred orientation of fine quartz aggregates within the matrix. The samples near the E margin of Taku Schist (T28, M05) in particular shows strong secondary transformation (M2). These include chlorite transformation from biotite minerals and sericitization of feldspars.

### 4.3 The Panau Formation

A localized exposure of oxidized, purplish orange sedimentary rocks showing original bed layering and devoid of cleavage is observed north of Tanah Merah adjacent to the Boundary Range Granite (Figure 4.1). The exposure composed of alternations of mudstone and fine-grained sandstone. The beds (S0) are striking NW-SE and dip about  $60^\circ$  toward NE (Figure 4.2; Figure 4.24). Some of the sandstone beds have graded bedding from a conglomeratic base to medium-grained sandstone at the top (Figure 4.23). These clasts are primarily comprised of polymict pebbles and gravels with maximum diameter about 15 cm.

The contact between the sedimentary rocks and Boundary Range Granite is along a sub-vertical NW-SE trending fault (Figure 4.2 and Figure 4.25). Kinematic analysis of the faults indicate a dextral normal oblique movement toward SE direction (Figure 4.3). The adjoining granite exposure shows a primary features devoid of any penetrative deformation.

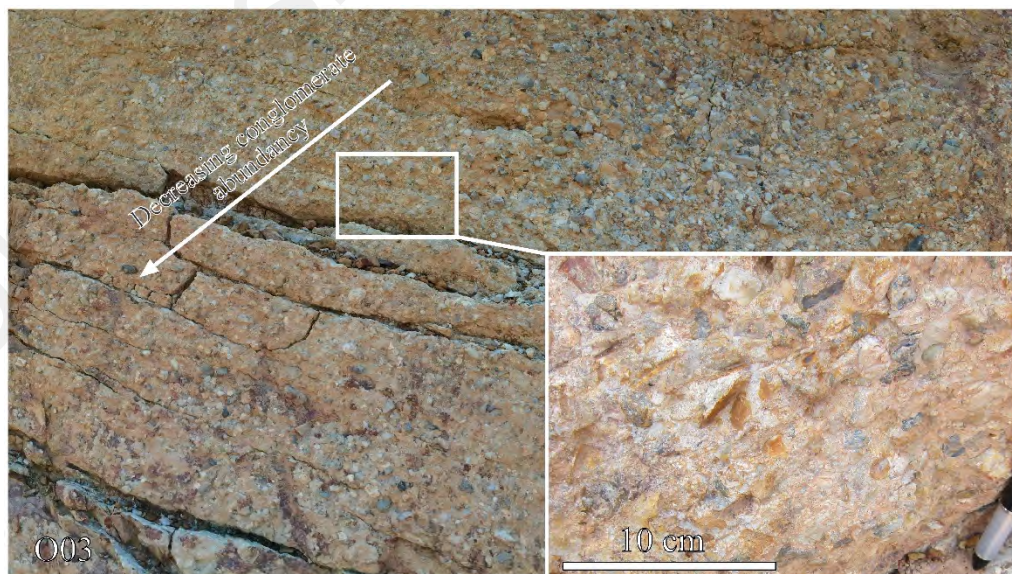


**Figure 4.23: Polymict conglomerates of Panau Formation. Notice the graded bedding showing with lateral changes of polymict conglomerates.**

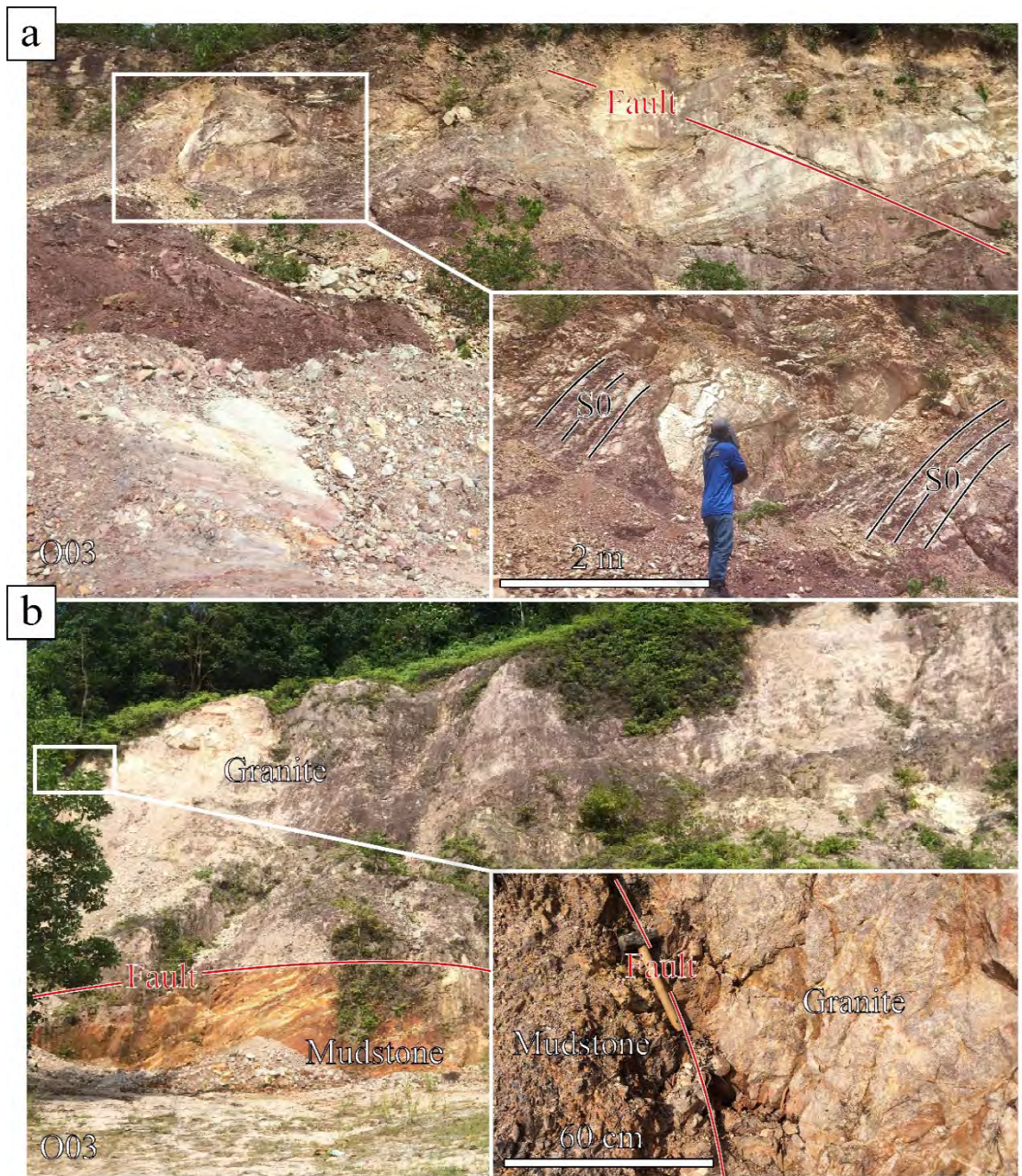


**Figure 4.24: Faults observed in the Panau Formation. (a) Steeply inclined bedding crosscut by a fault and, (b) fault contact between Panau Formation and the Boundary Range Granite.**

#### 4.4 The Boundary Range Granite

The granite exposed next to the Panau Formation near Bt. Panau display primary megacrystic texture composed of coarse-grained K-feldspar, plagioclase, biotite and hornblende. The granite is in contact with microgranite, and intruded by steep doleritic dykes (Figure 4.25). Generally, the granite is not affected by major deformation.

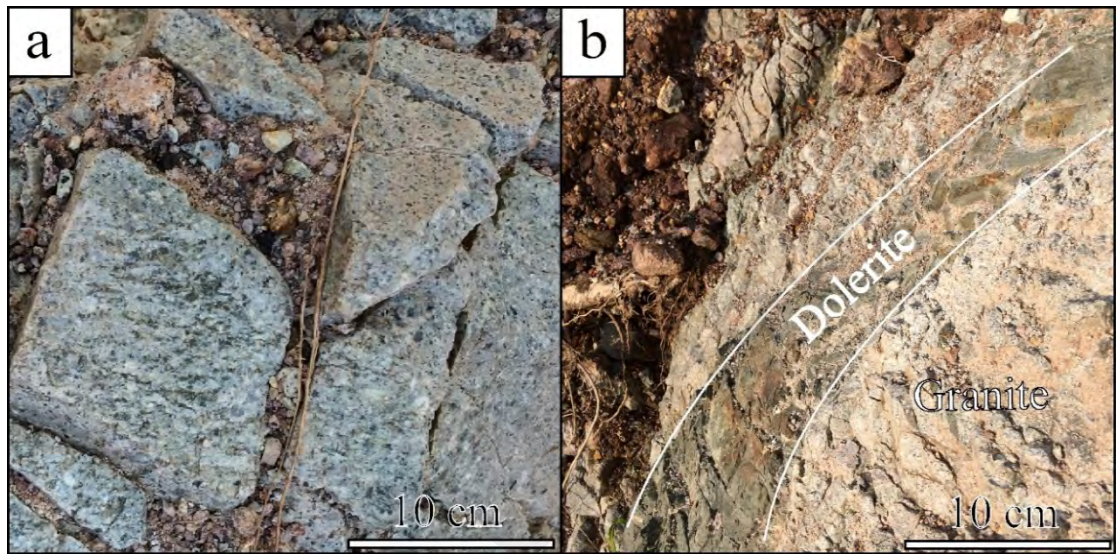


**Figure 4.25: Boundary Range Granite exposure in adjacent of Panau Formation; (a) Granite fabrics shows un-deformed coarse-grained biotite granite and (b) steep dolerite injection into the granite.**

In Lata Rek south of Kuala Krai, the granite exposure is in close proximity to Gua Musang Formation and they are separated by Lebir Fault zone (O02, Figure 4.1). The biotite granite is typified by coarse-grained and exhibit primary hypidiomorphic texture. A number of localize NNW-SSE trending shear zones about 20 centimeter in width crosscut the granite (Figure 4.25 c, d). The shear zone is cataclastic, containing granitic clasts and shows riedel shears. Kinematic analysis indicate dominant normal dextral oblique movement toward SE in addition to minor thrust sinistral oblique toward NW.

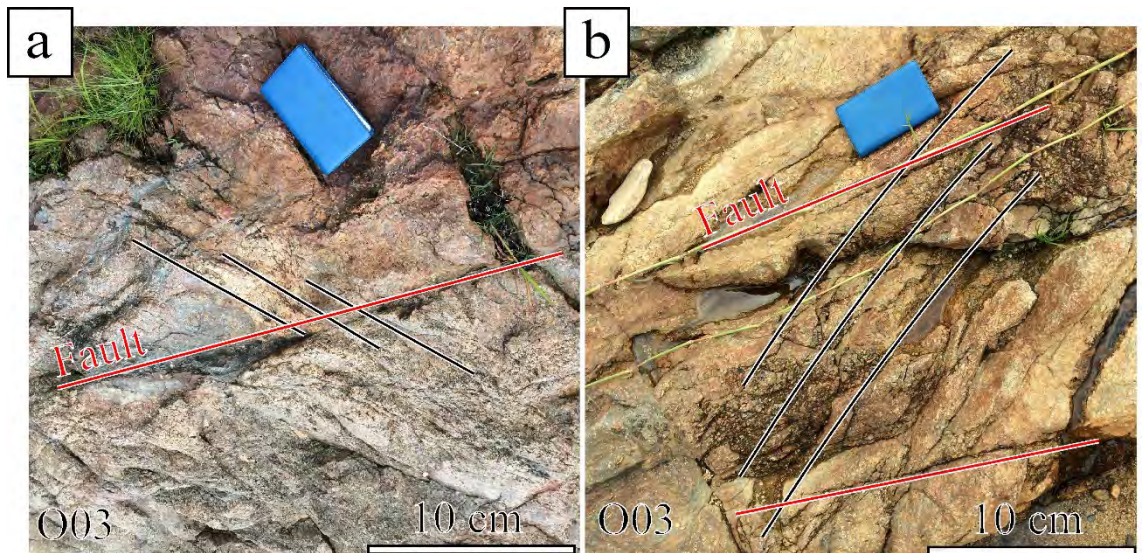


**Figure 4.26: Examples of granite rock exposures within the Lebir Fault zone at Lata Rek.**

## **4.5 The Kemahang Granite**

### **4.5.1 Field Observations**

The Kemahang Granite is situated in the northern part of study area. It is in contact with all other four units; Stong Complex, Taku Schist, Tiang Schist and Gua Musang Formation. The granite exposures can be observed along the EW- highway near Batu Melintang and continues eastward across Jeli – Ayer Lanas highway. The granite is in contact with the Stong Complex near Kg. Belahat – Jeli – Batu Melintang whereas on east, the unit is in contact with Taku Schist along Kg. Ipoh – Ayer Lanas road (Figure 4.1). In addition, the Kemahang granite continues northward across Thailand border as Buke Ta granite unit. Detailed geological analysis have been performed on about 20 stations with 10 samples collected for microstructural study. Parts of the granite exhibits metamorphic foliation (S1) particularly on the western part of the Taku Schist, trending NNW-SSE associated with low angle, SE to WNW plunging stretching lineation (L1) (Figure 4.2 and Figure 4.5).

#### 4.5.1.1 The Eastern Unit

The Kemahang granite intrudes into the NNW-part of Taku Schist, but the contact between two units are not exposed. Good exposures have been observed at Sebarang Bina Quarry (M01, Figure 4.1), typified by porphyritic granodiorite commonly displays large K-feldspar megacrysts within matrix of biotite and quartz. The K-feldspar megacrysts are mostly euhedral and exhibit a shape preferred orientation within matrix containing crystalline quartz- biotite minerals that defines a primary magmatic foliation (S<sub>0</sub>) (Figure 4.27a). Some of the granite exposures exhibit metamorphic foliation (S<sub>1</sub>) showing either completely foliated gneissic fabric or indistinctive S<sub>1</sub> foliation oriented obliquely to the former magmatic foliation (Figure 4.27b, c). In both cases, the foliations are sub-vertical striking along NW-SE direction associated with low-plunging stretching lineation (Figure 4.2 and Figure 4.5). The former fabric resemble an augen-gneissose texture characterized by sub-rounded, “eye-shape” K-feldspar prophyroclast enveloped within quartz-biotite matrix. This S<sub>1</sub> foliation is dipping towards SW-direction, where the kinematics inferred from  $\sigma$ -prophyroclast and S/C shear bands suggest top- WSW shears.

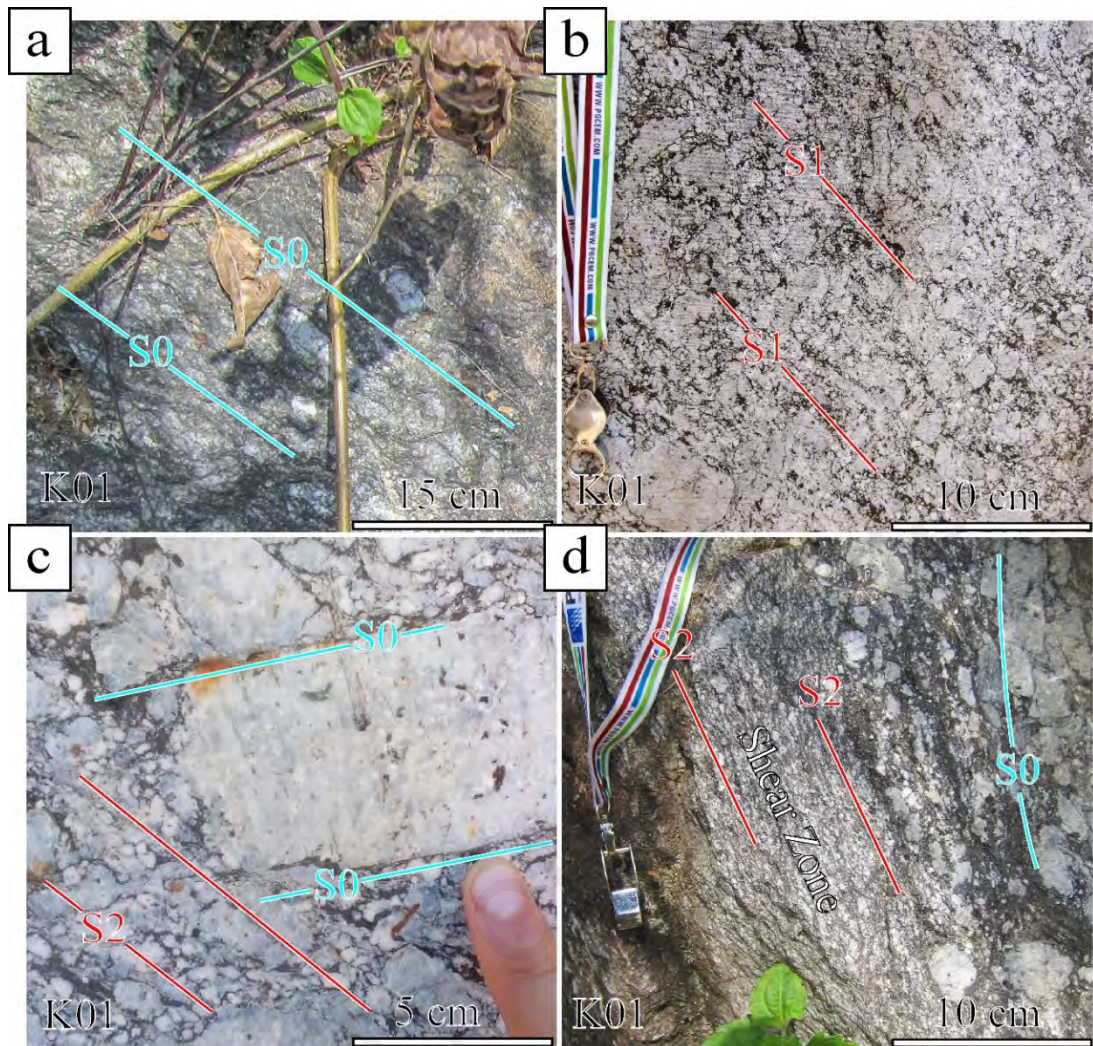


**Figure 4.27: Development of foliations in Kemahang granite; (a) primary magmatic foliation (S0), (b) an indistinctive S1 metamorphic foliation and (c) discontinuity between magmatic foliation (S0) with oblique S2 foliation and (d) localised shear zones development defining S2 foliation**

The second-type of foliation fabrics (S2) is indistinctive, observed by shapes preferred orientation of a medium-size K-feldspar enveloped within preferred align biotite micas. This is oriented oblique to former large, euhedral K-feldspar that demarcate the magmatic foliation (S0) (Figure 4.27c). Some of these smaller, sub-rounded K-feldspar show incipient prophyroclasts development whereas the large euhedral K-feldspar are fractured. Although the S2 foliation also strikes NW-SE, the planes are dipping towards NE- direction, as oppose to the dips of former S1 foliation (Figure 4.27b). Kinematic analysis using K-feldspar prophyroclasts suggests top-SE

shears ( $110^\circ \rightarrow 60^\circ$  in Figure 4.5). Minor parts of these exposures contain narrow  $\sim 1$  meter width shear zones containing both flattened and small, sub-rounded K-feldspar porphyroclasts that indicate top-SE shears ( $108^\circ \rightarrow 32^\circ$  in Figure 4.27d). In addition, there are a number of faults that are sub-parallel to S2 foliation. These faults indicate either normal oblique movement towards E-direction or sinistral movement towards SW-direction ( $135^\circ \rightarrow 18^\circ$  and  $234^\circ \rightarrow 52^\circ$ , Figure 4.3).

Apart from the exposures at Sebarang Bina quarry, most of the easterly domain is in forested area and exposures are not found. Granite exposures in the NNW domain of Taku Schist (near T51, Figure 3.2) show coarse-grained porphyritic granodiorite containing large euhedral K-feldspar megacrysts. This K-feldspar megacrysts show shape preferred orientation indicative of primary magmatic foliation (S0) and metamorphic fabric is absent (comparable to Figure 4.27a). The intrusional contact between granite and schist is not exposed in the NNW domain. There are quartz-mica schist exposures near to the pluton, but the schist is not affected by contact metamorphism. Schist in exposures nearest to granite margin are oriented along NS-strikes and displays compositional banding (Figure 3.27). The minerals are arranged in fine alternating layering about a centimeter thick defining pervasive foliation with stretching lineation that plunges at intermediate angles and indicates top-WNW shears ( $274^\circ \rightarrow 25^\circ$  in Figure 4.5). The schist exposures near granite margin are often cut by strike slip faults (Figure 4.3). The quartz-feldspar schist adjacent to the E-margin of granite is cut by NE-SW trending faults, whereas quartz-mica schist surrounding the SE margin is cut by NW-SE trending faults (Fp:  $235^\circ \rightarrow 80^\circ$ ;  $348^\circ \rightarrow 82^\circ$ ). Both of these faults indicate dextral kinematics toward -SSE direction.

#### 4.5.1.2 The Western Unit

Good exposures are observed in Polytechnic Jeli typified by grayish-colored megacrystic granodiorites-diorites (K02, Figure 4.1, Figure 4.28a). The granite contains high amount of biotite-hornblende in the matrix and elongated, flat K-feldspar megacrysts. While the megacrysts display shape preferred orientation, the biotite exhibits a strong preferred alignment defining the penetrative metamorphic foliation (S1) resembling an augen-gneiss textures (Figure 4.28d). The S1 foliation strikes NW-SE and is steeply dipping either towards SW or NE direction (Figure 4.2). Kinematics analysis on S/C shear bands and sigmoidal feldspar clasts indicates top-SW shears with low-angles plunges (Figure 4.5). Thin arrays of light colored, biotite-granite injected lit-par-lit/ parallel to metamorphic foliation (S1) of granodiorite (Figure 4.28a).

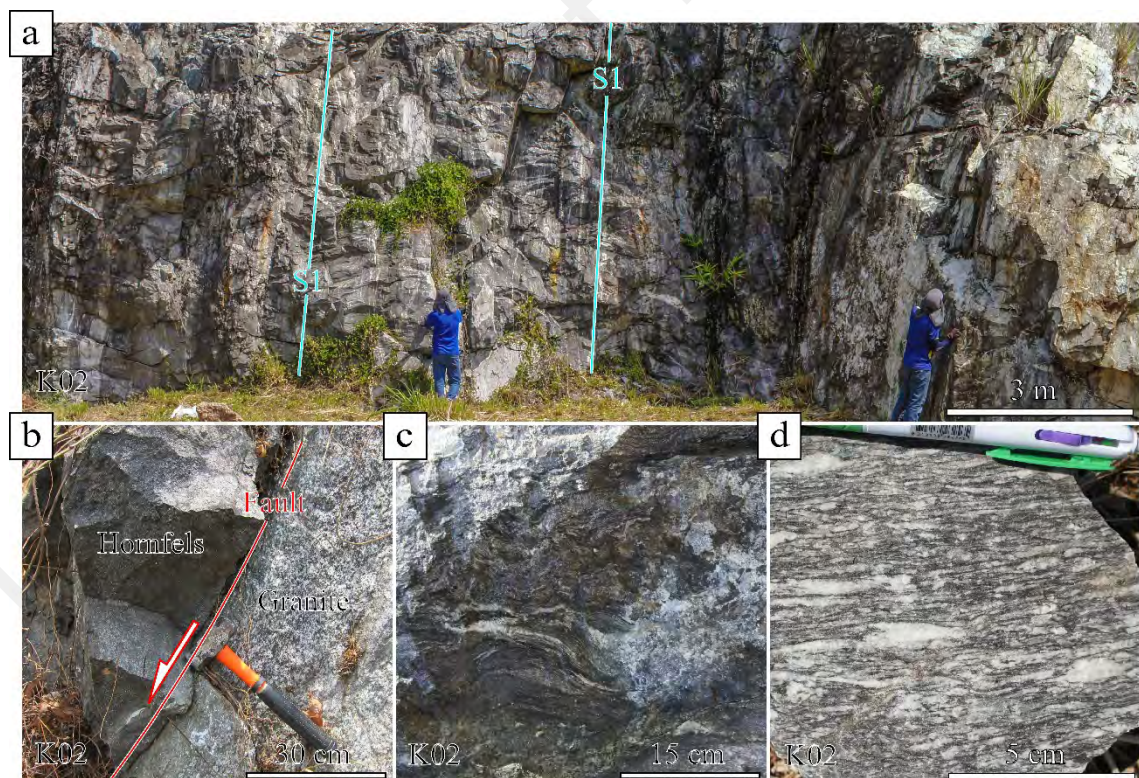


**Figure 4.28:** Kemahang granite exposure near Taku Schist, Polytechnic Jeli; (a) View of the granite exposure and lit-par-lit vein injections, (b) Normal fault contact separating country rocks from intruded granite, (c) fabrics of country rocks showing well-developed schistose layers and (d) strongly foliated granite near the fault contact.

A different foliation (S2) is observed in parts of the exposure, where it strikes NNE-SSW and steeply dipping towards the E. It often forms shear zones about 1 meter in width showing an increase of cleavage development where the pervasive mineral alignment define the stretching lineation. Kinematic analyses on sigmoidal K-feldspar prophyroclasts indicates low-angle top-SE shear ( $163^\circ \rightarrow 48^\circ$  in Figure 4.5). The biotite-granite vein injections in the granitic body show orientation similar to S2 foliation, which were latter boudinaged by dextral shear towards SE direction. The biotite contained within this fabric often display greenish color indicative of chlorite transformation likely resulted from this episode of shearing deformation.

The granodiorite and quartz-mica hornfels are in contact along a sub-vertical, NNW-SSE trending fault (Figure 4.28b). The latter still contain schistose relics, comparable to rocks fabric within the Taku Schist and represents the country rock of the intruded granite (Figure 4.25). Kinematic analysis of this fault indicates a dextral normal oblique movement towards E direction ( $94^\circ \rightarrow 52^\circ$ , Figure 4.3). The strike and kinematic movement of this contact fault is similar to surrounding fault arrays and shear zones. The surrounding faults are mostly dipping towards the E, although W-dipping faults are also observed. Minor strike-slip faults cut the biotite granite dykes are associated with dextral kinematics towards E-NE direction.

#### *Kg. Rual, Jeli*

The granitic exposures along the newly constructed highway at Kg. Rual, Jeli is in contact with both Tiang Schist and Noring granite (Stong Complex), and is situated in proximity with the overlying Gua Musang Formation (K08, Figure 4.1). The rocks is typified by dark colored, mafic granodiorite with foliations oriented along NS-strikes and is gently dipping towards E direction (Figure 4.2 and Figure 4.29b). The aligned elongated feldspar clasts define stretching lineation (L1) that plunges towards SE

direction at low angle. The granite intruded via lit-par-lit injections into meta-sedimentary layers comprising of quartz-mica and calc-silicate hornfels displaying well-developed relict schistosity (Figure 4.29b). The schistosity forms compositional banding with NS strike, similar to the granitic rocks that indicates top –SE shear ( $145^{\circ} \rightarrow 30^{\circ}$ , Figure 4.5). The layering/banding are further folded into symmetrical structure with sub-horizontal axial plane (Figure 4.29a). The fold axis plunges towards ESE direction subparallel to the stretching lineation (L1) ( $090^{\circ} \rightarrow 28^{\circ}$ ). Subsequent leucogranite vein intrusions discordant to the foliation (S1) are observed locally in the granitic exposures (Figure 4.29c). This later leuco/biotite-granite are light colored, fine-grained with phaneritic texture and devoid of metamorphic foliation (S1), similar to Noring granite.

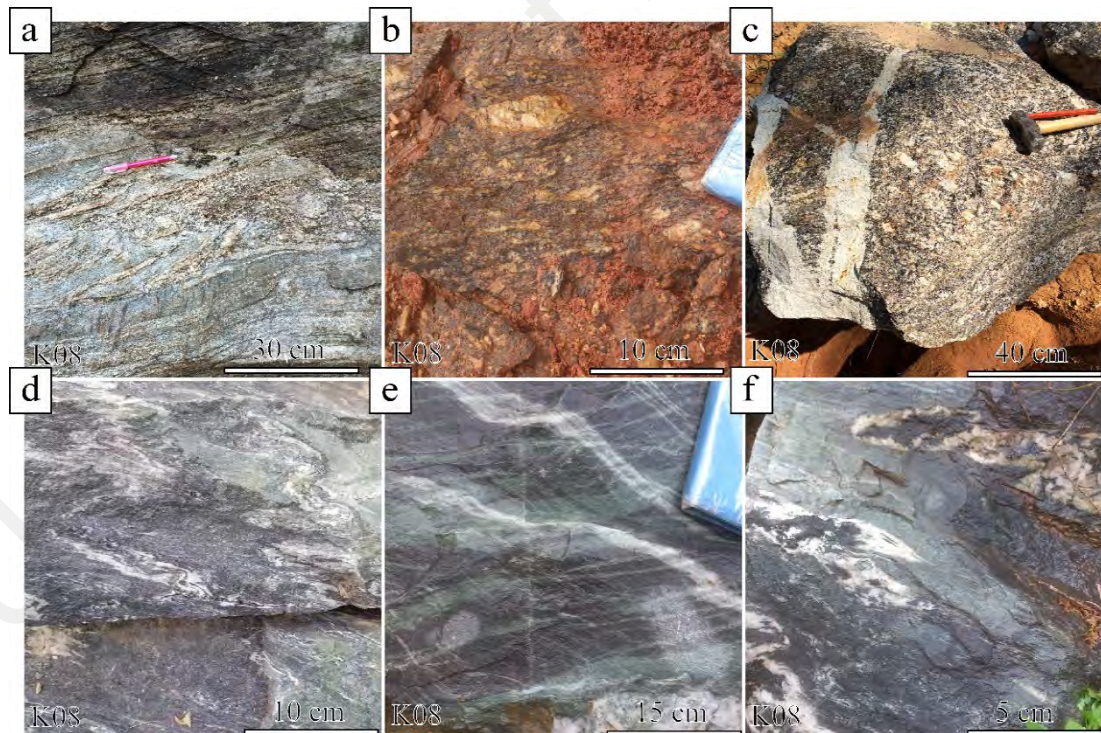


**Figure 4.29: Kemahang granite exposure near Noring Granite, Kg. Sg. Rual; (a) Granodiorite intrusion via lit-par-lit into meta sedimentary host rock affected by subsequent symmetrical folding, (b) Granodiorite with augen-gneiss fabric, (c) discordant intrusion of Stong leucogranitic veins, (d) asymmetrical folds of leucosome bands (e) migmatite rocks containing chloritic bands and (f) biotite-rich zone within leucosome bands.**

Migmatite exposure was observed nearest to the eastern margin of Kemahang Granite and is in close proximity to the phyllitic mudstone of Gua Musang Formation at about 100 meter in separation (S03, Figure 4.1 and Figure 4.29 d, e and f). This dark migmatite rocks display fine layering of quartz-feldspar-biotite minerals. The S1 foliation strikes NW-SE direction with intermediate dips towards E direction. The foliation is associated with low angle, SE plunging stretching lineation (L1) (Figure 4.2 and Figure 4.5). There are relics of highly elongated feldspar clasts with sigmoidal shapes as well as numerous light colored aplitic veins/quartz-rich veins forming ptygmatic fold. These veins are tightly folded into recumbent, Z- shape fold structures (Figure 4.29d) with fine biotite layering along fold curvatures. The sheet silicates surrounding the veins commonly shows dark-greenish bands indicative of chlorite (Figure 4.29e). Both the vein asymmetries and feldspar prophyroclasts indicate top –SE shear ( $150^{\circ} \rightarrow 30^{\circ}$  in Figure 4.5).

While the Kemahang granite exposures on the NW flanks are observed at Lata Janggut (K03, Figure 4.1). The exposure is consisting of biotite- microgranite displaying fine-grained phaneritic textures with observable metamorphic foliation (S1) trending along NNW-SSE strikes and gently dipping towards E- direction (Figure 4.2). The associated stretching lineation (L1) plunges towards northeast where kinematic transport observed from S/C shear fabric indicate top –WNW shear ( $320^{\circ} \rightarrow 10^{\circ}$  in Figure 4.5). The microgranite often contains dark-greenish enclaves of coarse- to fine-grained biotite. Thin injection of aplitic dykes into the microgranite observed to be folded into tight, upright folds with closure plunging towards S direction.

Minor granitic stocks have also been observed in NNW part of study area near Batu Melintang – Sg. Kalai area. The granite is in contact with Tiang Schist and Gua Musang Formation (K06, K07, Figure 4.1). The exposure is consisting of mafic granodiorite

with medium- to fine-grained phaneritic textures. It displays metamorphic foliation (S1) trending along NE-SW strikes and steeply dipping towards the SE (Figure 4.2). The rock commonly contains mafic enclaves or xenolith displaying well-developed schistosity with similar orientation to the foliation in the granite. Both rocks develop stretching lineations (L1) that plunge towards NW or SE direction at low angle. Kinematic analysis on feldspar prophyroclast and S/C shear band of both xenolith and granite indicates consistent top-SSE shear ( $170^\circ \rightarrow 10^\circ$  in Figure 4.5). A steep NS-trending fault cuts through S1 foliation where it develops chloritization associated with dextral normal oblique movement towards WNW direction (Figure 4.3,  $300^\circ \rightarrow 70^\circ$ ). The contact between the granite and Gua Musang Formation is not exposed (Figure 4.1). The Kemahang granite is also near the non-foliated Noring granite (Stong Complex) and are the enclaves of this latter granite observed in Lata Tubur exposure (G07, Figure 4.1).

#### 4.5.2 Microstructural Observation

- Migmatite; Sg. Rual. Lineation:  $165^\circ \rightarrow 10^\circ$ .

Major: Qtz, Kfs, Plg, Hbl, Bt.

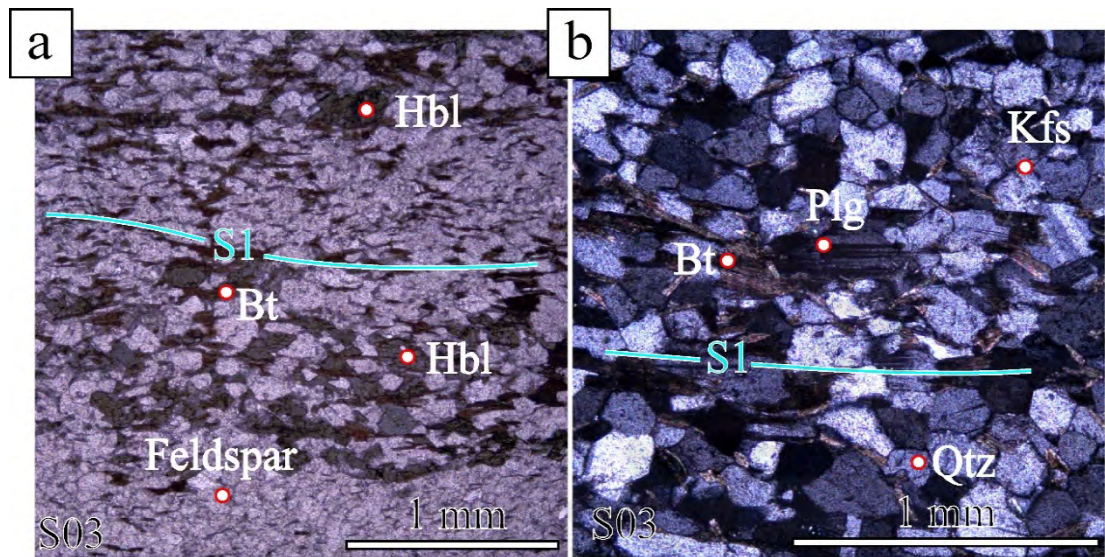


**Figure 4.30: Photomicrograph of migmatite (quartz-feldspar) in the western domain of Kemahang granite**

The migmatite sample is composed of fine to medium-grained polygonal aggregates of quartz, plagioclase and K-feldspar overgrown into hornblende and biotite within the matrix (Figure 4.30). The quartz-feldspar aggregates shows high angle contact or triple junction, where it is completely recrystallized under grain area boundary reduction (GBAR) mechanism. While the aggregates develop wavy-type of extinction, minor deformed twinning have also been observed within plagioclase minerals. The long axes aligned along the S1 foliation plane interlayered with biotite micas defining continuous disjunctive foliation fabric. The fabric also develops compositional layering between hornblende and biotite-rich domain alternating with quartz-feldspar-rich domain.

- Quartz-feldspathic hornfels; Sg. Rual. Lineation:  $145^\circ \rightarrow 30^\circ$ .

Major: Qtz, Kfs, Plg, Bt, Hbl. Minor: Chl, Adl, Src. Trace: Zr

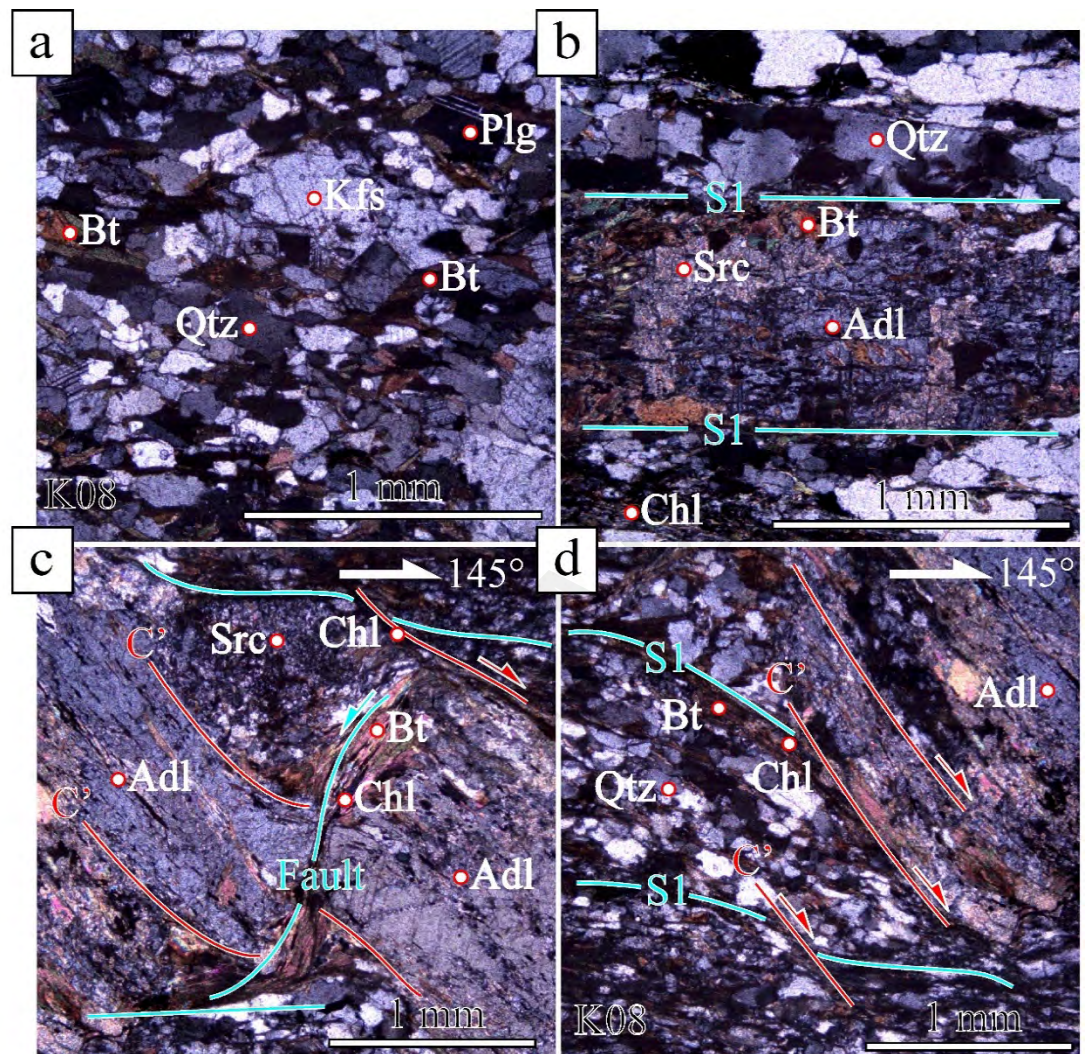


**Figure 4.31: Photomicrograph of quartz-feldspar enclave in the western domain of Kemahang granite unit.**

The sample is composed of coarse aggregates of quartz, K-feldspar and plagioclase as well as hornblende and biotite micas (Figure 4.31). In addition, minor tourmaline and zircon are also observed. The spaced disjunctive foliation fabric (S1) defined by the preferred orientation of the aggregates along the long axes and parallel alignment of sheet silicates. Individual grains in the quartz-feldspar aggregates display equigranular shapes with polygonal shapes. They show wavy extinction and the contact between the grains is strongly interlobated indicating both grain boundary migration (GBM) and

grain area boundary reduction (GBAR) mechanism of recrystallization. Large andalusite grown within masses of biotite and oriented parallel to the foliation. This blastose minerals also contain straight inclusions of biotite and quartz in symmetries with external foliation.

The former foliation fabrics containing andalusite is cut by wide, steeply inclined shear zone in alternation to C'-shear bands. Both of the biotite and chlorite within the shear zone form newly preferred orientation oblique to former S1 foliation. Both of the sheet silicates envelop the andalusite forming prophyroclast structures, where kinematic analysis on crosscutting C'- shear bands suggest top-right sense of shears towards SE direction ( $145^\circ \rightarrow 30^\circ$ ). The andalusite were subsequently faulted in later episode by an opposite, sinistral sense of shear, which is accompanied by internal fracturing. The biotite is chloritized and the andalusite is sericitized. In addition, the quartz aggregates contained within this C'-shear zones shows serrated boundaries indicating renewed bulging (BLG) recrystallization possibly related to fracturing of the K-feldspar minerals.

- Sheared quartz-feldspathic hornfels; Sg. Rual.

Lination:  $145^\circ \rightarrow 30^\circ$ . Major: Qtz, Plg, Kfs, Bt. Minor: Chl. Trace: Zr.

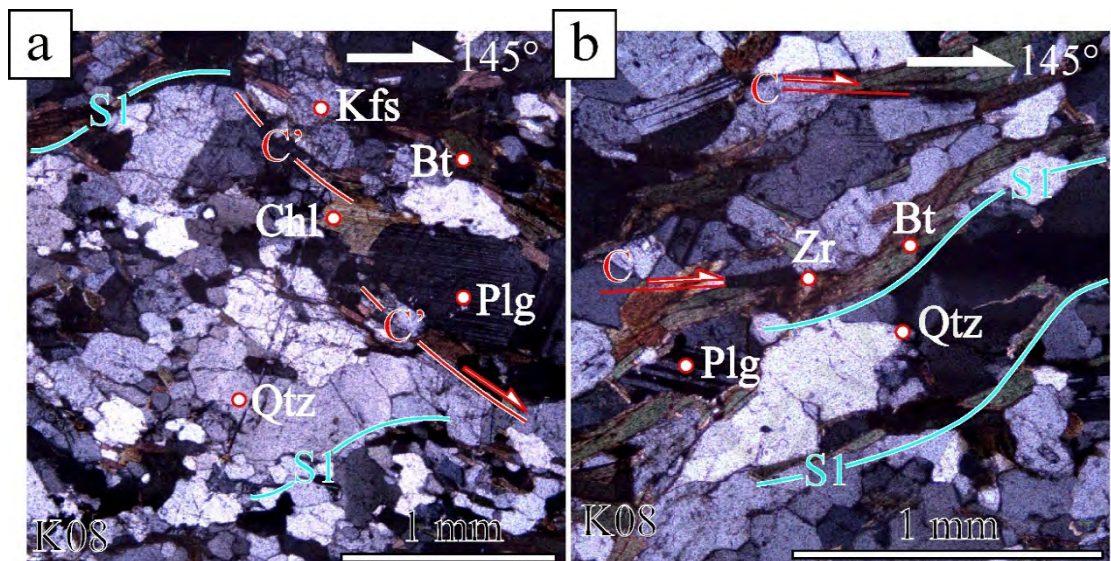


**Figure 4.32: Photomicrograph of sheared Kemahang granite in the western domain of the unit**

The rock is composed of quartz, plagioclase and K-feldspar as well as large biotite flakes, where it defines a weak continuous disjunctive foliation fabric. Individual grains in the quartz and feldspar aggregates are inequigranular with high angle contacts where in part the boundaries are interlobated. The long axes of these aggregates are oriented along foliation plane, interlayered with biotite. The quartz and feldspathic aggregates display dominantly wavy extinction. Minor patchy extinction was observed in K-feldspar, whereas plagioclase display both albite and deformation twinning indicating recrystallization mechanism by grain boundary rotation (SGR).

- Sheared Granodiorite; Dimensi Timal Sdn. Bhd. Lineation:  $120^\circ \rightarrow 48$ .

Major: Qtz, Plg, Kfs, Minor: Bt, Mcv. Trace: Zr

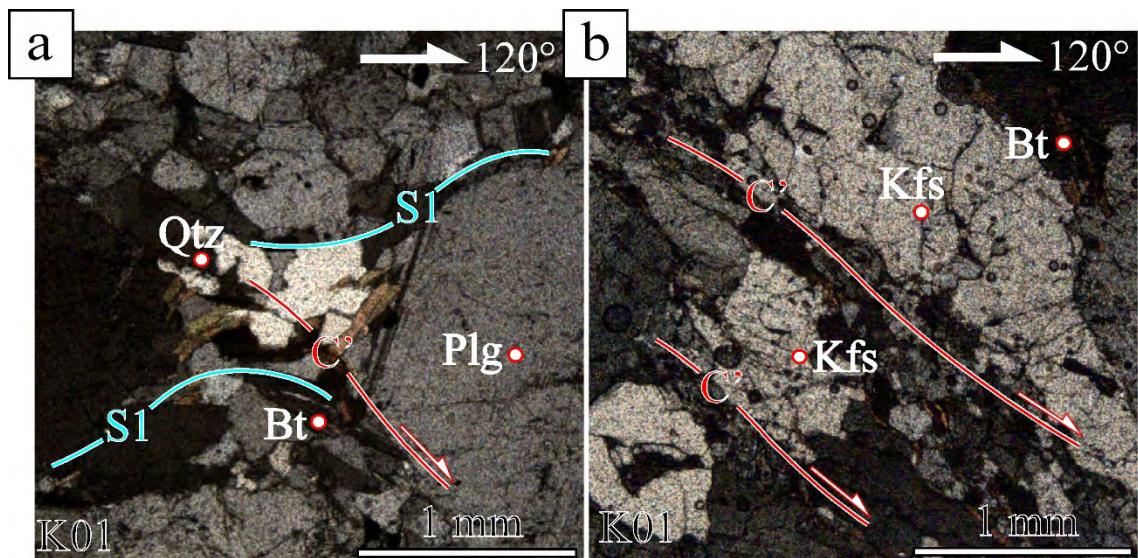


**Figure 4.33: Photomicrograph of sheared Kemahang granodiorite in the eastern domain of the unit.**

The granitic sample displays coarse quartz, plagioclase and K-feldspar as well as large biotite flakes and hornblende (Figure 4.33). The quartz and feldspar aggregates show shape preferred orientation, and biotite shows parallel alignment defining continuous disjunctive foliation fabric (S1). The quartz show wavy extinction, internally divided sub-grains and preferred orientation of neocryst indicating recrystallization mechanism via grain boundary rotation (SGR). The feldspars show patchy extinction, enveloped by biotite forming prophyroclasts, and some are fractured at right angles along cleavages. Incipient recrystallization was also observed within rims of the feldspars. The development of  $\sigma$ -shapes feldspar prophyroclasts are related to steeply inclined C'- shear bands that cut the foliation indicating top-right movement towards SE ( $120^\circ \rightarrow 48$ ).

- Quartz- mica hornfels; Polytechnic Jeli

Major: Qtz, Bt. Minor: Src, Chl

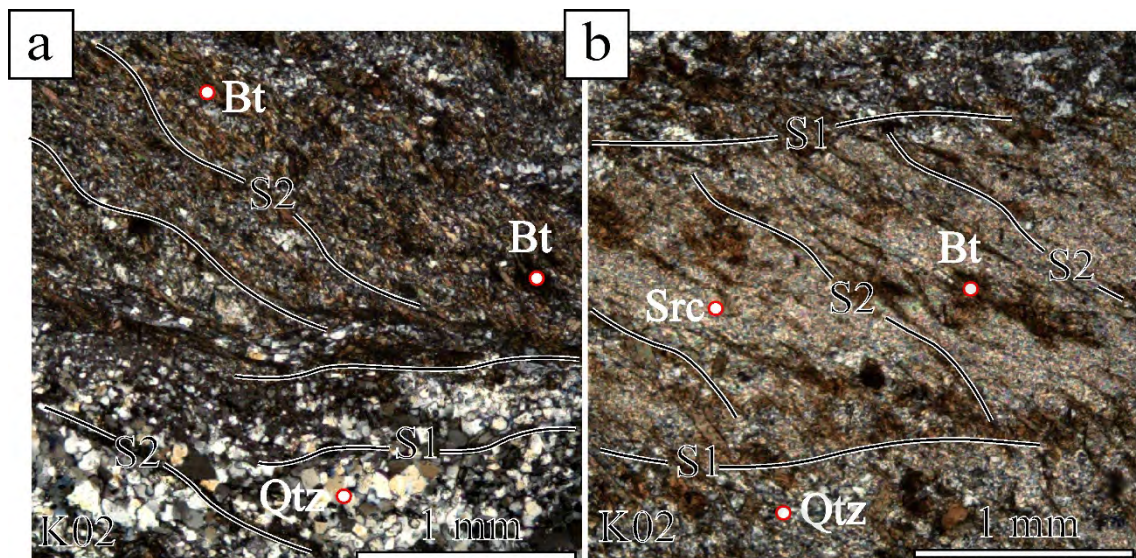


**Figure 4.34: Photomicrograph of quartz-mica enclaves (Taku Schist), in Kemahang granite at Polytechnic Jeli.**

The sample represents meta-sedimentary enclaves of the Taku Schist, which primarily composed of fine-grained quartz aggregates and biotite flakes (Figure 4.34). The disjunctive foliation fabric (S1) is define by compositional layering of quartz and mica. The rock also develops secondary foliation (S2), observed by preferred alignment of sericite with biotite oriented oblique to original S1 foliation. The quartz aggregates are fine and equigranular in part shows polygonal shapes that indicate recrystallization by grain boundary area reduction (GBAR) mechanism.

#### 4.5.3 Metamorphic Parageneses

The quartz-mica and quartz-feldspar schist samples display well-developed schistosity, in response to amphibolite-facies metamorphism (M1) by assemblages of muscovite-biotite-garnet minerals. Some of these samples show assemblages of andalusite-biotite-muscovite in response to medium-high temperature contact metamorphism (M2), likely by intrusion of Kemahang Granite. The second episode of

contact metamorphism (M3) was observed by occurrence of quartz-feldspar migmatite near to the unit boundary, whereas the quartz in granite samples shows recrystallization by high temperature grain boundary migration (GBM), likely as result from the intrusion of Stong Complex. The quartz-feldspathic samples within Kemahang granite near to Stong Complex (Noring Granite) also display evidence of retrogradational metamorphism (M4) by widespread occurrence of chlorite within biotite and muscovite. It indicates modification from upper amphibolite-facies to greenschist facies of metamorphism.

## **4.6 The Stong Complex**

### **4.6.1 Field Observation**

#### **4.6.1.1 Berangkat Tonalite**

In field, the exposures are primarily of hornblende-biotite-granite displaying coarse grained phaneritic texture. The granite composition and texture of the Berangkat pluton are similar to Kemahang granite in the north. Across Dabong- Gua Musang road, the granite is comparatively mafic and possesses metamorphic foliation (Figure 4.1 and Figure 4.35a). Many parts of the exposures contain dark greenish, prismatic actinolite enclaves devoid of definite orientation (Figure 4.35b). The preferred alignment of biotite and hornblende defines the S1 metamorphic foliation, striking NS with moderate dips towards East direction (Figure 4.2). There is incipient development of low angle stretching lineation (L1) plunging towards both SE and NW directions. Kinematic analysis of S/C' shear bands indicate top-SE shear ( $160^\circ \rightarrow 10^\circ$ , Figure 4.5). The granitic exposures are often cut by NW-SE trending faults, where kinematic analysis indicates normal dextral oblique movement towards E direction (Figure 4.3,  $90^\circ \rightarrow 28^\circ$ ).

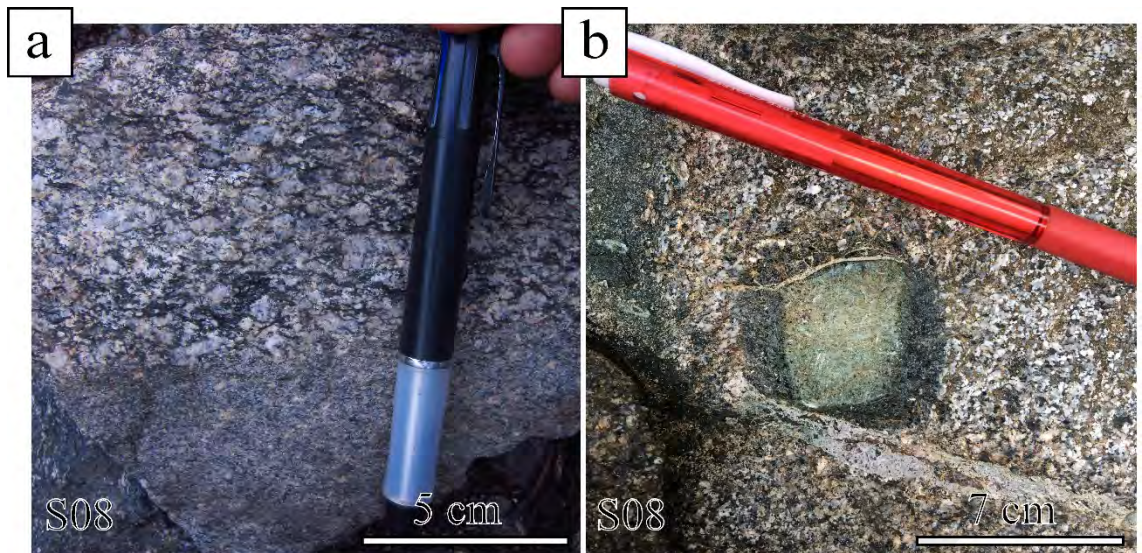


**Figure 4.35: Examples of Berangkat granodiorite exposures, showing (a) a weakly developed metamorphic foliation of granodiorite and (b) randomly aligned actinolite enclaves.**

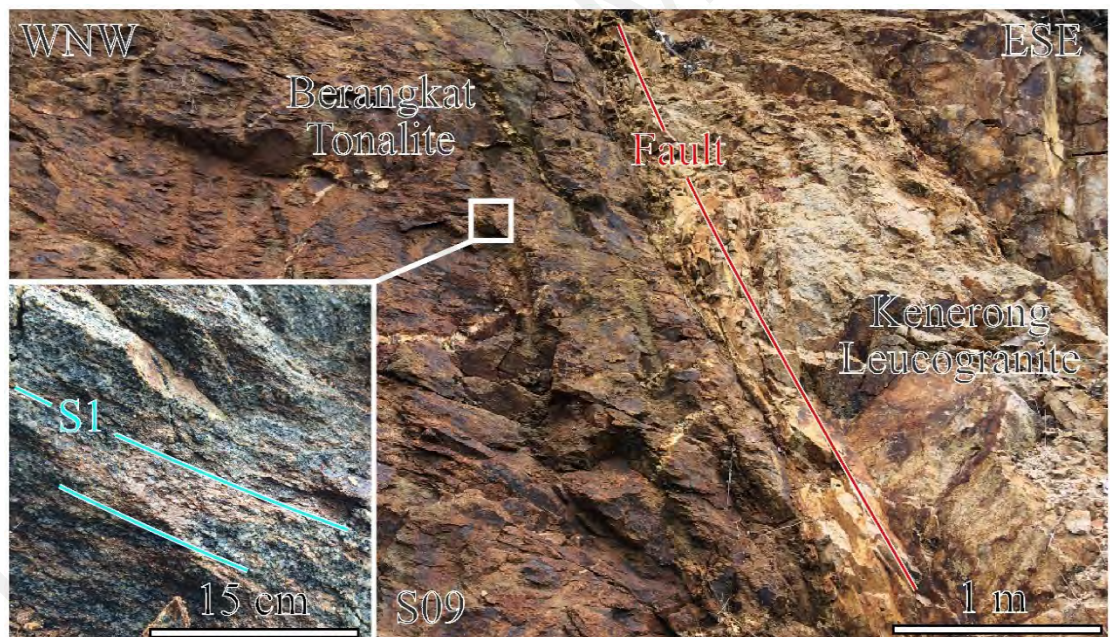


**Figure 4.36: Fault contact between Berangkat tonalite and Kenerong Leucogranite.**

#### 4.6.1.2 Kenerong Leucogranite

Field observations in the upstream of Kenerong River show the primary features of the leucogranite, characterized by light colored biotite-granite displaying coarse-grained phaneritic texture devoid of metamorphic foliation (Figure 4.1, Figure 4.37a). Toward the eastern margin of the granite pluton, the granite occurs as sequences of vein

injections in meta-sedimentary xenolith, in contact by faulting with sedimentary rocks of Gua Musang/Aring formation along Dabong – Kuala Balah road (Figure 4.1). The granitic injections form networks of crosscutting dykes and veins that indicate sequential episodes of granitic intrusions. The earliest injection occurs as lit-par-lit veins intrude parallel to S1 foliation of the meta-sedimentary xenoliths (Figure 4.37a). This results in compositional layered gneisses, oriented along NNE-SSW strikes with intermediate dips towards SE direction (Figure 4.2), accompanied by pervasive low angle stretching lineation plunging towards SE direction. This gneissic rock was further intruded by younger granite injections that subsequently became an enclave of larger granite intrusion (Figure 4.38b and Figure 4.38c). A minor part of the earlier granitic intrusion shows mylonitic texture, characterized by light colored leuco-granite displaying, flattened K-feldspar, quartz and biotite with pervasive stretching lineation. This mylonitic foliation strikes along NNE-SSW direction with gentle dips towards ESE direction (Figure 4.2). Kinematic analysis of this mylonite indicate top-SE shear ( $150^{\circ} \rightarrow 250^{\circ}$ ) (Figure 4.5). The final episode of dyke intrudes discordant to S1 foliation planes, which represents the major part of the exposures and the granite sub-unit (Figure 4.38c). This subsequent discordant intrusion of larger granitic dykes often contains fractured, disseminated enclaves.

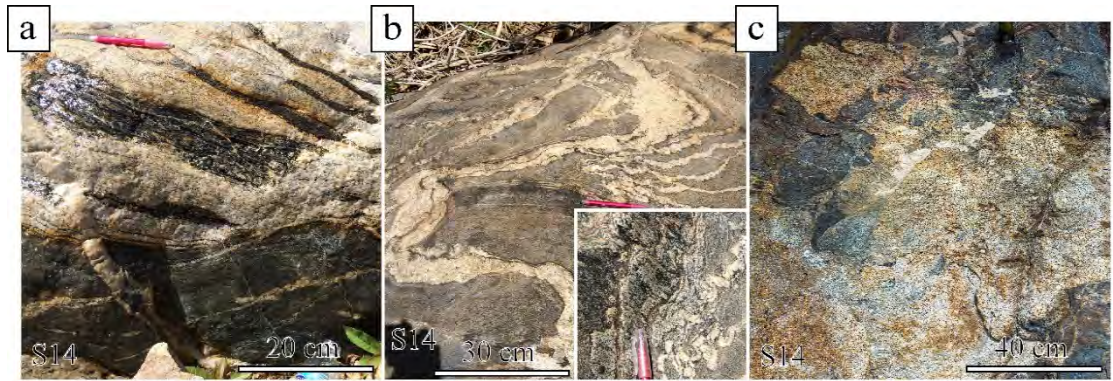


**Figure 4.37: Examples of styles of intrusion observed across Sg. Kenerong (a) A lit-par-lit granitic vein injections, (b) ptigmatic vein injections and (c) large, non- concordant dykes intruded to foliation planes.**

Enclaves in the leucogranitic dykes comprised dominantly of quartz-mica and quartz-feldspar, in addition to marble, calc-silicate, amphibolites and banded chert layers. The foliation in the xenolith consistently strike NNE-SSW to NNW-SSE with intermediate dips towards the E (Figure 4.2), accompanied by uniform stretching lineation (L1) that plunges towards SE direction at low angles. Both quartz-mica and quartz-feldspar contain numerous garnets (almandine) enveloped either as large porphyroblast or smaller grains overgrown onto the matrix. A dark-reddish brown blastose mineral was observed in the calc-silicate xenoliths. The xenoliths also contain intrafolial veins forming continuous boudinages and prophyroclast (Figure 4.40b), which indicates top-SE shears ( $150^\circ \rightarrow 10^\circ$ , Figure 4.5). The xenoliths also contain minor asymmetrical tight folds that plunge perpendicular to the stretching lineation. The foliation formed by parallel alignment of meta-sediments and the early generations of granitic veins are commonly cut by steeply inclined C' shear plane. This results in curved foliation fabric that indicates a top-SE shears ( $160^\circ \rightarrow 30^\circ$ ; Figure 4.38 b and c). Granitic injection into to the C'-shear planes are also observed, which is cut by later dextral faulting toward E-direction (Fp:  $155^\circ \rightarrow 80^\circ$ ). The development of ptigmatic folds is common in the downstream of Sg. Kenerong, situated nearest to plutonic

margin. Patches of chlorites were observed in biotite in close proximity with pygamic veins.

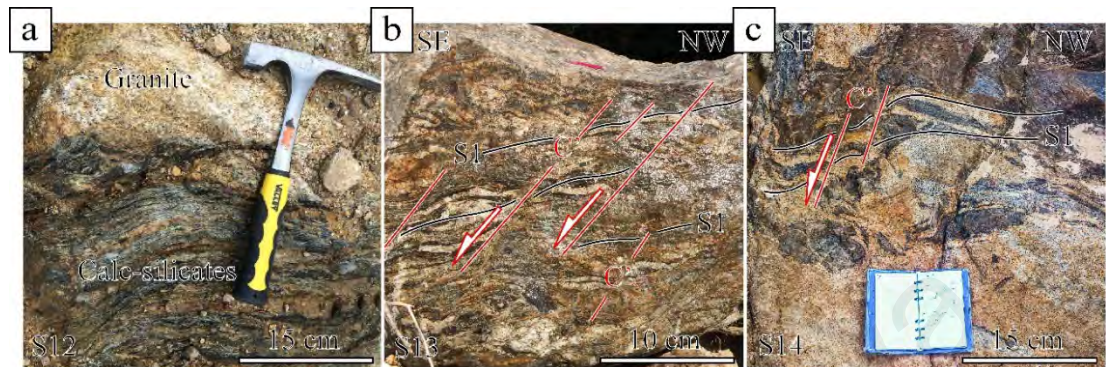


**Figure 4.38: Relations between meta-sedimentary xenoliths and granite at Sg. Kenerong. The meta-sediments include (a) calc-silicate, (b) quartz-mica and (c) quartz-feldspar showing well-developed gneissosity. Sinistral towards SE kinematic movements are inferred in (b) and (c) from crosscutting C'- shear planes.**

An exposure containing migmatite in contact with quartz-mica schist observed in the similar eastern margin of pluton near Bertam Lama. The migmatite develops thin, millimeter-scale compositional layering/ bands of white leucosome and dark-grey melanosome (Figure 4.39), where it shows a narrow but gradual transition to quartz-biotite schist. The foliation plane (S1) is almost horizontal, striking NNW-SSE and inclined towards WNW direction (Figure 4.2). The stretching lineations (L1) in quartz-biotite schist plunge towards both NE and WSW directions. Kinematic analysis of S/C shear bands in the quartz-mica schist indicates top-W shear ( $275^{\circ} \rightarrow 60^{\circ}$ , Figure 4.5). A steeply inclined, NW-SE trending fault cut the exposure where it indicates dextral normal oblique movement towards SSE direction ( $190^{\circ} \rightarrow 65^{\circ}$ , Figure 4.3). In the same exposure, light-colored quartz-feldspar schist is also observed showing similar kinematics as the quartz-biotite schist. About 500 meter towards the east, there is a change from schist-migmatite to sedimentary rocks of the Gua Musang Formation (Figure 4.1). The sedimentary rocks have sub-vertical beds (S0) striking NNW-SSE.

Contact metamorphism is absent and the rocks are cut by NW-SE trending normal fault with kinematic directed towards SE (Figure 4.3).

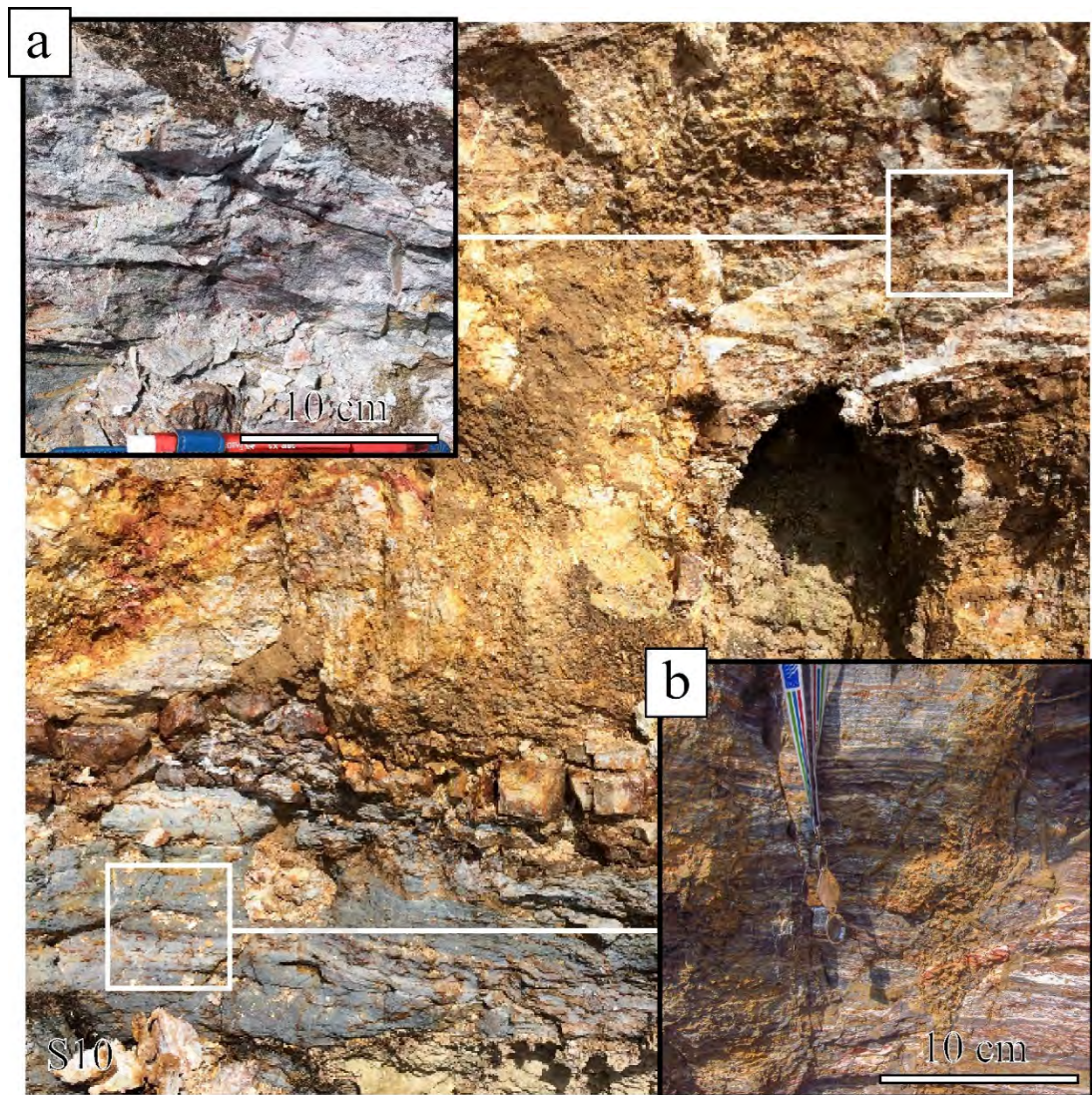


**Figure 4.39: Rock exposure near Kenerong Leucogranite showing transition of (a) quartz-mica schist into (b) migmatite melts**

An exposure situated parallel to eastern margin of pluton shows the presence of garnet-quartz-biotite schist striking NNW-SSE with gentle dips, accompanied by low angle stretching lineation plunging towards SW and NE directions (Figure 4.5). Kinematic analysis of well-developed S/C shear bands and garnet porphyroblasts indicates top-SW shears ( $265^{\circ} \rightarrow 15^{\circ}$ ). The quartz-mica schist is often accompanied by C'-shear plane that results in the development of asymmetrical tight folds plunge

towards ENE direction. Part of the quartz-mica schist displays pervasive crenulations accompanied by numerous small garnet (almandine) likely resulted from contact metamorphism by granitic intrusion.

*Sg. Renyok*

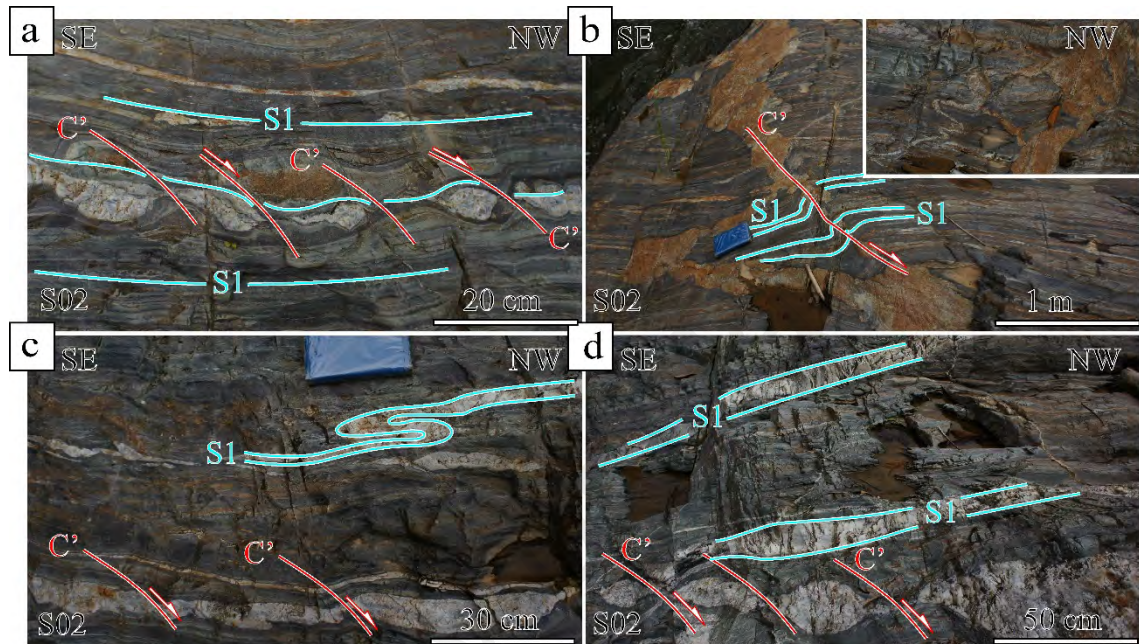


**Figure 4.40: Sheared meta-sedimentary and leucogranite rocks in Sg. Renyok, (a) Lit-par-lit injection of thin leucogranitic dykes, (b) Ptygmatic fold branches of larger leucogranite injection along C'-shear plane, (c) isoclinal fold structures of S1 foliation plane. (d) Stretched boudins crosscut by C'-shear indicates dextral kinematic towards NW.**

Exposure in Sg. Renyok displays pervasive lit-par-lit injections of leucogranitic dykes into meta-sedimentary xenoliths (S02, Figure 4.1). The meta-sedimentary rock is composed of millimeter scale layering of calc-silicate marble, where granitic injection has result in development of subsequent compositional layering with thin biotite-granites (Figure 4.40). The layering and injections define S1 foliation striking NW-SE with moderate dips towards NE direction (Figure 4.2), accompanied by pervasive low angle stretching lineation (L1) plunging towards SE (Figure 4.5). This is further intruded by larger granitic dykes/sill parallel to the foliation planes. The late granite

displays fine-grained phaneritic texture devoid of metamorphic foliation. Injection of ptygmatic veins oriented at oblique angle to the foliation plane of calc-silicate marble, where in part it branches out from larger sets of granitic dykes (Figure 4.40b). The fold axis of ptygmatic folds plunges towards SE and is sub-parallel to the stretching lineation (Figure 4.4). The final set of granitic dykes is the largest and intrude non-concordantly with foliation planes.

The calc-silicate marble contains transposed intra-folial bands of former bedding (S<sub>0</sub>), forming symmetrical isoclinal folds with an axial plane oriented sub-parallel to S<sub>1</sub> foliation (Figure 4.4, Figure 4.40a). A number of asymmetrical features observed in the thin leucogranite veins, such as boudinage, porphyroblast and foliation fishes varying from 10 to 100 centimeter in length that developed by crosscutting NNE-SSW striking C'-shear planes (Figure 4.40). Kinematic analysis of these structures indicate top-NW shear ( $318^\circ \rightarrow 28^\circ$  in Figure 4.5) although minor foliation fishes indicate top-SE shears ( $138^\circ \rightarrow 28^\circ$ ). The C'-shear plane is also associated with bending of the layers by sinistral kinematics towards NW direction. Some dykes are observed to intrude along the C'-shear planes and consequently sheared and result in pinch and swell structures.

#### **4.6.1.3 Noring Granite**

The northern-most sub-unit of the Stong Complex were primarily exposed along the East-West Highway near Batu Melintang area, as well as along the trunk road from Long River and towards Suda Dam in Gunung Basor Forest Reserve (S15; S17; Figure 4.1). The granite does not develop any penetrative metamorphic foliation and are largely non-deformed (Figure 4.41a).

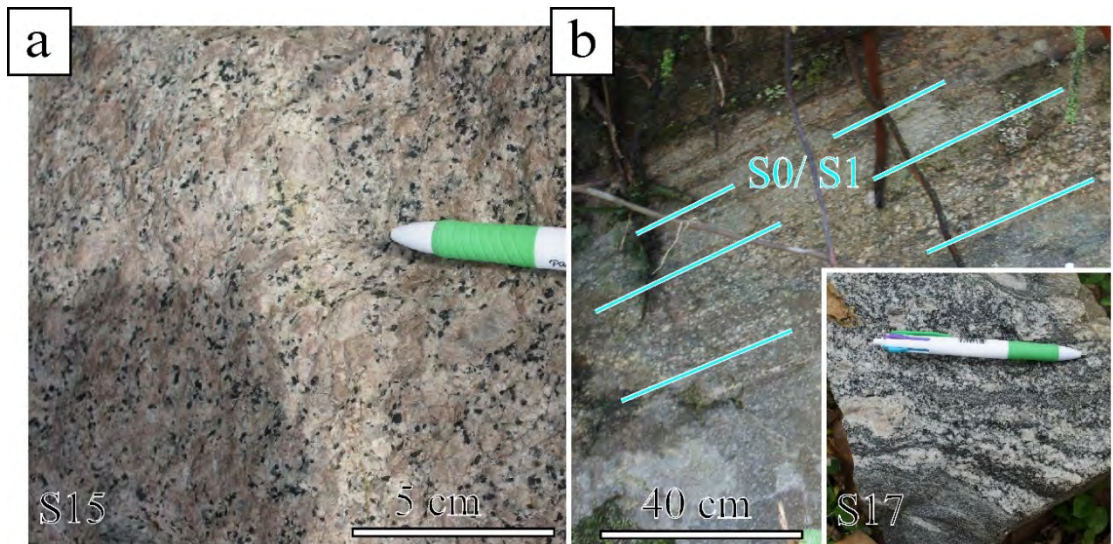


**Figure 4.41: Examples of Noring granite exposures in G. Basor Forest Reserve; (a) primary granitic fabric and (b) magmatic foliation with biotite- rich schlieren zone in gradation to porphyritic granite.**

Composed primarily of hornblende-biotite-granite, it displays coarse-grained porphyritic texture with large pinkish K-feldspar megacrysts showing shape preferred orientation representing magmatic foliation (S0). In the Gunung Basor Forest Reserve adjacent to Kenerong sub-unit, parts of the granite displays schlieren zones or layering with gradational transition from mafic biotite-hornblende to felsic-quartz feldspar zones (Figure 4.41b). The layering strikes NNW-SSE and dips towards ENE direction, oriented sub-parallel to magmatic foliation (S0) of Noring granite or metamorphic foliation (S1) of Tiang Schist/ Kemahang granite (Figure 4.2 and Figure 4.41b). Several exposures across the Forest Reserve are cut by NNE-SSW trending faults, with kinematic analysis indicates normal dextral oblique movement towards E-NE direction ( $65^\circ \rightarrow 15^\circ$ , Figure 4.3). A minor microgranite exposure containing fine-grained phaneritic biotite-granite was also observed within the central part of the Forest Reserve.

In the north, many exposures show the intrusion of Noring granite into an older Kemahang granite, for example: near Kg. Sg. Rual, along the EW- highway and at the

hydroelectric dam near Kg. Batu Melintang (G07, Figure 4.1). Despite well-defined contact metamorphism observed in the adjacent Gua Musang Formation, the contact between Noring granite and the sedimentary rocks is not observed in the field. Exposures at Lata Tubur near the hydroelectric dam in Batu Melintang contain large host rock xenoliths (Figure 4.42) intruded by Noring granite, where the granite similarly displays coarse-grained pinkish K-feldspar megacrysts (Figure 4.40a). Intrusion of granite is discordant to the foliation planes of the host rocks, where metasomatism occurs along the margin of granitic dykes (Figure 4.42a). This results in compositional difference between both rocks near to the contact. Aplitic veins further inject into both the granitic and country rocks discordant to foliation fabric in the final stages (Figure 4.42b).

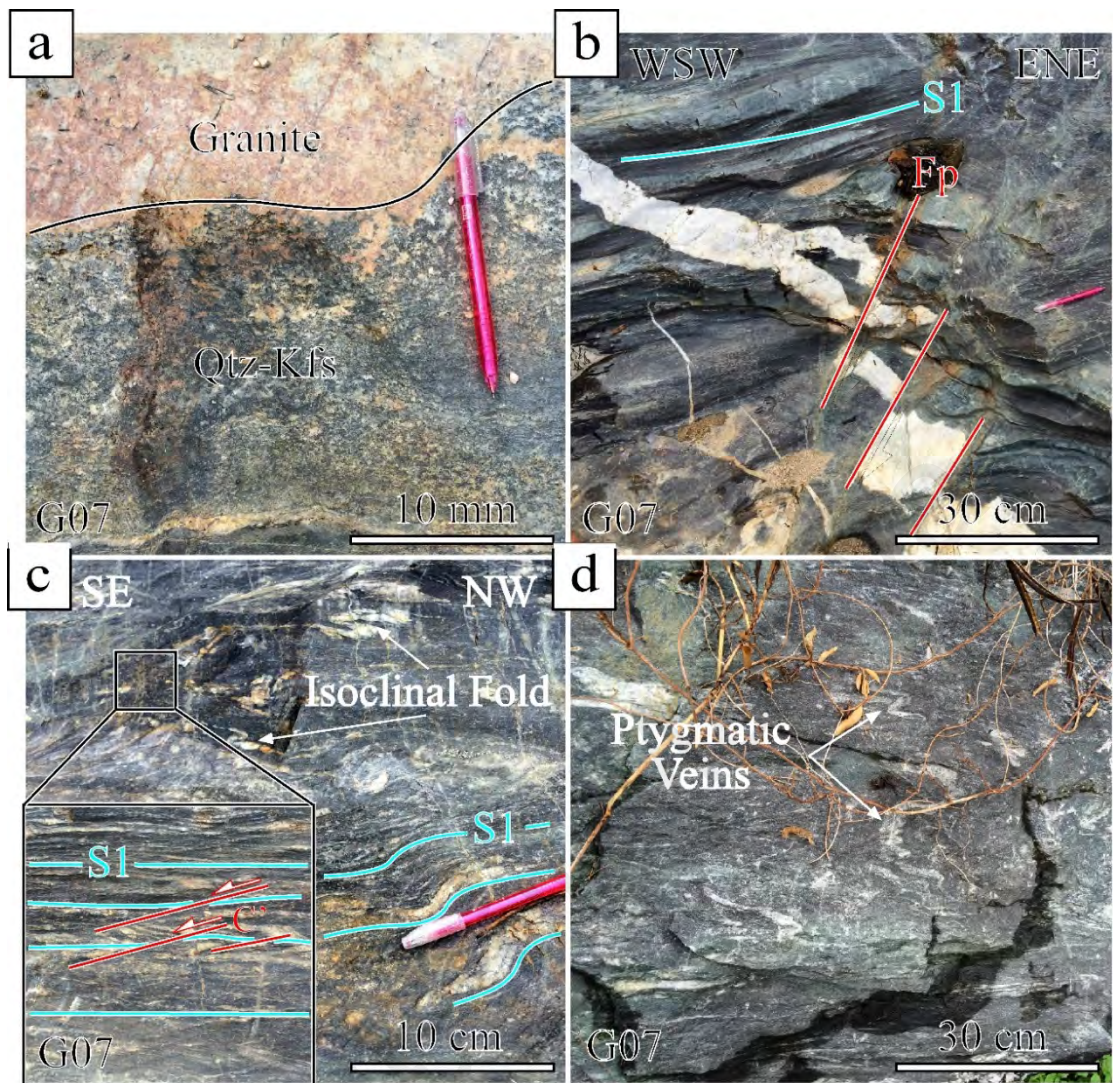


**Figure 4.42: Sheared meta-sedimentary xenolith exposure in Lata Tubur, (a) contact between granite and country rock, (b) late stage aplitic intrusion cut by dextral faulting, (c) quartz- feldspar gneiss and crosscutting C'- shear plane and (d) aplitic injection forming ptygmatic fold.**

The host rock forming xenolith in Lata Tubur, Batu Melintang composed dominantly of quartz-mica and quartz-feldspar gneiss in addition to amphibolite gneiss (Figure 4.42a, c). The NNE-SSW striking foliation planes (S1) dip towards E direction (Figure 4.2) and accompanied by pervasive low angle stretching lineation (L1) consistently plunges towards SSE direction. The quartz-biotite gneiss has elongated quartz ribbons interlayered with biotite forming compositional bands, and they envelop garnet (almandine) into porphyroblast structures. In comparison, the quartz-feldspar gneiss

display well-developed C'-shear bands, feldspar prophyroclast and (Figure 4.42c). On all cases, the kinematic analysis indicates top-SE shears ( $150^\circ \rightarrow 20^\circ$  in Figure 4.5). Some quartz-feldspar gneiss samples contain dark spotted andalusite that are flattened and display shapes preferred orientation parallel to S1 foliation. The quartz-biotite gneiss also contains injection of aplitic veins forming ptygmatic folds that crosscut the foliations. The ptygmatic folds plunge towards SSE direction, sub-parallel to L1 stretching lineation (Figure 4.42d). Patches of chlorite are observed surrounding the ptygmatic veins.

University of Malaya

## 4.6.2 Petrographic Study

### 4.6.2.1 Microstructural Observation

- Quartz-feldspathic hornfels; Sg. Kenerong. Lineation:  $120^\circ \rightarrow 30^\circ$ .  
(Xenolith) Major: Kfs, Plg, Qtz, Bt. Minor: Sil, Chl, Grt. Trace: Zr.  
(Veins) Major: Qtz, Kfs, Plg. Trace: Zr.

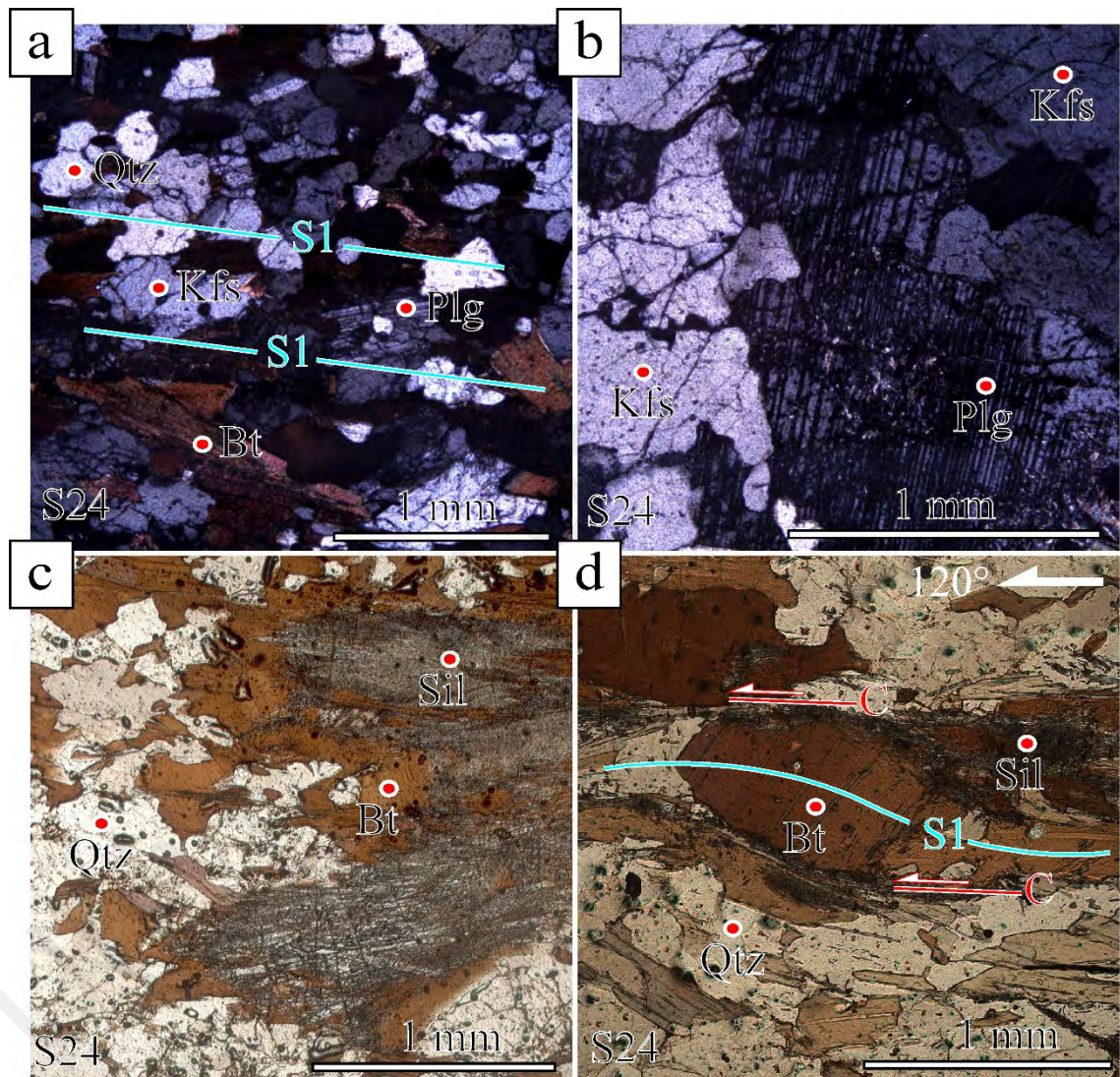


**Figure 4.43: Photomicrograph of quartz-feldspar hornfels, forming xenoliths in Kenerong Leucogranite at Sg. Kenerong. (a) Developed S1 foliation within the xenolith (b) Fabric of intruded pygmatic vein (c) biotite containing sillimanite within the core (d) biotite forming  $\sigma$ -prophyroblast**

The meta-sedimentary xenolith (Figure 4.43 a, c, d) is composed of coarse grains of quartz, plagioclase and K-feldspar interlayered with biotite micas forming continuous disjunctive foliation fabric, S1. Individual grains in the quartz and feldspar aggregates display amoeboid shapes with bulged outline, where the aggregates overgrown into the sheet silicates. Feldspars also occur as large, euhedral mineral surrounded by fine-grained recrystallized aggregates with polygonal outlines. The quartz displays strongly amoeboid shapes with bulged outline, where it shows internally divided sub-grain. These features indicate recrystallization mechanism operated within both quartz and feldspar controlled by grain boundary rotation (SGR). The garnet (almandine) contains numerous inclusions of fine quartz that results in poikiloblastic texture, although the inclusions lack a definite orientation. While some of the garnets are enveloped by biotite show evidence of being rotated, other garnets occur as static blastose minerals overgrown into the matrix. The rock also contains numerous sillimanite occurring as stacks of needles often observed within the core of biotite micas, oriented sub-parallel to the foliation plane (Figure 4.43c, d). Kinematic analysis of biotite C'-shear bands and prophyroclasts (Figure 4.43d) indicates dextral movement with minor oblique movement towards SE ( $120^\circ \rightarrow 30$ ).

In thin section, the ptigmatic vein (Figure 4.43b) is composed of large plagioclase, K-feldspar and quartz grains showing interlobate outlines. These minerals do not show any deformational or recrystallization features. Biotite near to the veins contains abundant sillimanite needles, where it developed near to the rims of biotite micas. Some of the biotite plates are chloritized and the feldspars are sericitized.

- Calc-silicate hornfels; Sg. Renyok. Lination:  $318^\circ \rightarrow 20^\circ$ .

Major: Ca, Plg, Kfs, Chl. Minor: Qtz, Hbl

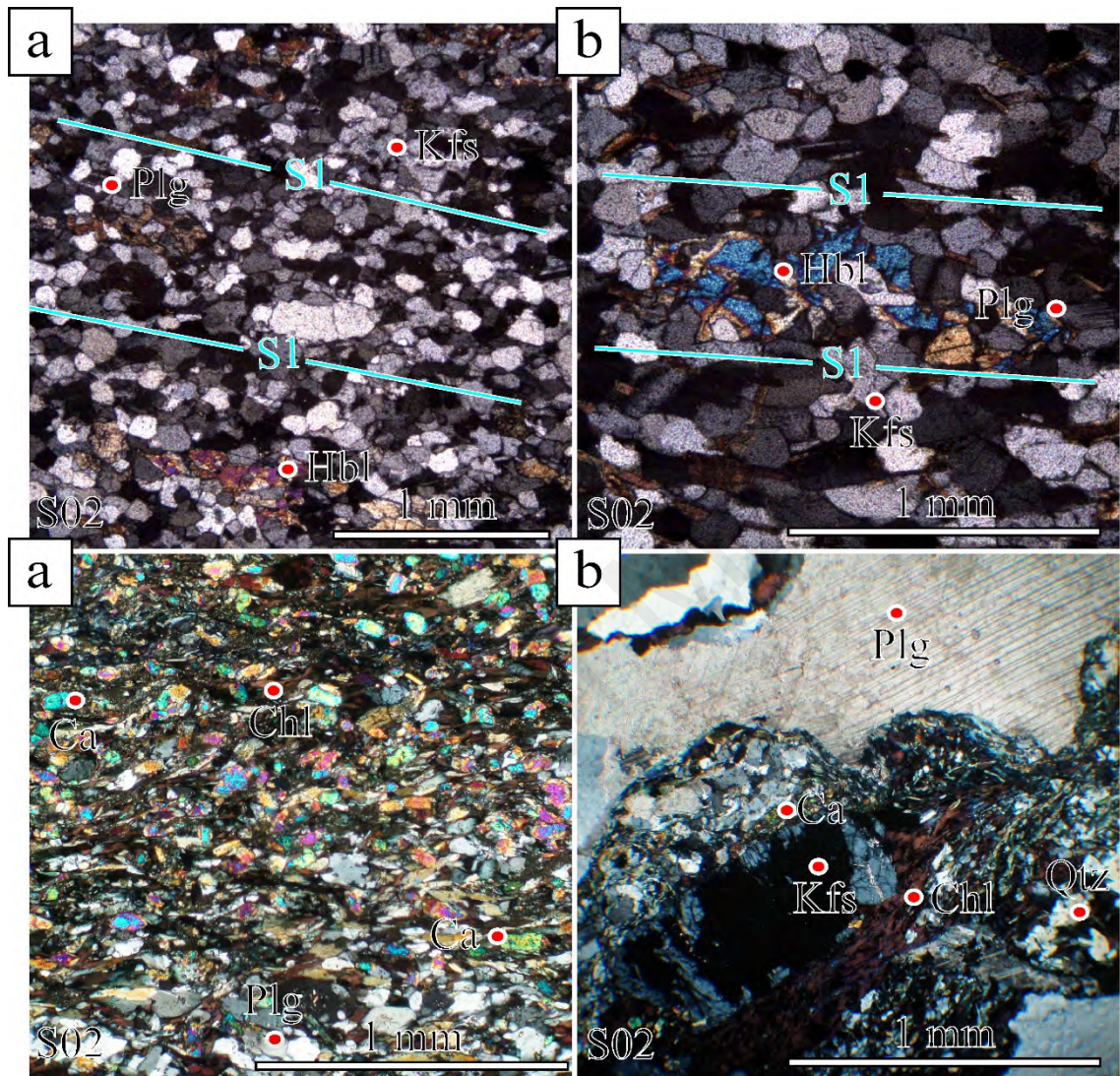


**Figure 4.44: Photomicrograph of calc-silicate hornfels xenolith in Kenerong Leucogranite at Sg. Renyok.**

The calc-silicate hornfels (Figure 4.44) is composed of layers of fine grained calcite, plagioclase, K-feldspar alternating with chlorite, hornblende and biotite-rich layers, which defined the foliation fabric (S1). Individual grains in the feldspar-epidote aggregates show equigranular, polygonal shapes overgrown into the biotite. A wavy extinction is observed in the feldspars, and primary albite twinning observed in plagioclase.

- Sheared Berangkat Tonalite; Gua Musang. Lineation:  $150^\circ \rightarrow 20^\circ$ .

Major: Qtz, Kfs, Hbl, Bt. Minor: Src, Chl. Trace: Titanite

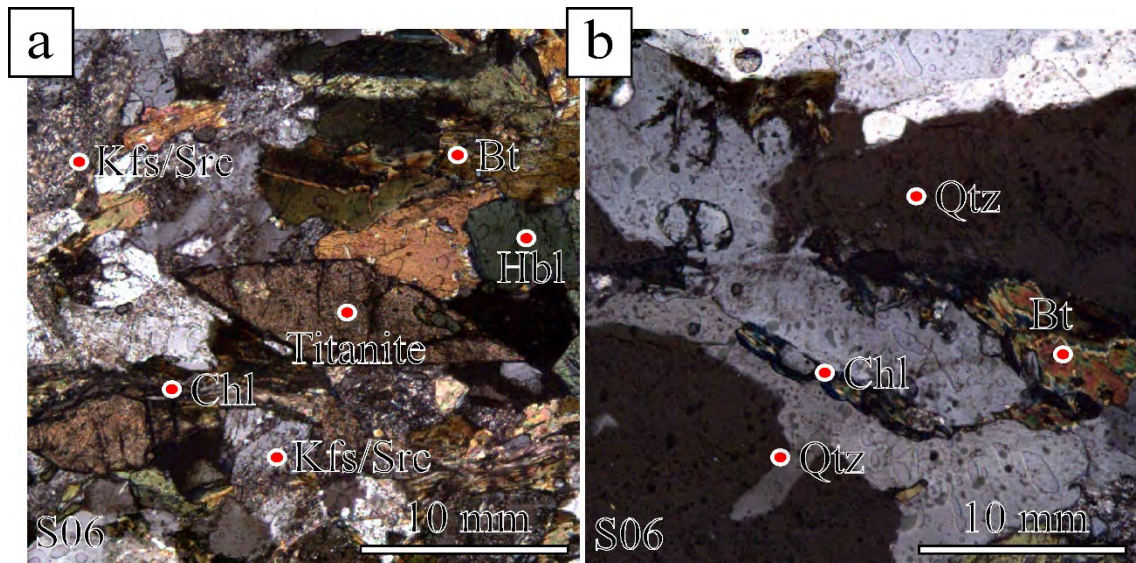


**Figure 4.45: Photomicrograph of sheared Berangkat tonalite at Gunung Stong, Dabong.**

The sheared granite (Figure 4.45) comprises of coarse-grained quartz, K-feldspar, plagioclase and biotite. It shows a weak development of penetrative foliation (S1) by preferred alignment of biotite. Individual grains in the quartz and feldspar aggregates shows strongly bulged outlines and indicate recrystallization by grain boundary migration (GBM) mechanism. The rock is affected by secondary alteration, such as intense chloritization of biotite along the foliation fabric as well as widespread sericitization of the K-feldspar.

- Quartz-feldspar, amphibole hornfels, Noring granite: Lata Tubur.

Lination:  $150^\circ \rightarrow 20^\circ$ .

(Amphibole hornfels) Major: Qtz, Hbl, Kfs, Plg, Bt.

(Quartz-feldspar hornfels) Major: Qtz, Plg, Kfs. Minor: Bt Hbl, Plg, Cal .Trace: Zr

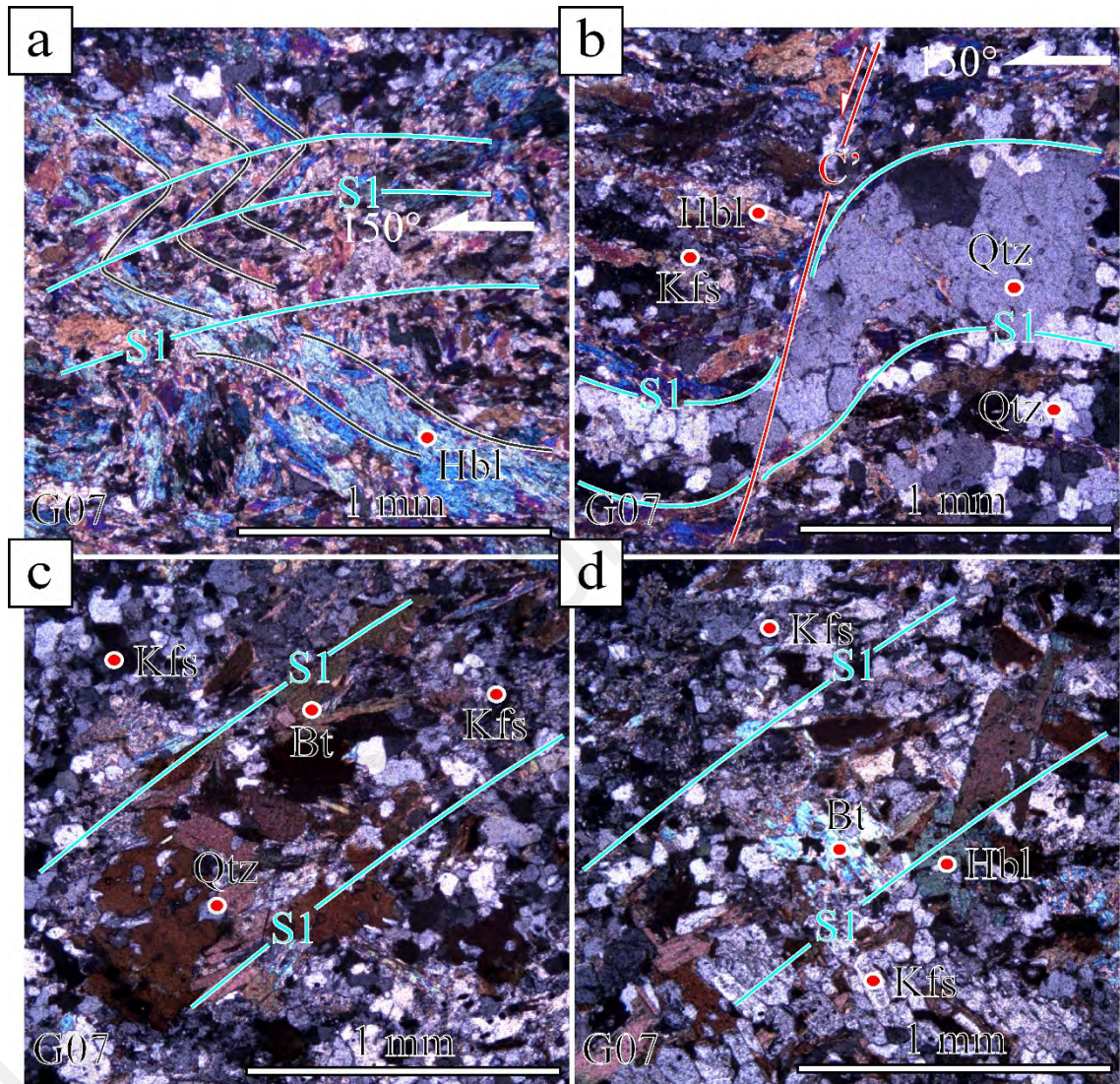


**Figure 4.46: Photomicrograph of amphibole hornfels. (a, b) and quartz-feldspar hornfels (c, d) xenolith of Noring Granite at Lata Tubur.**

In the amphibole hornfels (Figure 4.46a, b), the compositional banding between quartz-feldspar aggregates alternating with stacks of prismatic hornblende defines the spaced crenulated foliation fabric, S1. The crenulations are formed by development of hornblende minerals to spaced recumbent open fold structures. The quartz aggregates

show wavy extinction. They are fine- to medium-grained and the shapes outline are mostly lobate in parts are polygonal. Fine-grained, recrystallized K-feldspar and plagioclase are also observed within matrix typically surrounding hornblende. Both of quartz and feldspar indicate recrystallization mechanism dominated by grain boundary migration (GBM). Some of the hornblendes are oriented oblique to foliation (S1). This structure is interpreted as either wide C'- shear bands or narrow, steep micro-faults. The crosscutting C'-shear bands display dextral movement indicating top- SE shears ( $150^\circ \rightarrow 20^\circ$ ).

The quartz-feldspar hornfels (Figure 4.46c, d) is composed of fine-grained quartz, K-feldspar and plagioclase aggregates displaying an imperfect polygonal shapes with high angle contacts. Some feldspars show inequigranular-ameoboid shapes with strongly interlobated contacts. It indicates recrystallization within quartzo-feldspathic aggregates operated by grain boundary migration (GBM) mechanism. The biotite flakes stacked between the aggregates grow to large sizes, in part contain fine quartz inclusions and show weakly preferred alignment defining the foliation. Some biotite micas shows transformation to chlorite, where it shows stronger preferred alignment. In addition, the K-feldspar minerals are affected by sericitization.

#### **4.6.2.2 Metamorphic Parageneses**

The quartz-feldspar, quartz-mica, calc-silicate and amphibolite xenoliths show well-developed schistosity, where the general assemblages are made up of muscovite-biotite-garnet minerals that suggest prograde metamorphism (M1) to the amphibolite facies. The high temperature contact metamorphism (M2) is indicated by assemblage of sillimanite-biotite-muscovite in quartzo-feldspathic samples that indicate upper amphibolite facies metamorphism. This is related to the granitic injections that occur as ptygmatic veins as observed in the quartzo-feldspathic samples. The biotite and

muscovite in sheared granitic samples (Berangkat tonalite) show transformation to chlorite, whereas the feldspars are affected by sericitization. This indicates retrogradational metamorphism (M3) from upper amphibolite facies (M2) to greenschist facies.

## **4.7 Tiang Schist**

### **4.7.1 Field Observation**

The exposures are mainly observed along the East-West highway from Perak to Kelantan state border, as well as roads from Kg. Batu Melintang towards the Thailand border. Exposures near the Main Range Granite are less weathered but exposures degrade in distant due to tropical weathering (Figure 4.1).

Along the EW highway, the exposures are comprised dominantly of quartz-feldspar or quartz-mica schist associated with minor calc-silicate components (Figure 4.47a,b). The quartz-mica schist has preferred alignment of muscovite forming well-developed S/C and S/C' foliations. In quartz-feldspar schist, the feldspars are wrapped within foliated matrix forming prophyroclasts. Parts of foliation fabric (S1) develop mm-scale isoclinal fold that contain the former bedding plane (S1 on Figure 4.47a). The orientation of S1 strikes along NNW-SSE and is steeply dipping towards east direction (Figure 4.3). Well-developed stretching lineation defined by alignment of biotite and muscovite consistently plunges towards SW or NE directions. Both of feldspar prophyroclasts and S/C and S/C' shear bands suggest consistent top- SW shear ( $210^\circ \rightarrow 10^\circ$  on Figure 4.5).

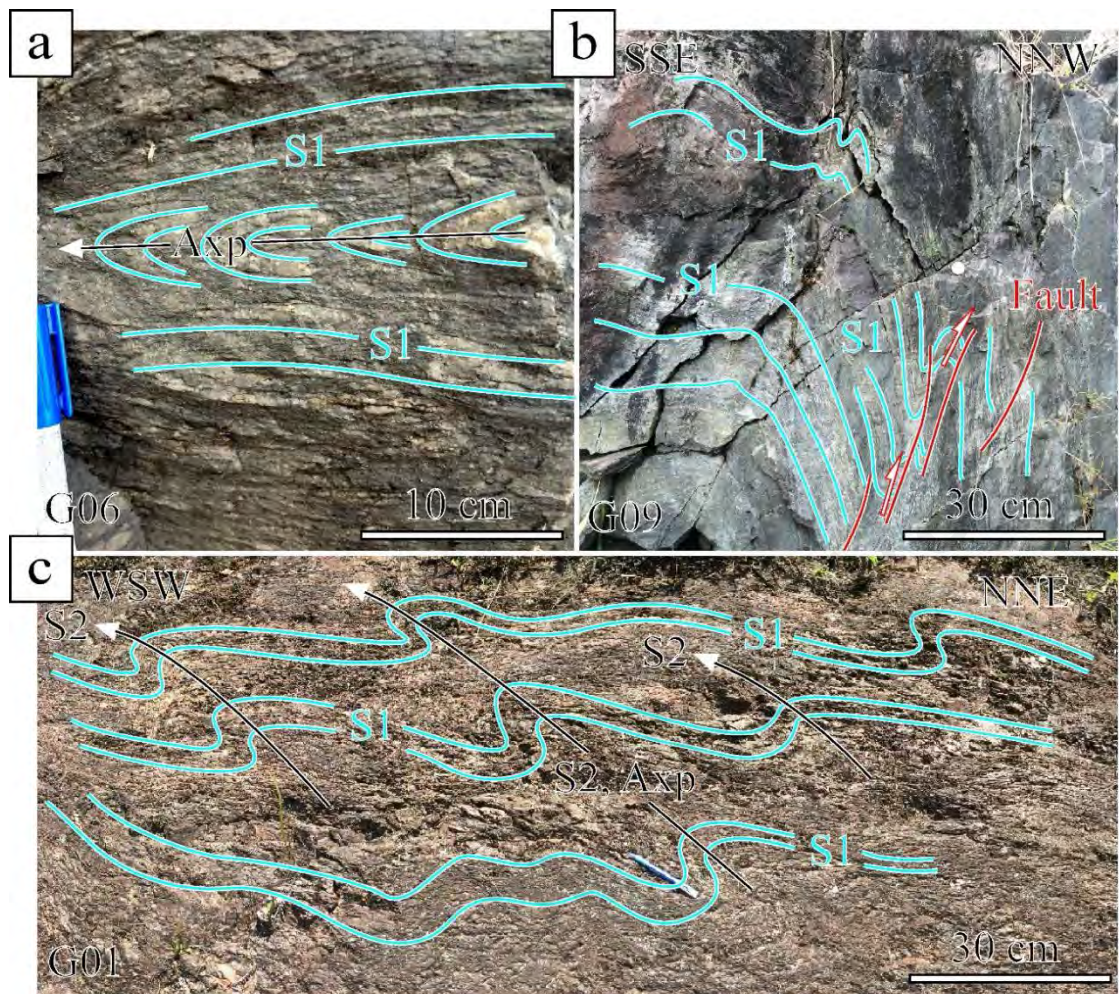


**Figure 4.47: Folded Tiang Schist exposure on EW-highway showing (a) symmetrical tight to isoclinal folding and (b) reverse faulting in quartz-feldspar schist, and (c) pervasive asymmetrical folding of quartz-mica schist.**

One of the exposures across EW-highway displays strongly contorted S1 foliation caused by crosscutting C'- shear plane subsequently resulted in pervasive asymmetrical folds (Figure 4.47c). The shear planes are steeply oriented and strike along NNE-SSW direction. The asymmetrical folds are of centimeter-meter scale with steeply dipping axial plane and tight to isoclinal hinges consistently verges towards westerly direction (Figure 4.47c). In addition, the axis of these folds plunges towards NE and is sub-parallel to the stretching lineation ( $30^\circ \rightarrow 10^\circ$  Figure 4.5).

The quartz-feldspar schist exposures nearest to the Main Range granite are noticeably hard in comparison to other exposures. The S1 foliation plane strikes NW-SE

and dipping at low angle towards SW direction (Figure 4.2). There is pervasive stretching lineation (L1) plunges towards NE at low angles. Kinematic analysis of boudinaged quartz veins and feldspar prophyroclasts indicate shears towards NE direction ( $30^\circ \rightarrow 20^\circ$  in Figure 4.5). Numerous centimeters-scale transposed folds with symmetrical, tight hinge closures oriented parallel to the foliation planes (S1) and plunge towards NNE direction sub-parallel to the stretching lineation (L1). The exposure is also cut by a low-angle, NW-SE striking fault dipping towards SW direction. Kinematic analysis of this fault suggests sinistral strike-slip movement towards SSE direction.

## 4.7.2 Petrographic Study

### 4.7.2.1 Microstructural Observation

- Quartz-mica schist; E-W Highway. Lineation:  $220^\circ \rightarrow 10^\circ$ .

Major: Qtz, Bt, Mcv. Minor: Kfs

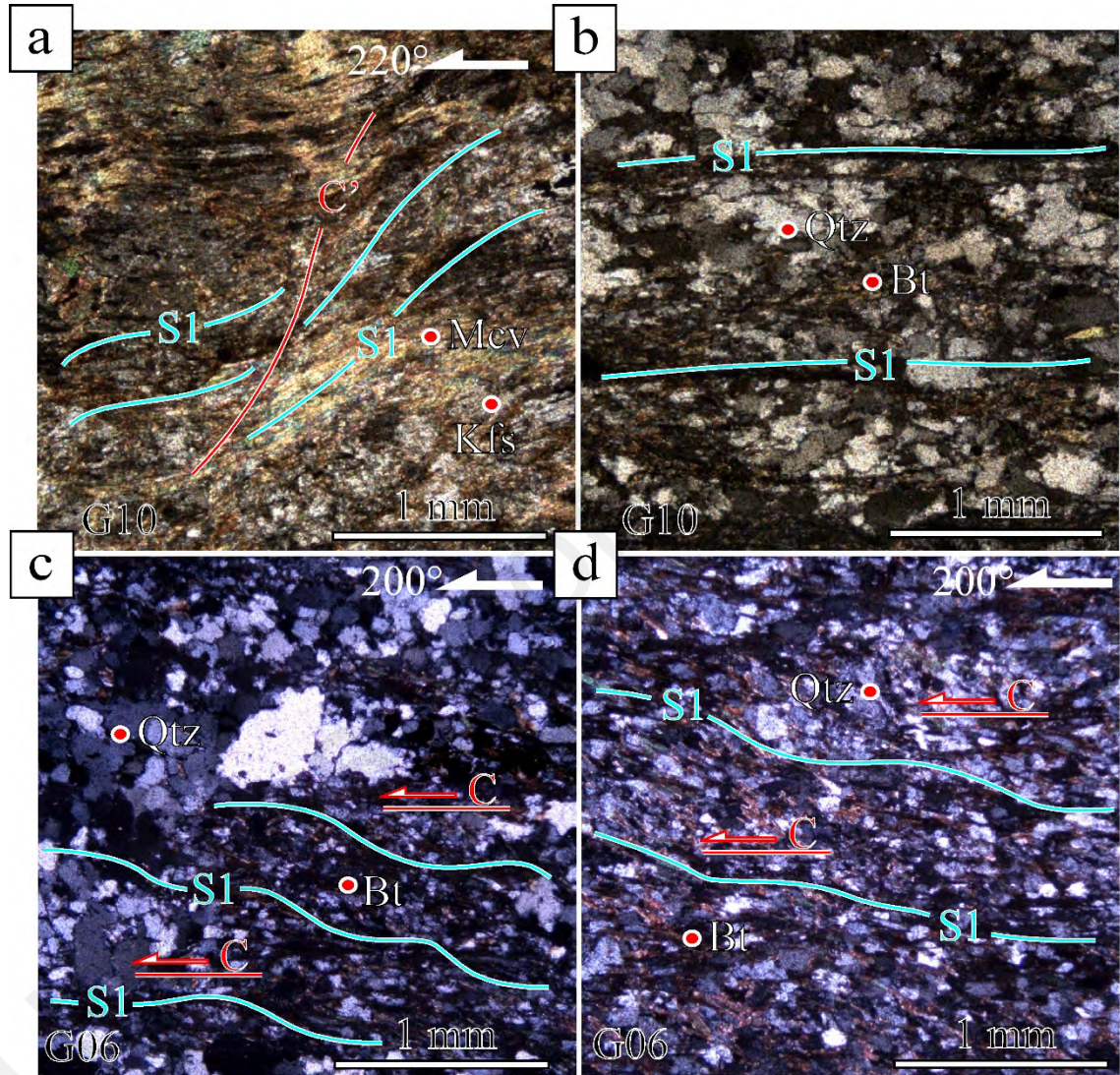


Figure 4.48: Photomicrograph of quartz-mica schist with pervasive shear fabrics (a, b) and contact metamorphosed quartz-mica-schist near Main Range Granite (c, d).

The quartz-mica schist sample in Figure 4.48 a, b is located about 8 km to the east of Main Range Granite. It is composed of muscovite and biotite with preferred alignment interlayer with quartz aggregates forming continuous crenulated schistosity. It is often cut by steeply inclined C'-shear bands which indicates sinistral sense of shear towards WSW direction ( $220^{\circ} \rightarrow 10^{\circ}$ ).

The schist near the Main Range Granite in Figure 4.48c, d is composed of fine to medium quartz and K-feldspar aggregates interlayered with fine biotite and muscovite. The preferred alignment of biotite along sub-horizontal plane defines the continuous disjunctive foliation fabric. Individual grains in the quartz and K-feldspar aggregates shows a dominantly polygonal shapes and possess wavy extinction. Bulged outlines with high angle contact suggest recrystallization by grain boundary migration (GBM) mechanism. Gradational transitions between quartz/K-feldspar-rich and mica-rich domain forms compositional layering. Relics of tight, S-shape asymmetrical folds within biotite are also observed. Relics S/C shear bands indicates sinistral sense of shear towards SW direction ( $200^{\circ} \rightarrow 10^{\circ}$ ).

- Quartz-mica schist; Sg. Kalai. Lination:  $120^\circ \rightarrow 20^\circ$

Major: Qtz, Bt, Mcv. Minor: Adl

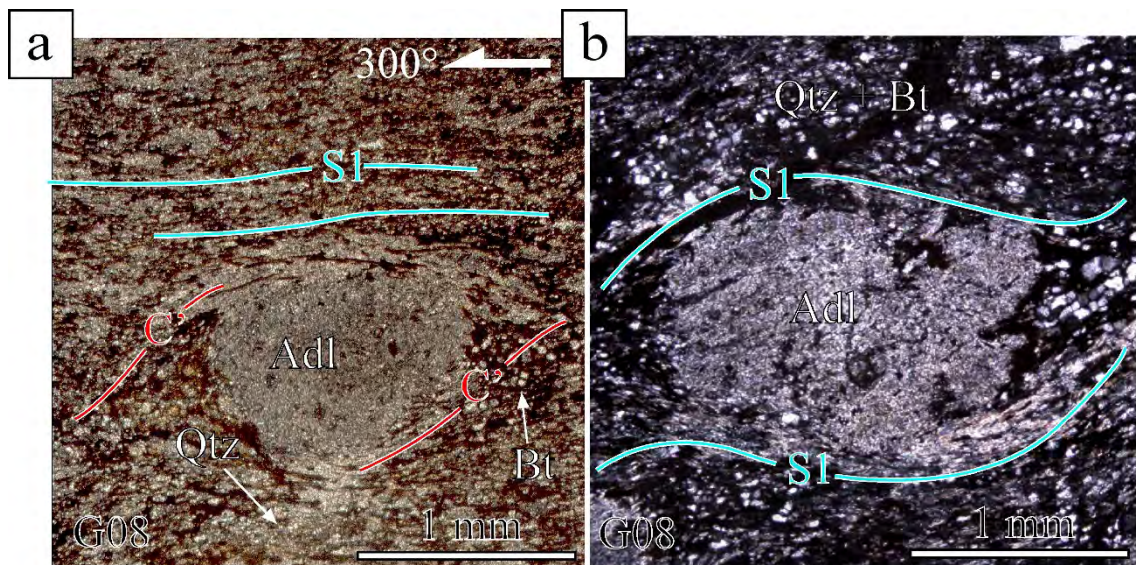


**Figure 4.49: Photomicrograph of andalusite-mica-schist near Kemahang Granite.**

The quartz-mica schist shown in Figure 4.49a, b is composed of fine quartz aggregates interlayered with biotite and muscovite with preferred alignment forming continuous disjunctive schistosity. The rock also contains medium to large andalusite that contains quartz inclusions arranged in straight layers with a spiral end towards the rim. The andalusite enveloped within foliated matrix forming  $\sigma$ -porphyroblasts, which indicate sinistral senses of shears (Figure 4.49a, b). There are well-developed S/C shear bands that indicate similar sense of shear. Both of these kinematic indicators suggest sinistral shear towards SW direction ( $120^\circ \rightarrow 20^\circ$ ).

- Quartz-feldspathic, amphibolite; E- W Highway. Lineation:  $20^\circ \rightarrow 20^\circ$ .  
 (Quartz-feldspar Schist) Major: Qtz, Kfs, Bt. Minor: Chl,  
 (Amphibole Schist) Major: Hbl, Kfs. Minor: Qtz.

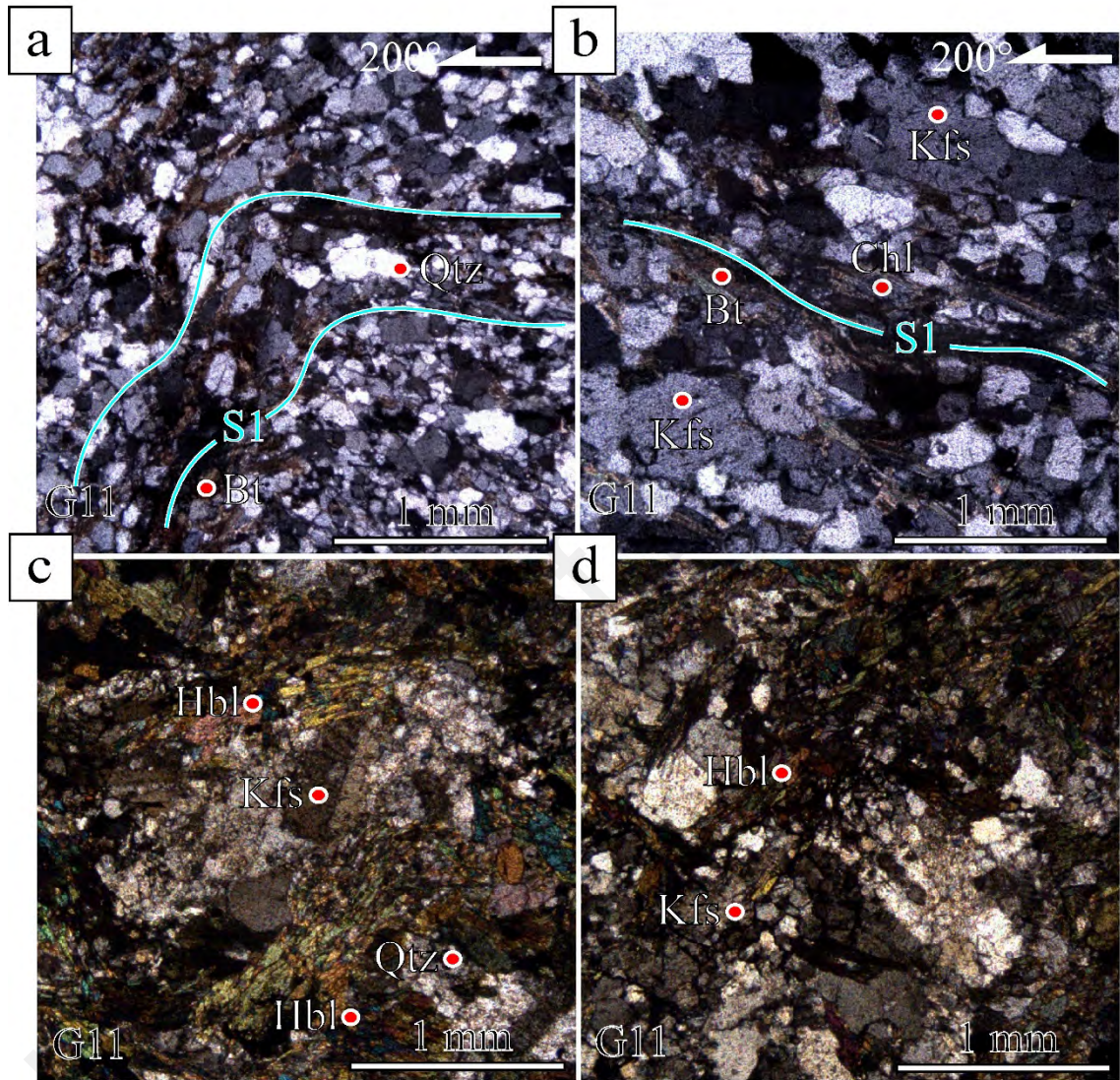


**Figure 4.50: Photomicrograph of contact metamorphosed quartz-feldspathic schist near Noring Granite.**

The schist in the western flank of Stong Complex (Noring granite) is composed of fine to medium quartz and K-feldspar aggregates interlayered with aligned biotite and minor muscovite defining foliation fabric, S1 (Figure 4.50a, b).

Incipient chlorite developed within biotite are aligned along the foliation. The micas are folded into asymmetrical structure, which shows a steeply inclined hinge and gentle closure. Muscovite fishes observed indicates top-SW shears.

#### **4.7.2.2 Metamorphic Parageneses**

The assemblages of biotite-muscovite minerals observed in Tiang Schist samples suggest that the prograde metamorphism (M1) to the lower amphibolite-facies. Intrusion of Kemahang granite has likely resulted in contact metamorphism (M2 (a)) in schist samples near to the pluton, which is indicated by assemblage of andalusite-biotite-muscovite minerals. The contact metamorphism has also been observed in samples near to the Main Range Granite (M2 (b)). In samples nearest to Stong Complex, occurrence of biotite and muscovite that have been transformed to chlorite suggest a retrograde metamorphism (M3) to greenschist facies.

## CHAPTER 5: STRUCTURAL ANALYSIS

### 5.1 Introduction

The orientation and structural styles of the Taku Schist and the surrounding units are shown in Figure 5.1 and Figure 5.3. This study also demonstrates the kinematic of deformations observed across the study area with the tectonic interpretation shown in Figure 5.2 and Figure 5.4.

Four deformation events (D1 – D4) have been interpreted and are discussed in this chapter. The first deformation D1 is related to initial burial and metamorphism of the followed by top – WSW shearing and asymmetric shearing in the second episode of deformation (D2). Symmetric contraction and open folding is inferred as the third deformation event (D3). The final episode of deformation (D4) involve the formation of extensional deformation and large scale exhumation.

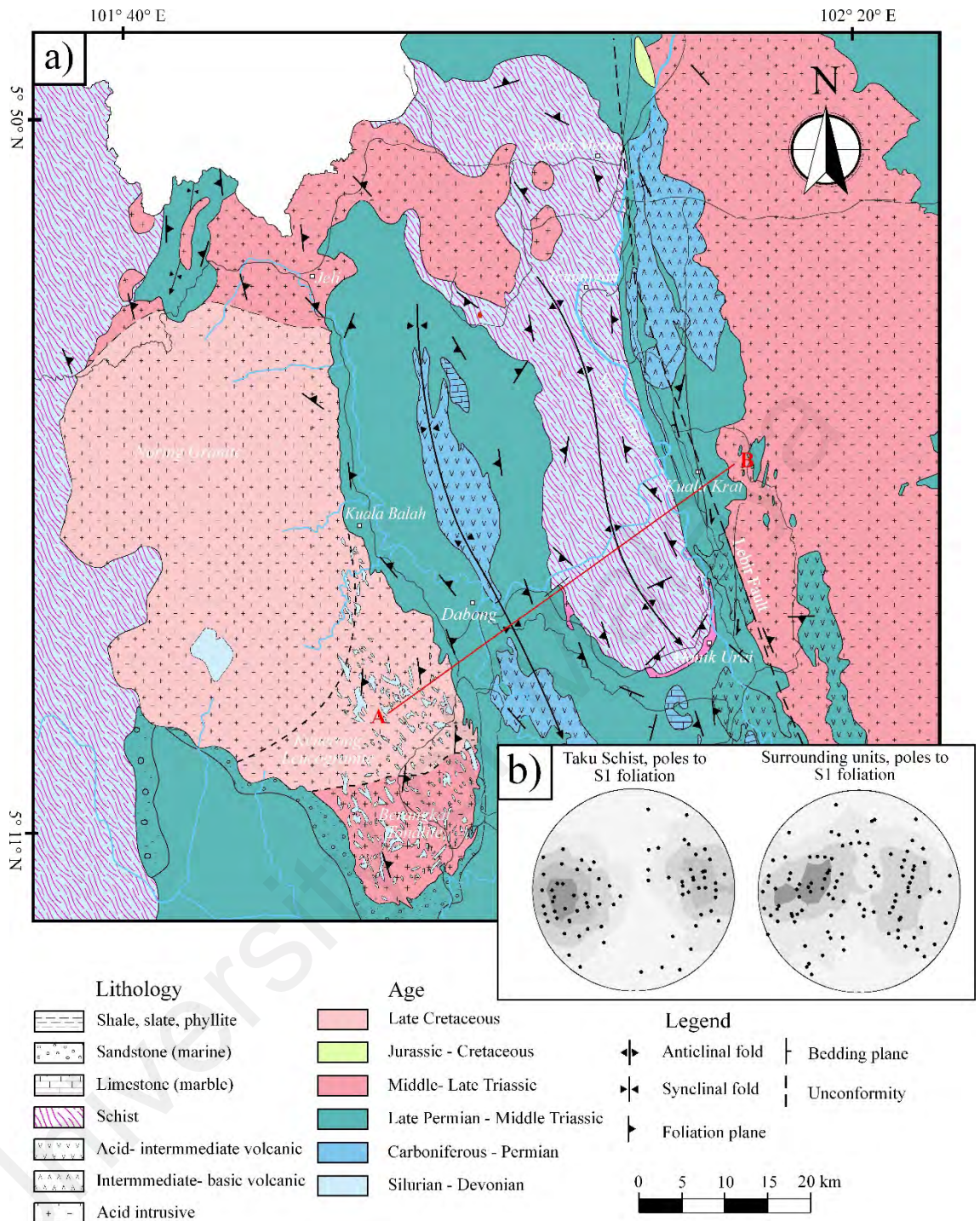


**Figure 5.1:** a) Structural geology map of the study area (modified after *MacDonald, 1968*) with orientation of overall S1 foliation and interpreted antiform-synform structures. b) Stereoplots and contour plots of poles to S1 foliation in Taku Schist and surrounding units.

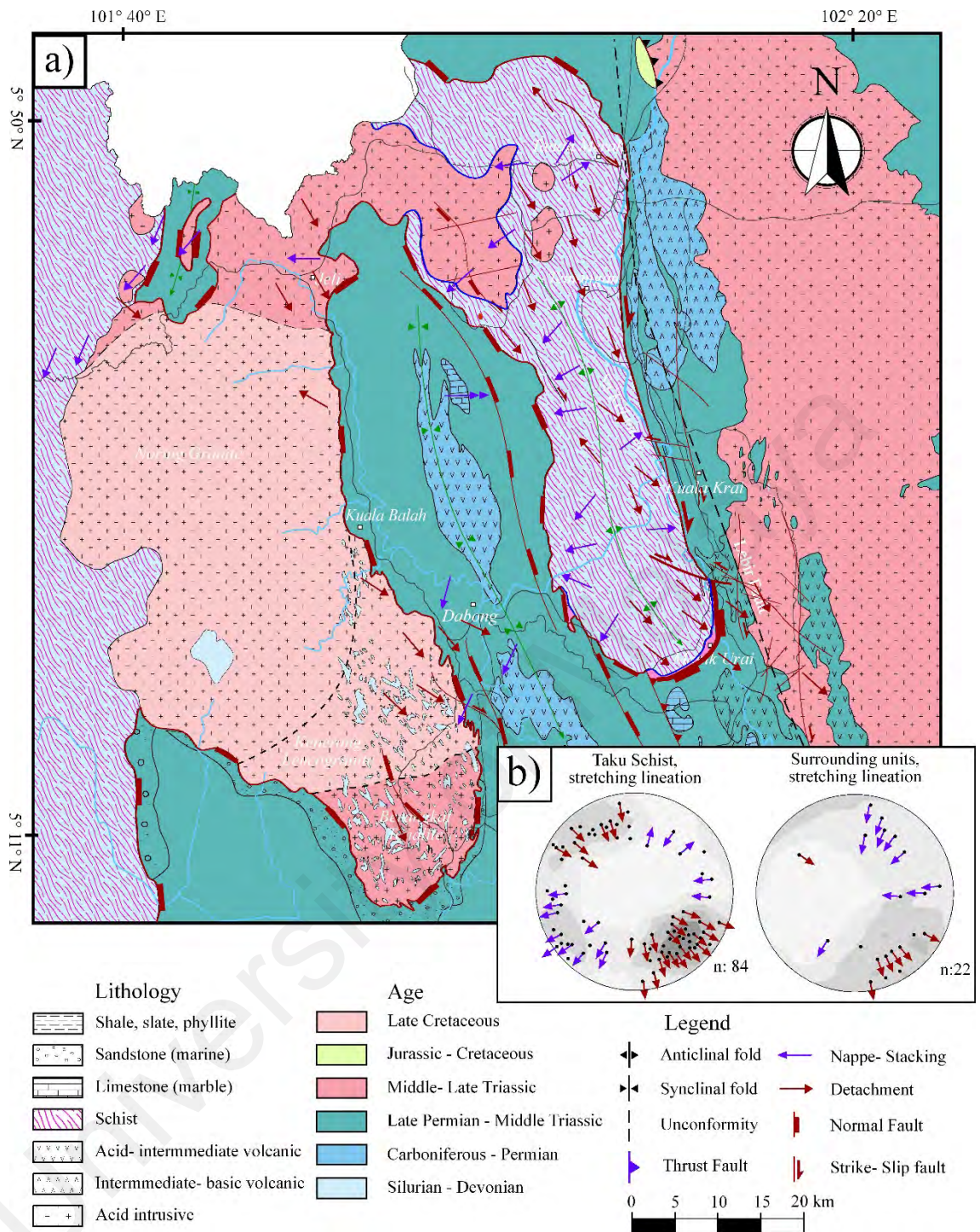


**Figure 5.2:** a) Structural geology map of the study area (modified after MacDonald, 1968) with kinematic results of this study and interpreted tectonic omission. Blue arrows indicate the direction of shearing related to nappe-stacking whereas red arrows indicate shearing related to extension. b) Stereoplots and contour plots of stretching lineation for nappe-stacking and extensional shearing.

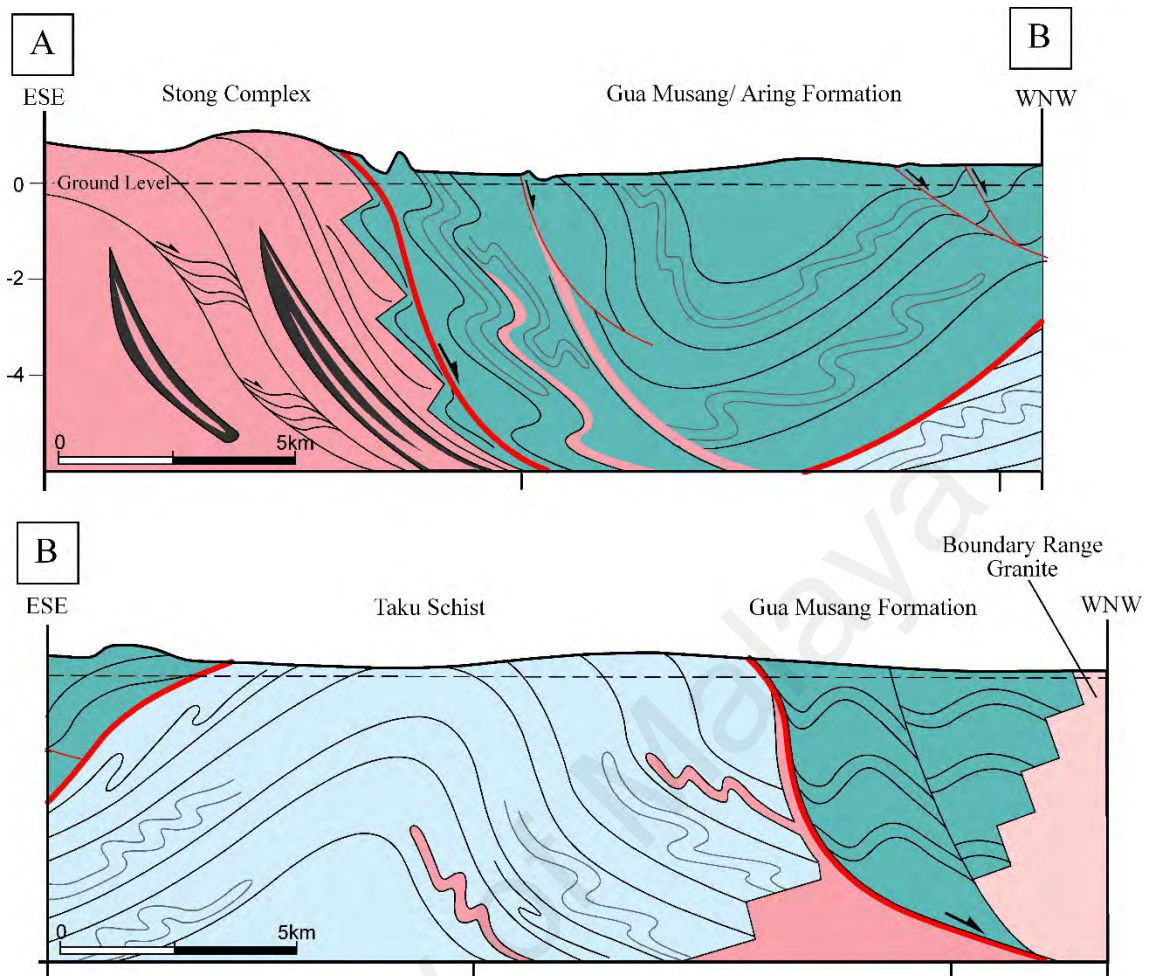


**Figure 5.3: Structural and geological cross-section of the Taku Schist and surrounding units across an east-west transect. The Taku Schist and Stong Complex represent the footwall separated from Gua Musang/ Aring Formation hanging-wall by extensional detachment.**

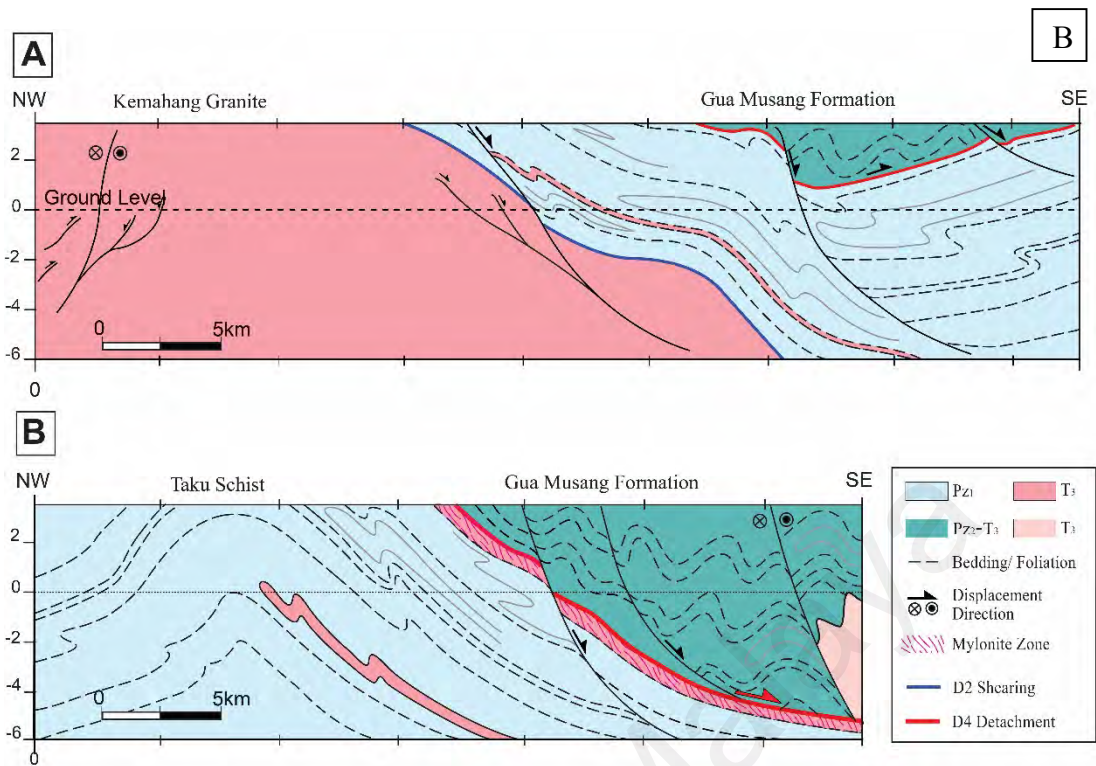


**Figure 5.4: Structural and geological cross-section of the Taku Schist and surrounding unit across northwest-southeast transect. The Taku Schist and intruded Kemahang granite are separated by an extensional detachment from the hanging-wall Gua Musang Formation by extensional detachment. In the Taku Schist footwall, shearing changes from brittle-fault to mylonitic detachment.**

## 5.2 Initial Burial Compression and Metamorphism, D1

### 5.2.1 Field Observation

#### 1. *The Taku Schist*

Throughout the unit, the quartz-mica schist displays well-developed, penetrative disjunctive schistosity (S1) interpreted as product of initial burial and metamorphism (D1). The metamorphic foliation (S1) generally strikes NNW-SSE and dips towards both E and W directions forming an anticlinal structures observed in map view (Figure 5.1 a, b). In addition to dominant quartz-mica and garnet-mica schists, minor lithological components includes quartz-feldspar-, quartz-rich-, graphite-, calc-silicate- and amphibole- schist and marble (Figure 3.14; Figure 3.17). The schist also contains inter-foliated quartz and marble layers oriented sub-parallel to foliation planes (Figure 3.16 b, Figure 3.17 b and Figure 3.24 c). The wide variations of lithologies observed in the field suggest that the original protolith of the Taku Schist are heterogeneous, but with dominant input of pelitic materials. Field observations indicate that the schist shows variation in the quartz-mica compositions, which controls the development of certain minerals i.e. garnet (almandine) as well as the morphology of the penetrative cleavages. Such example includes in the NNE part of unit, where the occurrence of garnet is mostly observed within chlorite-rich schist (Figure 3.23) but is weakly developed in the quartz-rich schist. This mica-rich schist often develop pronounced schistosity containing numerous garnet minerals, in parts grows to large sizes (~10mm) as observed in SSE parts of unit (Figure 3.6).

The orientation of the S1 foliation is parallel to the axial plane of millimeter-scale intrafolial folds (F1). The original layering of bedding planes (S0) are folded into symmetrical, transposed limbs and isoclinal hinge closures (Figure 3.7 and Figure 3.24).

The folds generally plunge towards N-S direction and along the regional antiformal trend (Figure 3.4a and Figure 5.1). These structures often observed as intra-folial layers within the quartz-rich schist as well as in the fine marble layers intercalated within the schist. It is inferred that the contraction or flattening deformation responsible for creation of F1 folds is coeval with the initial burial and metamorphism.

## *2. The Surrounding Units*

The development of penetrative disjunctive schistosity, S1 dominantly in quartz-mica and quartz-feldspar schist similarly observed in many parts of surrounding western units. This includes Tiang Schist, or the host rocks of both Kemahang granite and Stong Complex, where in part occur along the eastern margin of the Stong Complex (Figure 4.39, Figure 4.40 and Figure 4.42). The lithologies observed within these units are heterogeneous, which comprised dominantly of quartz-mica and quartz-feldspar schists, in addition to minor amphibolite, calc-silicate and banded cherts. In particular, the heterogenous lithologies are widely observed in xenoliths in the Stong Complex. The metamorphism led to general orientation of schist fabric (S1) along NNW-SSE trending planes with steep dips towards both E and W directions (Figure 5.1). The occurrence of millimeter-scale isoclinal folds (F1) of former bedding planes (S0) striking parallel to S1 foliation planes are common throughout these exposures (Figure 4.12a and Figure 4.4a). The intrafolial layers are particularly observed in Sg. Renyok exposures situated east of the Kenerong Leucogranite (Figure 4.40). Overall, field observations indicate that the first stage of deformation (D1) resulted in development of S1 schistosity contemporaneous with symmetrical contraction during the burial metamorphism of the Taku Schist unit together with Tiang Schist and host rocks of Stong-Kemahang granite. These structures are further re-folded and affected by subsequent deformations.

The overlying sedimentary units of Gua Musang and Aring Formation are composed predominantly of carbonaceous argillitic mudstones (Figure 4.6 a, b, Figure 4.10 a, c). This is further influenced by compositional variation observed across the formation. On the eastern and southern flanks of the Taku Schist, occurrences of carbonaceous shales and tuffaceous shales are common in addition to minor rhyolite and andesites (Figure 4.6 c, d), suggesting components of acidic to intermediate volcanic and volcanoclastics. The amount of these materials decreases toward the western-northwestern flank, in presence of more arenaceous sandstone materials (Figure 4.10b). In contrast to pervasive schistosity in both Taku Schist and Tiang Schist, the development of penetrative cleavage within Gua Musang and Aring Formations varies from from slaty to fine phyllitic cleavage (compare Figure 4.10a and b). The sedimentary rock exposures on the eastern and southern flanks of Taku Schist display slaty cleavage containing original sedimentary relics (Figure 4.6a and Figure 4.15) whereas exposures on the western flank display higher degrees phyllite (Figure 4.10a and Figure 4.11), signifying the Aring Formation. In both cases, the degrees of penetrative cleavage development within overlying sedimentary unit are significantly low to absent, in comparison to the fabric observed in the Taku Schist (Figure 3.6). This suggests that deposition of Gua Musang Formation are weakly affected, or postdate the burial metamorphism affecting the Taku Schist. In similar relationship to the above describe contraction during burial metamorphism, occurrence of tight to isoclinal folding (F1) of former bedding plane (S0) are widely observed as millimeter-centimeter scale structures (Figure 4.12). Notable increase of penetrative cleavage development of quartzofeldspathic phyllite occurred near the SE- margin of the Taku Schist unit, as results of subsequent deformation event.

### 5.2.2 Microstructural Study

Microstructural study shows that the schistosity is defined by preferred alignment of micas, i.e. muscovite and biotite minerals alternated with ribbon quartz in either disjunctive or continuous spacing defining the compositional layering (Figure 3.12 d Figure 3.21 d and Figure 3.29). In part, stronger development of penetrative disjunctive cleavage is observed in mica-rich schists (Figure 3.21c). The common assemblages within schist are comprising of quartz, K-feldspar, muscovite, biotite, and garnet (almandine) that confirm the pelitic protolith (Figure 3.21c), with quartz-rich layers (Figure 3.22), likely tuffaceous sandstone that is still visible through subsequent metamorphism. The protolith was subjected to burial flattening and prograde metamorphism to the amphibolite facies. Likewise, the flattened quartz aggregates displays an interlobated outline, recrystallize under subgrain rotation and grain boundary migration (SGR and GBM) that indicates metamorphic condition around 400°-700° C. This period of metamorphism is likely correspond to straight internal foliation of quartz inclusions within garnet (almandine) porphyroblast (Figure 3.10c and Figure 3.21a, c). This internal foliation is overprinted and discontinued with the external foliation in subsequent deformation events. The above described micro-structural features are similarly observed within xenoliths in Kemahang granite and Stong Complex, although samples within the Tiang Schist are devoid of garnet (i.e. Figure 4.48). The most probable interpretation is that the degree of burial metamorphism in Tiang Schist is lower than the Taku Schist, the hosting Stong Complex and Kemahang granite (Figure 5.5).

### 5.2.3 Top- West Directed Shearing, D2

#### 5.2.3.1 Field Observation

##### 1. *The Taku Schist*

Strong developments of asymmetrical folds observed in western flank and along the anticlinal crest of Taku Schist (Figure 3.15 and Figure 3.25) resulted in inconsistency in the orientation of primary metamorphic foliation, S1. Kinematic analysis in this area indicates a dominant top-SW shear, inferred from well-developed S/C and S/C' shear bands (e.g. Figure 3.14 e; Figure 5.2). Notable presence is an opposite sense of shears towards NE within some parts of the Taku Schist (Figure 3.14 c), which indicates the shearing is associated with co-axial flattening. The development of asymmetrical folds is often controlled by steeply dipping, C'- shear plane striking EW-direction that cut the primary foliation (S1). This results in the formation of meter-scale asymmetrical folds with steeply inclined axial plane, tight-open hinges and consistent westerly vergence direction (Figure 3.25; Figure 5.2), confirming the top-W/SW directed shearing. The crosscutting C'-shear plane also results in crenulated foliation fabrics as well as lenses of foliation fishes in mica-rich schists. A renewed foliation resulted from the last stage of deformation (D4) overprints this top-SW shear but still retained the asymmetrical fold relics. These folds usually plunge perpendicular to newly developed stretching lineation (L2) and are mostly occurred in NNW-domain of the Taku Schist (Figure 5.2).

Occurrences of lit-par-lit biotite granite intrusions into the schist have been observed in a few parts of the Taku Schist where larger stock intrusions is present near the SE-margin (Figure 3.3 and Figure 5.1). Field observation of the lit-par-lit biotite granite in NNW domain (T67, Figure 3.2) suggest a subsequent folding into Z-shape asymmetries proceeding the intrusions (Figure 3.17a), where the kinematic analysis on surrounding fabric suggest top-SW shears (Figure 5.2). Near to the contact with the Kemahang

Granite, a mylonitic quartz-feldspar band indicates top-SW shear (Figure 3.27, Figure 5.2), although the granitic fabric of Kemahang granite does not indicate the presence of metamorphic foliation. This indicates the syn-kinematic characters of Kemahang granite and the relationship with former lit-par-lit biotite granite injection across the Taku Schist.

## 2. *The Surrounding Units*

Close to the Bentong-Raub suture zone, the Tiang Schist exhibits pervasive sheared fabrics that correspond to second deformation (D2) episodes comparable to Taku Schist unit (compare Figure 3.25 with Figure 4.47a). Kinematic analysis derived from S/C and S/C' shear bands in strongly contorted quartz-mica and quartz-feldspar schists indicates consistent top-SW directed kinematics (Figure 5.2). The kinematic is similarly interpreted mostly from arrays of crosscutting NNE-SSW trending C'- shear planes forming pervasive asymmetrical folding. These folds characterized by steeply inclined, tight to isoclinal asymmetrical folds plunging towards NE, sub-parallel to the stretching lineation. The consistent W- directed vergence of these folds also support the asymmetrical WSW directed kinematics (Figure 4.47).

In the western domain of Kemahang granite, the granite emplaced syn-kinematically by lit-par-lit injection into quartz-feldspar schist (Figure 4.29a), where both units display S1 metamorphic foliation associated with top SW directed kinematics. The continuous period of shear deformation resulted in the folding of these compositionally layered granites/ quartz-feldspar schist into Z- shape asymmetrical folds (Figure 4.29a). Similar fabrics have been observed within xenoliths in the Stong Complex (Kenerong Leucogranite and Noring granite) such as Sg. Renyok, where granitic injection into calc-silicate hornfels are subsequently folded isoclinally and forms intra-folial layering (Figure 4.40a). Given that both Kemahang granite and Berangkat tonalite (Stong

Complex) show comparable mafic composition and texture, it is inferred that emplacement of both units are likely coeval.

The presence of meta-sedimentary xenoliths within the Stong Complex comprises of wide protolith ranges showing well- developed schistosity, suggesting that the country rocks have been similarly affected by top –SW directed shearing. Part of the quartz-mica schist exposures located on the E margin of Kenerong Leucogranite indicates top –SW shears, where it is in contact with migmatite and separated from phyllitic mudstones/ shales exposures within less than 100 meter in distance (Figure 4.2 and Figure 4.39). It is speculated that the migmatite forms as result of emplacement of Kemahang granite by lit-par-lit injections within deep-seated environment that involves high temperature metamorphism reaches up to partial melting. The separation with weakly metamorphosed sediment however is resulted by latest extensional deformation event (D4; Figure 5.2 and Figure 5.3).

### **5.2.3.2 Microstructural Study**

#### *1. The Taku Schist*

In WNW and NNE part of the unit, the kinematic analysis on S/C and S/C' shear bands from both biotite and muscovite micas indicates dominant top –SW shears in addition to minor top –NE shears (Figure 3.21, Figure 3.22, Figure 3.28 and Figure 3.30). The garnet porphyroblasts show similar kinematics, which also show the continuation between internal foliation with external foliation fabric in the surrounding matrix (Figure 3.21a, c). This internal foliation is defined by layers of quartz inclusion where it forms either straight or spiral shapes. The presence of muscovite and biotite forming S/C and S/C' shear bands as well as quartz inclusions within garnet porphyroblasts suggest that the burial metamorphism is followed by top-SW directed

shearing occurring within amphibolite facies. Comparable sinistral kinematics is also observed in amphibole schist in the central domain of the Taku Schist.

The quartz aggregates are dominantly coarse-grained with equigranular shapes and possess wavy extinction. Individual grains in the aggregates also show weak oblique shapes preferred orientation along C-axis indicating sinistral sense of shear towards W/SW direction (Figure 3.22). The recrystallization mechanism operated within quartz aggregates within WNW domain is mainly by subgrain rotation (SGR), with variances of temperatures in order of 400°C to 500°C. In many parts of the areas, these aggregates shows serrated outline boundaries and patchy type-of extinction suggesting a renewed recrystallization by grain boundary bulging (Figure 3.11), pertaining to top-SE deformation.

Despite the continuation between internal foliation of garnet porphyroblast structure with the surrounding S1 foliation as observed in WNW domain, many samples across the unit do not indicate the concordance between the two foliation structures (compare Figure 3.21a and c). The internal foliation structures observed in SSE domain in particular is discontinuous to external foliation suggesting overprinting of S1 foliation fabric by subsequent ductile deformation (Figure 3.10c). In other cases, the former S1 foliation was folded into isoclinal structure within a renewed foliation fabric (S2).

## *2. The Surrounding Units*

Kinematic analysis of the quartz-mica and quartz-feldspar schist samples from the Tiang Schist shows consistent sense of shear towards WSW direction. The kinematic indicators are derived from the S/C and S/C' shear bands, the oblique quartz aggregates (SSPO) as well as the andalusite porphyroblasts (Figure 4.48 and Figure 4.49). The sample containing andalusite are obtained near to the Kemahang granite unit, and is

resulted from contact metamorphism of the intrusion (Figure 5.1). The andalusite enveloped in the muscovite and biotite of the matrix, forming porphyroblasts that indicate top-SW shears (Figure 4.49). It indicates syn-kinematic characters of Kemahang granite, where the emplacement of the granite occurred during continuous period of top-SW directed shearing deformation. The schist sample obtained in proximity to the Main Range Granite similarly shows evidences of contact metamorphism (Figure 4.48c, d). The samples contain polygonal quartz aggregates showing triple junction contact, interlayered with biotite/muscovite-rich domain forming compositionally layered foliation fabric. The samples also contain relic of asymmetrical fold of S1 foliation and fine recrystallized biotite flakes. It indicates that the emplacement of Main Range Granite is not strongly affected by top-SW directed shearing in comparison to the Kemahang granite, which possibly occur during the final stages of top-SW shearing deformation.

## 5.2.4 Late E-W Contraction, D3

### 5.2.4.1 Field Observation

The folds related to D3 are particularly observed in the southern and eastern flanks of the Taku Schist within argillaceous lithology. They are characterized by open symmetrical folds about 100 meter in amplitude, such as those exposed near Kg. Slow Pak Long (Figure 4.15). The shale beds are folded into S-shape antiformal structures with steeply dipping axial plane cleavage (S3) striking NE-SW, which crosscut bedding plane (S0) at high angle (Figure 4.15a). In Kuala Krai, this deformation event is responsible for development of NE-SW trending foliation (S3) widely observed in carbonaceous and tuffaceous shales (Figure 4.2 and Figure 4.6a). The deformation is responsible for the occurrence of symmetric buckle fold superposed on equivalent larger fold that range about 50 to 200 meters in amplitude (Figure 4.8). They also contain relics of Z-shape asymmetrical folds that develop during former D2 deformation event. The D3 folds are cut by normal and strike-slip faults formed in subsequent D4 deformation, which tilted the fold axes and affect the originally symmetrical fold limbs. This indicates that the D3 folds occurred during intermediate event, which contain an older D2 relics but were truncated by later D4 deformation.

Detailed analysis of D3 folds in Gua Musang Formation indicates that the fold axis is generally oriented along NNW-SSE direction associated with steeply-dipping plunges. Despite the nearly symmetrical orientation of both flanks, the easterly flanks in general are steeper by few degrees than the westerly flanks indicating slight easterly vergence, directed away from Taku Schist unit (Figure 5.3). In contrast to Gua Musang Formation, D3 folds are less common and unrecognizable within the Taku Schist, which possibly affected or crosscut by D4 deformation event. Given that the fold shows large-scale structures occurring at regional scale, this deformation is likely responsible for the development of NNW-SSE trending regional anticlinal-synclinal-anticlinal structures of

the Taku Schist- Gua Musang Formation- Stong Complex observed in map view (Figure 5.1, Figure 5.3 and Figure 5.4). The above evidences also suggest that the D3 fold deformation involve symmetrical horizontal contraction not associated with significant shearing.

University of Malaya

## 5.2.5 Top- SE Detachment, D4

### 5.2.5.1 Field Observation

#### 1. *The Taku Schist*

A uniform, pervasive occurrence of top-SE directed kinematics throughout the Taku Schist signify the last stage of deformation (D4). It results in a newly developed metamorphic foliation (S4) and pervasive low-plunging stretching lineation (L2) associated with strong kinematic indicators, including S/C' shear bands, rotated porphyroblast and foliation fishes (Figure 5.1b, Figure 5.2b). The development of stretching lineation is concurrent with increase of shearing intensity toward the south by appearance of mylonitic shear zone at anticlinal culmination near the SSE-margin of the Taku Schist (Figure 3.8a). The mylonite is comprised of compositionally layered biotite-granite and quartz-mica schist, the former intruded by lit-par-lit injection during second deformation (D2). The top-SE directed kinematics subsequently sheared both rocks during this last stage of deformation. The crosscutting C'- shear bands controls the development of feldspar porphyroblast and mica-fishes within both mylonitic leucogranite and mica-schist (Figure 3.8b). The shear zone in the SSE margin is also responsible for sudden increase of penetrative cleavage development within sedimentary rocks of Gua Musang Formation (Figure 3.9a). The exposures comprise of both quartz-feldspar phyllite and phyllitic mudstone that display pervasive mineral alignment and strongly contorted fabrics controlled by crosscutting C'- shear band that indicate top-SE directed kinematics. The above evidence indicates that the top-SE directed shearing is responsible for the major metamorphic offset between the Taku Schist and overlying Gua Musang Formation (Figure 5.2 and Figure 5.5).

Notable contradicting sense of shears observed in a few parts of Taku Schist, including parts of the mylonitized leuco-granite at the SSE-margin and exposures in the

NNW area suggest localized co-axial shearing (Figure 5.2). The deformation also corresponds to the development of gentle symmetrical folds with sub-horizontal axial plane, likely to be collapse folds (Figure 3.7b). These folds have been similarly observed in the overlying Gua Musang Formation, which plunges parallel to stretching lineation (L2). The degrees of deformation are noticeably weaker within the NNW domain, usually occurring as transition between brittle-ductile deformations. Relics of D2 asymmetrical folds are cut by newly developed metamorphic foliation (S4) associated with top- SE or -NW shear (Figure 3.15). Otherwise, the older primary metamorphic foliation (S1) is still preserved and are cut by steep brittle-normal faults (Figure 3.26). In some cases, the occurrence of foliation fishes indicating a dextral sense of shear toward SE is also related to this brittle-ductile deformation. Altogether, the top-SE directed shearing largely involve some degrees of asymmetrical deformation, from a brittle-ductile deformation in the NNW and NNE parts of unit toward more ductile, intensive shearing in the direction approaching the SSE-margin of the unit (Figure 5.2 and Figure 5.4).

Field study indicates that the ductile deformation progressively changes to brittle-dominated shearing. For example, the occurrence of NNW-SSE trending normal faults crosscut the S4 foliation in number of exposures including the mylonite in the SSE-margin (Figure 3.8a). The strike of these fault planes are oriented sub-parallel to the direction of shear deformation, where the kinematics mostly indicate dextral-normal oblique movement towards SE. The quartz-mica schist is either drag folded or brecciated by the crosscutting faults, such as in the exposure in NNE-domain (Figure 3.26). The brittle deformation episode is followed by major NS-trending strike-slip faults where kinematic analysis indicates a dextral sense of shear towards SE (Figure 5.2).

The occurrence of major N-S trending strike-slip fault in the easterly margin of unit near Temangan iron mine separates the staurolite-bearing mica schist from mudstones of overlying sequence (Figure 3.18, Figure 5.1 and Figure 5.5). An aerial view of the pattern of Kelantan River also indicate a sudden EW-bend near Temangan possibly arise from this strike-slip fault. This strike slip fault continues southwards where it cuts through the earlier normal faults (Figure 5.2). Kinematic analysis indicate dextral sense of shears towards SE direction, comparable to transport of former ductile deformation. It is inferred that the strike-slip fault occurred after the ductile-shearing and brittle normal faults, which resulted in sudden change in metamorphic condition from high amphibolite-facies to sub-greenschist facies observed in overlying Gua Musang Formation (Figure 5.2).

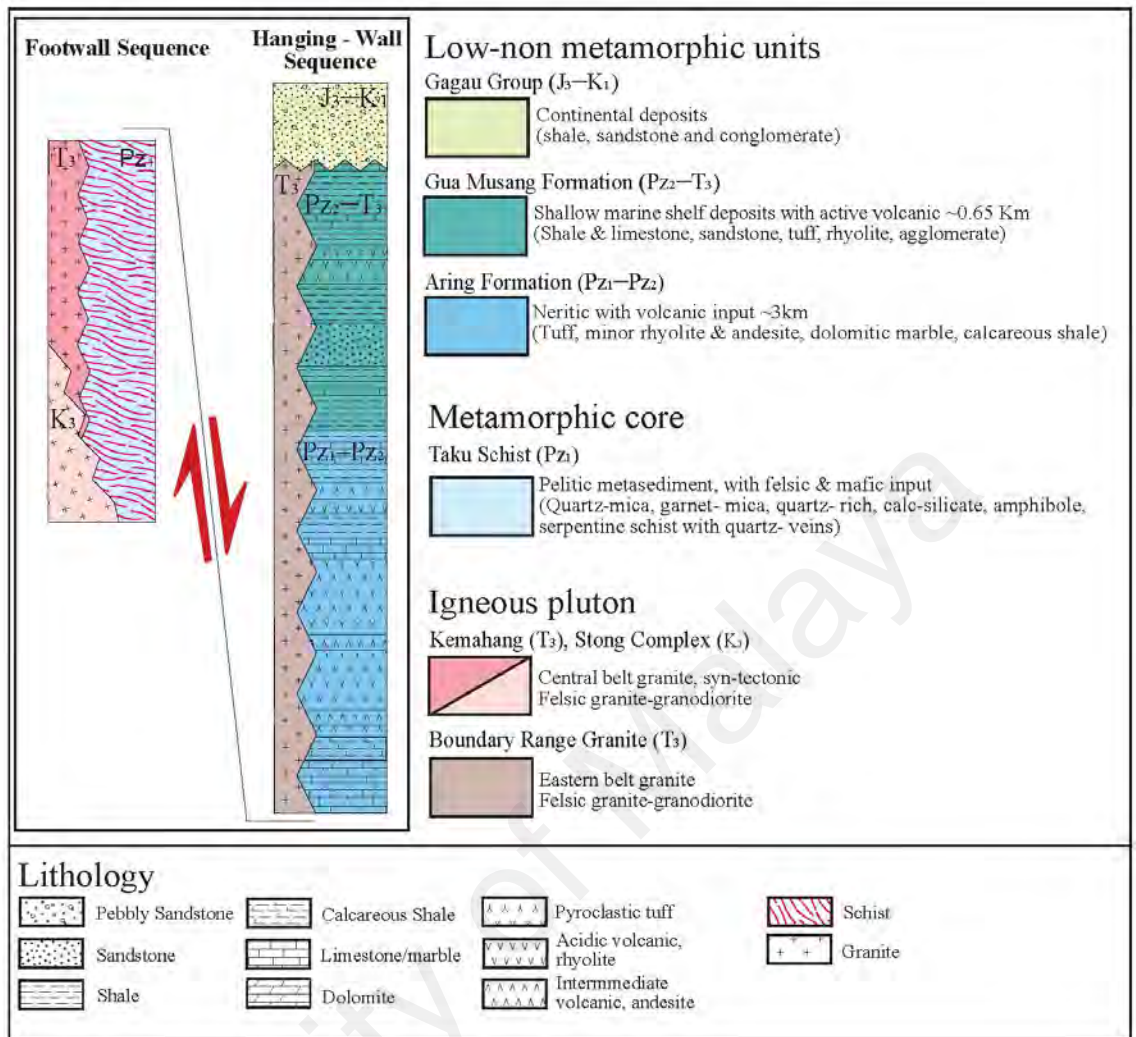


**Figure 5.5: Summarize tectonic-stratigraphic plot of the Taku Schist and the surrounding units.**

## 2. The Overlying Units

A prominent NNW-SSE trending fault zone occur within the eastern domain of the overlying Gua Musang Formation has been recognized previously as Lebir Fault Zone (Figure 4.3). Field study shows that the fault zone stretches more than 100 km in distance where kinematic analysis indicates dominant normal dextral oblique movement directed towards SE as well as minor sinistral oblique movement towards NW direction. This deformation is contemporaneous with the brittle-ductile episode of top –SE directed shearing observed in the Taku Schist (Figure 5.2). The brittle-ductile faults result in the occurrence of arrays of anastomosed faults sub-parallel to the shear zone,

which crosscut the weakly metamorphosed, tuffaceous mudstone exposures and result in sudden phyllitic cleavage development affected by deep chloritization (Figure 4.7, Figure 4.8 and Figure 4.26). The fault zones form the geological contact with Boundary Range Granite and similarly affect the granite in the proximities by similar kinematic movements (Figure 4.25).

### 3. *The Stong Complex*

On eastern margin of pluton, the presence of mylonitic leucogranite with pervasive stretching lineation within gneissic xenoliths associated with top –SE sense of shears suggest that the intrusion of Kenerong Leucogranite was emplaced into shear zones. The syn-kinematic injection episodes comprises of an initially millimeter-scale lit-par-lit injection, followed by a later episode of centimeter to meter scale veins injection which subsequently becomes enclaves of larger dyke intrusions (Figure 4.37a). The earlier stages of intrusions form compositionally layered granite-gneisses, which displays migmatitic features by presence of ptygmatic veins (Figure 4.37a, b). The veins branches out from granitic dykes and plunges towards SE direction parallel to the stretching lineation (L2). Thin section analysis of ptygmatic veins suggest a granitic origin unaffected by ductile shear deformation, in contrast with the gneissic xenoliths (Figure 4.43b). The latter meta-sedimentary xenoliths develop both sillimanite and chlorite minerals (Figure 4.43c), suggesting that the intrusion is associated with high temperature metamorphism that reaches up to partial melting likely upper amphibolite facies, and sharply reduced afterward to the sub-greenschist facies by retrograde metamorphism. The final episodes of intrusion forms major part of sub-unit are discordant to country rocks and unaffected by ductile shear deformation (Figure 4.43c).

The country rock of intruded granite displays well-developed schistosity/gneissosity with an assemblage of muscovite-biotite-garnet minerals. This indicates that the rocks

were regionally metamorphosed to the amphibolite facies comparable to the neighboring Taku Schist unit. The top –SE directed shear deformation is responsible for the creation of S4 foliation, with average NE-SW strike and pervasive SE-directed stretching lineation that overprints an older S1 foliation fabric (Figure 5.1 and Figure 5.2). The syn-kinematic injection is contemporaneous with shear deformation that results in formation of asymmetrical boudinages and prophyroclasts within both the country rocks and granitic veins (Figure 4.38b, c and Figure 4.40), indicating dextral sense of shear toward SE direction. Occurrences of minor exposures showing different sense of shears (sinistral in Sg. Renyok) suggest localized co-axial shearing within dominant top –SE directed shear deformation. The development of these asymmetrical structures arises from crosscutting C'- shear planes oriented at oblique angle to the S4 foliations (Figure 4.40d).

The development of shear zones with mylonitic top-SE directed shear separates the quartz-mica schist along the E-margin of Kenerong Leucogranite from the phyllitic mudstones of Gua Musang Formation (Figure 5.2). The phyllitic mudstone metamorphosed up to lower greenschist facies are separated from migmatite and garnet bearing quartz-mica schist (compare Figure 4.39 with Figure 4.12b, c). The latter indicate metamorphism to the high amphibolite facies that reaches up to partial melting. This indicates that the top-SE deformation is responsible for the significant metamorphic offset, which exposed the deep-seated, highly metamorphosed schist and migmatite in contact with weakly metamorphosed rocks (Figure 5.2).

Near the eastern margin of Kenerong Leucogranite, the phyllitic mudstones metamorphosed sub- greenschist facies shows well developed mineral lineation, where kinematic analysis indicate top-SE shears (Figure 4.13). Also exposed is the intrusions of leuco-granite along the fault planes, which was concordantly sheared into quartz-

feldspathic schist with top-SE kinematics (Figure 4.13). The sedimentary rocks are separated from (garnet-) quartz-mica schist metamorphosed amphibolite facies situated nearest to the pluton by a steeply dipping NW-SE trending fault associated with dextral normal oblique movement towards E/SE. This schist exposure is in contact with migmatite (Figure 4.39b). It indicates that the top-SE deformation affect both of the schist-gneiss and overlying phyllitic mudstone exposing the deep seated, highly metamorphosed schist and migmatite within footwall in contact with low-metamorphosed sediment in the hanging-wall (Figure 5.2). Thus, the deformation covers a continuous episode from ductile shearing toward brittle faulting responsible for significant metamorphic offset. The ductile shearing and normal brittle faulting marks the geological contact between the Stong Complex (E-margin of pluton) and Gua Musang Formation, showing consistent top-SE directed kinematics (Figure 5.2).

## CHAPTER 6: DISCUSSION

### 6.1 The Evolution of the Taku Schist and the Surrounding Units

Event	Evidences	Tectonic Implication
D1	Transposition of bedding planes into isoclinal folds and creation of S1 metamorphic foliation Assemblages of Mcv- Bt- Grt- Kfs minerals under amphibole- facies metamorphism. Straight, internal foliation within garnet.	<div style="display: flex; justify-content: space-between; align-items: center;"> <div style="writing-mode: vertical-rl; transform: rotate(180deg);">Prograde Metamorphism</div> <div style="writing-mode: vertical-rl; transform: rotate(180deg);">Retrograde Metamorphism</div> <div style="writing-mode: vertical-rl; transform: rotate(180deg);">Extension</div> </div> <p style="text-align: center;">           Initial burial metamorphism and nappe-stacking in the onset of continental subduction during Late Permian to Early Triassic            ↓            WSW directed shearing/ flattening in the late stage of nappe-stacking. Onset of continental collision (Late Triassic).            ↓            Late-stages of collision and large scale S-type magmatism during Jurassic - Early Cretaceous            ↓            Low-angle extensional detachment by top-SE shearing, crustal exhumation and coeval sedimentary basins during Late Cretaceous - Eocene         </p>
D2	W/SW- directed shearing, asymmetric fold deformation and period of syn-kinematic intrusion of Kemahang Granite S-C, C-C' shear bands and d-prophyroblast. Weak SSPO of quartz sub-grains	
D3	Upright symmetric fold and initial creation of Taku antiform	
D4	Uniform, SE- directed shearing toward shear zones in contact with overlying sediment, followed by episodes of major faulting. Overprinted fabric, brittle-ductile shearing w. straining intensification toward SE direction by C/C' shear bands, SSPO quartz subgrains, sericitization and chloritization.	

**Figure 6.1: Summarize of evidences detailed by this study and the interpreted tectonic implication.**

Following the first three stages of contractional deformations observed in the Taku Schist and surrounding units (i.e. the Tiang Schist, the hosting Kemahang and Stong Complex and the Gua Musang Formation), it is inferred that this events are coeval with the evolution of continental subduction and collision between Sibumasu and Indochina terranes of Peninsular Malaysia (Figure 6.3 a, b; Metacalfe, 2000, 2013). This includes an initial burial and nappe-stacking followed by asymmetric shearing toward W/SW direction and symmetric upright folding in the late stage of contraction (Figure 5.2). In agreement with MacDonald (1968) and Hutchison (1973), this study indicates that the Taku Schist is composed dominantly of quartz-mica, garnet-mica and quartz-feldspar, in addition to quartz-rich, amphibole and serpentinite (i.e Figure 3.11, Figure 3.12, Figure 3.13 and Figure 3.19). The heterogenous composition of the Taku Schist suggests that

the unit is made of original pelitic succession locally intercalated with meta-turbidites, meta-acid and meta-mafic materials. In addition, both of the Tiang Schist and hosting Kemahang and Stong Complex shows heterogenous composition (Figure 4.31, Figure 4.43, Figure 4.44 c, d and Figure 4.46), in similar relationship to the Taku Schist. It is likely that these units together with the Taku Schist are of similar origin, which were separated by subsequent deformation events. This evidences is in agreement with previous studies, which indicate that these units represent original succession of lower Paleozoic materials (MacDonald, 1968, Lee et al., 2004) forming an accretionary prism in the Permo-Triassic continental subduction of Sibumasu plate underneath Indochina terrane (Metcalf, 2000).

The nappe-stacking episode of deformation (D1) involves a combination of burial metamorphism and symmetric flattening (Figure 6.3a). This results in creation of metamorphic foliation, S1 synchronous with development of symmetric isoclinal folding (F1) or intrafolial fold structures observed within the fabric of the Taku Schist and the hosting Tiang Schist (i.e. Figure 3.24 and Figure 4.46a). The development of isoclinal fold structure is also in agreement with previous studies of MacDonald (1968), Richardson (1946) and Singh (1984), interpreted to form as result of regional metamorphism (i.e the burial metamorphism in this study). While the sediments of Gua Musang Formation similarly displays similar isoclinal fold structures formed as results of D1 symmetric contraction, the development of penetrative cleavage only results in formation up to slates or phyllite, which is in contrast with the well-developed penetrative schistosity cleavage observed in the Taku Schist or the Tiang Schist (compare Figure 4.11 with Figure 3.24). This indicates that the sediments and volcanics of Gua Musang Formation was least unaffected by burial metamorphism, and is in agreement with previous interpretation of shallow marine environment of a forearc basin formed during Permo-Triassic times (Lee et al., 2004).

In agreement with MacDonald (1968), this study indicates that both of the Taku Schist and the Tiang Schist attained amphibolite-facies metamorphism during this burial metamorphism, significantly higher than the greenschist-facies metamorphosed sediments of the Gua Musang Formation. The high metamorphic degree of the Taku and Tiang Schist also support the interpretation of nappe-stacking that result in thickened accretionary prism during the continental subduction (Figure 6.3a, Metcalfe, 2000).

The initial symmetric contraction of nappe -stacking deformation (D1) is proceeded by top-WSW shearing and asymmetric folding (D2) in the late stage of burial metamorphism (Figure 6.3 a). In the Taku Schist, this deformation involves coaxial flattening toward WNW or NE direction as observed in the respective westerly and easterly flank (Figure 5.2). The fabric pertaining to this deformation however, is often overprinted by subsequent D4 deformation (Figure 3.15, Figure 3.25) and is less clear in comparison to the fabric observed in the Tiang Schist. This study indicates that the Tiang Schist documented pervasive top-SW directed shearing associated with strong development of asymmetric folding (Figure 5.2, Figure 4.47c), which is in agreement with mylonitic sinistral/top-SW directed shearing of Shuib (2009) or the pervasive fold development observed by Richardson (1946). Previous studies of Hutchison (1973) and Metcalfe (2000) indicate that the Tiang Schist unit represent the lateral prolongation of the Karak Formation to the south and is part of the Bentong-Raub suture zone (Fig. 5.1). When compared, the Taku Schist is also represent a part of the Bentong-Raub suture zone, such that the formation of accretionary prism involve intense shearing and thrusting toward W/SW direction in response to the eastward collision of Sibumasu plate toward Indochina plate during late Triassic (Figure 5.2 and Figure 6.3 b). This is supported by the presence of kyanite in the easterly flank of the Taku Schist (MacDonald, 1968) that indicates high-pressure metamorphism. This suggest that the Taku Schist unit is located in close proximity to the subduction plane or near to the

contact between two major units in nappe-stack sequence (Figure 6.3 b). Field observation in the Taku Schist and the hosting Stong Complex indicate the presence of large amount of meta-mafic materials i.e. sheared amphibolite rocks intercalated with minor band chert and marble layers (Figure 4.42). The presence of these mafic to ultramafic rocks (amphibolite, serpentinite etc.) have also been recognised in previous studies (Hutchison, 1973; MacDonald, 1968 and Shuib, 2009). According to Hutchison (1973), the rocks sequences represent a part of an ophiolite suite widely observed in suture zone rocks. This interpretation is in agreement with occurrence of pillow basalt intercalated with serpentinite and chert layers in Ku Mung Igneous Complex at southern Thailand about 30 km to the north of the Taku Schist, where the exposures have been severely fractured and folded (JMGSC, 2006).

Both of field and micro-structural observation indicate that the emplacement of Kemahang granite into the Taku Schist and the Tiang schist occurred during period of D2 shear deformation, which characterize the syn-kinematic granitic intrusions. The top-WSW directed kinematic have been observed in schist fabric closest to Kemahang granite, such as in quartz-feldspar mylonite located in the NE flank in the Taku Schist or quartz-mica schist fabric in the adjacent Tiang Schist (Figure 5.2, Figure 4.49 and Figure 4.47). The latter contains andalusite porphyroblast that indicates synchronous contact metamorphism with shear deformation. Exposure containing lit-par-lit granite intrusion within the Taku Schist were also folded into asymmetric structure and shows comparable top-WSW sense of shear (Figure 4.49). This syn-kinematic evidences of Kemahang Granite indicate the intrusion is synchronous with shearing toward WSW direction (D2), which also signifies the period of continental collision (i.e. Indosinian orogeny) between the Sibumasu and Indochina continental plate (Figure 6.3 b). Recent U-Pb zircon analysis by Ng et. al (2015) indicates a middle/late Triassic (~226 Ma) age of emplacement of Kemahang Granite (Figure 2.4), reflecting the timing of continental

collision. This time constraint also suggests that onset of continental subduction (Figure 6.3a) observed by nappe stacking and burial metamorphism is older, which commences from late(st) Paleozoic onward until early Triassic times. These period is in agreement with continental subduction and collision of Metcalfe (2000) and the age of forearc basin of Gua Musang Formation (Lee et al., 2004).

Following the top-SW asymmetric shearing (D2), the third contractional stage of deformation (D3) proceeds and is represented by symmetric horizontal compression that results in formation of regional antiformal-synformal-antiformal fold structure in the studied area (the Taku Schist-Gua Musang Formation-Stong Complex/Tiang Schist in Figure 5.1; Figure 4.4c). Field observation on argillaceous sediments of the Gua Musang Formation indicates that the symmetric upright fold structures (Figure 4.7 and Figure 4.8) crosscut the former asymmetric inclined fold structures (F2, D2), but is crosscut by later normal and strike slip fault (D4). This suggest that the D3 fold deformation occurs as an intermediate event, which post-date the D2 top-SW asymmetric shear deformation in middle/late Triassic but pre-date the D4 top-SE extensional shear deformation in late Cretaceous (Figure 6.3 b). Both of the symmetric to asymmetric upright fold structure were similarly observed by Shuib (2009) within sediment exposures in the Semantan Formation of the Central belt, where the fold structures were similarly crosscut by latest strike-slip fault. He indicates that this fold deformation was resulted from dextral transpression in the late Triassic-early Jurassic time followed by transtension that results in deposition of Jurassic and Cretaceous sediments.

This study infers that the D3 contractional deformation occurred during the late stage of continental collision, likely in the Jurassic-early Cretaceous time. This period is largely unconstrained in Peninsular Malaysia, where another possible hypotheses is that

the open folding is responsible for steep inclination of Jurassic and Cretaceous strata in the central belt (Shuib, 2009). The interpretation of symmetric contraction is in agreement with studies in the other orogenic areas, where the entrance of buoyant continental material into the subduction systems results in locking of the subduction zones and symmetrical out of sequence contraction (Ziegler et. al., 1995). In the case of studied area, the locking of subduction system in late Triassic results in symmetric contraction coeval with major S-type granite intrusion (the Main Range Granite) into the accretionary prism as well as part of thickened Sibumasu lithospheric crust (Figure 6.3 b; Ghani, 2009, Metcalfe, 2000).

Detail structural interpretations as described from above are compatible with the processes of Indosinian orogeny through the convergence between the Sibumasu continental unit and the Sukhothai arc (Metcalfe, 2009; 2013). The continental subduction initiating in late Permian results in burial metamorphism and nappe-stacking (D1) of deeply-buried amphibolite-facies of Taku Schist equivalent of Bentong-Raub suture zone and the lower greenschist-facies of the Tiang Schist (Figure 6.1; Figure 6.3). The initial symmetrical contraction during burial metamorphism is followed by top-WSW shearing (D2) and syn-kinematic granite in late Triassic. This indicates a continuous process of burial and thrusting that took places gradually as the rocks approached toward the continental subduction inferred as the thrusting of Sukhothai over the Sibumasu plate. The subsequent episodes of Indosinian orogen lead to locking of the subduction during the continental collision resulting in symmetrical contraction (D3).

The processes of Indosinian orogeny through the convergence between the Sibumasu continental unit and the Sukhothai arc (Metcalfe, 2009; 2013) are compatible with the structural interpretation of this study. The continental subduction initiating in late

Permian results in burial metamorphism and nappe-stacking (D1) of deeply-buried amphibolite-facies of Taku Schist equivalent of Bentong-Raub suture zone and the lower greenschist-facies of the Tiang Schist (Figure 6.1; Figure 6.3). The continuous processes of continental subduction results in thrusting of the rocks toward the Sukhothai over the Sibumasu plate by top-WSW shearing (D2) and syn-kinematic intrusion in the late Triassic. The consequent locking of the subduction plate and continental collision results in formation of symmetrical contraction (D3).

This study indicates a formation of never described extensional tectonic represented by low-angle shearing deformation (D4) toward SE direction, resulting the separation of the Taku Schist, Stong Complex and Kemahang Granite units from the overlying Gua Musang Formation (Figure 5.2 and Figure 6.3 c). The top-SE shear deformation covers period of ductile- mylonitic shearing towards brittle- normal and strike-slip faulting (Figure 3.8, Figure 3.13 and Figure 3.18). It results in formation of low-angle, recumbent fold structures (Figure 3.7, Figure 3.15 and Figure 4.12 c) interpreted as collapse fold of steeply inclined foliation planes inherited from previous deformation events. The continuation of ductile shearing toward brittle faulting is in accordance with retrograde metamorphism from amphibolite-facies to greenschist-facies). This is particularly observed near the SE margin of the Taku Schist , where the observed quartz recrystallization by both grain boundary bulging (BLG) and rotation (SGR) is accompanied with the formation of chlorite and sericite minerals (Figure 3.10 f and Figure 3.12b). This indicates that the top-SE shearing is responsible for the exhumation of the Taku Schist metamorphic body, which likely occurred in late Cretaceous onwards, post-dating the previous three stages of contractional event (Figure 6.3 b).

The unroofing of the Taku metamorphic body results in significant tectonic omission with the overlying Gua Musang Formation in the order of 300°C, which indicates 12-15 km of differential vertical exhumation during the extension. Thus, this study infers that the nature of contact between the Taku Schist and Gua Musang Formation is large-scale detachment (Figure 5.2). The interpretation is in agreement with tectonic contact of MacDonald (1968) and Hutchison (1973), and disregards the previous interpretation of gradational Barrovian Isograd succession as described by Khoo and Lim (1983). Both field and microstructural observation indicates that the style of deformation changes across the Taku Schist, from brittle-ductile shear transition in NNW and NNE domain to a ductile-mylonitic shearing in the direction toward the SSE margin of the unit (Figure 5.2).

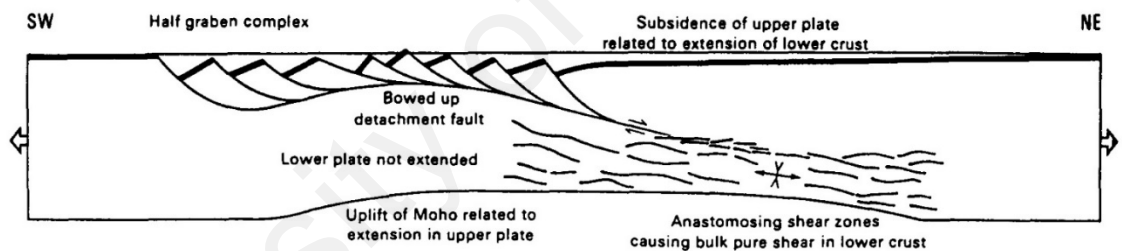


**Figure 6.2: The formation of low-angle detachment fault by the formation of metamorphic core complex (Lister, 1989).**

The mechanics of top-SE shear deformation resulting the formation of large-scale detachment described above demonstrates the formation of metamorphic core complex (Figure 6.2, Lister, 1989). Both field and microstructural evidence indicates the asymmetries of top-SE deformation from brittle-ductile shear transition in NNW domain (Figure 3.29), which shifted toward ductile shearing in the direction toward SE direction (Figure 3.10). The relative shear transport is directed toward a single, shallow dipping- mylonitic shear zones in SSE margin that represents a master detachment fault (Figure 3.8 and Figure 3.13). The initial ductile detachment shearing continues as brittle

normal and strike-slip faulting in the late stages of deformation, suggesting that the latest strike-slip fault accommodates the top-SE detachment (Figure 3.18 and Figure 5.2). The observed shifting from ductile toward brittle deformation is also in agreement with retrograde metamorphism to the greenschist-facies as indicated by microstructural analysis. According to Lister (1989), the formation by metamorphic core complex by bowing up movement of the lower crust is the result of isostatic adjustment in an extensional tectonic settings. This is responsible for the exhumation of Taku Schist together with the footwall units of the Taku Detachment (Figure 6.3c).

## **6.2 Implication of Taku Extensional Detachment**

### *1. Development of Extensional Detachment in NE Peninsular Malaysia*

The latest strike-slip faulting accommodates the evolution of top-SE extensional detachment in the Gua Musang hanging-wall. Field observation indicates that the strike-slip fault on E-margin of Taku Schist form major NNW-SSE trending fault zone with dominant dextral normal oblique sense of shears (Figure 2.2). The interpretation of normal dextral oblique component justify the steep inclination of foliation planes observed in the Taku Schist (see contour plot of Figure 5.2), which is unusual for formation of metamorphic core complex. The observed strike-slip faults have been previously interpreted as Lebir Fault Zone by the lineament studies (Aw, 1974; Tjia 1969), where it stretches more than 100 kilometers along the N-S lineament forming the transcurrent boundary between Central and the Eastern belt of Peninsular Malaysia (Figure 2.2). Previous kinematic studies shows sinistral thrust kinematic of Lebir Fault (Tjia, 1969; Aw, 1974; Shuib, 2000; Zaiton, 2002), which is against the interpretation of dextral normal oblique kinematic shown by this study. Noticeable present of sinistral thrust kinematic have been observed in parts of exposures, although the crosscutting relationship with the dextral kinematic is unclear.

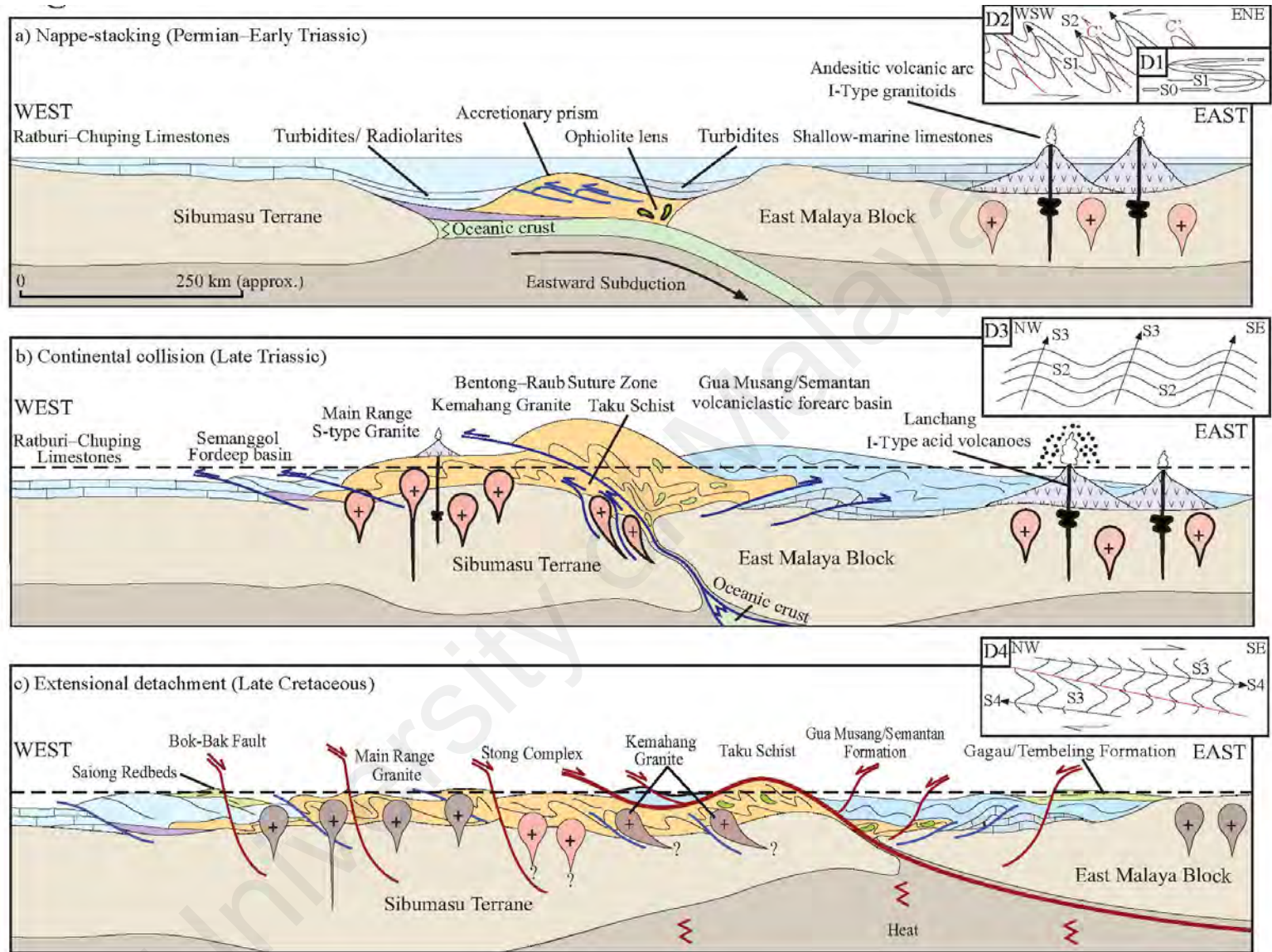


Figure 6.3: Interpreted tectonic model for the Taku Schist following modification of Metcalfe, 2002. (a) Continental subduction of Sibumasu underneath Indochina block, (b) Continental collision of Sibumasu and Indochina in late Triassic and (c) Continental extension resulted from the Taku Detachment in late Cretaceous - Eocene

The study interpret that the Taku Schist, together with Kemahang Granite, Stong Complex and the Tiang Schist form the footwall of the Taku detachment that was separated from the Gua Musang hanging-wall by a similar top-SE shear deformation (Figure 5.2 and Figure 5.5). This study also implies that the Tiang Schist is the lateral prolongation of the Taku Schist, which was intruded by both Kemahang Granite and Stong Complex and forms another set of anticlinal dome (Figure 5.1). The formation of Taku Detachment by SE directed shearing result in unroofing of both domes in the footwall. This is observed in map view by changing of strike direction, from NNW-SSE direction in the Taku Schist to E-W direction and finally back to NNW-SSE direction in the Tiang Schist following the antiformal-synformal-antiformal plunges of the dome structures (Figure 5.1).

The interpretation of regional folding that result in formation of two anticlinal dome structures indicates that the NW-SE directed extension was followed by subsequent contraction along E-W direction. The latest contractional episodes will justify the steep inclinations of foliation planes in the Taku Schist (Figure 5.1b) as well as the bedding planes of Jurassic and Cretaceous sediments (i.e. Gagau and Tembeling Formation; Figure 4.24a). This is in agreement with previous studies (e.g. Shuib, 2009; Tjia, 1996; Zaiton, 2002) suggesting that the formation of regional folds structures and the steep inclinations of foliation/bedding planes are the results sinistral thrust kinematic of Lebir Fault system. According to Shuib (2009), the deformation observed in the Lebir Fault is an expression of late Cretaceous transpressional event, coeval with intrusion of Stong Complex and folding of Jurassic and Cretaceous sediments. The interpretation are mainly derived from gravity anomaly studies of Ryall (1982) by transition of thick crust to thin crust from Eastern to Central belt of Peninsular Malaysia. Kinematic analysis shown by this study indicates that the Lebir Fault is an expression of later top-SE shear deformation with dominant normal dextral oblique movement (Figure 5.2). Although

the late Cretaceous time constraint can be disregarded, it is possible that the sinistral reverse kinematic toward NW direction observed in field observation and previous studies (e.g. Shuib, 2009; Tjia, 1996; Zaiton, 2002) resulted from fault reactivation by subsequent contractional deformation in Eocene time (Cottam, 2013). The contractional deformation results in tilting of the Jurassic and Cretaceous sediment and subsequent exhumation of this hanging-wall unit (see below).

This study interprets that both of the Taku Schist and the Tiang Schist as well as the hosting Stong and Kemahang Granite are composed of equivalent heterogeneous materials of lower Paleozoic in age that were metamorphosed to the amphibolite facies (Figure 5.5). It indicates that the materials were likely derived from remnants of Paleotethys Ocean accreted forming the accretionary prism which were metamorphosed by burial nappe-stacking during the progressing eastward subduction of Sibumasu block underneath Indochina block (Figure 6.3a). It also suggests that both of the Taku Schist and Tiang Schist represent the deeply buried equivalent of Bentong-Raub suture zones that were exposed in the north of Peninsular Malaysia. When correlated, the structures are more complex and cannot merely be formed as a result of regional anticlinal-synclinal-anticlinal fold structures interpreted by previous studies (e.g. Khoo and Lim, 1983). The overall structures support the conclusion that the Taku Detachment exhumes the deeply buried Bentong-Raub suture zone during this major extension possibly reactivating the former subduction/thrust plane (Figure 6.3c).

This study demonstrates that the emplacement of the Stong Complex (i.e. Kenerong Leucogranite and Noring Granite) is syn-kinematic in agreement with previous studies (i.e. Shuib, 2000, Singh, 1984). The Stong Complex intrudes into gneissic host rocks (Tiang Schist) in another set of anticline of the footwall units (Figure 5.1). The extensional detachment shearing toward SE direction is accompanied with initial high-

temperature intrusion of Stong Complex (Figure 4.37). This is observed by lit-par-lit injection into gneissic host rock showing top-SE sense of shears, where in part shows an occurrence of migmatite bands and ptymatic veins (of igneous origin, Figure 4.37). The shifting of ductile to brittle of top-SE deformation is accompanied with retrogradational metamorphism to the green-schist facies (Figure 4.30) synchronous with further young intrusion of Stong Complex (i.e. Noring Granite). This interpretation is in accordance with observation of brittle normal faults crosscutting former ductile mylonites showing similar top-SE sense of shear, as well as the absence of metamorphic foliation in young granite exposures. The evidence also suggests that the formation of Taku detachment is responsible for the unroofing and exhumation of deeply buried Stong Complex, which initially lies beneath the sediments of Gua Musang Formation (Figure 5.1). Microstructural analysis indicates that the separation between the Stong Complex and the Gua Musang Formation involve metamorphic offset that ranges about 600°C, suggesting vertical exhumation in the order of 20-30 km. This indicates that the degree of exhumation in Stong Complex is significantly higher than the Taku Schist.

The post-orogenic, continental extension observed in the Taku Schist of NE Peninsular Malaysia is expressed by formation of large-scale detachment that results in significant exhumation in the footwall units (Figure 6.3c). Thermochronological studies on granitic rocks across Peninsular Malaysia by apatite and fission track analysis (Cottam et. al, 2013) indicates that the major exhumation in entire Peninsular Malaysia occur during the late Early Cretaceous and Early Cenozoic (Late Paleocene-Oligocene). The late Cretaceous exhumation is interpreted to occur as result of dynamic topographic response to the termination of subduction along the Sunda margin following the continental collision of Australian micro continent fragement with the southern margin of Sundaland (Cottam et. al, 2013; Hall, 2011). Subsequent resumption of the subduction processes along the Sundaland margin in the Eocene brought the region into

compressional deformation and results in regional exhumation. In the absence of thermochronological studies in the Taku Schist or the surrounding units, the timing of exhumation resulted from formation of the extensional detachment interpreted by this study is likely occurred during the late Cretaceous. The time constraint is coeval with intrusion of Stong Complex (Ng et. al, 2015; Singh, 1984; Figure 2.4) and formation of Lebir Fault (Shuib, 2009; Zaiton, 2002). Further exhumation of the Central Belt region possibly continues during the Eocene time by subsequent resumption to contractional deformation as interpreted by Cottam (2013). This will also justify the reactivation of Lebir Fault by sinistral transpressive movement responsible for tilting of Jurassic and Cretaceous basin (Shuib, 2009). In addition, the period of exhumation in Eocene is coeval with initiation of basin subsidence in the offshore of Peninsular Malaysia.

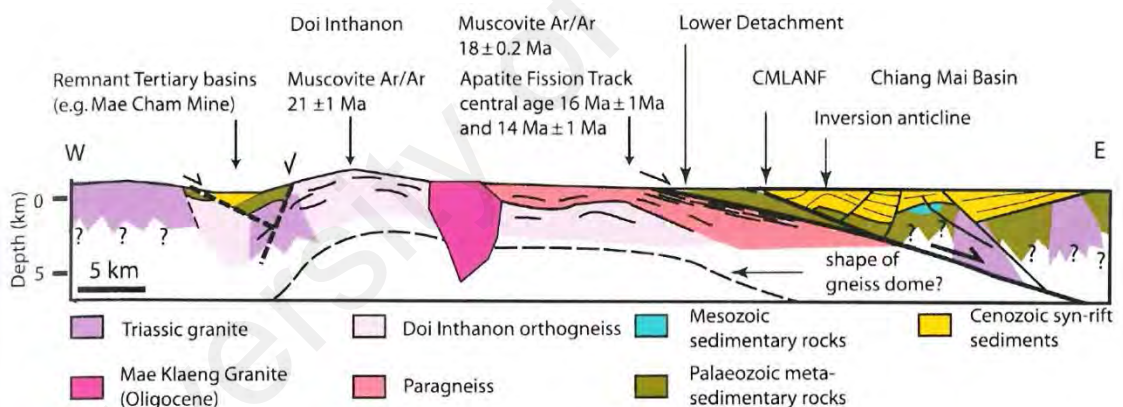


**Figure 6.4: Cross-section in the Northern Thailand from Chiang Mai Basin across Doi Intahonon Core Complex showing main structural and stratigraphic features, after Searle and Morley (2011). CMLANF is Chiang Mai Low Angle Normal Fault**

The orogenic and post-orogenic structure observed by the formation of Doi Intahonon Core Complex in the northern Thailand is comparable to the evolution of the Taku metamorphic core complex in NE Peninsular Malaysia (compare Figure 5.4 with Figure 6.4). The Doi Intahonon Core Complex forms an asymmetric anticlinal dome structures, showing three stages of folding that correspond to compressional deformation of the

Triassic Indosinian Orogeny (i.e Baum et. al, 1973). The master detachment fault shows pervasive low angle, top-E directed kinematic (MacDonald, 1993), which separates the amphibolite-facies gneisses from an overlying greenschist-facies sediments and schist. The post-orogenic, crustal extension covers an initial high temperature intrusion during late Cretaceous –Tertiary times (Teggin, 1975; Braun et al. 1976, Cobbing et al, 1992) that proceed with formation of low-angle detachment during late Cretaceous-early Paleogene times. In the NE Peninsular Malaysia, covers an initial high temperature Stong Complex intrusion into the footwall of the Taku Detachment proceeded with large-scale detachment and formation of Taku-Stong metamorphic core complex that result in significant tectonic omission with overlying Gua Musang Formation of the hanging-wall unit (Figure 6.1).

## CHAPTER 7: CONCLUSION

By implementing detailed structural and kinematic analyses, this study has demonstrated the structural evolution in the Taku Schist and the surrounding units (the Gua Musang Formation, Kemahang Granite, Stong Complex and the Tiang Schist) in the NE of Peninsular Malaysia. The first three-stage succession of contractional deformation are interpreted to developed during the orogenic stages (latest Permian – Late Triassic), followed by formation of newly detected post-orogenic, extensional deformation that is expressed by the formation of Taku Detachment (Late Cretaceous). All of this deformation stages observed in the Taku Schist and the surrounding units are in general agreement with previous studies as the product of Indosinian orogenic and post-orogenic structures of the SE Asia, resulting from the collision of Sibumasu and Indochina blocks during Permo-Triassic times (Metcalf, 2013 and references therein).

In general agreement with previous results, this study indicates that the Taku Schist represents an original lower Paleozoic protolith with high mafic intercalations that were metamorphosed to the amphibolite facies during the burial stages of the Indosinian orogeny (Aw, 1974; Lee et al., 2004; Hutchison, 1973; Khoo and Lim, 1983; Shuib, 2009 and references therein). The burial and metamorphism represents the first stage of deformation (D1) synchronous with development of isoclinal fold (F1) structures and is demonstrated by nappe-stacking of Paleo-Tethys succession within an accretionary prism developed during the Permo-Triassic continental subduction.

This is proceeded by late stages of burial metamorphism in the second stage of deformation (D2), which is observed in the Taku Schist by flattening along WSW and NE direction and development of asymmetric fold structure (F2) with similar vergence structure. This study interpret that the top-WSW shearing is the product of continental collision (Metcalf, 2000), where the primary feature is observed in the Tiang Schist

representing the northern extension of the Bentong-Raub suture zone (Hutchison, 1973). This is supported by presence of Kyanite as high pressure metamorphism indicators (MacDonald, 1968) and intercalation of pillow basalt with chert layers in the adjacent areas (JMGSC, 2006). The syn-kinematic character of the Kemahang Granite allow the timing of the deformation i.e. the continental collision, which occurred in middle late Triassic (220 Ma) as indicated by U-Pb analysis of Ng et. al (2015), in Figure 2.4. This is proceeded with symmetric contractional folding in the third stage of deformation (D3) and formation of regional anticlinal-synclinal in the studied area. This open upright folds structures has also been observed at the scale of the entire peninsula (Shuib, 2000; 2009), interpreted to occurred in late stages of continental collision in late Triassic by symmetric out-of-sequence contraction coeval with the locking of subduction zone and large scale emplacement of S-type Main Range Granite.

This study demonstrates the formation of extensional stage of deformation (D4) that has not yet been described to present date in Peninsular Malaysia. The deformation is characterized by pervasive low angle shearing toward SE direction that results in creation of Taku Detachment. The formation of this large scale detachment is responsible for the separation between the Taku Schist together with Stong Complex, Kemahang Granite and Tiang Schist from the overlying Gua Musang Formation by a significant 15-30 kilometres tectonic omission. This study interprets that the mechanics resembles the formation of metamorphic core complex that develop during late Cretaceous-Eocene time. The time constraint is in agreement with the intrusion of the high temperature Stong Complex (Ng et. al, 2015 in Figure 2.4) into the footwall of the Taku Detachment and period of major exhumation in the entire Peninsular Malaysia as indicated by Cottam et. al, (2013). It is likely that this major exhumation affects the footwall of detachment exposed across Bentong-Raub suture zone of Peninsular Malaysia in a similar relationship to the Taku Schist and Stong Complex. This supports

the post-orogenic extensional tectonic settings in NE Peninsular Malaysia during late Cretaceous-Eocene where the primary feature is the Taku Detachment.

The discovery of this newly detected extensional detachment recorded by this study indicates that NE Peninsular Malaysia was similarly affected by post-orogenic extensions that have been previously recorded in Thailand (e.g. Searle and Morley, 2011; Morley, 2012; Pubellier and Morley, 2014). It indicates that the Taku Detachment reactivates the former subduction plane and exhumes the former deeply buried Bentong-Raub suture zone. A number of inferences on development of post-orogenic extensional tectonic settings in Peninsular Malaysia remain speculative in the absence of low-temperature thermochronology in the Taku Schist and the regional kinematics correlation. The top-SE detachment may have occurred as results from termination of subduction along the Sundaland margin in late Cretaceous followed by subsequent resumption in Eocene (Cottam et. al, 2013). The latter can possibly related to the sinistral transpression of Lebir Fault interpreted in previous studies (Shuib, 2009; Tjia, 1996; Zaiton, 2002) that results in steepening of Jurassic and Cretaceous basins. In addition, the formation of core complex and coeval sedimentary basins widely observed in Thailand (e.g. Morley, 2012) can be related to Tertiary basins in offshore Peninsular Malaysia otherwise the Jurassic-Cretaceous basin of Peninsular Malaysia.

## REFERENCES

- Aw, P.C. (1974). Geology of the Sungai Nenggiri–Sungai Betis Area. *Geological Survey of Malaysia Annual Report 1972*, 115–119.
- Bignell, J.D. & Snelling, N.J. (1977). K-Ar Ages on Some Basic Igneous Rocks from Peninsula Malaysia and Thailand. *Geological Society of Malaysia Bulletin*, 8, 89–93.
- Braun, E. von., Besang, C., Eberle, W., Harre, W., Kreuzer, H., Lenz, H., Muller, P. & Wendt, I. (1976). Radiometric age determinations of granites in northern Thailand. *Geol. Jahrbuch. B21*, 171-204.
- Burton, C. K. (1973). Mesozoic. In: Gobbett, D. J. & Hutchison, C. S., (Eds). *Geology of the Malay Peninsula*, Wiley-Interscience, New York, 97-141.
- Cobbing, E. J. & Pitfield, P. E. J. (1986). South-East Asia Granite. *Project Field Report for Thailand 1985*. B.G.S. Overseas Dh., Report MP/86/16/R.
- Cobbing, E. J., Pitfield, P. E. J., Darbyshire, D. B. F., & Mallik, D. I. J. (1992). *The granites of the South East Asian tin belt, (Vol. 10)*. London: British Geological Survey.
- Cottam, M.A., Hall, R. & Ghani, A.A. (2013). Late Cretaceous and Cenozoic tectonics of the Malay Peninsula constrained by thermochronology. *Journal of Asian Earth Sciences*, 76, 241–257.
- Dawson, J., MacDonald, S., Paton, J.R., Slater, D. & Singh, D. S. (1968). *Geological map of Northwest Malaya, 1:250,000*, Geological Survey Department, West Malaysia.
- Ghani, A.A. (2000). The Western Belt granite of Peninsular Malaysia: some emergent problems on granite classification and its implication. *Geosciences Journal*, 4, 283–293.
- Ghani, A. A. (2009). Plutonism. In C. S. Hutchison & D. N. K. Tan (Eds.), *Geology of Peninsular Malaysia* (pp. 211-232): University of Malaya and Geological Society of Malaysia, Kuala Lumpur, Malaysia.
- Hall, R. (2011). Australia–SE Asia collision: plate tectonics and crustal flow. *Geological Society, London, Special Publications 355(1)*, 75–109.
- Harbury, N.A., Jones, M.E., Audley–Charles, M.G., Metcalfe, I. & Mohamed, K.R. (1990). Structural evolution of Mesozoic peninsular Malaysia. *Journal of the Geological Society*, 147(1), 11-26.
- Hutchison, C.S. (1973). Metamorphism. In D. J. Gobbett & C. S. Hutchison (Eds.), *Geology of the Malay Peninsula* (pp. 253-303). New York: Wiley – Interscience.
- Hutchison, C.S., Tan, D.N.K. (2009). *Geology of Peninsular Malaysia*. University of Malaya and Geological Society of Malaysia, Kuala Lumpur, Malaysia.

- Ibrahim Abdullah. & Jatmika Setiawan. (2003). The kinematics of deformation of the Kenerong Leucogranite and its enclaves at Renyok waterfall, Jeli, Kelantan, *Geological Society of Malaysia Bulletin*, 26, 307-312.
- Khoo, T.T. (1980). Some comments on the emplacement level of the Kemahang granite, Kelantan. *Geological Society of Malaysia Bulletin* 13, 93–101.
- Khoo, T.T. & Lim, S.P. (1983). Nature of the contact between the Taku Schist and adjacent rocks in the Manek Urai area, Kelantan and its implications. *Geological Society of Malaysia Bulletin*, 16, 139–158.
- Lee, C. P. (2009). Paleozoic stratigraphy. In: Hutchison, C.S. & Tan, D.N.K. (Eds.), *Geology of Peninsular Malaysia* (pp. 55–86). University of Malaya and Geological Society of Malaysia, Kuala Lumpur.
- Lee, C. P., M. S. Leman, K. Hassan, B. M. Nasib. & R. Karim. (2004). *Stratigraphic Lexicon of Malaysia*. Geological Society of Malaysia, Kuala Lumpur, Malaysia.
- Lister, G.S. & Davis, G.A. (1989). The origin of metamorphic core complexes and detachment faults formed during Tertiary continental extension in the northern Colorado River region, USA. *Journal of Structural Geology*, 11(1-2), 65-94.
- MacDonald, S. (1968). *The geology and mineral resources of north Kelantan and north Terengganu*. Geological Survey West Malaysia, Ipoh, Malaysia.
- MacDonald, A. S., Barr, S. M., Dunning, G. R. & Yaowanoyothin, W. (1993). The Doi Inthanon metamorphic core complex in NW Thailand: age and tectonic significance. *Journal of Southeast Asian Earth Science* 8, 117-125.
- Metcalf, I. (2000). The Bentong–Raub Suture Zone. *Journal of Asian Earth Sciences* 18, 691–712.
- Metcalf, I. (2013). Tectonic evolution of the Malay Peninsula. *Journal of Asian Earth Sciences* 76, 195–213.
- Moore, A.C. (1970). Descriptive terminology for the textures of rocks in granulite facies terrains. *Lithos*, 3(2), 23-127.
- Searle, M.P. & Morley, C.K. (2011). Tectonic and thermal evolution of Thailand in the regional context of SE Asia. *The Geology of Thailand*. Geological Society, London.
- Morley, C.K. (2012). Late Cretaceous–Early Palaeogene tectonic development of SE Asia. *Earth Science Reviews* 115, 37–75.
- Ng, S.W.P., Whitehouse, M.J., Searle, M.P., Robb, L.J., Ghani, A.A., Chung, S.L., Oliver, G.J.H., Sone, M., Gardiner, N.J. & Roselee, M.H. (2015). Petrogenesis of Malaysian granitoids in the Southeast Asian tin belt: Part 2. U-Pb zircon geochronology and tectonic model. *Geological Society of America Bulletin*, 127.
- Passchier, C. W. & Trouw, R. A. J. (2005). *Microtectonics*. Springer Berlin Heidelberg.

- Pubellier, M., & Morley, C.K. (2014). The basins of Sundaland (SE Asia): Evolution and boundary conditions. *Marine and Petroleum Geology*, 58(Part B), 555–578.
- Richardson, J. A., 1946. The stratigraphy and structure of the Aranecous Formation of the Main Range Foothills. F. M. S. *Geological Magazine*, 83, 217-229.
- Richter, B., Schmidtke, E., Fuller, M., Harbury, N. & Samsudin, A. R., (1999). Palomagnetism of Peninsular Malaysia. *Journal of Asian Earth Sciences*, 17, 477-519.
- Rishworth, D. E. H. (1974). The Upper Mesozoic terrigenous Gagau Group of Peninsular Malaysia. *Geological Survey of Malaysia Special Paper*, 1, 1-78.
- Ryall, P. J. C. (1982). Some thoughts on the crustal structure of Peninsular Malaysia—results of gravity traverse, *Geological Society of Malaysia Bulletin*, 15, 9–18.
- Shuib, M. K. (2000). The Mesozoic Tectonics of Peninsular Malaysia – An overview. In: GSM Dynamic Stratigraphy & Tectonics of Peninsular Malaysia – Seminar III. The Mesozoic of Peninsular Malaysia. *Geological Society of Malaysia Warta Geologi*, 26, 23-29.
- Shuib, M. K. (2009). Structures and deformation. In C. S. Hutchinson & B. K. Tan (Eds.), *Geology of Peninsular Malaysia*. Kuala Lumpur: University of Malaya.
- Simpson, C. & Schmid, S.M. (1983). An evaluation of criteria to determine the sense of movement in sheared rocks. *Geological Society of America Bulletin*, 94, 1281–1288.
- Singh, D.S., Chu, L.H., Teoh, L.H., Looanathan, P., Cobbing, E.J. & Mallick, D.U. (1984). The Stong Complex: A reassessment. *Geological Society of Malaysia Bulletin*, 17, 61–78.
- Tate, R.B., Tan, D.N.K., Ng, T.F. (2008). *Geological Map of Peninsular Malaysia*. Scale 1:1,000,000. Geological Society of Malaysia.
- Teggin, D. R. (1975). *The granites of northern Thailand*. Ph.D. thesis, University of Manchester, U.K.
- The Malaysian and Thai Working Groups. (2006). *Geology of the Batu Melintang – Sungai Kolok transect area along the Malaysia – Thailand border*. Minerals and Geoscience Department Malaysia and Department of Mineral Resources, Thailand.
- Tjia, H.D. (1969). Regional implication of Lebir fault zone. *Geological Society of Malaysia Newsletter*, 19, 6–7.
- Tjia, H.D. (1996). Tectonics of deformed and undeformed Jurassic–Cretaceous strata of Peninsular Malaysia. *Geological Society of Malaysia Bulletin*, 39, 131–156.
- Umor, M.R. & Mohamad, H., 2002. Tren unsur-unsur nadir bumi (REE) Suit Stong, Jeli, Kelantan. *Bulletin of Geological Society of Malaysia*, 45, 51-58.

- Zaiton, H. (2002). Late Mesozoic–Early Tertiary faults of Peninsular Malaysia. *Geological Society of Malaysia Bulletin*, 45, 117–120.
- Ziegler, P. A., S. Cloetingh & J.D. van Wees. (1995). Dynamics of intra-plate compressional deformation: the Alpine foreland and other examples. *Tectonophysics*, 252 (1–4), 7–22.

University of Malaya

## LIST OF PUBLICATIONS AND PAPERS PRESENTED

### A. Publications

M.A. Md Ali., E. Willingshofer., L. Matenco., T. Francois., T.P. Daanen., T.F. Ng., N.I. Taib. & M.K. Shuib (2016). Kinematics of post-orogenic extension and exhumation of the Taku Schist, NE Peninsular Malaysia. *Journal of Asian Earth Sciences*, 127, 63 – 75.

T. François., M.A. Md Ali., L. Matenco., E. Willingshofer., T.F. Ng., N.I. Taib. & M.K. Shuib. (2017) Late Cretaceous extension and exhumation of the Stong and Taku magmatic and metamorphic complexes, NE Peninsular Malaysia, *Journal of Asian Earth Sciences*, 143, 296-314.

### B. Papers Presented

Title: The Kinematics Retrograde Deformation in Taku Schist, NE Peninsular Malaysia: Implications to Post-Orogenic Extension and Exhumation.

Oral Presentation

GEOSEA XIV CONGRESS and 45<sup>th</sup> IAGI ANNUAL CONVENTION, 10-13<sup>th</sup> October 2016. Trans Luxury Hotel Bandung, Indonesia.